7-10-75

THE GAWLER RANGES VOLCANIC COMPLEX

ASH FLOW DEPOSITS IN CAULDRON SUBSIDENCE AREAS

by

A.R. Turner B.Sc., Canterbury N.Z.

A thesis submitted to the Geology Department, University of Adelaide for the Degree of Master of Science.

Australian Mineral Development Laboratories
Anaconda Australia Inc.

September 1974

STATEMENT

This thesis contains no material which has been submitted for the award of any degree or diploma in any University.

To the best of my knowledge and belief this thesis does not contain any material previously published or written by another person, except where due acknowledgement is made either in the text, or in the bibliography.

This thesis was submitted in candidate's absence, his signature is being obtained

A.R. Turner

1st September 1974

CONTENTS

		Page
1.	INTRODUCTION	1
	1.1 Regional Physiography	2
	1.1.1 Mapped Area	3
2.	PREVIOUS INVESTIGATIONS	4
	2.1 Field Occurrence and Structure	4
	2.2 Geological Setting	5
	2.3 Petrography	7
	2.4 Age of the Gawler Range Rocks	8
	2.5 Field Work	9
	2.6 Laboratory Techniques	10
3.	INTRUSIVE ROCKS SOUTH OF THE SOUTHERN BOUNDARY	12
	3.1 Rocks of the Gawler Ranges Petrogenetic Province	12
	3.2 Intrusive Granites	14
	3.3 Basic Rocks	15
4.	STRUCTURE	15
	4.1 The Southern Boundary	15
	4.2 The Arc Structure	18
	4.2.1 Jointing	20
	Blocky Joint System	20
	Flaggy Jointing	21
	Fracture Jointing	21
	4.2.2 Faulting	22
	4.2.3 Folding	23
	4.3 Welded Tuff Sheet ($p\epsilon v_3$)	24
	4.3.1 Internal Structure	24

CONTENTS

		Page
4.3.2	Jointing	24
	Platy Jointing	24
	Columnar Jointing	25
4.4.	Tectonic Map	27
4.4.1	Statistical Analysis of Joint Sets	27
	Western Ridge	27
	Ring Structure	27
	Ridge North of Ring Structure	28
	Eastern Block	28
4.4.2	Results	29
4.4.3	Conclusions	31
5.	STRATIGRAPHY	
5.1	Lithic and Lapilli Tuff (pЄt)	34
5.1.1	Field Observations	34
5.1.2	Petrography	38
	Altered Fragments	37
	Rhyolitic Rock Fragments	37
	Lithic Tuff Rock Fragments	38
	Pumice Fragments	38
	Siliceous Vitric Tuff Fragments	39
	Devitrified Obsidian Fragments	39
	Quartz Fragments	39
	Feldspar Fragments	39
	Altered Crystal Fragments	40
	Accessory Minerals	40
	Eastern Region	40
	Central Region	40
	Western Region	41
5.1.3	Petrochemistry	42
5.2	Porphyritic Rhyolite ($p\epsilon l_1$)	45
5.2.1	Field Observations	45
5.2.2	Petrography	46
5.3	Welded Tuff ($p\epsilon v_1$)	48
5.3.1	Field Observations	48

CONTENTS

		Page
5.3.2	Petrography	49
	Eastern Region	49
5.3.3	Petrochemistry	60
5.4	Porphyritic Rhyolite ($p\epsilon 1_2$)	63
5.4.1	Field Observations	63
5.4.2	Petrography	65
	Snowflake Textured Porphyritic Rhyolites	65
	Perlitic Textured Porphyritic Rhyolites	68
	Lithic Vitric Tuffs	73
5.4.3	Petrochemistry	74
5.5	Crystal Tuff ($p\epsilon ct$)	74
5.5.1	Field Observations	74
5.5.2	Petrography	75
5.5.3	Petrochemistry	78
5.6	Pumiceous Tuff ($p\epsilon pt$)	80
5.6.1	Field Observations	80
5.6.2	Petrography	81
	Pumice Fragments and Ash	81
	Devitrified Perlitic Fragments	82
	Rock Fragments	83
	Crystal Fragments	84
5.7	Welded Tuff ($p\epsilon v_2$)	87
5.7.1	Field Relationships	87
5.7.2	Petrography	88
5.8	Porphyritic Amygdaloidal Rhyolite ($p\epsilon al$)	93
5.8.1	Field Observations	93
5.8.2	Petrography	95
	Basal Welded Tuffs	95
	Massive, Banded and Perlitic "Rhyolites"	96
	Amygdaloidal Rhyolites	100
5.8.3	Petrochemistry	103
5.9	Porphyritic Rhyolite ($p\epsilon 1_3$)	105
5.9.1	Field Observations	105
5.9.2	Petrography	106
	Massive Porphyritic Phase	106

CONTENTS

	Page
Banded Porphyritic Phase	109
Breccia Member	111
5.9.3 Petrochemistry	112
5.10 Fluidal Banded Porphyritic Rhyolite (pЄfbl)	116
5.10.1 Field Observations	116
5.10.2 Petrography	117
5.10.3 Petrochemistry	121
5.11 Vitric Tuff (pЄvt)	122
5.11.1 Field Observations	122
5.11.2 Petrography	123
5.11.3 Petrochemistry	126
5.12 Welded Lithic Tuff (pCwt)	127
5.12.1 Field Observations	127
5.12.2 Petrography	128
Welded Vitric Crystal Tuffs	130
Massive Rhyolites	131
Devitrified Obsidian	131
Siliceous Vitric Tuff Fragments	131
Fluidal Banded Rhyolites	131
Altered Vesciculated Fragments	132
5.13 Welded Tuff Sheet ($pЄv_3$)	134
5.13.1 Field Observations	134
5.13.2 Petrography	135
Groundmass	135
Quartz Phenocrysts	138
Ferromagnesian Minerals	139
Accessory Minerals	142
Feldspar Phenocrysts	143
5.13.3 Petrochemistry	143
5.13.4 Modal Distribution of Phenocrysts in Welded Tuff Sheet ($pЄv_3$)	143
Results	144
Conclusions	151

6. CHEMISTRY AND PHYSICAL CONDITIONS OF CRYSTALLIZATION

6.1 Major Element Variations 152
6.2 Trace Elements 154
6.3 Physico Chemical Conditions of Crystallization 156
6.3.1 Water Vapour Pressure at Time of Differentiation 156
6.3.2 Water Content, Temperature, Depth of Magma During Crystallization and Differentiation 158
6.3.3 Crystallization History 160

7. THE PRIMARY ROCK TYPES AND THEIR POST EMPLACEMENT HISTORIES. 164

7.1 Crystallization Textures 164
7.1.1 The Snowflake Texture 165
7.1.2 Fluidal Banding 166
7.1.3 Lava Textures 168
7.2 Vapour Phase Crystallization 168
7.3 Granophyric Crystallization 170
7.4 The Primary Rock Types 171
7.4.1 Lithic and Lapilli Tuffs (pЄt) 172
7.4.2 Porphyritic Rhyolite ($pЄl_1$) 172
7.4.3 Welded Tuff ($pЄv_1$) 173
7.4.4 Porphyritic Rhyolite ($pЄl_2$) 174
7.4.5 Crystal Tuff (pЄct) 175
7.4.6 Pumiceous Tuff (pЄpt) 176
7.4.7 Welded Tuff 177
7.4.8 Porphyritic Amygdaloidal Rhyolite (pЄal) 178
7.4.9 Porphyritic Rhyolite ($pЄl_3$) 179
7.4.10 Vitric Tuff (pЄvt) 180
7.4.11 Welded Tuff Sheet ($pЄv_3$) 181
7.5 Discussion 182

8. THE GAWLER RANGES VOLCANIC COMPLEX 185

8.1 Basement Relationships 186

9. THE SOURCE MAGMA 188

10. BACKGROUND AND ACKNOWLEDGMENTS 190

11. REFERENCES 191

TABLES 1 to 13

FIGURES 1 to 15

PLATES 1 to 32

APPENDICES A to E

ATTACHMENTS - Map 1 Map 2

LIST OF TABLES

Table 1	GENERALIZED STRATIGRAPHIC SECTION	follows 34
Table 2	LITHIC TUFF ($p\epsilon t$)	
	Chemical and C.I.P.W. Normative Analyses	43
Table 3	WELDED TUFF ($p\epsilon v_1$)	
	Chemical and C.I.P.W. Normative Analyses	61
Table 4	CRYSTAL TUFF ($p\epsilon ct$)	
	Chemical and C.I.P.W. Normative Analyses	79
Table 5	AMYGDALOIDAL RHYOLITE ($p\epsilon al$)	
	Chemical and C.I.P.W. Normative Analyses	104
Table 6	PORPHYRITIC RHYOLITE ($p\epsilon 1_3$)	
	Chemical and C.I.P.W. Normative Analyses	113
Table 7	FLUIDAL BANDED RHYOLITE ($p\epsilon fbl$)	
	Chemical and C.I.P.W. Normative Analyses	121
Table 8	VITRIC TUFF ($p\epsilon vt$)	
	Chemical and C.I.P.W. Normative Analyses	126
Table 9	WELDED TUFF SHEET ($p\epsilon v_3$)	
	Chemical Analyses	Appendix C
Table 10	WELDED TUFF SHEET ($p\epsilon v_3$)	
	C.I.P.W. Normative Analyses	Appendix D
Table 11	TREND SURFACE ANALYSIS	145
Table 12	BARIUM ANALYSES	155
Table 13	SUMMARY OF MAJOR LITHOLOGIES	164

LIST OF FIGURES

		follows page
Figure 1a	EYRE PENINSULA - SOUTH AUSTRALIA Gawler Ranges - Location and Access Routes	1
Figure 1b	GAWLER RANGES VOLCANIC COMPLEX Structural Boundaries Eastern Limits	2
Figure 2	TREND SURFACE ANALYSIS Sample Numbers and Locations	143
Figure 3	CONTOUR PLOT - PLAGIOCLASE	143
Figure 4	TREND SURFACE ANALYSIS Feldspar Run 1	144
Figure 5	TREND SURFACE ANALYSIS Feldspars Run 2	146
Figure 6	TREND SURFACE ANALYSIS Feldspars Run 3	147
Figure 7	TREND SURFACE ANALYSIS Mafics and Total Crystal Run 3	147
Figure 8	TREND SURFACE ANALYSIS Ratio Feldspars/Total Crystal Run 3	149
Figure 9	DIAGRAMMATIC CROSS SECTION A-A' (Fig.2)	151
Figure 10	CHEMICALLY ANALYSED SAMPLES Numbers and Localities	151
Figure 11	NORMATIVE Or-Ab-An RECALCULATED TO 100% (after O'Connor 1965)	152
Figure 12	MAJOR ELEMENT VARIATION DIAGRAMS	152
Figure 13	POTASSIUM AND BARIUM VARIATION	155
Figure 14	NORMATIVE Q-Or-Ab TERNARY DIAGRAM Adapted from Tuttle & Bowen (1958) Luth, Johns & Tuttle (1964)	157

LIST OF PLATES

		follows page
Plate 1	BLOCKY JOINT SYSTEM	20
Plate 2	FRACTURE JOINTING	21
Plate 3	FLAGGY JOINTING	21
Plate 4	TIGHT FOLD STRUCTURES	23
Plate 5	TIGHT FOLD STRUCTURES	23
Plate 6	OPEN STYLE FOLDING	23
Plate 7	PLATY JOINTING	24
Plate 8	COLUMNAR JOINTING	26
Plate 9	COLUMNAR JOINTING	26
Plate 10	COLUMNAR JOINTING	26
Plate 11	LITHIC TUFF (pЄt)	37
Plate 12	LITHIC TUFF (pЄt)	37
Plate 13	LITHIC TUFF (pЄt)	37
Plate 14	LAPILLI TUFF (pЄt)	41
Plate 15	MASSIVE PORPHYRITIC RHYOLITE ($pЄl_1$)	47
Plate 16	WELDED TUFF ($pЄv_1$)	51
Plate 17	PORPHYRITIC RHYOLITE ($pЄl_2$)	72
Plate 18	CRYSTAL TUFF (pЄct)	74b
Plate 18a	CRYSTAL TUFF (pЄct)	75
Plate 19	PUMICEOUS TUFF (pЄpt)	81
Plate 19a	PUMICEOUS TUFF (pЄpt)	81
Plate 20	WELDED TUFF ($pЄv_2$)	88
Plate 21	PORPHYRITIC AMYGDALOIDAL RHYOLITE (pЄal)	98
Plate 22	PORPHYRITIC AMYGDALOIDAL RHYOLITE (pЄal)	102
Plate 23	PORPHYRITIC RHYOLITE ($pЄl_3$)	108
Plate 24	PORPHYRITIC RHYOLITE ($pЄl_3$)	108
Plate 25	PORPHYRITIC RHYOLITE ($pЄl_3$)	110

LIST OF PLATES

		follows page
Plate 25a	PORPHYRITIC RHYOLITE ($p\epsilon l_3$)	111
Plate 26	FLUIDAL BANDED RHYOLITE ($p\epsilon fbl$)	119
Plate 27	VITRIC TUFF ($p\epsilon vt$)	122
Plate 28	VITRIC TUFF ($p\epsilon vt$)	123
Plate 29	WELDED LITHIC TUFF ($p\epsilon wt$)	132
Plate 30	WELDED TUFF SHEET ($p\epsilon v_3$)	136
Plate 31	WELDED TUFF SHEET ($p\epsilon v_3$)	137
Plate 32	WELDED TUFF SHEET ($p\epsilon v_3$)	139

APPENDICES

		page
Appendix A	CONTOUR MAPS AND STATISTICAL EVALUATION OF GEOLOGICAL DATA.	A1 - A5
Appendix B	CALCULATION OF WATER PRESSURES DURING FORMATION OF THE MAGMA	B1 - B2
Appendix C	TABLE 9 - WELDED TUFF SHEET ($p\epsilon v_3$) Chemical Analyses	
Appendix D	TABLE 10 - WELDED TUFF SHEET ($p\epsilon v_3$) C.I.P.W. Normative Analyses	
Appendix E	SAMPLED LOCATIONS ROCK UNITS Examined in Thin Section	E1 - E2

ATTACHMENTS

Map 1	GEOLOGY ARC AND ENVIRONS Gawler Range Volcanic Complex S.A.
Map 2	TECTONIC MAP ARC AND ENVIRONS Gawler Range Volcanic Complex S.A.

ABSTRACT

The Gawler Ranges of South Australia extend across Northern Eyre Peninsula and comprise extensive tracts of superficially similar acid extrusive rocks of dominantly rhyolitic character. The volcanics were extruded in the Middle Proterozoic but for the most part are sub-horizontal. Cauldron subsidence along peripheral ring fractures and pre-existing basement lineaments exposes a partial cross-section through the pile.

At the eastern end of the Ranges three volcanic cycles are recognized. Each cycle is initiated by the explosive eruption of ash-fall tuffs which are structurally zoned according to their mechanics of emplacement. Each of these initial ash-falls is over-lain by volatile-enriched ash flows. The volume of extruded material is greater in each succeeding cycle and culminates in the outpouring of a vast, ash-flow, tuff-sheet at least 460 metres thick and over 1500 square kilometres in extent.

The less welded, more porous formations of each cycle crystallize in the zone of vapour phase crystallization (Smith 1960). Fluidal, banded and snowflake textures develop in these zones. Some of the magmatic textures may represent original lava flows. The introduction of potash and silica displaces soda, magnesia, lime and iron the latter three of which are redistributed, but soda is expelled from the system. The zone of vapour-phase crystallization grades upwards into a zone of granophyric crystallization (Smith op. cit) manifested in the ash-flow tuffs where most primary textures are destroyed and where the lime, magnesia and iron are relocated.

The welded tuff sheet is rhyodacitic at the base and rhyolitic at the surface. A continuous out-pouring of pyroclastic ejecta shows a progressive increase in potash feldspar phenocrysts at the expense of plagioclase and ferromagnesians upwards through the sheet.

The internal structure is dominated by a tectonic joint set developed in response to block faulting which trends north-north-west and east-north-east. The blocks are tilted to the south-west and subsidence is greater near the southern margin where a fissure may be the source for much of the erupted material.

In the western part of the Gawler Ranges basic rocks are known at Kokatha and basic xenoliths are found in ash-flow tuffs at Hiltaba and Yarna. These rocks probably represent the base of the extruded pile and are domed by granites which are intruded as high level stocks by underground cauldron subsidence. Contemporaneous trachyandesite, trachyte and basalt are, however, rare.

Comparison of normative analyses with experimentally determined isobars suggests that the water-vapour pressure at the time of differentiation was about 600 bars. If the total confining pressure was lithostatic the equilbrium water content of the magma was approximately 3.5 weight percent, the temperature 730^{o} and the depth to the top of the magma chamber 2.5 kilometres.

These data are consistent with a rhyolitic magma occupying a shallow chamber and forming ash-flow eruptions by the rapid expulsion of large, shallow magma bodies. The preponderance of acid magma is similar to most other high level magmatic provinces.

The magma was probably generated at the base of the crust during the orogenic phase of the development of the Adelaide Geosyncline and was injected under tension into the upper levels of the crust prior to crystallization, then enriched in volatiles, and erupted from fissure vents primarily as immense ash flows.

1. INTRODUCTION

The Gawler Ranges were discovered and named by the explorer E.J. Eyre in 1839 who, on his return from the Great Australian Bight, passed along their southern boundary. To describe the area Eyre annotated his map "Bar(re)n range of porpheritic granite" (sic).

South Australia's first Government Geologist, H.Y.L. Brown, briefly examined the rocks of the Gawler Ranges in 1885 and noted -

> "low hills of red feldspar porphyry rising 200 to 500 feet above the plains, extending westward for 100 miles from near Corunna Station (5 miles north of Iron Knob) and north for an unknown distance".

Reconnaissance mapping by geologists from the South Australian Government Department of Mines has shown that the dominant rock type (rhyolitic welded tuff) outcrops over an area of some 190,000 square kilometres extending from near Wartaka Homestead westwards for almost 480 kilometres. The bulk of the outcrop comprises the Gawler Ranges, with a north-south dimension averaging 48 kilometres but outliers at Tarcoola give a maximum north-south extent of about 256 kilometres. Figure 1 shows the location and geographic extent of rocks which comprise the Gawler Ranges Volcanic Complex.

In the 130 years since their discovery the Ranges have been subjected to cursory examinations which have confirmed their volcanic character (Jack 1917, Crawford 1963) and established, within fairly close limits, their age by isotopic age-determinations (Compston et. al., 1966).

Prior to the present study no part of the Complex had been critically examined in an attempt to establish the true nature of the rocks, their habit, petrogenesis and detailed structure and stratigraphy.

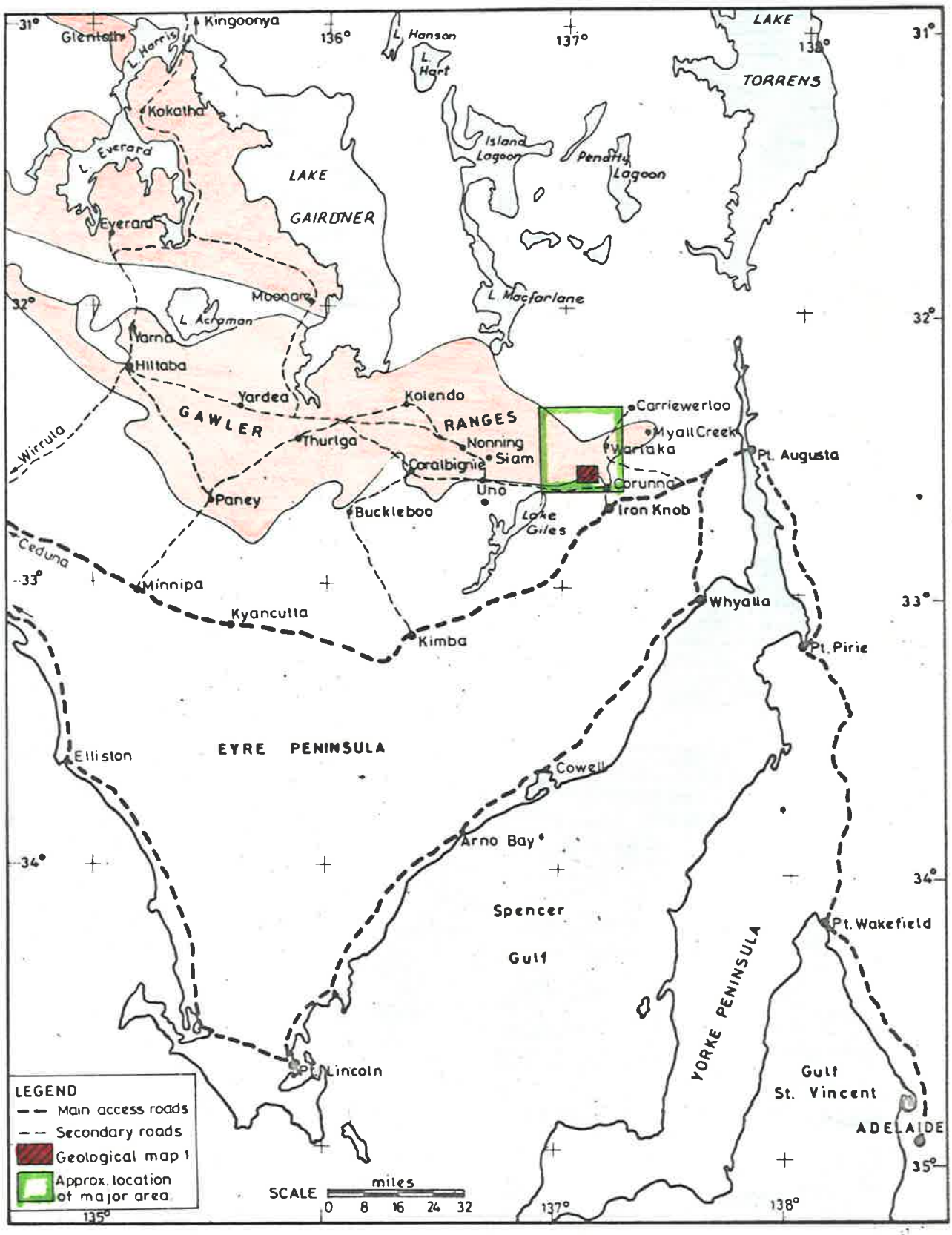


FIGURE 1: EYRE PENINSULA. SOUTH AUSTRALIA
Gawler Ranges: Location and Access Routes.

In this study an area of about 900 square kilometres, situated in that portion of the Port Augusta 1:250,000 Geological Map area bounded by longitudes 136 degrees 31 minutes to 137 degrees 04 minutes west and latitudes 32 degrees 14 minutes to 32 degrees 40 minutes south (Figures 1 and 1B) has been investigated in some detail. Maps 1 and 2 show the geology and structure respectively of the southern part of this area.

The collected data are applied to the whole Complex in an attempt to establish its petrogenesis.

1.1 Regional Physiography

The Gawler Ranges form a dissected plateau which attains an elevation of over 500 metres in several places. In the south the ranges rise abruptly from a vast, scrub-covered, sandy plain with numerous granite inselbergs (?Charlestonian phase granites) and local gneiss outcrops (Cleve Metamorphics). The plain is about 150 to 300 metres above sea level and the Gawler Ranges attain an elevation of as much as 230 to 350 metres above that. The Ranges form low, rocky hills covered with spinifex and stunted trees separated by numerous flat-bottomed, grassy valleys usually dotted with salt and blue bush. No permanent streams exist. The rainfall is approximately 12 inches per annum in the south but northwards the country deteriorates and sand cover becomes dominant with a rainfall of 10 or even 8 inches. To the west are immense spreads of dunes trending west-nor-west. In the general area of the Gawler Ranges and to the east are several very large and innumerable, smaller salt lakes. Lake Gairdner, by far the largest, covers about 3,200 square kilometres.

The area is remote and, except for local pastoralists, is seldom visited. Access is by way of the main Adelaide - West Australian highway

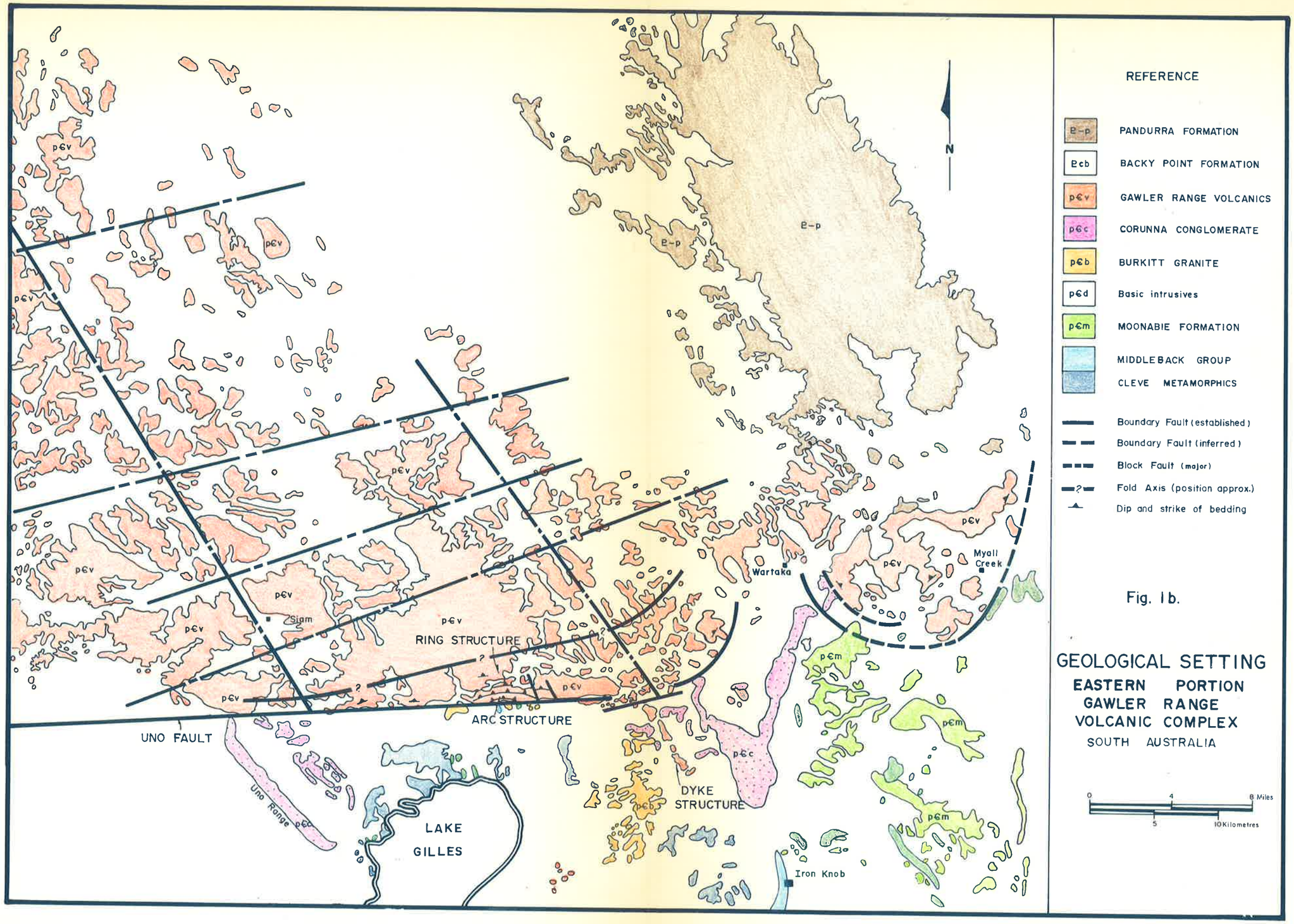


Fig. 1b.

GEOLOGICAL SETTING

EASTERN PORTION GAWLER RANGE VOLCANIC COMPLEX

SOUTH AUSTRALIA

from which several all-weather secondary roads provide good access to most portions of the Complex. Numerous station tracks provide supplementary access. The Trans-Continental Railway between Perth and Sydney is sited along the northern limits of the Complex.

1.1.1 Mapped Area (See Fig. 1)

The rocks of the Complex, adjacent to the Uno Fault, are not characteristic of the main mass. Flow structures are common, contacts between flows are generally recognizable, welding foliation in tuffaceous rocks can be mapped and multiple cooling units can be recognized.

Of all the volcanics exposed along the Uno Fault, those exposed in an Arc Structure on the southern margin of the mapped area afford the best exposures and the most mappable volcanic succession. They are in striking contrast to the megascopically homogenous rocks to the north of this area.

The Arc Structure is formed of three rows of low hills alternating with shallow troughs. The higher areas are formed of a massive, resistant, red welded tuff and the troughs develop over more readily weathered, non-welded tuffs and flow-banded rocks.

The major drainage is essentially consequent and radially disposed with respect to the Arc's profile. A subsidiary, concentric drainage system draining into the radial system has formed along major lithologicaly contacts and over more readily weathered tuffaceous and flow-banded rocks.

Variations in lithology within the Arc are manifested in aerial photographs by vegetation differences. The more resistant massive, red, welded tuffs support a vegetation of Spinifex and poorly developed Mallee scrub. The less-resistant tuffs and flow-banded rocks support blue-bush vegetation, more luxuriant Mallee scrub, Arcacias and indigenous grasses and wild flowers in the wet season. In some areas contacts are sharply

delineated by the contrasting vegetation which provides an excellent aid to mapping in areas of poor exposure.

The outcrop in the mapped area is poor. The welded tuffs are moderately well exposed but the non-welded tuffs and flow-banded rocks are poorly exposed and small discontinuous and sporadic outcrops are characteristic.

To the north of the Arc the outcrop is better, although the lithologies are monotonously uniform.

2. PREVIOUS INVESTIGATIONS

2.1 Field Occurrence and Structure

Apart from the observations of Brown in 1885, little geological work was carried out until Lockhart Jack (1912) commented on the habit of the "porphyry". He regarded the main mass of the Gawler Ranges as "either an enormous sill or an extensive surface flow".

Jack (1917) observed that the eastern end of the Gawler Ranges "porphyry" rested upon Precambrian Gneisses (Cleve Metamorphics). He also commented that "although the mass has been deeply dissected the great lateral extent and the remarkably even skyline suggest that the rock is effusive rather than intrusive". Jack equated the copper bearing Moonta Porphyry to that of the Gawler Ranges, as an intrusive equivalent of an effusive mass.

Brown (1899, p.11) recorded the wide distribution of "feldspar porphyry" to the north and north-west of Glenloth and up to 50 kilometres past Tarcoola and regarded this as a continuation of that of the Gawler Ranges.

In about 1900 lode gold was found at Tarcoola and Glenloth. Brown (1902) noted that the lodes "partake of the nature of dykes". He added that "dykes of diorite and amygdaloidal trap (related to the Complex) probably have some influence on the occurrence of gold".

Segnit (1932) noted "characteristic feldspar porphyry" in the Yarna area (?massive, red, welded tuff) and the restricted occurrence of granite porphyry (?porphyritic microgranite) a rock type which was also described by Jack as a variant of the basement granites.

Crawford (1961) produced a reconnaissance map in which the outcrop area of rocks of the Complex was delineated together with major structural features as determined from an examination of aerial photo mosaics. He also described ring structures near the Arc of the writer's mapped area which he suggested were "vents with diameters of about 1 mile".

Geologists from the Department of Mines mapped the eastern limits of the Complex as part of the Port Augusta 1:250,000 Sheet (1968).

2.2 Geological Setting

The regional geology of Eyre Peninsula has been described in the Handbook of South Australian Geology (Ed. Parkin, 1969).

The Gawler Range Volcanic Complex overlies the crystalline gneissic basement of the Gawler Platform which is composed of a metasedimentary sequence of gneisses (Cleve Metamorphics, Thomson, 1968) intruded by granitoid rocks. Isotopic age determinations (Compston et. al., 1966) show that the Cleve Metamorphics were deformed and re-crystallized during the Kimbian tectonic phase of Carpentarian age (1,600 to 1,800 million years).

Unconformably overlying the older basement, is the Moonabie Formation, a metaquartzite with conglomerate and tuffaceous members (Smale, 1965) that

is itself intruded by the Moonabie Porphyry (porphyritic rhyolite).

The Charlestonian Phase of folding and plutonism affected the region after the deposition of the Moonabie Formation. This phase is marked by the intrusion of numerous granites which extend across north-eastern Eyre Peninsula. The largest of these is the Charleston granite in the Moonabie Range, the intrusion of which marked the end of the Charlestonian Phase of folding (1,590 million years; Thomson, 1966; Compston et. al., 1966).

Unconformably overlying the granites of the Charlestonian phase of plutonism is the Corunna Conglomerate which is more than 170 metres thick. A shale from the conglomerate has been dated at 1,550 million years (Compston et. al., op cit).

Subsequent to its sedimentation in the Upper Carpentarian the Corunna Conglomerate was moderately folded. This event was followed by the extrusion of the great volume of acid Gawler Range Volcanics at about 1,535 million years, with volcanism continuing until at least 1,470 or 1,480 million years (Compston et. al., op cit); this being the date of emplacement of the porphyritic rhyolite dykes intruding the Corunna Conglomerate sequence (Whitten, 1966, 1969; Johns and Solomon, 1953) and of the related Moonta Porphyry. The Wartaken Phase of folding and acid volcanism marks the beginning of stability of the Gawler Platform in the Gawler Ranges area although it is possible that folding and magmatism continued into Adelaidean time in the concealed northern and western parts. Further east along the margin of the Gawler Platform the sedimentation in the Adelaide Geosyncline was yet to begin.

The Gawler Range Volcanic Complex is undoubtedly greater in extent than its exposed massif, the extension probably being greatest in the west where exposure is restricted by Quaternary sand. Rocks of the Complex may also extend further to the north and east and be overlain by sediments of the Adelaide Geosyncline.

The southern boundary of the Complex is discordant to, and in faulted contact with,the steeply dipping, nor-west striking,meta-sedimentary Cleve Metamorphics.

Several granite bodies in the region are thought to be petrologically similar to rocks of the volcanic episode. Such are found at Wilgenna, Gibralter Rocks (Segnit 1937) and elsewhere to the north-west, within the Complex at Hiltaba and Kokatha, and to the south the Charleston granite, the Buckleboo granite, the Burkitt granite and several others extending across Northern Eyre Peninsula. These granites have all been tentatively correlated with the Charlestonian Phase of plutonism on the basis of radiometric age-determinations (Compston et. al., op cit).

2.3 Petrography

Jack (1917) stated that the porphyritic rocks of the Gawler Ranges -

> "invariably show a cryptocrystalline groundmass. In some cases there are numerous acicular microlites and the groundmass when examined under cross nicols, shows, in some instances, well defined aggregate polarisation. Both plagioclase and orthoclase appear to be represented amongst the feldspars but without exception the feldspars have suffered considerable alteration. Hematite is abundantly distributed in the form of dust throughout the groundmass, and in cleavages of feldspar crystals of the reddish varieties, and is the cause of their red colour. The ferromagnesian constituent is a colourless pyroxene when unaltered, but in almost every instance it is chloritized. The occasional quartz phenocrysts show rounded outlines and a corona in the groundmass surrounding them is clearly defined, perhaps marking the effect of resorbtion".

Mawson (1926) briefly examined some rocks from the Gawler Ranges and states -

> "sericitization of the feldspar phenocrysts is a common feature. Grains of yellowish-green epidote are often abundant. Whisps of a

secondary greenish amphibole and grains of leucoxene from the complete alteration of ilmenite are frequent. In the fine-grained base, apparently recrystallized after solidification, one frequently finds a marked micrographic intergrowth between the feldspar and the quartz which constitutes the mass of such base".

2.4 Age of the Gawler Ranges Rocks

Jack (1922) regarded the mass of the Gawler Ranges as being effusive over the Precambrian gneisses (Cleve Metamorphics) of Eyre Peninsula. Mawson (1926) stated that -

"the acid porphyries of the Gawler Ranges and of the Mount Painter Block are probably effusives of the middle Proterozoic (a period when granite intruded on a grand scale, thick sedimentary strata in South Australia)".

Johns and Solomon (1953) were able to demonstrate that some of the Gawler Ranges Volcanics intruded the supposedly Cambrian (now Carpentarian) sediments of the Corunna Conglomerate. Intrusive bodies and plugs were found 5 kilometres south of Wartaka Homestead and 3 kilometres south-west of Roopena Homestead.

Compston et. al. (1966) stated that -

"with one exception, radiometric age determination data on all samples of the Gawler Ranges Volcanics so far analysed, including the plug (Wartakan Neck) are consistent with a single period of extrusion for these lavas. The data obtained confirm the approximate contemporaniety of the volcanics and the Corunna Conglomerate proposed on field evidence. Their determined age is 1,535 ± 25 million years".

Thomson (1966) stated that -

"no positive geological field evidence has yet been found that clearly resolves the age relationships of the Corunna Conglomerate to the Adelaide system. The age determination of Compston et. al. (1966), however, established that the Corunna Conglomerate and the Gawler

Range Volcanics are older than any rocks yet dated within the Adelaide system and younger than granites that intrude the older Precambrian basement in the region". (Charlestonian granites).

2.5 Field Work

Geological mapping was based on 60 chains to 1 inch (65:391 F Series) base maps prepared by the South Australian Government Department of Mines. The maps locate the drainage patterns, access tracks (sometimes erroneously), fences, dams and station properties together with principal geographic features. No relief is indicated except for several Trig stations. Subsequently, sample locations were transferred to a topographic base of the Port Augusta 1:250,000 geological sheet (S.A. Govt. Dept. Mines, 1968) for the interpretation of trend surface analysis results.

Vertical air photographs flown from a height of 5,000 metres and reproduced at a scale of about 60 chains to 1 inch (Survey 137 UNO Run 2, Photos 120, 121 and 122), together with an enlargement of one of these to a scale of about 10 chains to 1 inch, were employed for detailed mapping. The uncorrected photo enlargement was used as a topographic base for the geological map. The map was then photographically enlarged and redrawn at a corrected scale.

Hand specimens were geographically orientated. This allowed a study of the rocks in the laboratory in order to establish whether or not there were textural and/or petrographic data which could be related to joint directions and other structural features. In some cases structures, not apparent in hand specimen but evident in thin section, could be used to advantage.

2.6 Laboratory Techniques

Approximately 800 rocks were collected and about 700 thin sections were prepared and examined with a polarising microscope.

The most common rock type is a massive welded tuff. The comparatively coarse grain size of the phenocrysts and their random distribution does not allow modal analyses to be completed by the usual techniques viz: point counter or intergrating stage. Both of these techniques were tried but because of the area available in a standard thin section the results could not be reproduced between two thin sections taken from the same hand specimen.

The percentage of each feldspar phenocryst type [distinguished by staining with sodium cobaltinitrite according to the method of Gabriel and Cox (1929) and Williams (1960)] were estimated with the aid of a transparent glass plate ruled in a 2 mm grid containing 800 squares, and a binocular microscope set at times 16 magnification.

No modal analyses were performed on other than homogeneous, massive rocks. Mineral percentages in rocks with an internal structure are visually estimated and hence only approximate.

The application of the sodium cobaltinitrite staining technique to uncovered thin sections (Chayes, 1952) was also found useful for the identification and distribution of potash feldspar in the groundmass. About one hundred slides were thus stained.

In most cases the composition of the plagioclase feldspars was determined in thin section using extinction angles in grains cut perpendicular to A. The nature of the potash feldspars was roughly determined by estimating the optic axial angle on suitably oriented

sections. In addition, measurements of the optic axial angle of both potash feldspars and plagioclase feldspars were made on the Leitz 4-Axis Universal Stage. The determinations of anorthite content were made using the method described by Turner (1947) and the refined curves of Slemmons (1962). The latter author believed the anorthite content could be ascertained to within 3% by this method.

The identity of several alteration products was determined by X-ray powder diffraction using cobalt Kα radiation.

Four new silicate analyses were completed using conventional techniques.

Five published analyses are also used together with forty-eight whole rock analyses (one -S128- a repeat of a rock analysed by standard techniques for cross-checking purposes) determined on a Direct Reading Emission Spectograph. In this case total iron was calculated as Fe_2O_3 and FeO was determined colormetrically. Trace elements from five samples were determined semiquantitatively using spectrographic techniques.

Specific gravities of five rock samples were measured by the wax-immersion method described by Milner (1958).

CIPW normative analyses were calculated on the University of Adelaide computer. Trend-surface analyses of the modal distribution of phenocrysts in the Welded Tuff Sheet were calculated on the University of Adelaide computer using a programme modified by Amdel from that of Peikert (1973). The results were contoured in some cases and printed out on the line printer in others (the latter technique is less expensive and quite adequate). The plots were traced onto a suitable enlarged topographic base map and then photographically reduced for this study.

3. INTRUSIVE ROCKS SOUTH OF THE SOUTHERN BOUNDARY

Several intrusive bodies both related and unrelated to the Gawler Ranges Volcanic Complex occur to the south of, and along the main boundary of the Complex.

3.1 Rocks of the Gawler Ranges Petrogenetic Province

Small intrusions of characteristic, massive, red, porphyritic rhyolite are found:

1. in the Corunna Conglomerate 5 kilometres south of Wartaka Homestead (Wartakan Neck - Johns and Solomon 1953);
2. in the axis of the north plunging syncline of the Corunna Conglomerate, 10 kilometres north-north-west of Corunna Homestead; and
3. 3 kilometres south-west of Roopena Homestead.

In addition, plugs of the same porphyritic rhyolite have been mapped to the east of Lake Gilles (Johnson, J. pers. com.) 16 kilometres west of Iron Knob; and 6 kilometres west of Pandurra Homestead (Johns and Solomon, op cit., Dalgarno, pers. com.)

The relationship of these rocks to the country rocks is best shown at Wartakan Neck where the outcrop of the intrusion is irregular in plan and covers an area of about 0.5 square kilometres. The structure is a volcanic neck which has punched up through the Corunna Conglomerate. The core of the neck is made of material indistinguishable from the main mass of the complex. A trachyte forms a chilled margin to the intrusion and a contact breccia is composed, in the main, of partially digested sediment fragments.

Intrusive relationships have also been described from the Corunna Syncline (Johns and Solomon 1953).

Within the rocks of the Dyke Structure (Map 1B, Johns and Solomon op cit) there are granite xenoliths that range up to 1 cm in diameter and have petrographic affinities with the nearby Burkett Granite which is considered to be their source. The Corunna Conglomerate is exposed to the east and west of the structure. In the west, between the Dyke and the Corunna Conglomerate a small exposure of an intrusion breccia has been recognized. This breccia is medium-grained and composed of pink, buff and green rock fragments set,with quartz,in a fine-grained, quartzo-feldspathic groundmass. The rock fragments are both rhyolitic rocks and metasedimentary gneisses; the groundmass is graphic, microcrystalline quartz and potash feldspar. This breccia shows close affinities to that developed around the margins of the Wartakan Neck intrusion to the north-west.

Quartz-deficient Burkett Granite outcrops to the west. In the vicinity of the Corunna Conglomerate - Burkett Granite contact, the granite is traversed by a network of veins of red porphyritic, rhyolite of the Gawler Ranges Province. The veins range up to 4 cm in width and locally chilled margins develop against the granite. Nearby, massive veins of crystalline barite intrude the Burkett Granite - Corunna Conglomerate contact. Crystalline quartz is associated with the barite and in places exceeds barite in amount. The most pure barite is a vein 1.5 metres wide and 20 metres long. Intergrown quartz and barite outcrops over an area 0.75 kilometres long and about 100 metres wide to the east of the pure barite. Fluorite, chalcopyrite, galena, pyrite and hematite occur in trace amounts in the quartz and barite.

3.2 Intrusive Granites

The Burkett Granite is composed of coarse-grained, euhedral to subhedral crystals of orthoclase which display a pronounced alignment. The crystals are set in a crystalline mass of quartz, (minor) feldspar and hornblende. Crystals of sphene are abundant.

Although the contact between the Corunna Conglomerate and the Burkett Granite is nowhere exposed, the contact is almost certainly an unconformity because abundant, rounded to sub-angular fragments of the Burkett Granite are found within the conglomerate near the contact.

Other granitic intrusive rocks are found along the Uno Fault about 20 kilometres to the west of the neck of the Dyke and to the south of the main Complex. These are correlated with the Burkett Granite on the Port Augusta 1:250,000 geological map and their outcrop is mapped on the geological map appended to this report (Map 1).

The granite in the vicinity of the Uno Fault has a subdued outcrop, in contrast to that of the tors further east. In places it is extensively weathered and in others sub-outcrop has to be relied on for mapping purposes.

The weathered varieties are friable and sandy with gritty quartz set in a mass of kaolinized feldspar and a few flakes of partially decomposed muscovite. The fresher varieties are composed of a medium - (in places coarse) grained aggregate of quartz and pink potash feldspar through which are distributed a few crystals of plagioclase and flakes of muscovite.

The rock has been cataclastically deformed and partially recrystallized with the intensity of deformation reaching a maximum in the vicinity of the inferred trace of the Uno Fault. Shear planes strike east-west.

3.3 Basic Rocks

Three dolerite dykes intrude the metamorphics south of the Uno Fault (see Map 1). These dykes, for the most part, are poorly exposed. The vegetation on the basement and granitic rocks is the ubiquitous South Australian blue-bush. On the basic dykes grasses do not grow and the natural herbage is predominantly salt bush.

The outcrops of the dykes trend-north-west, parallel to prominent lineaments within the Complex to the north. The rocks are variable but the most typical variety is massive, coarse-grained and composed of an aggregate of greenish-black, ferromagnesian minerals through which are distributed laths of altered feldspar that bear an ophitic relationship to the ferromagnesian minerals. The feldspar may comprise as little as 5% of the rock or as much as 30%. Some samples contain large clots (up to 1 cm) of very fine-grained micaceous minerals in addition to the feldspars and ferromagnesians.

4. STRUCTURE

4.1 The Southern Boundary

The outcrop of the eastern portion of the main mass of the Complex is limited in the south by an east-west trending fault. This fault is named the Uno Fault and is mapped on the Port Augusta 1:250,000 Geological Map (S.A. Govt. Dept. Mines, 1968) as extending due west for 20 kilometres from the neck of the Dyke Structure (Map 1B). Thomson, in Parkin (1969, Fig. 5 p 26) interpreted the fault to extend for some 280 kilometres along the southern boundary of the Complex.

The fault trace is obliterated along most of its length by a thin veneer of recent alluvium derived in the main from the Volcanic Complex to the north and also from the nearby granites and underlying basement. However, it can be traced by means of isolated exposures cataclastically deformed by movement along the fault, by adjacent exposures of volcanics and basement gneiss, and by the distribution of sub-outcrop characterising the volcanics to the north and the basement gneiss and granites to the south.

The fault plane strikes east-west and dips steeply to the north or in some areas approaches the vertical.

Observations or oriented thin sections strongly suggest that movement is in the vertical direction rather than laterally. Porphyroclasts are rotated within shear planes and ribbon-like streaks of dimmensionally oriented quartz bend and swirl around these relicts defining their direction of rotation.

A pediment developed on the basement rocks slopes gently away from the fault and drains into Lake Gilles some 10 kilometres distant to the south. To the north the volcanics drop away sharply and are dissected by numerous drainage channels. The more youthful drainage pattern in the volcanics contrasts with that of the basement pediment. The available evidence suggests that the Uno Fault is a normal dip-slip fault formed as a result of differential subsidence to the north.

Deformation adjacent to the fault is not as marked in the rocks of the Complex as in the rocks of the older basement. A flinty rock, formed by brecciation and replacement by quartz of a fine-grained igneous rock, outcrops intermittently along the fault. Where the flinty rock is not found there is no obvious megascopic evidence for shearing or deformation of the wall of the Complex.

There is no shearing of the country rock parallel to the margins of the flinty breccia; instead the contacts are sharp and, in many localities, irregular. The breccia appears to have been locally emplaced as a fluid. Similar, although finer-grained rocks, have been described from the Glen Coe cauldron subsidence area in Scotland (c.f. Clough et. al., 1909; Reynolds, 1956; Hardie, 1963; Taubeneck, 1968).

A north-west striking dolerite dyke intrudes the basement to the south of the fault (see Map 1) and minor occurrences of intrusive dolerite are recorded within the Complex. A massive vein of quartz and flinty breccia also strikes north-west, south of the Uno fault. The resemblance of this quartz and breccia to the mobile breccia to the north is striking. Both the quartz vein and breccia and the dolerite dyke are thought to be emplaced along tension fractures related to the Uno fault.

The south-east trending Dyke Structure (Fig. 1B) is apparently radially disposed with respect to the curved boundary of the main mass of the Complex, and in alignment with one of several prominent, north-westerly lineaments within it. The structure is flanked on either side by narrow strips of Corunna Conglomerate. To the south-west is an area of low tors of white, fine-grained granite (Burkett Hill Granite). Field evidence suggests the Dyke Structure post-dates the Uno Fault and isotopic age determinations (Compston et. al., op cit) confirm that it is intrusive and probably represents a late phase of the material which forms the main mass of the Complex in the Uno, Siam and Corunna 1:63,360 map areas. Further east the Southern Boundary of the Complex is less well defined. The implication that the Uno Fault has moved prior to termination of the volcanic activity is significant (see Section 4.1).

The outcrops of the Gawler Ranges volcanic rocks mapped on the

published 1:63,360 Corunna sheets (Johns and Solomon, S.A. Govt. Dept. Mines, 1952), between the neck of the Dyke Structure in the south and Wartaka Homestead in the north, when outlined, have an arcuate boundary (Fig. 1B). To the south and east of Wartaka Homestead an arcuate fault is mapped on the Port Augusta 1:250,000 mile sheet (S.A. Govt. Dept. Mines, 1968).

This fault intersects the northerly extension of the Corunna Conglomerate and separates the rocks of the Complex to the north-west from the older Moonabie Formation of the basement to the south-east. A second fault extends from due south of Myall Creek Homestead in a crudely arcuate pattern south-westwards for about 6 kilometres. This fault also separates the younger rocks of the Gawler Ranges to the north from basic rocks, intrusive into the basement, in the south.

It seems probable that the southerly limits of the faults are linked beneath a Quarternary soil cover to form a faulted and arcuate boundary to the Gawler Ranges Volcanic Complex in this area.

Thus, the main mass of the Gawler Ranges Volcanic Complex is limited in the south by the east-west trending Uno Fault, along which differential subsidence has occurred with concomitant cataclastic deformation of the basement rocks and the intrusion of a mobile breccia along the fault zone. The younger rocks of the Complex are down-faulted against the older basement rocks. The easterly margins of the main mass are possibly limited in the south and east by two arcuate faults bearing similar relationships to the Complex as does the Uno Fault observed to the south of the main mass.

4.2 The Arc Structure

The Arc Structure is about 7.2 kilometres long and about 1.2 kilometres

wide at the central and widest part. The structure is a steeply dipping, steeply north-plunging, anticlinal flexure truncated by erosion to expose a conformable series of tuffs and their welded equivalents. To the west of the main structure a series of smaller, subsidiary, flexures are developed.

In the east the conformable rock series of the Arc is abruptly terminated by a hinge fault which has its maximum throw to the south, adjacent to the Uno Fault.

The structure can be divided into three Regions:

1. The Eastern Region lying mainly to the east of Margoon Creek;
2. The Central Region lying between Margoon Creek and a subsidiary hinge fault in the west; and
3. The Western Region lying west of the subsidiary hinge fault.

Although there is some lensing along strikes of the various units a generalised stratigraphic column (Table 1) shows the distribution of the major formations with respect to the three Regions of the Arc.

Flow and compaction layering adjacent to the Uno Fault is almost vertical or steeply dipping to the north (85 degrees). In the western part of the main structure the rocks, locally dip, steeply to the south. To the north dips decrease slightly to about 75 degrees.

The tops and bottoms of some units can be determined by mechanical sorting (resulting from subaerial deposition of ejecta) and by the distinction between the flow-brecciated base and the agglomeratic surface of lavas (the latter formed by a process of attrition involving the chilled outer surface and the fluidal lava below).

Crawford (1962) suggested that the structure is a part of a volcanic vent cut off by the Uno Fault. However, the attitudes of the rocks are

considerably steeper than the angle of repose of pyroclastic ejecta and fluidal lavas. In some places the rocks are even overturned, indicating that tectonism is, in part, responsible for the present structure. A subsidiary arcuate structure is not a subsidiary cone but an anticlinal flexure bordering the main structure. Further west a conformable rock series representing the lower parts of the exposed volcanic succesion continues to strike east-west and dip steeply to the north. To the east the volcanic succession is represented only by the Welded Tuff Sheet ($p\epsilon v_3$) in faulted contact with rocks from the lower levels exposed in the Arc.

The attitude of contorted flow-layering about solid phenocrysts (thin sections) indicates that the direction of flow has been to the south rather than to the north as would be expected if the Arc formed a part of a crater whose centre was sited on the edge of Lake Gilles. The major control in the south of the Complex is tectonic and the structure is due to peripheral upturning as a result of differential subsidence along the Uno Fault. It is of interest to note that the dips recorded here are steeper than those from subsidence studied elsewhere (Clough et. al., 1901; Anderson, 1936; Rittman, 1958; Branch, 1966; and others).

4.2.1 Jointing

Blocky Joint System (Plate 1) A blocky joint system is confined to those rocks which, for the most part, are massive, viz welded tuffs and the crystal and vitric tuffs. It is defined by two joint sets, a dominant east-west set which is generally tangential, and a sub-dominant north-south set which is generally radial with respect to the Arc. Both sets are usually closed although the dominant east-west set may open and develop measurable displacements between adjacent faces as a result of slumping. The dominant set is

PLATE 1 BLOCKY JOINT SYSTEM

Welded Tuff ($p\epsilon v_1$) showing dominant joint set striking east-west and dipping steeply to the north (view looking west). The subdominant set is 90^{o} to the first, is discontinuous and strikes north-south (Locality 266).

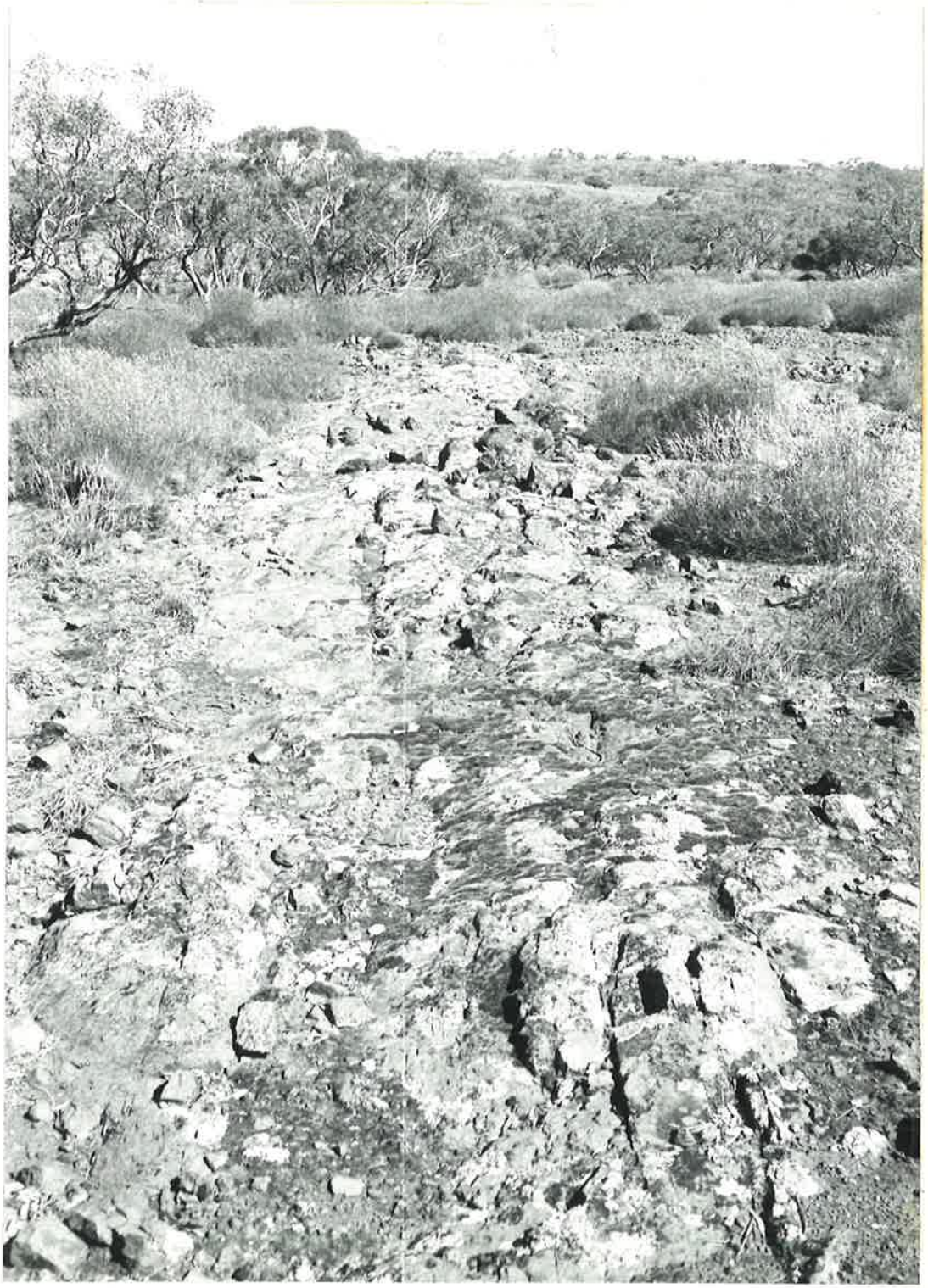


PLATE I

persistent along strike and the major joints are usually regularly spaced at about 20 cm intervals. However, subsidiary, discontinuous joints, within the plane of the principal set may be spaced at 3 to 5 cm intervals.

The dominant joint-set dips consistently at a high angle to the north and is concordant with the flow and compaction layering of the interbedded tuffs and lavas. The joints of the sub-dominant set, at 90 degrees to the first set, are vertical and are spaced at intervals of from about 20 to 50 cm. They are more discontinuous than those of the dominant east-west set. The complete homogeneity of the rock implies that the blocky joint system is tectonic and formed by extension.

Flaggy Jointing (Plate 3A) A principal joint set defines the flaggy jointing and this has a similar orientation to the dominant set of the blocky joint-system.

The spacing of these joints is controlled by the internal structure of the rocks and ranges from a few millimetres to several centimetres. The spacing of the joints of a sub-dominant set normal to the flaggy jointing is irregular but usually of the order of 5 to 20 cm. Although both the blocky and flaggy joint systems are tectonic the distinction is in the restriction of the flaggy jointing to those rocks which possess a strong internal structure (viz fluidal rocks, tuffs, layered pyroclastics), and of the blocky jointing to those rocks which generally lack an internal structure (welded tuffs).

Fracture Jointing (Plate 2) Fracture jointing is distinctive in that it is restricted to broad belts which trend north-north-west and which are sub-parallel to other linear, regional features to the north. (see Tectonic Map - Map 1). The joint planes are irregularly spaced and have variable strikes,

PLATE 2 FRACTURE JOINTING

Fracture jointing in Welded Tuff ($p\epsilon v_2$) showing predominant strike with cross fracturing at acute angles to the main cleavage (view looking south, Locality 162).

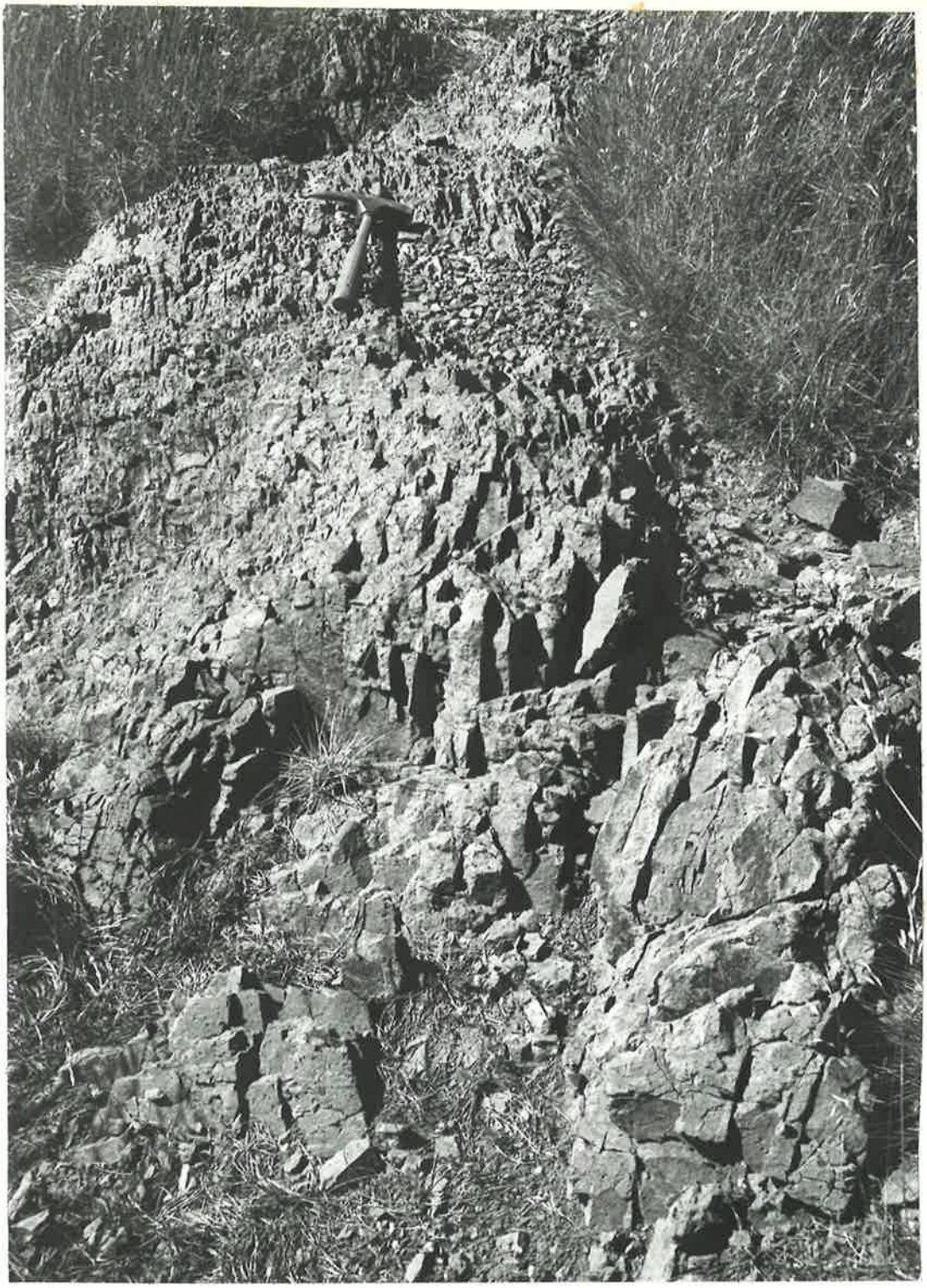


PLATE 2.

PLATE 3 FLAGGY JOINTING

A. Flaggy Jointing showing dominant east-west joint set and subdominant north-south set. The dominant joint set is controlled by the internal structure of the rocks. Porphyritic Rhyolite ($p\epsilon 1_3$) (Locality 253).

B. Large-scale open folding of flaggy jointing in Porphyritic Rhyolites ($p\epsilon 1_3$) (Locality 212).



A

PLATE 3.



B

the north-north-west one of which, however, generally predominates. The belts of irregular jointing are, in places, related to faulting but in most cases displacement is not apparent.

4.2.2 Faulting

The anticlinal Arc is broken by a series of hinge faults (Maps 1 and 2) which have their maximum throw in the south adjacent to the Uno Fault. Their trace is marked by the displacement of rock units and by distinctive joint patterns (Plate 2).

The welded tuffs are mainly massive and distinctions between platy jointing and fracture jointing are difficult to discern because of the absence of reference planes.

Along the fault planes the dominant jointing strikes due north-south rather than east-west and thus transects and is unrelated to primary depositional features.

Textural or mineralogical features do not exercise a control on this jointing, hence it is interpreted as tectonic. Relative displacement along the planes of fracture jointing cannot be determined in the massive rocks. Displacement is clear where faults transect interbedded tuffs and lavas; although these are folded into the plane of displacement rather than ruptured. Where rupture occurs in the massive rocks the jointing takes the form of a crush zone.

The eastern-most fault marks the termination of the conformable sequence of tuffs and lavas and here they abutt against the overlying Welded Tuff Sheet ($p\mathcal{E}v_3$). In this case the eastern side of the fault is downfaulted with respect to the western side.

The fault which trends north-west and lies to the west of Margoon Creek shows measurable horizontal displacements of about 80 m in the south

and 12 m in the north. The absolute displacement cannot be determined.

The fault which trends north-north-east in the west of the Arc Structure also has a measurable displacement of about 50 m in the south and 12 m in the north. The absolute displacement cannot be determined.

4.2.3 Folding

In addition to the regional, tectonic folding, small-scale folding is common in the units which possess an internal structure and particularly in the Fluidal Banded Rhyolites (pЄfbl) and the Porphyritic Rhyolites ($pЄl_3$) (Plate 3b). These latter folds affect only a few feet of strata and, within the limits of available outcrop, appear to be contained within undisturbed beds above and below.

The folds are of two principal types. One type forms as small-scale, structures which have an amplitude ranging from about 20 cm to 1.5 m and extend along strike for 0.5 to 1 m (Plate 4a, 4b, 5b). Some of this type can, in places, be ascribed to contortion due to the flow of a viscous magma, but others probably represent pressure ridges imparted by compressive forces on the crust of a fluidal magma caused by the viscous drag of slowly moving sub-crustal lava. In extreme cases the pressure ridges rupture and have sharp, broken crests which result from the extreme puckering of the surface of the lava.

The second type forms larger-scale, open folds which may have an amplitude of several metres but which are still contained within undisturbed beds above and below (Plate 5a and 6). These structures are generally more regular and symmetrical than those of the first group. However, the distinction is probably morphological rather than genetic. All are thought to be contortions due to flow.

PLATE 4 TIGHT FOLD STRUCTURES

A. Ruptured pressure ridge in Porphyritic Rhyolite ($p\epsilon 1_3$) - note that the structure sits within undisturbed beds above and below. (Locality 224).

B. Extreme puckering of Flow Banded Porphyritic Rhyolite ($p\epsilon fb1$) in plane of bedding. (Locality 224).



A

PLATE 4.



B

PLATE 5 TIGHT FOLD STRUCTURES

A. Folded Bedding in Porphyritic Rhyolite ($p\epsilon l_3$). Fold possibly represents pressure ridge formed by compressive forces on a fluidal magma. (Locality 223).

B. Contorted folding in Porphyritic Rhyolite ($p\epsilon l_3$). (Locality 223).



A

PLATE 5.



B

PLATE 6 OPEN STYLE FOLDING

Localised fold in bedded Porphyritic Rhyolite (pЄ13) - note continuity of strike to east (view looking east, Locality 212) and northerly fold-plunge.



PLATE 6.

4.3 Welded Tuff Sheet ($p\epsilon v3$)

4.3.1 Internal Structure

Flow banding and features akin to crystal settling are recognized from only two localities. In one area (Locality U180) north of the Ring, (Fig. 1b) the feldspar phenocrysts are concentrated into laminae about 3 to 4 mm in width and spaced at intervals of about 2 to 3 cm. This structure is only repeated for a distance of about 2m across strike and extends about 10 m along strike, which is here east-west. The two dimensional exposure does not allow a determination of the attitude.

At Locality U183 on the northern lip of the Ring Structure and in its vicinity, layering is evident in the groundmass of the porphyritic rocks. The layers are defined by subtle variations in colour from brick red to dull brown and are continuous over a strike length of about 200 m. The layering strikes east-west and dips at about 70 degrees to the north. Apart from these isolated occurrences primary depositional features are lacking and regional structure of the Welded Tuff Sheet is difficult to determine.

4.3.2 Jointing

Platy Jointing Platy jointing is apparently confined to the area between the Arc and the Ring Structure in the Welded Tuff Sheet ($p\epsilon v_3$). It differs from the flaggy jointing displayed in the Arc Structure in that it cannot be related to internal reference planes. On fresh surfaces the jointing is in the form of closely-spaced parallel planes (Plates 7B). On any one outcrop the spacing is regular but it tends to vary between outcrops. It ranges from 1 to 3 cm. In fresh outcrops the joints are closed but on weathered outcrops chemical weathering may open the joint set (Plate 7A).

PLATE 7 PLATY JOINTING

A. Platy jointing in massive, Welded Tuff Sheet ($p\epsilon v_3$). Note persistant strike and weak, subdominant joint set emphasized by weathering (Locality U165).

B. Close-spaced, parallel planes of platy joint system in massive, Welded Tuff Sheet ($p\epsilon v_3$). (Locality U165).



A



B

PLATE 7.

The principal set can be traced over extensive areas and has a strike which fluctuates about a west-south-west, east-north-east trend. The joint planes dip at steep angles (70 to 80 degrees) to the north. A secondary, vertical joint set at 90 degrees to the platy jointing is barely evidenced in fresh exposures but is enhanced in the weathered outcrops. This set is discontinuous and spaced at irregular intervals of up to 20 cm. Both sets of joint planes intersect phenocrysts but there is no significant displacement along them.

The platy jointing in the Welded Tuff Sheet ($p\mathfrak{G}v_3$) can be related to deposition planes because of:

a. The similarity of the platy jointing to the flaggy jointing in the rocks with internal structures in the Arc Structure;

b. The Conformable contacts between the volcanic successions exposed in the Arc Structure; and

c. The general concordance of strike between the platy jointing of the Welded Tuff Sheet and the flaggy jointing of the rocks with internal structures in the Arc.

The origin of platy jointing in extrusive rocks is not known (Hills, 1963) but the writer considers that the present joint system results from torsional stress as a consequence of peripheral upturning along the Uno Fault and is related to primary depositional planes.

Columnar Jointing Columnar jointing is the most consistent and spectacular feature of the Welded Tuff Sheet. The occurrence of columnar jointing in extrusive rocks has been widely investigated (Iddings, 1886; James, 1920; Hunt, 1938; Beloussov, 1962; Hills, 1963).

Typically the columns are four, five or six-sided (Plate 8). Seldom are a greater number of faces found and the five-sided columns are the most common. The columns normally range from about 1 m to 20 m in height although in any one area the column height and width is usually fairly consistent (Plate 9A). They range from 20 cm to 1.5 to 2 m in width. A low-angle joint set intersects the columnar structures. Unlike the classical columnar structure described from elsewhere, the low angle joints are, for the most part, flat and do not display the cup and ball jointing normally attributed to lengthwise contraction on cooling. However, the columns often display 'chisel marks' (Plate 9B) which are attributed to growth stages and to deviations in the direction of cracking at each stage.

Whereas the high angle joint sets, which define the sides of the columns, may be persistent over considerable distances (at least 50 m or more) the low-angle joint set tends to be more discontinuous (Plate 9B). On the sides of hill slopes a series of benches develop (Plate 10B) along the major, low-angle joint planes but in addition to these there are subordinate, parallel, low-angle joints spaced at intervals of as little as 10 cm and off-set with respect to similar planes in adjacent columns.

The general absence of internal structures does not permit the attitude of the columns to be determined but it is assumed that the high-angle joints develop at about 90 degrees to the cooling surfaces and that the low-angle joints form in the plane of the cooling surfaces as in recent extrusives. It is further assumed that the cooling surfaces thus determined are sub-parallel to the planes of primary deposition. These assumptions are employed in an attempt to unravel the regional structure of the Welded Tuff Sheet.

Joint directions were measured throughout the area and are presented as contoured projections of the perpendicular to each joint plane on a Schmidt equal area net (lower hemisphere) on the Tectonic Map (Map 2).

The four projections use data from restricted areas, viz the Western Ridge, the Ring Structure, a ridge to the north of the Ring Structure, and the Eastern Block.

4.4 Tectonic Map

4.4.1 Statistical Analysis of Joint Sets

Western Ridge A general analysis of the joints from the western ridge shows six principal joint sets: a low-angle set striking at 035 degrees east and dipping 8 degrees east, and five, high-angle, joint sets the orientations of which are tabulated below:

Strike	Dip
044°	approx. vertical
080°	87° north
005°	approx. vertical
060°	approx. vertical
040°	approx. vertical

The ten girdle point-maxima represent the sides of the columns and the low-angle point-maximum represents the horizontal joint set intersecting the columnar joint system. A subsidiary, low-angle joint-maximum represents a joint set striking at 285 degrees and dipping 30 degrees south.

The ridge is bounded by two prominent, parallel, linear features which strike at 140 degrees and which are sub-parallel to other linear features to the north and east in the mapped area. One of the high-angle joint sets parallels these regional, linear trends.

Ring Structure A different distribution is shown by the statistical analysis of joints from the Ring Structure. Here, when all joint directions are

PLATE 8 COLUMNAR JOINTING

Vertical view of polygonal joint system in massive Welded Tuff Sheet ($p\epsilon v_3$) which defines five and more rarely six sided columns (Locality U168).



PLATE 8.

PLATE 9 COLUMNAR JOINTING

A. Incipient development of benches formed along the low-angle joint set. Note the uniform size and height of columns. (Locality U180).

B. Chisel marks on the faces of columns. Note the persistence of high-angle joint set and the discontinuous pattern of the low-angle joint set (Locality U185).



A

PLATE 9.

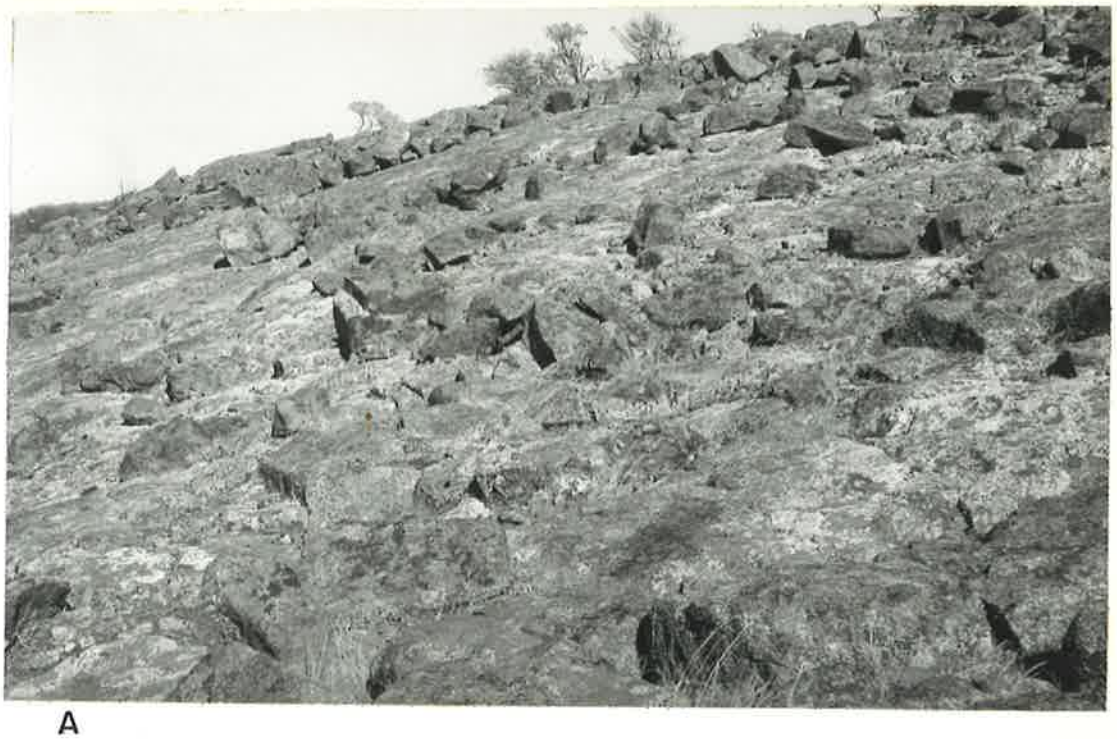


B

PLATE 10 COLUMNAR JOINTING

A. Sheeting along low angle joint set on Ring Structure. Illustrating down-slope, gravity slumping of columns (Locality U168).

B. Prominent Bench developed along a low angle joint set (Locality U179).



A

PLATE 10.



B

are considered, there are four point-maxima within a weak peripherial girdle and a somewhat diffuse low-angle, point maximum. The peripheral point maxima represent two essentially vertical joint sets which strike at 095 degrees and north-south respectively. The low-angle point-maximum represents jointing with an average strike of about 150 degrees and an average dip of about 5 degrees west.

A multi-directional joint set consistently dips at an average angle of about 50 degrees in towards the central depression of the Ring Structure which is bounded by two sub-parallel, regional, linear features, one of which strikes 135 degrees and the other at 150 degrees. Neither of these directions is parallel to any of the preferred strike directions of the joints measured from the Ring Structure.

Ridge North of Ring Structure The spherical projection indicates a girdle with six maxima which correspond to almost vertical joint sets that strike 005 degrees, 138 degrees, and 110 degrees. The joint giving the low-angle point maximum are almost horizontal, although with a slightly preferred dip of 10 degrees south. The ridge is bounded by two regional linear features, one of which trends 150 degrees and the other of which trends 140 degrees.

The latter direction is almost parallel to the 138 degrees near-vertical joint set. As before the girdle and related point maxima represent the columnar joint system and the low-angle point maximum represents a perpendicular joint set intersecting the columnar joint system.

Eastern Block A statistical analysis indicates four high-angle point maxima within a girdle and a low-angle point maximum. In contrast to the other areas the columns are horizontal and the perpendicular to the sides

of the columns plot as three maxima, viz in the centre of the stereogram and at 90 degrees and 260 degrees on the periphery. The joint set perpendicular to the length of the columns is in this case vertical and plots on the periphery of the stereogram at 0 degrees and 180 degrees, neither of which is parallel to the bounding, regional, linear features that trend at 155 degrees and 150 degrees.

4.4.2 Results

In two areas (the Western Ridge and the Ridge North of the Ring Structure) one of the joint sets which comprise the columnar joint system is parallel to regional, linear features but in the other two areas the regional, linear trends are not apparently related to the columnar joint system.

Assuming that the columnar structure originally formed at 90 degrees to the cooling surface and that the cooling surface, on a regional scale, was approximately horizontal then it appears that the Western Ridge has been regionally tilted such that the former horizontal joint set now dips between 5 and 20 degrees to the south and east and that the block was tilted to the south-east about an axis striking between 035 degrees and 040 degrees. Using the same assumptions, the ridge to the north of the Ring Structure was tilted such that the horizontal joint set now dips between 5 and 15 degrees to the south and the block has been tilted to the south about an axis that strikes somewhat north of west. The Eastern Block, on the other hand, would appear to have been tilted to the north through almost 90 degrees about an east-west axis so that the columns now lie on their side and dip between 0 and 15 degrees to the south.

The Ring Structure has a crude cone and crater habit. The columns are perpendicular to the topographic surface. Those in the centre of the structure are almost vertical or tilted at a slight angle away from the crater, whereas those towards the outer margins or base of the cone dip at an angle of about 50 degrees into the crater.

The geomorphic expression of the Ring Structure is today a poorly displayed dome structure. Hack (1966) has described circular dome structures formed as a result of exfoliation in crystalline rocks. At first sight the Ring Structure could be the result of exfoliation but a study of the jointing indicates otherwise. The structure has formed as a result of sheeting along the joint set which intersects the columnar joint structures at 90 degrees (Plate 10A). Except in the higher levels of the Ring Structure this joint set is concordant with the slope of the domal structure and blocks of rock slide, under the effects of gravity, downslope in a manner akin to that of exfoliation. The important point is that the joint set along which the sheeting occurs is not tectonic or formed in response to load relief on a pre-existing topographic surface but is developed by contraction on cooling.

Exfoliation has been described previously (Gilbert, 1904; Matthes, 1930; Jahns, 1943; Chapman and Rioux, 1958; Bradley, 1963) and is found on a small scale in the crystalline rocks of the Complex. It is, however, only a secondary phenomena which takes the form of 'onion skin' weathering on the tops of exposed columns. The flat-topped columns become rounded knolls as small sheets of rock (5 mm to 1 cm in thickness) peel from the exposed surface. This exfoliation has developed in response to thermal expansion and contraction rather than by dilation of rocks that have previously been deeply buried.

4.4.3 Conclusions

An intensive study of the columnar jointing and its relationship to the regional linear features so characteristic of the Complex enables the following conclusions to be drawn:

1. The regional, linear features are not necessarily related to the columnar joint system.
2. The attitudes of the columnar joints in three of the four zones bounded by regional linear features can be explained as a result of tilting of the zones or blocks (see also Results, Section 4.4.2).
3. The regional linear features are faults bounding fault blocks which have moved differentially.
4. The domal shape is a geomorphologic feature formed in response to sheet erosion which is governed by the pre-existing columnar joint system.

It has been suggested that the volcanics are upturned along the Uno Fault, although a fold axis has not been found. The prominent drainage channel which traverses the mapped area is not related to a joint set but could have a structural control. Major structural features change their attitudes on either side of the channel. The regional linear features (block faults) trend in significantly different directions on either side of the drainage channel. In addition, to the north and west of the main drainage channel the fault blocks appear to be tilted about axes which trend due north-west, whereas the Eastern Block to the south and east of the channel is tilted about an east-west axis. The blocks to the north are tilted to the south and the block in the south is tilted to the north.

In the absence of better information it is suggested that the fold axis trends north-east (Tectonic Map - Map 2) and follows the approximate course of the principal drainage feature and separates the two, structurally dissimilar, environments. Its extension to the north and east is unknown. The distribution of platy jointing supports the interpretation. Platy jointing which by analogy with the Flaggy jointing in the underlying tuffs is thought to parallel a depositional surface is found only in the vicinity of the main drainage. Here, it is maintained that the rocks have been rotated almost 90 degrees exposing a section through the rock pile. The absence of platy jointing further north is a function of the regional, more nearly horizontal attitude of the volcanic succession.

The regional features bounding fault blocks, are now occupied by large drainage depressions and evidence for shear deformation is generally lacking. However, at two localities (U146 and S118) quartz-cemented breccias are found. These breccias are restricted to, and form in linear zones which parallel the drainage depressions. In most cases they are formed of sharp angular chips of red welded tuff set in white, crystalline, quartz. That the quartz is magmatic is evidenced by chilled margins and accessory minerals such as apatite. Rarely the quartz forms long needles which penetrate the brecciated host giving a slaggy texture. These breccia zones are considered to be related to the block faulting and to develop concomitantly with extrusion and cooling.

A limited study of joint systems further north tends to confirm the observations and interpretations made within the mapped area. Joint measurements, when plotted on a spherical projection, disclose an average

regional dip of the columns between 70 and 85 degrees to the north and for the low-angle joint set, dips between 5 and 15 degrees to the south-east, although there is considerable scatter about these means.

The outcrop of the northern area is traversed by a rectilinear drainage pattern trending north-north-west and east-north-east. A study of the modal distribution of phenocrysts across one block defined by the drainage has shown that there is an increase in the abundance of phenocrysts from the south-west corner to the north-east corner.

The phenocryst content is thought to increase with depth in the Welded Tuff Sheet. If so, these data suggest that the block has been tilted to the south-west about a north-west trending axis. A study of the distribution of phenocrysts and joint patterns in other blocks may show a similar pattern.

A structural interpretation for the northern part of the Welded Tuff Sheet is that there is a series of elongate fault blocks trending due north-west and bounded by major north-west trending drainages. These fault blocks are believed to be broken into a series of sub-blocks that are now bounded by major east-north-east drainage basins.

The sub-blocks subside en-echelon fashion and are tilted to the south and west about a west-north-west trending axis. Blocks further to the south subside to a greater extent than those in the north. Subsidence is accompanied by rotation about axes parallel to the inferred fold axis in the mapped area. The folded and subsided pile has since been truncated by erosion to expose a section through the Welded Tuff Sheet.

5. STRATIGRAPHY

The oldest rocks in the eastern area of the Complex are not exposed and therefore the earliest parts of the volcanic history are not known.

Peripheral upturning of the volcanics along the margins of the Complex, permits a study of the upper levels of the stratigraphy exposed in the Arc Structure (Table 1).

The contacts between tuffs and recrystallized welded rocks are often gradational but colour changes are abrupt and allow arbitrary boundaries to be defined and facilitate mapping. Primary depositional features enable the attitudes of the rocks to be determined and most units can be sub-divided into a series of members on the basis of textural and post-depositional re-crystallization features (Table 13).

There are no erosional contacts within the Arc Structure and the absence of subaqueous and/or subaerial sediments interbedded with the volcanics indicates that the volcanic succession is the product of a virtually continuous outpouring of magma erupted over a geologically short timespan.

The field relationships, macroscopic features, petrography and petrochemistry of each unit are discussed in the following sections.

5.1 Lithic and Lapilli Tuff (pЄt)

5.1.1 Field Observations

Much of the exposure is formed of sub-outcrop* or is partly concealed by debris derived from a red, massive, welded tuff to the north. The best exposures are west of Margoon Creek.

---

* Sub-outcrop - insitu rubble derived from fresh rock immediately below the surface.

TABLE 1 GENERALISED STRATIGRAPHIC SECTION

		Symbol	Region		
			East	Central	West
Top	Welded Tuff Sheet	$p\epsilon v_3$	**	**	**
	Welded Lithic Tuff	$p\epsilon wt_2$	**	**	-
	Silicified Vitric Tuff	$p\epsilon vt$	**	**	**
	Fluidal Banded Rhyolite	$p\epsilon fbl$	**	**	-
	Massive, Rhyolite	$p\epsilon l_3$	**	**	**
	Massive, Welded Tuff	$p\epsilon v_{1_c}$	-	**	-
	Amygdaloidal Rhyolite	$p\epsilon al$	-	**	-
	Massive, Welded Tuff	$p\epsilon v_2$	-	**	-
	Pumiceous Tuff	$p\epsilon pt$	-	**	-
	Crystal Tuff	$p\epsilon ct$	-	**	-
	Massive and Banded Rhyolite	$p\epsilon l_2$	-	**	-
	Massive, Welded Tuff	$p\epsilon v_1$	**	**	**
	Massive, Porphyritic Rhyolite	$p\epsilon l_1$	**	-	-
Bottom	Lithic and Lapilli Tuff	$p\epsilon t$	**	-	**

Note : ** - Outcrop present

\- - Not represented

The basal member is a coarse-grained lithic tuff which gives way upwards to a fine-grained lapilli tuff. The lithic tuff is a massive, medium, light-grey rock composed of volcanic rock fragments embedded in a fine-grained matrix.

The fragments range in size from 8 to 2 mm in diameter although fragments up to 5 or 6 cm in diameter may be found. The most conspicuous are pale-grey, reddish-brown, and yellowish-green in colour with the last predominating. Other fragments are dark-grey or black. The majority are massive although many of the reddened fragments exhibit flow banding. All are microcrystalline. Although well consolidated the fragments show no indication of elongation and distortion. A parallelism of the long axes due to settling of the smaller fragments is evident in some areas.

When weathering is advanced (Sample 17) the rock assumes a yellowish-brown coloration and is strongly pitted where rock fragments are preferentially weathered.

The coarse-grained lithic tuff is essentially massive although locally, minor bedding is developed. The bedding becomes more pronounced in the finer-grained horizons. An overall decrease in grain size towards the top of the unit is accompanied by a decrease in the ratio of fragments to groundmass from approximately 1:06 to 1:15.

The lapilli tuff is a distinct lithological entity but also represents a transition member between the lithic tuff and the overlying lower breccia of the succeeding lava flow ($p\epsilon 1_1$). In some places (e.g. Locality 6) the transition from the lithic tuff to the lapilli tuff is gradational but in other areas (e.g. Locality 15) the lithic tuff interfingers on a fine scale with the lapilli tuff.

The lapilli tuff is reddish to brownish-grey in colour and composed of small, rounded to sub-rounded lapilli, aggregates of which are drawn out

into lenticular shapes displaying a pronounced parallelism. The individual lapilli are commonly less than 0.5 mm in diameter, are equigranular and range in colour from creamish-white to buff yellow. A few coarse-grained rock fragments have a random distribution. These range from pale greenish-grey to deep reddish-brown and in size from about 18 to 2 mm. Rotation of the larger fragments is indicated by the contorted nature of the lenticular aggregates of lapilli about them. The direction of rotation suggests southerly movement. This is a local feature possibly resulting from minor, down-slope slumping rather than general flow.

The lithic tuffs from the Central and Western Zones differ from those in the Eastern Zone in that they are welded* and contain a more limited variety of rock fragments.

The pyroclastic rocks are closely jointed adjacent to the Uno Fault. Some of the joint planes and minor fractures are cemented with secondary or late-stage silica in the first instance and more recently with caliche. The jointing, although less intense away from the fault, is a persistant feature of the Lithic and Lapilli Tuffs and retains a strike of 080 degrees through most of its outcrop.

Internal structures are not an obvious macroscopic feature though bedding, as indicated, is weakly developed. In some areas weak flow-layering is developed (Locality 6). The flow structures dip at an angle of about 85 degrees to the north and strike between 065 and 085 degrees. The folds are open and generally asymmetrical, have an amplitude of about 8 to 12 mm and may extend over a strike length of 1 to 2 m. These folds are not

---

* Welding - Flattening of shard and pumice structures due to load compaction and internal heat without obliteration of the characteristic ash structure. Intense welding may result in extreme flattening and slight flowage and may partially obscure the original structure.

consistent over large areas and affect only a few metres of strata. The folds appear to be contained within undisturbed beds above and below.

5.1.2 Petrography

In the lithic tuff the rock fragments are variable in lithology but all are from an acid igneous provenance and related to extrusive activity.

Altered Fragments These fragments are especially characteristic of the lithic tuff and are largely responsible for the greyish-green colour. The fragments are composed essentially of fibrous illite* associated with minor, microcrystalline quartz. Fragments of this type are thought to represent an altered volcanic glass.

A few preserve a shadowy, relict banding defined by sub-parallel variations in the degree of crystallinity of the clay minerals and micas, enhanced by sub-parallel concentrations of disseminated opaques.

Rhyolitic Rock Fragments These display numerous textural variations (Plates 11, 12 and 13) but are essentially composed of a micro-crystalline aggregate of quartz and partially kaolinized potash feldspar# set in fibrous illite.

The characteristic types include:

a. Massive fragments composed of a mass of small (less than 0.15 mm) reddened snowflakes (Snyder, 1962) which may be compact and comprise the whole rock fragment or which may be loosely packed and set in cryptocrystalline, colourless illite.

---

* Illite - Where specifically named in this thesis its identity has been confirmed by X-ray powder photography.

Potash feldspar - Where specifically named in this thesis its identity has been confirmed by microchemical staining (Chayes, 1952)

PLATE 11 LITHIC TUFF (pEt)

A. Sample 1;PPL x 40

A lithic tuff fragment composed of angular chips of quartz (colourless), quartz and illite (colourless and grey) and illite (grey, after ?potash feldspar) set in a reddened, cryptocrystalline matrix of potash feldspar with fine crystal chips and fragments.

B. Sample 3:XN x 40

An angular fragment composed of partially reddened, cryptocrystalline, potash feldspar and quartz. The fragment could represent devitrified obsidian.

C. Sample 3:PPL x 40

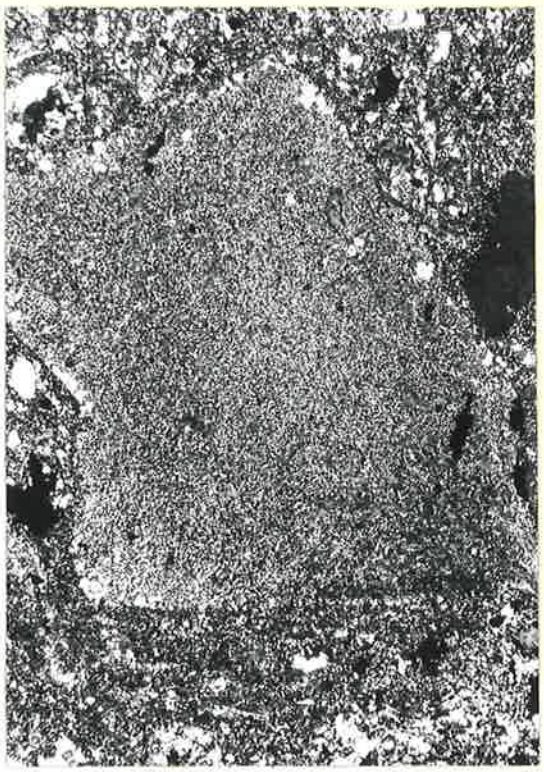
A portion of a collapsed and incipiently welded pumice fragment with collapsed, elongate pore structure (pale grey areas are quartz, dark grey potash feldspar and alteration products).

D. Sample 3:XN x 40

Some field of view as for Plate 11C showing the effects of devitrification to crypto- and microcrystalline quartz and potash feldspar. The potash feldspar tends to form the walls of the tubular structures with quartz infilling the pore spaces.



A

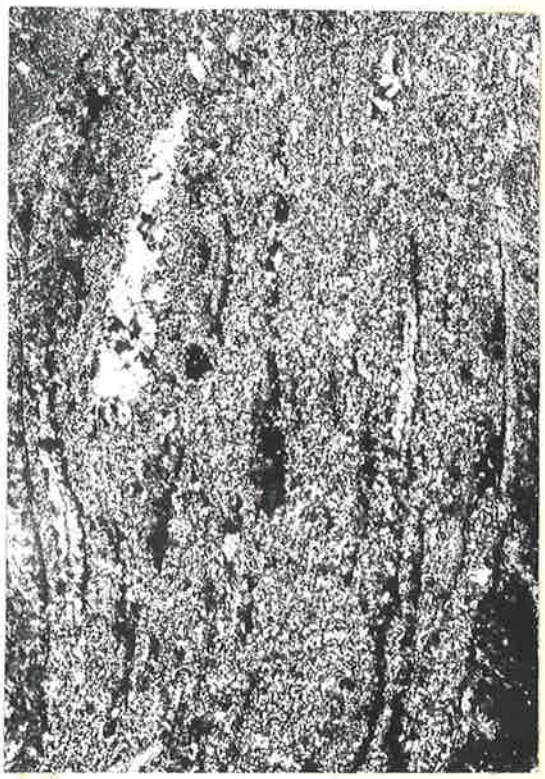


B

PLATE II.



C



D

PLATE 12 LITHIC TUFF (pCt)

A. Sample 1:XN x 100

Fragmented quartz crystal. Note the sharply angular outline and the fine, hair-like fractures. The flecks in the quartz represent dirt on the thin section and not inclusions.

B. Sample 1:XN x 50

Elongate fragment composed predominantly of microcrystalline quartz (white and black) and potash feldspar partially replaced by illite (grey and stippled). The fragment probably represents a devitrified, rhyolitic glass.

C. Sample 1:XN x 100

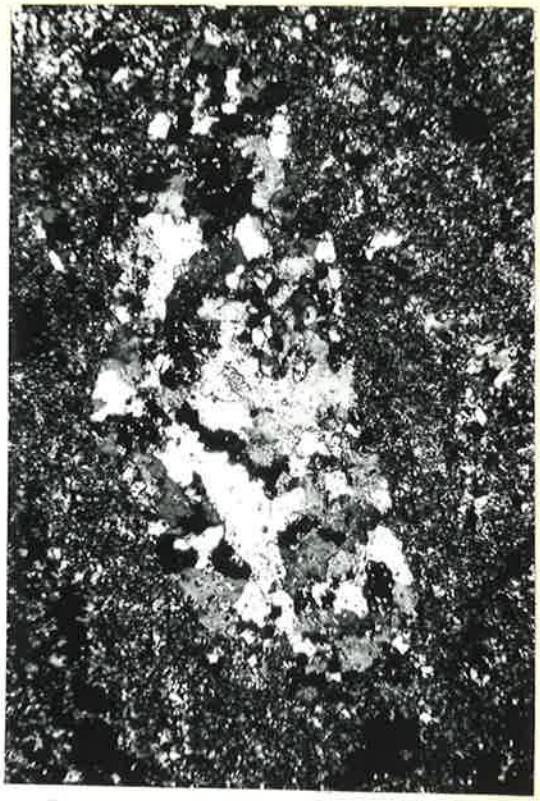
Elongate fragment composed essentially of microcrystalline, granular quartz (white and black) set in a groundmass of cryptocrystalline illite (stippled). The fragment is similar to that of Plate 2B but the alteration to illite of the potash feldspar is more advanced.

D. Sample 3:XN x 40

A rock fragment composed of a feathery mosaic of potash feldspar.



A



B

PLATE 12.



C



D

PLATE 13 LITHIC TUFF (pЄt)

A. Sample 1:XN x 40

Rhyolitic rock fragment composed of rounded aggregates of microcrystalline illite (after ?potash feldspar) set in a network of microcrystalline, granular quartz. A veinlet of secondary quartz traverses the fragment (left of centre of photomicrograph). Black areas are holes in the thin section.

B. Sample 3:PPL x 100

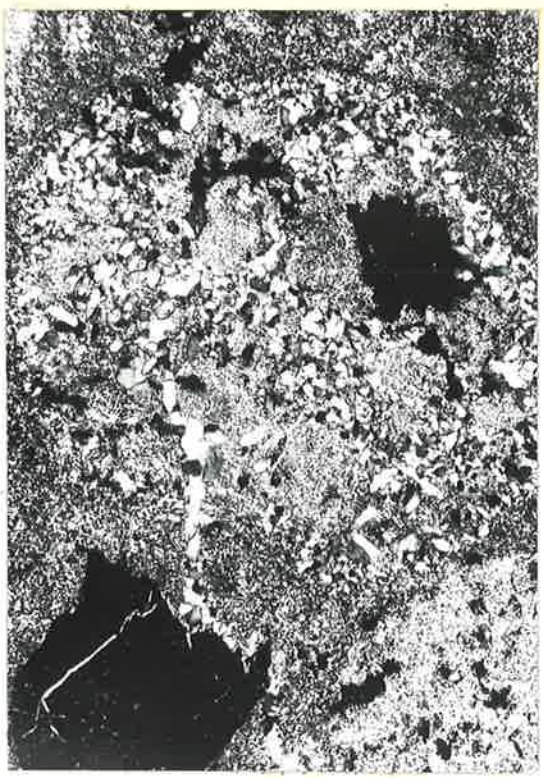
A portion of a fragment composed of partly altered, cryptocrystalline potash-feldspar. The fragment is traversed by a network of relict, perlitic cracks defined by iron-oxides.

C. Sample 1:PPL x 100

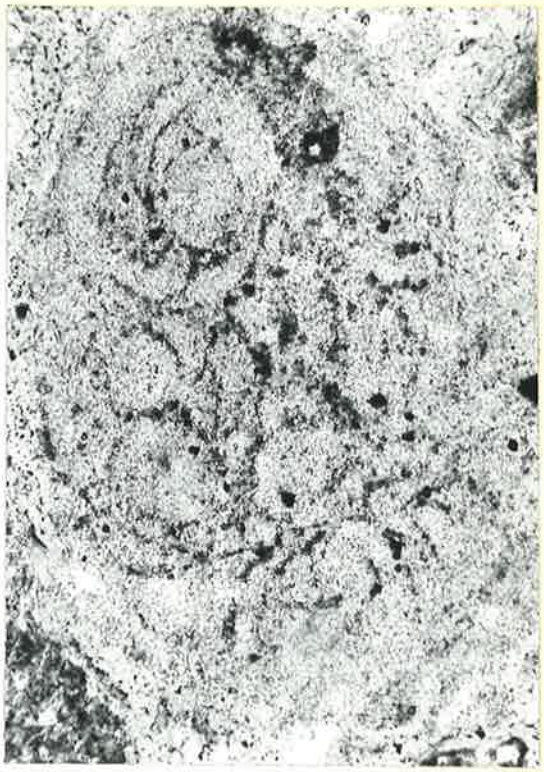
A shard in a vitric tuff fragment. The shard has formed by the explosive brecciation of a vesciculate, siliceous glass and represents a part of the wall of a former bubble. Note the absence of distortion.

D. Sample 1:XN x 100

Same field of view as for Plate 13C in doubly polarized light. The shard is the product of devitrification of a glass and is now composed of microcrystalline quartz the elements of which have crystallized transverse to the shard structure.



A

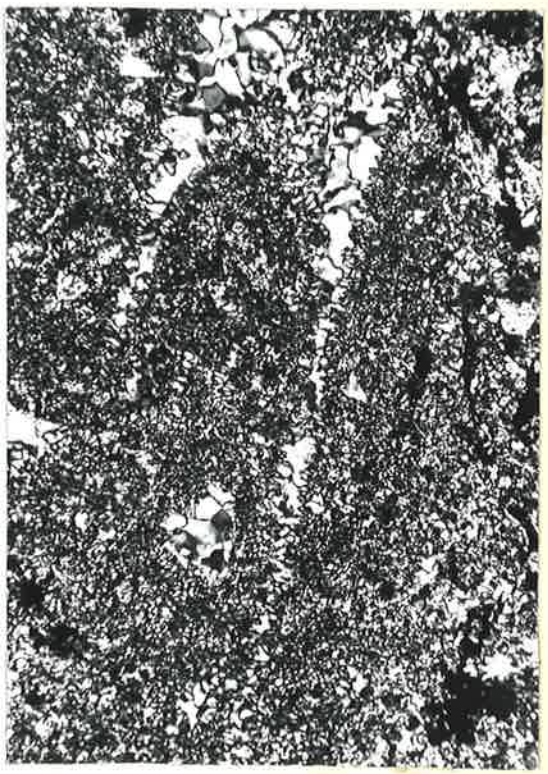


B

PLATE 13.



C



D

b. • Fluidal-banded porphyritic rhyolites composed of phenocrysts of potash feldspar set in a strongly banded groundmass. The phenocrysts (orthoclase (-ve 2V 71°)) * are partially replaced by iron oxides and sericite. The crystals are subhedral to euhedral and range in size from 0.2 to 0.4 mm. The groundmass is composed of alternate, linear segregations of reddened quartz and colourless, cryptocrystalline illite (Plate 15,c, d). A few snowflakes (Snyder, op. cit.) may occur within the illite. The banding is sub-parallel on a fine scale and contorted about phenocrysts. A second type is composed of microcrystalline quartz through which is scattered cryptocrystalline illite and disseminated opaques. In places the illite and opaques are segregated into narrow, sub-parallel zones set in microcrystalline quartz. These zones cut across the quartz crystal boundaries and define the relict, primary banding.

Lithic Tuff Rock Fragments (Plate 11A) The most common is formed of angular rock fragments (up to 0.5 mm) of microcrystalline quartz and separate fragments of fibrous illite set in cryptocrystalline matrix of reddened, potash feldspar. Variations are due to differences in grain size. The fragments were not welded prior to incorporation in the present tuff.

Pumice Fragments (Plates 11C, 11D) Pumice fragments composed of a micro- and cryptocrystalline aggregate of quartz and partly reddened potash feldspar which crystallise by devitrification from a vesiculate, acid

---

* orthoclase - Where optical properties are specifically stated the measurements have been made using a Leitz 4-axis Universal Stage.

glass. There has been an almost complete collapse of the pore spaces and welding into a compact glass prior to devitrification but the vesicular nature of the fragment is still evident.

Siliceous Vitric Tuff Fragments (Plates 13C, 13D) The tuff fragments are composed of brecciated, vesiculate glass. Abundant lune, Y-shaped and crescentic shards are randomly distributed through a microcrystalline groundmass of quartz. The groundmass quartz is dusted and discoloured with finely disseminated opaques. There is no distortion or flattening of the shard shapes.

Devitrified Obsidian Fragments These fragments are featureless and composed of cryptocrystalline quartz and potash feldspar traversed by a network of fine fractures along which cryptocrystalline illite has crystallised.

Crystal fragments are much less abundant than rock fragments but are consistantly present throughout the unit.

Quartz Fragments (Plate 12A) These are little more than accessory. The crystals are usually shattered and broken relicts of former hexagonal bipyramids. The crystal fragments range to 0.6 mm in diameter and have sharp convex and concave edges; they are not embayed. The quartz is water clear, but displays a weakly undulose extinction and the fragments may be traversed by a network of fine fractures.

Feldspar Fragments Feldspar fragments are similar to those found in the fluidal-banded, rhyolitic rock fragments. They are partially replaced by iron oxides, illite and rare quartz.

Altered Crystal Fragments These fragments are compositionally identical to the altered rock fragments. However, their origin is indicated by relict, crystal habits. Some are euhedral and resemble potash feldspar crystals. Others are deeply embayed to form lobate shapes which could not have formed by the fragmentation of solid rock but are resorbed plagioclase phenocrysts now pseudomorphed by potash-rich alteration products.

Accessory Minerals Zircon, rutile and leucoxenised opaques are comparatively abundant. Angular chips and broken fragments of anhedral zircon crystals range up to 0.15 mm in diameter; most are colourless but a few are zoned. Rutile is honey-coloured and forms small euhedral and prismatic crystals which are partially decomposed to leucoxene. Opaques are the most abundant of the accessories as sub-angular to rounded, anhedral, crystals up to 0.3 mm in diameter and which are almost completely leucoxenized.

Although the rock and crystal fragments are constant throughout the three Zones the groundmass textures of the Lithic Tuffs differ in their degree of welding.

Eastern Region The matrix displays a modified (by welding) vitroclastic texture. Devitrified shards are randomly oriented. They tend towards a platy habit, although lune, crescentric and Y-shaped shards are common. The shards have a wide size distribution in the range 0.1 to 0.5 mm and are now composed of parallel, small quartz crystals transverse to the shard structure (Plate 13D) . They are set in a micro-crystalline intergrowth of quartz and reddened, potash feldspar. The potash feldspar is extensively replaced by fine-grained illite.

Central Region The matrix is cryptocrystalline and eutaxitic being composed of elongate, discontinuous streaks which have a sub-parallel orientation and which are moulded about phenocrysts to resemble flow banding.

The streaks represent flattened shards and are composed of cryptocrystalline, potash feldspar which forms the outer walls and surrounds a core of white, cryptocrystalline illite. The lenticular and elongate, modified shards are further enhanced by concentrations of disseminated opaques about their outer margins. They are set in massive, cryptocrystalline, reddened, potash-feldspar.

Western Region Shard-shapes are clearly preserved although partly distorted and flattened. For the most part they are formed of an outer selvedge of iron oxides bounding a core of inwardly directed, microcrystalline quartz and flakes of potash-rich*, colourless clay minerals.

A feature of the welded rocks in both the Central and Western Regions is the development of a reaction rim about the rock fragments. The reaction rim is no more than 0.1mm in width and is continuous about the fragment. It is formed of radially disposed snowflakes which are elongate perpendicular to the wall of the fragment.

The overlying lapilli tuff is composed of a compacted mass of well-rounded to sub-angular lapilli set in a dense matrix. The structure evident in the hand specimen is a function of compositional layering (Plate 14A, 14B).

The lapilli are homogeneous, similar in size and grouped into two types. The first is composed of a dense mass of cryptocrystalline illite through which are distributed a few small crystals of quartz, and the second is composed of a complex intergrowth of cryptocrystalline illite and quartz (Plate 14C, 14D). The two types tend to be restricted to particular layers.

---

* Where clay minerals are stated to be potash-rich the identification is based on microchemical staining techniques (Chayes 1959). X-ray diffraction was used to confirm that potash-rich clay minerals were selectively stained by a sodium cobaltinitrite solution.

PLATE 14 LAPILLI TUFF (pЄt)

A. Sample 6:PPL x 25

General field of view of lapilli tuff composed of sub-angular fragments of devitrified glass. Note the close compaction of the fragments and the laminated structure defined by hydrated iron-oxides.

B. Sample 6:XN x 25

Same field of view for Plate 14A in doubly polarized light.

C. Sample 6:PPL x 100

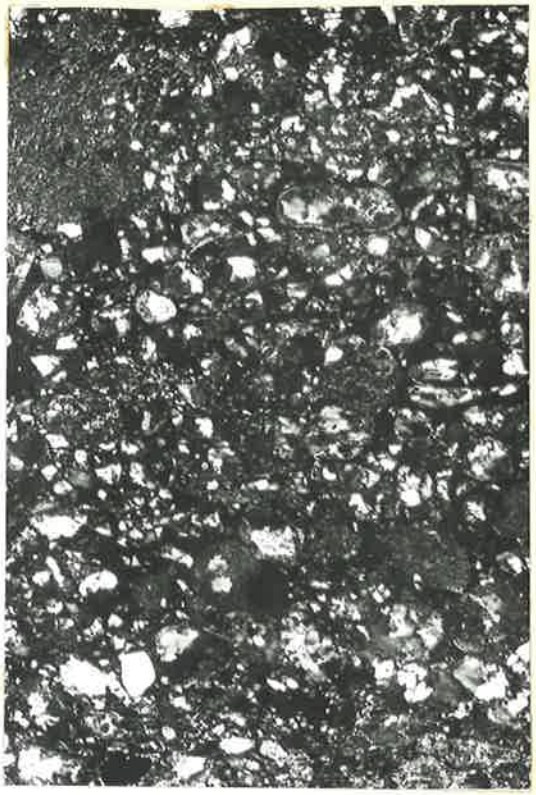
Typical lapilli in the lapilli tuff, closely compacted but not distorted, and set in a cryptocrystalline reddened groundmass.

D. Sample 6:XN x 100

Same field of view as for Plate 14C in doubly polarized light showing the results of devitrification and partial alteration of the potash feldspar phase by illite. Note the absence of contact effects around the margins of the fragments.



A



B

PLATE 14.



C



D

Lapilli which contain an appreciable amount of quartz tend to be more angular than those that contain only minor amounts of quartz. Both lapilli types are uniform in size. Some range to 3 mm in diameter, but more usually are in the range 1 to 2 mm. There is no apparent variation in grain size between one layer and another. The layering is defined by variations in the mineralogy of the fragments and also by the ratio to rock fragments, and by the presence or absence of comminuted glass fragments.

In those layers composed essentially of illite-rich lapilli, the matrix is cryptocrystalline and almost opaque due to an abundance of iron oxides. The mineralogy cannot be determined optically. On the other hand, in those layers composed essentially of fragments formed of intergrown illite and quartz, iron oxides are lacking and the matrix is seen to be composed of numerous, devitrified shards. These are usually short and stubby in habit but range to lune and crescentic shapes in places.

Larger rock fragments include:

a. Partially welded, devitrified vitric-tuff fragments composed of a mass of microcrystalline, deep red potash-feldspar in which are set recognizable although welded (flattened) shards.

b. Rhyolitic fragments composed of a mass of microcrystalline deeply reddened, alkali feldspar in which are set grains of quartz.

c. Siliceous, vitric-tuff fragments which are indistinguishable from those incorporated in the lithic tuff.

d. Flow-banded rhyolites composed of segregated layers of quartz and reddened, microcrystalline potash feldspar.

5.1.3 Petrochemistry

Two samples of the Lithic Tuffs from the Central Region (Localities 281, 297) have been chemically analysed. The results and the recalculat-

ed CIPW molecular norms are presented in Table 2.

TABLE 2: LITHIC TUFF (pЄt)

Analysis, %			CIPW Norm, %		
	A281	A297		A281	A297
SiO_2	74.70	77.90	Q	56.09	58.50
Al_2O_3	11.50	12.30	Co	9.11	6.74
Fe_2O_3	0.84	0.96	Or	26.59	27.78
FeO	0.56	0.64	Ab	0.25	1.02
MnO	0.01	0.01	An	1.29	0.76
MgO	0.44	0.26	En	1.10	0.65
CaO	0.30	0.18	Mn	1.17	1.11
Na_2O	0.03	0.12	I1	0.44	0.65
K_2O	4.50	4.70	He	0.03	0.19
TiO_2	0.23	0.34	Ap	0.07	0.05
P_2O_5	0.03	0.02			
			Sub-Total	96.14	97.43
LOI*	3.25	2.25	LOI*	3.25	2.25
	99.39	99.68		99.39	99.68

* LOI - Loss on ignition.

Sample A281 is representative of the welded varieties of lithic tuff and is composed of about 50% rhyolitic rock fragments (banded, massive and altered) and about 10% quartz, altered feldspar, and opaque mineral fragments set in a cryptocrystalline, eutaxitic matrix.

The silica value of the analysis and the quartz of the norm is somewhat higher than would be anticipated by inspection of the thin section. Modal quartz is evident as snowflakes and as quartz crystal fragments but these are not sufficiently abundant to account for the silica and quartz of the analyses. The cryptocrystalline matrix must contain appreciable quartz in addition to potash feldspar.

The high potash to soda ratio in the analysis is reflected by high orthoclase and low albite in the norm and in thin section by the abundance of potash-rich micas and by the replacement of former plagioclase (presumably sodic) by potash-rich, clay minerals.

The lime and magnesia recorded in the analysis and reflected in the norm as anorthite and enstatite are not so readily explained. There are no calcium- or magnesium-rich mineral phases visible in the thin section. It is assumed, therefore, that a little of the lime and magnesia are incorporated within the crystal lattice of the clay mineral (?illite) and that the remainder is included within the matrix.

The normative iron and titanium-bearing minerals are present as altered titano-magnetite, rutile and hematite in the mode.

The sample from Locality 297 resembles that from Locality 281 in most respects. It differs in that the eutaxitic texture is much less well displayed and in that some of the rock and crystal fragments are partly replaced by quartz. The groundmass is essentially crypto- and microcrystalline-granular although eutaxitic texture is incipiently developed in some specimens.

The mineralogy compared with Sample 281 is reflected in the chemical analysis and norm. Silica and normative quartz are somewhat higher than in Sample 281. The lower value for normative corundum in Sample 297 is reflected in the greater abundance of alkalies in the analysis and of normative feldspars. Although the soda content of Sample 297 is somewhat higher than that of Sample 281 this difference is not significant and the relative proportions of alkalies in both samples are such as to suggest that these rocks have been relatively enriched in potash and depleted in soda. Calcium- and magnesium-rich mineral phases are not visible in Sample 297. Magnesia and normative enstatite are somewhat

lower in the rock that has been more enriched in silica (Sample 297).

5.2 Porphyritic Rhyolite ($p\epsilon 1_1$)

5.2.1 Field Observations

The unit is restricted to the Eastern Region. It displays a structural zonation; a basal breccia is overlain by a weakly flow-banded porphyritic rhyolite which is capped by a flow breccia. The Formation is poorly exposed and the contact with the underlying Formation was not found. However, the presence of lithic tuff fragments in the basal member together with the concordant nature of the two rock formations suggests that the contact is conformable.

The basal breccia is a dark-grey, fragmental rock composed of a few reddish, massive and banded rhyolitic rock fragments, indistinguishable from those in the underlying tuff, and numerous dark-greyish-green fragments set in a dark-grey groundmass. The fragments are angular to subrounded and range from 30 to 4 mm in diameter. Perlitic texture is developed locally. The breccia grades to the north into a banded dark-grey porphyritic rhyolite lacking the reddish fragments that characterise the breccia. The phenocrysts have a random distribution and range from 5 to 2mm in size. Both glassy quartz and white, pink and buff, extensively altered, feldspar phenocrysts are present. The flow banding is defined by parallel layers which alternate between mid-grey and dark-grey and which are contorted around phenocrysts.

The overlying flow breccia is a distinctive rock. It is formed of comparatively large, incomplete ovoid and globular particles which range to 40 mm in diameter and which are enclosed in a porphyritic, pale-grey or fawn, aphanitic groundmass. The upper surface of the 1 to 2 m thick breccia body is composed wholly of the ovoids which gradually decrease

in size down through the breccia until the rock passes into solid rhyolite. The globules contain relict flow banding but there is no systematic orientation between the banding in adjacent globules. One half of each globule surface is smooth (rounded and mammillated) and the other is indistinct and rough.

Jointing is less well displayed in these rocks than elsewhere within the Arc Structure. Flaggy jointing, dipping steeply to the north, and conforming with the depositional banding within the main Porphyritic Rhyolite ($p\epsilon l_1$), is present locally.

Folding was not seen within the unit except in the vicinity of the mapped fault. Locally the rocks are traversed by a network of fine fractures, along a few of which brecciation has occurred. The breccias and small vugs are recemented with secondary or late-stage silica.

5.2.2 Petrography

Tuff fragments derived from the underlying Formation comprise about 10% of the basal breccia. The remainder of the rock consists of fragments of the overlying porphyritic rhyolite (Zone 2, Table 13) composed of a few phenocrysts of quartz and altered feldspar set in a microcrystalline groundmass which displays a shadowy banding. The feldspar phenocrysts are potash-rich and almost completely replaced by a crypto- and microcrystalline mass of sericite and clay minerals. A little secondary quartz accompanies the alteration products. The groundmass is made up of small, reddened, snowflakes set in a cryptocrystalline, potash-rich groundmass in which are set sub-parallel flakes of shredded and fibrous, colourless micas. The alternation of layers composed of snowflakes and of cryptocrystalline material, together with concordant, sub-parallel alternations in the degree of reddening, define the shadowy banding.

Cracks and fractures serve as locii for the onset of devitrification. The glass has devitrified into microcrystalline snowflakes composed of smoky quartz crystals in which are set cryptocrystalline, potash-rich feldspar about the margins of the fragments and also along a network of fine fractures within them. The remainder is composed of cryptocrystalline illite and quartz which is believed to have formed directly from the glass, as a result of potash enrichment, before devitrification was complete.

Crystals of quartz (Plates 15C and 15D) and accessory crystals of zircon, rutile and partially leucoxenized titano-magnetite have a sporadic distribution.

The upper flow breccia is formed of rounded and globular fragments which are thought to have formed by rolling of the chilled crust by the advancing, fluid magma below. The globules range up to 30 mm in diameter. The original internal structure of the globules is that of a series of shells concentric with the outer surface, now poorly defined against a devitrified, microcrystalline mosaic of reddened potash feldspar (Plates 15 A and 15 B). In some cases a radial structure is superimposed upon this concentric structure. Individual crystals of potash feldspar and fine-grained opaque mineral phases have a radial disposition with respect to the globule surface. The globules do not contain phenocrysts.

Surrounding the globules is a later phase of the same magma which does contain phenocrysts of both quartz and feldspar. The quartz phenocrysts are equigranular and commonly terminated, although modified to a sub-rounded habit due to resorbtion. The feldspar phenocrysts are potash-rich and most are partially to completely replaced by sericite.

The enclosing matrix is prominently banded. The banding is similar to that in the underlying flow and formed of linear segregations of quartz and potash feldspar and the latter's alteration products.

PLATE 15 MASSIVE PORPHYRITIC RHYOLITE ($p\epsilon 1_1$)

A. Sample 12:PPL x 25

A portion of a globule of devitrified glass from the upper brecciated surface (Zone 1) of a fluidized rhyolitic tuff ($p\epsilon 1_1$). Note the poorly defined concentric structure concordant with the outer surface.

B. Sample 12:XN x 25

Same field of view as for Plate 15A in doubly polarized light. The glass has devitrified to a mosaic of reddened snowflakes composed of a polycrystalline mosaic of quartz included with numerous cryptocrystalline, crystallites of potash feldspar.

C. Sample 14:XN x 100

A rounded (?formerly terminated) phenocryst of quartz mantled by quartz which has nucleated from the surrounding groundmass. The quartz of the mantle crystallizes in optical continuity with the parent crystal and includes numerous, cryptocrystalline crystals of potash feldspar. Note the relict crystal faces preserved between the quartz phenocryst and the mantle.

D. Sample 14:XN x 25

General field of view of Massive Porphyritic Rhyolite. Quartz phenocrysts, one at extinction (top right), and one exhibiting maximum birefringence (bottom left), are mantled by quartz as for Plate 15C and set in a snowflake-textured groundmass.

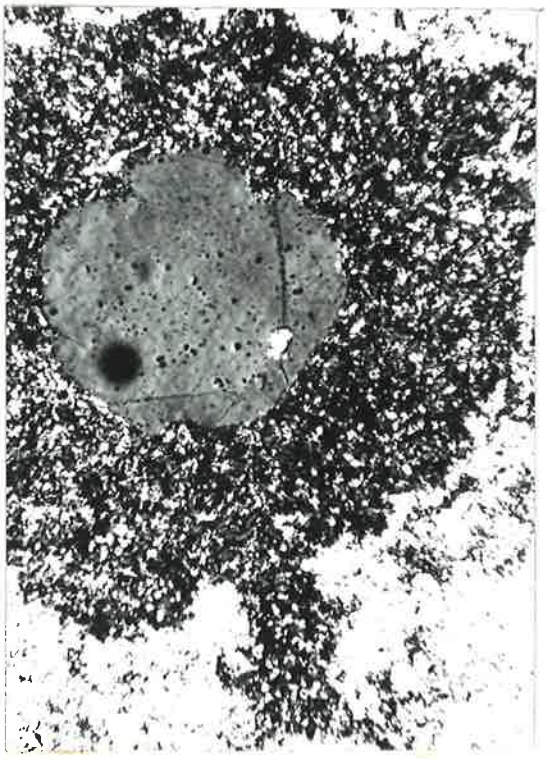


A

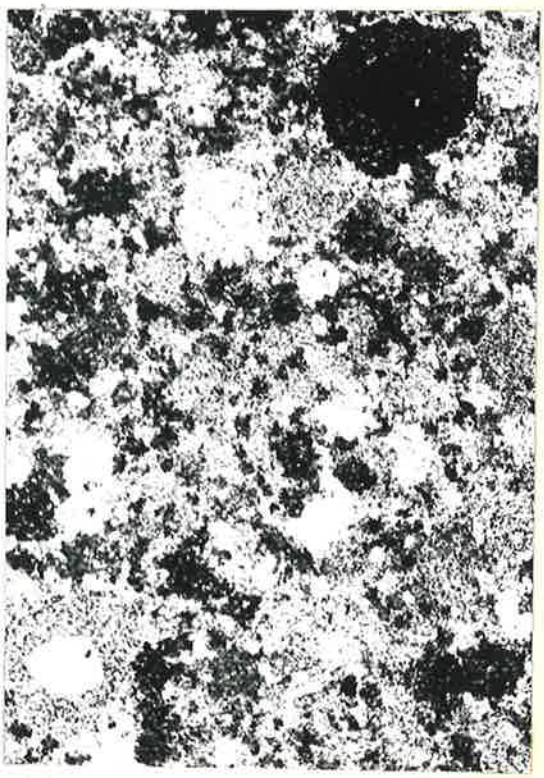


B

PLATE 15.



C



D

Locally the consolidated lava flow is faulted and sharply angular chips and fragments of the host are embedded in secondary or late-stage quartz (e.g. Locality 11). The quartz is cryptocrystalline adjacent to the rock fragments and coarser-grained in the central regions of the fractures. Flakes of sericite are included within the quartz, which in places has a smoky colouration. These features suggest that the quartz is magmatic rather than supergene.

5.3 Welded Tuff ($p\epsilon v_1$)

5.3.1 Field Observations

In the Eastern Region the Welded Tuff ($p\epsilon v_1$) conformably overlies the upper breccia surface of the Porphyritic Rhyolite ($p\epsilon l_1$). A rhyolitic lapilli-tuff (Zone 6, Table 13), composed of spheroidal lapilli set in a dark reddish-brown microcrystalline, porphyritic groundmass, outcrops sporadically along the lower contact (e.g. Localities 4 and 10).

The lapilli-member gradually gives way to a pink or pale red, massive welded tuff composed of phenocrysts of quartz and feldspar distributed through a massive, aphanitic groundmass. Most phenocrysts are less than 4 mm in diameter and the feldspars are pale greenish-grey and the quartz glassy. Upwards through the unit the only change is the progressive darkening of the groundmass until in the central regions the rock is very hard and dark reddish-brown. The colour again lightens to a pale pink towards the northern contact. The bleached zones are confined to the contact regions (perhaps 7 metres).

In the Central and Western Regions the Welded Tuff is separated from the Uno Fault by sporadic outcrops of the Silicified Breccia ($p\epsilon s$).

The lowermost Zone of the Welded Tuff exposed in these Regions is Zone 4 (Table 13); it differs from Zone 4 in the Eastern Region in that a weak

internal structure is present. This structure (sinuous, partly contorted banding which resembles fluidal flow banding) is generally confined to the vicinity of the contact with the Silicified Breccia, and is only rarely found higher in the Formation. It cannot be traced for any distance along strike but consistently strikes east-west and dips at a high angle to the north. It is defined by subtle variations in colour and is usually better displayed on weathered surfaces. At the upper surface of the Formation a rhyolitic agglomerate is a prominent marker. It outcrops poorly but overlying weathered material contains numerous spherical blocks or geodes. The rock is composed of spherical blocks ranging up to 10 cm in diameter set in a massive, red, welded tuff. Most geodes consist of a wall of welded tuff surrounding an irregular cavity lined with quartz. In a few cases the cavities are completely infilled with quartz and in rare instances the geodes are quite solid, and formed of poorly defined concentric zones. The outer surfaces of the blocks are mammillated rather than smooth.

5.3.2 Petrography

Eastern Region. The morphology of the lapilli in the basal tuff (Zone 6) is variable but in general the lapilli are composed of two parts; a wall and a core. The wall may be further subdivided into an inner and an outer shell, both of which are porphyritic. The inner shell is composed of a mass of reddened, microcrystalline, potash feldspar crystallites set in small crystals of quartz which display a patchy extinction. The feldspar crystallites have a radial distribution with respect to the core. The outer shell of the wall is distinguished from the inner by an abrupt increase in the degree of crystallinity and in the degree of reddening. Disseminated opaques and acicular crystals of apatite are found in both shells. The outer surfaces of the lapilli are sharp and may be marked by the develop-

ment of clusters of small spherulites.

Feldspar phenocrysts in the walls of the lapilli range in size from 2.5 to 0.5 mm and are subhedral to anhedral. Three crystal types are represented. The first is subhedral, strongly embayed and corroded crystals of plagioclase (well twinned albite - An_5Ab_{95}) mantled by potash feldspar. These crystals are extensively replaced by sericite oriented along the cleavage traces of the parent. The cores of the albites have a corroded appearance; the embayments being occupied by groundmass. The outer surface of the mantles assumes a tabular habit suggesting that they were formerly sanidine but now are composed of orthoclase microperthite. The perthite is of the patch type, the exsolved blebs varying in concentration from place to place in the crystal. In most cases the blebs are aligned along crystallographic directions in the reddened host.

The second phenocryst type is a sodic plagioclase (An_5Ab_{95})which is subhedral to euhedral and extensively sericitised. These crystals differ from the first in that they generally lack mantles and the appearance of corrosion and are partially replaced by a mosaic of quartz included with acicular apatite crystals.

The third feldspar is orthoclase perthite as discrete crystals. These are less extensively altered and reddened and lack the exsolution textures of the mantle feldspars.

Other alteration products of the feldspars include a brownish-yellow chlorite and iron oxides (?hematite), indicating the addition of magnesium and iron as well as silica and potash.

The few quartz phenocrysts are subhedral with high temperature, hexagonal symmetry, have a uniform extinction and minor corrosion. Other quartz phenocrysts,which are elliptical and display an undulose extinction, have perhaps crystallized at a later stage.

The core of the lapilli is composed of irregular quartz crystals clouded with opaque minerals. The centre of some cores consists of a globular or lobate-shaped mass of cryptocrystalline, colourless chlorite and a yellowish-brown, pleochroic, biotite-like mineral. The chlorite contains small,round crystals of iron oxides (?hematite). This mass is enveloped in a veneer of colloform quartz.

The lapilli are set in a glomeroporphyritic groundmass which is coarser-grained, more siliceous and less intensely reddened than the material forming the lapilli. The phenocryst assemblage is similar to that in the lapilli except that the apparently corroded and embayed albite crystals mantled with alkali feldspar, are lacking. Whereas the discrete albite phenocrysts in the lapilli are seldom embayed, those in the groundmass display widespread corrosion. In addition, some are partially replaced by a mosaic of quartz and accessory apatite crystals.

Rarely, late-stage quartz infills the interstices between the lapilli (Locality 4) or forms an aggregate of subspherical to elliptical globule shapes composed of a mosaic of quartz crystals outlines by a concentration of clay minerals. A relict axiolitic texture suggests crystallization from a siliceous glass.

Traversing the walls of the lapilli is a system of sub-radial cracks infilled with barite. In most rocks the cracks do not extend beyond the wall (Locality 10) but some fractures cut the quartz-rich interstitial material (Locality 4).

The overlying tuffs (Zone 5, Table 13) are sparsely porphyritic at the base. Feldspar phenocrysts have a size in the range 0.2 to 5 mm with a mean diameter of about 3 mm. There are two types. One is an altered, faintly reddened, sodic plagioclase (An_5Ab_{95}). Replacement by shredded sericite, aligned along crystallographic planes is common and a few are

replaced by cryptocrystalline albite. These albite phenocrysts contrast with those in the lapilli tuff in that they are generally untwinned and lack widespread corrosion. However, they are usually mantled by intensely reddened, cryptoperthites with the optical properties of orthoclase (-ve $2V \approx 71^{o}$). The mantle feldspar, generally has a tabular habit and it is probable that it inverted from the high temperature modification. The mantles show minor alteration to sericitic micas.

Solitary crystals of orthoclase cryptoperthite are less common than the albite phenocrysts. They may be subhedral but more usually are the broken relicts of euhedral crystals twinned according to the Carlsbad Law.

Quartz phenocrysts are abundant and have a variety of shapes ranging from rounded and embayed, to rectangular and prismatic. They have a size in the range 0.1 to 1 mm, a uniform extinction, are water clear and have the high temperature, hexagonal symmetry. Each quartz phenocryst is rimmed by a corona which has crystallized in optical continuity with the phenocryst and contains numerous crystallites of potash feldspar.

A few skeletal remains of former titanomagnetite consist of leucoxene and ilmenite crystallized along octahedral planes of the parent. These relicts are filled with colourless sericite and are often associated with or included within the feldspar phenocrysts. Colourless euhedral to subhedral zircon and minor apatite are accessory.

Rare, hair-like, discontinuous fractures filled with late-stage quartz traverse the rock.

The matrix of the lowermost Welded Tuff (Zone 5) is composed of small crystallites of reddened potash feldspar set in granular, microcrystalline quartz. Snowflake texture characterises the central part of Zone 5. The nature and extent of late-stage alteration also varies throughout this Zone (e.g. Locality27).

Developments in the central, compared with the lower levels of Zone 5 include:

1. A decrease in the degree of replacement of the albite phenocrysts by potash-rich alteration products (sericite).
2. A marked increase in the amount of alkali feldspar exsolution. The solitary crystals are patch perthites with irregular, untwinned blebs of sodic feldspar in the potash-rich host. The mantle feldspar is also extensively exsolved but the perthite tends towards the ribbon type and the sodic feldspar blebs are twinned according to the albite law.
3. The presence of a pale yellowish-green, weakly pleochroic, micaceous chlorite replacing sodic feldspar.
4. The presence of fine fractures infilled with iron oxides (?hematite) and minor amounts of ?hematite replacing the feldspar phenocrysts.
5. The presence of pseudomorphs after primary ferromagnesian silicate minerals. These are anhedral and composed of crypto- to microcrystalline chlorite similar to that replacing the feldspars. A little colourless carbonate or quartz accompanies the chlorite. Euhedral to subhedral crystals of leucoxene (after ?ilmenite) and a few colourless, euhedral to subhedral zircon crystals occur within or associated with the pseudomorphs. The leucoxene, in places, is partially replaced by ?hematite. The leucoxenised opaques, unlike those found in the lower levels, are not skeletal and do not have potash-rich minerals among their alteration products.
6. The groundmass is almost identical to that of the rocks from the lower horizons, except for a much increased intensity of redden-

ing. Locally (e.g. Locality 350) there are spherulites which range up to 0.4 mm in diameter.

At higher levels in Zone 5, i.e. above the horizon (e.g. Locality 203) which contains chlorite (see 3 and 5 above) the snowflake texture persists but the grain size of the quartz mosaic decreases and the included potash feldspar becomes cryptocrystalline. The potash feldspars are still extensively exsolved and the plagioclase (albite), corroded. However, there is no evidence for their replacement by chlorite and iron oxides; instead a reversion to replacement by sericitic micas is a feature of both the potash- and soda-rich feldspars. The quartz phenocrysts are identical to those in the lower horizons but may be somewhat more abundant. The pseudomorphs after primary ferromagnesian minerals vary from 1-3% by volume and consist of a felted matte of iron-rich, finely fibrous, yellowish-green micas which are stained with disseminated hematite. In places a potash-rich clay mineral(?illite) may be associated with the chlorite. Relict cleavage traces, suggest the mineral was probably a pyroxene. Acicular apatite and partly leucoxenised rutile together with altered titanomagnetite are associated with or included within the mafic pseudomorphs.

At one locality (Locality 29) carbonate and a blue-green chlorite pseudomorph primary ferromagnesians and also partially replace feldspar (preferentailly albite).

At the top of Zone 5 the groundmass changes from the fine-grained modification of the snowflake texture to the microcrystalline granular texture of Zone 4. (e.g. Localities 9 and 87). A change in the nature of the feldspar phenocrysts accompanies the textural change. The feldspars are compositionally similar but are broken and splintered relicts. A few crystals are partially replaced by quartz and minor potash-rich alteration

products, in contrast to those in the lower horizons which are extensively replaced by sericitic micas and iron oxides. Albite crystals, unlike the potash-rich crystals, are usually associated with, or enclose, acicular apatite and euhedral leucoxene (after ?ilmenite or titanomagnetite). The mantling of plagioclase feldspar by potash feldspar appears to be less general in this horizon. A few "fragments" composed of a polycrystalline mosaic of quartz, which is dusted with iron oxides and acicular apatite, are usually associated, or included with crystals of leucoxene (after titanomagnetite). It is possible that these represent former ferromagnesian minerals replaced by quartz but direct evidence is lacking.

The groundmass of Zone 4 is microcrystalline granular, and formed of colourless quartz containing crystallites and small anhedral crystals of deeply reddened potash feldspar and discrete, small crystals of iron oxides (?hematite). The feldspar is partially replaced by fine-grained illite and/or a lemon-yellow chlorite. This groundmass texture contrasts sharply with the fully developed snowflake texture.

In the microcrystalline granular groundmass the quartz and feldspar are interstitial to one another, whereas with the snowflake texture the feldspar is included within the quartz. Zone 4 grades upwards into Zone 3 which has a coarse-grained, granophyric texture. The phenocryst assemblage remains the same but there is no indication of late stage alteration.

The above sequence, (Zones 5, 4, 3) is reversed towards the top of the Formation. The granophyric textured Zone 3 grades upwards into a microcrystalline texture (Zone 2) and further up into the snowflake textured Zone 1. Within the latter zone distinct horizons characterized by chlorite and iron enrichment can be identified. The transition from horizon to

horizon is more rapid than it is in the lower horizons.

In the Central and Western Zones the phenocryst assemblages are similar to those found in the Eastern Zone although:

a. Sodi-potassic feldspars (e.g. Locality 10) are distinctive and common. The centre of a crystal is water-clear albite but the margins are discoloured, faintly reddened and partly altered orthoclase. Potash feldspar has crystallized along cracks in the core and the replacement becomes gradually more extensive towards the peripheries such that the junction between the albite and potash feldspar zones is diffuse. Shadowy albite twinning may develop adjacent to the potash feldspar, but this is not universal. The albite is not antiperthitic but the orthoclase is weakly perthitic (20% inclusions). It is important to note that the sodi-potassic feldspars differ from the albite phenocrysts which have a discrete potash feldspar mantle.

b. Colourless albite phenocrysts are present in the Central Region but are not recognized from the Eastern Region. In the Central Region these crystals decrease in abundance upwards through the Formation. At the base they are partially replaced by orthoclase but the extent of the alteration decreases upwards.

c. Deeply corroded, twinned, albite phenocrysts which are partially to completely replaced by sericite are recognized from both zones but whereas in the Eastern Region the crystals are often mantled by potash feldspar, the mantles are not recognized in the Central Region. In both Regions these crystals decrease in amount upwards through the Formation.

d. Ferromagnesian phenocrysts are more abundant. Fresh crystals (e.g. Locality 295), are colourless to very pale, lemon-yellow clinopyroxene with the optical properties of ferro-augite and possibly a sub-calcic, ferro-augite. The ferro-augite forms anhedral crystals which are usually associated with titano-magnetite and may be enclosed within, or associated with, plagioclase crystals. Inclusions of titanomagnetite are rimmed by small overgrowths of pink, pleochroic titanaugite. Elsewhere, dull green, pleochroic crystals of aegirene-augite form overgrowths on the ferro-augite. Both the parent crystals and the overgrowths are partially replaced by cryptocrystalline uralite and an iron-rich, brownish-green chlorite. Many are stained yellowish-brown by iron oxides (?hematite). Rarely the clinopyroxene and titanomagnetite form a mass of minute globules included within glomeroporpyritic clusters of plagioclase crystals. The clinopyroxene and its alteration products may compose up to 5% of a single sample and the crystals range up to 2 mm. Relict pyroxene cleavages may be preserved by sub-parallel concentrations of disseminated opaques (e.g. Locality 295) in chlorite and amphibole pseudomorphs. Iron oxides (hematite) crystallize along fracture networks and partially replace the feldspar phenocrysts. However, in those rocks in which pyroxene is only partly replaced the network of fractures is infilled with a yellowish-green, microcrystalline chlorite and chlorite may partially replace the feldspar phenocrysts.

The groundmass of the rocks from the lower horizon (Zone 4) in the Central and Western Regions is composed of a microcrystalline granular intergrowth of quartz and reddened potash feldspar, although locally there is an incipient development of a snowflake texture (e.g. Locality 127). Weak banding is generally evident in thin section (e.g. Localities 10 and 32). The banding is irregularly spaced and most bands are contorted, although they are continuous and sub-parallel, and in this respect resemble flow banding. The banding is defined by variations in grain size and in the quartz to feldspar ratio. The broader layers are finer-grained and tend to be less quartz-rich than the finer layers. In a few places (e.g. Locality 32) the banding is defined by variations in the degree of reddening of the feldspar in the groundmass. Elsewhere (e.g. Localities 266 and 244) alternation of snowflakes and microcrystalline textures defines the banding. In one sample (Locality 266) the granular layers form wispy sub-parallel streaks and bolder aggregates which could be interpreted as representing either relict flow banding or eutaxitic foliation. Elsewhere they form continuous but contorted sub-parallel lines. In the second sample (Locality 244) definite broad layers up to 30 mm in width are formed. In either case the layers are clearly defined and have sharp contacts.

The banding in the groundmass of the surface horizons (Zone 1) is more strongly developed than that of the rocks from the middle horizons but not usually as well as those from the lower horizons. The predominant texture is snowflake.

Some rocks have a contorted sub-parallel banding (e.g. Locality 231) formed of alternate layers of feathery, microcrystalline potash feldspar interspersed with sinuous, lens-shaped segregations of residual quartz

enclosing reddened potash feldspar. The layering is further enhanced by varying degrees of reddening and of crystallinity in the potash feldspar layers.

Elsewhere (e.g. Locality 29) the banding is solely dependent on the varying degrees of reddening of the potash feldspar.

The groundmass of most rocks is traversed by a series of discontinuous fractures lined with iron oxides or, (Locality 29) microcrystalline quartz with carbonate along the margins.

The geodes in the surface agglomerate of Zone 1 are composed of a wall of porphyritic rhyolite enclosing an irregular cavity lined with quartz. The principal phenocrysts in the walls are plagioclase (albite) many of which are corroded. Some of the crystals form glomeroporphyritic clusters and are associated with pseudomorphs of ferromagnesians which are composed of lemon-yellow intergrowths of sericite and chlorite. Crystals of leucoxenised opaques, apatite and zircon are associated with the pseudomorphs and also occur as discrete crystals.

Sub-rounded quartz phenocrysts dot the walls of the geodes mainly as single crystals but a few multicrystalline aggregates also occur.

Much of the groundmass of the wall is composed of irregularly shaped but equant, interlocking quartz which contains intensely reddened, acicular potash feldspar. In most places the included feldspar is radially disposed with respect to the core. In some places quartz may form some 40 to 50% of the groundmass whereas in others it is almost absent. The overall texture has a feathery appearance.

The cores are formed of inwardly directed, bladed quartz crystals. The crystals have an undulose extinction and contain growth lines defined by

lines of disseminated hematite. A few fragments of the walls, rimmed by a selvedge of microcrystalline quartz, are incorporated within the core.

The outer surfaces of the geodes are mamillated rather than smooth, and are set in a groundmass which resembles that of the walls but displays the snowflake texture.

5.3.3 Petrochemistry

Analyses of three samples of Porphyritic Rhyolite ($p\epsilon v_1$) from the Central Region (Localities A244, A266 and A295) and their recalculated CIPW molecular norms are presented in Table 3, (Page 62).

The three samples are from the middle of the outcrop; Sample A244 from the eastern limits, A247 from the central limits and A295 from the western limits.

The analysis of Sample A295 is in contrast with many from the Arcuate Structure in that the alkali balance is compatible with primary crystallization in a natural system. The normative feldspars equate with the modal feldspars.

The comparatively high soda content of 3.50% and the normative albite of 29.62% is reflected in the abundance of unaltered modal albite phenocrysts. The abundance of potash (5.90%) is reflected in the norm as orthoclase and in the mode by the abundance of potash feldspar in the groundmass and to a lesser extent in the potash-rich alteration products of the groundmass feldspars. The presence of iron- and titanium-rich pyroxenes is reflected to some extent by the comparatively high iron and titanium values of the analysis. In the norm, in addition to enstatite, ferrosilite is also recorded among the metasilicates.

TABLE 3: WELDED TUFF ($p\epsilon v_1$)

Analysis, %				CIPW Norm, %			
	A244	A247	A295		A244	A247	A295
SiO_2	72.20	73.30	72.10	Q	34.31	37.05	27.21
Al_2O_3	13.40	13.50	14.00	Co	2.28	3.11	0.44
Fe_2O_3	1.56	1.44	1.62	Or	28.37	37.82	34.87
FeO	1.04	0.96	1.08	Ab	26.23	16.08	29.62
MnO	0.08	0.01	0.05	An	2.25	0.91	3.87
MgO	0.25	0.12	0.17	En	0.62	0.30	0.42
CaO	0.48	0.25	0.86	Fs	0.31	0.28	0.04
Na_2O	3.10	1.90	3.50	Mn	2.26	2.09	2.35
K_2O	4.80	6.40	5.90	I1	0.53	0.36	0.80
TiO_2	0.28	0.19	0.42	He	-	-	-
P_2O_5	0.02	0.05	0.06	Ap	0.05	0.12	0.14
LOI	1.80	1.45	1.18	Sub-total	97.21	98.12	99.76
	99.01	99.52	100.94	LOI*	1.80	1.40	1.18
	-	-	-		99.01	99.52	100.94

* LOI - Loss on ignition.

Aegirine-augite is present in only small proportions in the modal minerals but even so would account for some of the normative albite.

The high magnetite of the norm can be accounted for by the modal titanomagnetite, with the ilmenite of the norm recording that titanium in the analysis which is present in titanomagnetite and titanaugite of the mode.

The low value of 0.17% magnesium in the analysis indicates that the chlorite which forms in veinlets through the rock is an iron-rich rather than a magnesium-rich variety. The comparatively high value of 0.86% CaO in the analysis is reflected in the comparatively high anorthite content of the norm and by the presence of ferromagnesian minerals in the mode.

Sample A244 differs from A295 in that it is bright brick red rather than dull brown. Sample A244 contains pseudomorphs after ferromagnesian minerals but these are much less common than the fresh crystals and pseudomorphs in A295. This difference is reflected in the reduced lime of the analysis and the lower anorthite of the norm. The presence of ferromagnesian pseudomorphs is, however, reflected in the enstatite and ferrosilite values of the norm. Sample A244 also contains a lower phenocryst to groundmass ratio than A295 and thus the lower values for soda in the analysis and albite in the norm are readily explained. Lower potash is a function of the degree of alteration; Sample A244 has been subjected to less potash enrichment, and crystallization of secondary, potash-rich phases than A295. In other respects the analysis and recalculated norms do not differ significantly.

The differences between the analysis and calculated norm of A247 and those of A244 can be explained by differences in the modal proportion of primary minerals and by slight differences in the degree of late-stage alteration. The most anomalous feature of A247 lies in the alkali imbalance and in the low lime content. The sample has pseudomorphs after primary ferromagnesian minerals, but they are composed entirely of an iron-rich chlorite, with no amphibole, reflecting the low calcium of the analysis and comparatively low anorthite content of the norm. The anomalous alkali

balance with high potash and low soda is a reflection of the degree of replacement of the albite phenocrysts by potash-rich secondary products.

No samples from the Welded Tuff ($p\epsilon v_1$) of the Eastern Region have been analysed but the petrography indicates that there is a continuous chemical zonation from bottom to top within the Formation as follows:

1. a potash-enriched horizon deficient in mafic silicates or their pseudormorphed equivalents (Zone 5).
2. A magnesium, iron- and calcium-enriched horizon with common pseudomorphs after mafic silicates and increased exsolution of potash feldspar phenocrysts (Zone 5).
3. a silica enriched horizon (Zone 5).
4. A series of horizons (Zones 4, 3, and 2) in which chemical alteration is barely evidenced. In Zone 3 the rocks are the least altered and most closely represent the magmatic composition of this Formation.
5. A magnesium, iron and calcium enriched horizon (Zone 1).
6. A potash enriched horizon (Zone 1).

In the Central and Western Regions the chemical variation is less distinct but appears to follow a similar pattern. The base is enriched to a minor degree in potash and this gives way to magnesium, iron and perhaps a carbonate-enriched horizon before encountering comparatively fresh rocks. An iron-enriched horizon is evident in the surface layers.

5.4 Porphyritic Rhyolite ($p\epsilon l_2$)

5.4.1 Field Observations

The unit is poorly exposed and much of the outcrop is concealed beneath sub-outcrop and scree derived from the underlying Welded Tuff ($p\epsilon v_1$).

The rock is composed of phenocrysts of quartz and feldspar set in a pale-brown or fawn, massive and aphanitic groundmass. The feldspar phenocrysts range from deep red to pale pink and from 2 to 4 mm in size. They are present in variable proportions but compose some 25% by volume of most examples. Quartz phenocrysts compose less than 5% of the rock. In the lower levels the quartz phenocrysts are very small and usually less than 1 mm in diameter. Upwards the anhedral, glassy quartz phenocrysts have a bimodal distribution of less than 1 mm and between 2 and 3 mm in diameter. The larger crystals are identical to those from the overlying Crystal Tuff (pЄct).

The groundmass has a mottled appearance and in places is streaked with red iron oxides and green alteration products. Elsewhere a weak and subtle banding is defined by sub-parallel variations in colour.

A very fine-grained tuffaceous rock appears towards the top of the unit. This rock is streaked due to the sub-parallel alignment of the pyroclastic components and the colour ranges from reddish fawn to reddish grey in colour. It appears to pass upwards rather abruptly into a dark reddish-brown somewhat coarser-grained lithic-vitric tuff that contains crystal fragments not represented in the finer-grained rock. The coarser tuff has a restricted distribution and is found to the east of the Central Region and appears to form a basal unit to the overlying Crystal Tuff to which it may be more closely affiliated.

In the vicinity of the contact between the Porphyritic Rhyolites ($p\epsilon l_2$) and the Crystal Tuff (pЄct), lenses of late-stage quartz are injected along the fractures in the country rock. These lenses are discontinuous but persistent along strike. In some respects the quartz masses resemble the Fluidized Breccia (pЄs) along the Uno Fault zone, although rock fragments

are generally lacking. The quartz has a jasperoidal appearance and is streaked in sub-parallel lines which are concordant with the walls of the intrusive masses. The streakiness is due to combined iron oxides which stain the quartz a deep red colour. Locally the quartz is jointed in the same direction as the country rocks. The margins of the intrusions are vuggy and infilled with colourfully zoned agates. Many of the intrusive bodies attain 2 m in width and are continuous for as much as 15 m along strike.

5.4.2 Petrography

Distinctive micro-textures enable the unit to be sub-divided into three conformable members from top to bottom as follows (see also Table 13):

1. lithic-vitric tuffs,
2. perlitic-textured porphyritic rhyolites,
3. snowflake-textured porphyritic rhyolites.

Snowflake-Textured Porphyritic Rhyolites The snowflake-textured rhyolites, at the base, are composed of phenocrysts of quartz, feldspar and pseudomorphs after phenocrysts set in a massive, or in places (e.g. Locality 298) weakly banded groundmass which displays a snowflake texture (Snyder, 1962).

Some of the quartz phenocrysts have the hexagonal symmetry of high temperature crystallization but most are rounded and embayed. A few have splintered habit. The crystals have sharp margins, are water clear and have a uniform extinction. A few contain small (a few microns) fluid inclusions within which are colourless mineral phases.

In a few samples (e.g. Localities 248, 249) the feldspars are partially preserved, whereas in others (e.g. Localities 166, 167) they are almost

entirely pseudomorphed. The main feldspar recognized is orthoclase ($2V=71^{o}$). The crystals are subhedral and range up to 3 mm in diameter with a mean crystal size of about 2 mm. The relict orthoclase is deeply reddened (?hematite) and in places exsolves to cryptoperthite. The replacement products are almost exclusively a cryptocrystalline matte of colourless sericitic mica but in a few rocks (e.g. Localities 248, 298) iron oxides and quartz are also present.

A fourth replacement product of the potash feldspars is barite (+ ve $2v=37^{o}$, R.I. about 1.64) (e.g. Locality 248). This mineral is generally confined to the core regions of the relict phenocrysts and forms a subradiating mass of prismatic crystals up to 0.2 mm in length. The outer regions of these phenocrysts are sericitic.

Plagioclase phenocrysts were identified from only one sample (locality 60). The plagioclase (albite An_6 Ab_{94}) phenocrysts are relatively coarse grained (up to 5 mm) and lamellar twinning is well developed. The margins of each phenocrysts are deeply embayed; the embayments and corroded cores of the phenocrysts are infilled with groudmass. The relict phenocrysts are partially replaced by sericite and clay minerals and iron oxides (?hematite). A few grains consist of a core of sericite and a mantle of partially-replaced potash feldspar. The sericite core is thought to be albite by analogy with less altered potash-feldspar mantled albites elsewhere. They are less abundant than the potash feldspar phenocrysts.

A third phenocryst phase composed of fibrous, microcrystalline sericite has a subrounded habit, in contrast to the more euhedral outlines of the feldspar pseudomorphs and is interpreted as former ferromagnesian silicates completely replaced by potash-rich alteration products. In some cases a little iron oxide (presumably from iron in the crystal lattice of the

primary mineral phase) is preserved along former cleavage traces.

A second type of pseudomorph is composed of relict hematite and leucoxene crystallizing along octahedral planes, with interstitial areas of sericitic mica. This type is thought to represent titano-magnetite crystals also replaced by potassic alteration products.

The partial replacement of feldspar phenocrysts by iron oxides only occurs in those rocks in which the pseudomorphs after probable ferromagnesian minerals are found. The supposed ferromagnesian phenocrysts could have provided a source of iron as a result of their replacement by potassic alteration products.

The groundmass is variable in textural detail but is compositionally consistent throughout, being some modification of the snowflake texture. The snowflakes have a mean size of between about 0.8 mm (e.g. Locality 248) and 0.1 mm (e.g. Locality 167) and the larger size predominates. In most samples the snowflakes form the complete groundmass but in others (e.g. Locality 298) the snowflakes are loosely packed with interstitial, colourless, clay mineral phases and disseminated iron oxides (?hematite) or smaller snowflakes.

Most rocks exhibit a banding or layering, even though it is not always visible in the hand specimen. The banding is due to:

1. relative concentrations of iron oxides (e.g. Locality 167), in interstitial areas between adjacent snowflakes. The texture is further enhanced by small parting fractures which parallel the layering and along which late-stage quartz crystallizes;
2. the sub-parallel alignment of segregations of residual quartz and sericite (e.g. Locality 166). This texture is reminiscent of fluidal-banded lavas, the banding being closely spaced, forming lines, and being contorted and bent about solid phenocrysts.

The more massive varieties (Localities 298 and 248) have structures formed of sub-parallel, lenticular shapes defined by the shadowy concentrations of opaque mineral phases. The texture is not clear in thin section and is better displayed in hand specimen; it resembles that of extensively welded tuffaceous rocks.

Amygdules are comparatively abundant (Locality 60 and 167) and form about 5% by volume of the whole rock. The amygdules range in size from 0.1 to 0.4 mm and are ragged although generally sub-spherical. They are composed wholly of a polycrystalline quartz mosaic which displays shadowy growth lines delineated by trains of disseminated opaques. Concentrations of sericite adjacent to the amygdules indicates high potash enrichment in these areas.

Almost all samples are traversed by a series of fractures along which secondary minerals crystallize. In several cases the fractures are parallel to the banding but in others they are cross cutting. In either case they are infilled with colourless, microcrystalline quartz, projecting in from the walls to the centre of the fracture. The centre of most fractures is infilled with colourless crystals of flaky sericite but iron oxides (?hematite) and minor chlorite are found in a few samples. Alteration of feldspar phenocrysts is more advanced adjacent to cross cutting fractures.

Perlitic-Textured Porphyritic Rhyolites (Zone 2 of $p\epsilon 1_2$, Table 13) The change from a snowflake texture to a perlitic texture is a gradational one.

In general the phenocryst phases are better preserved in the perlitic-textured than in the snowflake-textured rhyolites. They are best displayed in the sample collected from Locality 249.

Quartz, potash and plagioclase phenocrysts are represented but there is no indication of the ferromagnesian silicate minerals postulated as being present in the lower horizon.

Two quartz phenocryst types are found. The first type is large (up to 4 mm in diameter). The second type is smaller than the first (up to 1.55 mm in diameter) and has a more nearly idiomorphic habit and straight extinction. Most of these were terminated crystals or broken relicts of terminated crystals somewhat rounded and embayed, which crystallized with the symmetry of high quartz.

Potash feldspar phenocrysts are more abundant than plagioclase (albite). The crystals are euhedral to subhedral and have a size distribution in the range 1.5 to 0.4 mm. Usually they form as discrete crystals but glomeroporphyritic aggregates are also found. The crystals have the optical properties of sanidine (-ve 2V = 8^{o}) and are faintly to deeply reddened by disseminated iron oxides (?hematite). Most crystals are comparatively fresh although minute crystals of colourless mica are present along the cleavage traces. There is only minor exsolution.

Discrete albite crystals are untwinned, subhedral and differ from the potash feldspar in that they are somewhat embayed. Other albite grains mantled by potash feldspar have lamella twinning and a composition of $Ab_{96}An_{4}$. A few of the crystals are fresh but most are partially replaced by sericite and clay minerals. The mantle potash-feldspar often assumes an euhedral habit. In some crystals of this type quartz appears to have crystallized along the boundary between the albite core and the potash feldspar mantle.

In addition to the lesser alteration of the feldspars compared with those of the underlying rhyolites (Zone 3, $p\epsilon 1_{2}$) these rocks are further characterised by the development of spherulites. In some places the spherulites enclose or partially enclose single phenocrysts; in other places they unit several phenocrysts and yet in others they appear to be unrelated to the feldspar phenocrysts. They range in size from 6 to 2 mm and are

formed of a mosaic of quartz crystals in which are set crystallites of sub-radiating, reddened, potash feldspar. In general the quartz mosaic is coarser-grained in the core regions than towards the rim of the spherulites and the feldspar crystallites are more abundant towards the rim than they are at the cores. The net result is a weak concentric zonation of the spherulites.

The rim of a spherulite is formed of a thin layer of polycrystalline quartz, with disseminated clay minerals covered by a veneer of iron oxides. Opaque mineral crystals (leucoxene after ?titano-magnetite) and quartz phenocrysts are included within some spherulites.

The cores of spherulites which are unrelated to feldspar phenocrysts are formed of a small globular mass of colourless microcrystalline quartz.

Another phenocryst type with a sporadic distribution may represent a former ferromagnesian silicate phase. The crystals usually have a sub-rounded to lobate outline and are composed of a polycrystalline mosaic of quartz through which are distributed fine-grained,yellowish clay minerals and abundant, dusty iron oxides. The iron oxides are concentrated about the outer margins of the relict crystals and along relict cleavage traces.

The groundmass of Zone 2 ($p\epsilon 1_2$) is characterized by a network or perlitic cracks. These and the texture of intervening areas varies as follows:

1. Perlitic cracks defined by colourless, crystalline quartz enclosing mottled aggregates of microcrystalline quartz and potash feldspar. The feldspar is discoloured by iron oxides and partially replaced by yellowish-green clay minerals (e.g. Locality 249).

2. Perlitic cracks defined by smoky brown, microcrystalline quartz and cryptocrystalline illite (?) enclosing reddened and partially altered potash feldspar (e.g. Locality 285).

A few euhedral and anhedral crystals of leucoxene (pseudomorphs after titano-magnetite) have a sporadic distribution, with minor crystals of colourless zircon, apatite and secondary barite.

Towards the top of Zone 2 ($p\epsilon 1_2$) there is an absence of spherulites and better preservation of perlitic cracking. Also the feldspar phenocrysts are more extensively altered to sericite (e.g. Locality 1999). A little quartz may accompany the alteration. Plagioclase (albite) is possibly more abundant in this than in the lower horizons. The crystals display lamella twinning are sericitized and are generally anhedral, although a few subhedral crystals occur. The albite phenocrysts are seldom rimmed or mantled by potash feldspar as in the lower levels of Zone 2. However, a few crystals are mantled by a feldspar phase which has the optical properties of anorthoclase (Plate 17B). The mineral has a cross-hatched twin pattern which is somewhat coarser than that usually ascribed to anorthoclase, is optically negative, has a small extinction angle on (001) of 4 degrees and a moderate 2V of 48 degrees. It is patchily reddened by disseminated opaque mineral phases (?hematite). As well as mantling a few albite phenocrysts it also occurs as discrete euhedral crystals in small amounts. The occurence of this mineral is somewhat unusual, in that it has not been identified as a mantle phase elsewhere in the Arcuate Structure.

Two amygdule-like structures have a sporadic distribution (e.g. Locality 267). The first and most abundant is elliptical in cross section and formed of concentrically zoned quartz. The outer margins are sharp and lined with a veneer of shadowy quartz crystals which have a radial distribution with respect to the ellipse. The core regions are infilled with microcrystalline quartz. The concentric banding is further enhanced by zones of very fine dusty opaques and clay minerals ranging up to 0.2 mm in diameter. The second type is coarser-grained, irregular in outline and

composed of a rim of quartz, the inner surface of which is lined with very fine-grained, colourless ?illite. The core is formed of a single crystal of quartz which displays shadowy extinction and is discoloured by disseminated opaque mineral phases.

The groundmass towards the top of Zone 2 shows a variety of modifications of perlitic texture, including those found at lower levels together with:

1. Perlitic cracks defined by a microcrystalline aggregate of reddened potash feldspar enclosing masses of potash-rich, cryptocrystalline material in which are set blotchy discoloured crystals of quartz (e.g. Locality 199).
2. Perlitic cracking formed of colourless quartz enclosing areas of discoloured quartz and potash feldspar (e.g. Locality 229). This variety is important for it is accompanied by amygdules that are composed of cryptocrystalline, emerald green chlorite (Plate 17C) rather than the common quartz. The high proportion of quartz in the groundmass is significant.

The rocks are traversed by a series of fractures similar to those found in the lower horizons. Most of the fractures are fine and infilled with colourless quartz and more rarely by disseminated, colourless, clay minerals. A second fracture type (Locality 199) occurs as sub-parallel sets. They have irregular boundaries and are formed of angular chips and fragments of the host rock set in a microcrystalline groundmass of reddened potash feldspar, suggesting some minor deformation (Plate 17A). The fractures are variable but in places attain 4 mm in width.

In contrast to the rocks towards the base of Zone 2 ($p\epsilon 1_2$) those from the higher levels show:

PLATE 17 PORPHYRITIC RHYOLITE ($p\epsilon 1_2$)

A. Sample 199:PPL x 10

A fracture zone traversing a perlitic textured (upper right) porphyritic rhyolite. The fracture has an irregular boundary and contains fragments of the host set in a microcrystalline mass of reddened potash feldspar. This relationship illustrates the late stage introduction of potash-rich minerals.

B. Sample 267:XN x 35

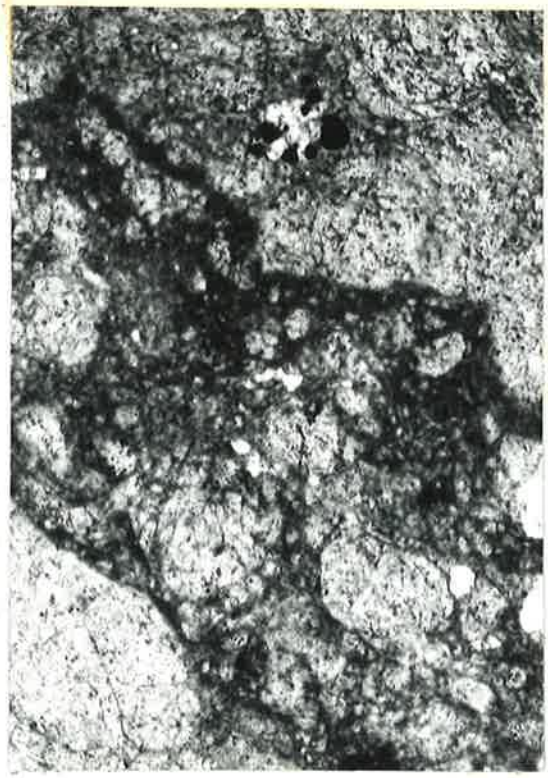
Corroded crystal of albite (lamella twinning) mantled by anorthoclase (cross-hatched twin pattern) set in a micro-granular groundmass composed of quartz (maximum birefringence) and reddened feldspar (dark).

C. Sample 229:XN x 35

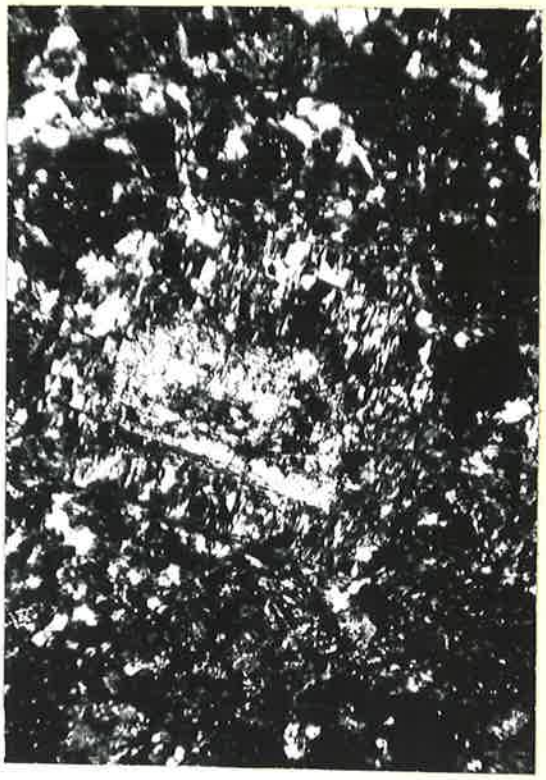
An elliptical amygdule (upper left) composed of a rim of quartz plates enclosing cryptocrystalline chlorite. The groundmass displays convolute perlitic cracks (lower). The cracks are infilled with plates of colourless quartz (q) associated with disseminated, potash-rich clay minerals (speckled) and enclose a microcrystalline mosaic of discoloured quartz (bright) and potash feldspar (dark). The abundance of quartz and the association with chlorite bearing amygdules is significant.

D. Sample 59:XN x 35

A silicified vitric tuff fragment set in a very fine grained siliceous matrix. The fragment has a diffuse margin and is composed of microcrystalline quartz (bright) disseminated iron-oxides (?hematite) and sericitic micas. In plane polarized light iron-oxides and micas define shadowy, relict shard shapes.



A

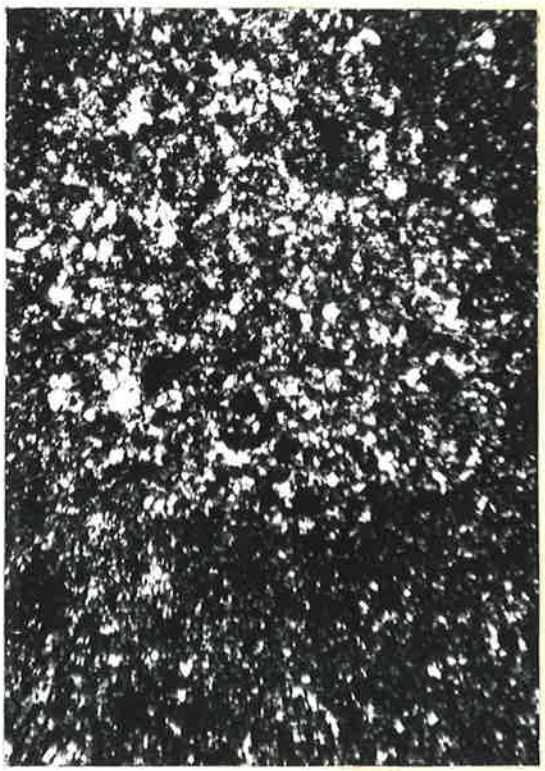


B

PLATE 17.



C



D

1. evidence for deformation;
2. evidence for enrichment in magnesia as suggested by the comparative abundance of chlorite in the sample collected from Locality 229;
3. evidence for enrichment in silica in all samples.

Lithic-Vitric Tuffs [Zone 1 ($p\epsilon 1_2$)] The rocks are composed of fragments of vitric tuff set in a very fine-grained siliceous matrix. The vitric tuff fragments (Plate 17D) are composed in large measure of microcrystalline quartz through which are distributed disseminated iron oxides (?hematite) and very fine-grained, colourless and pale-yellow sericitic micas. The dusty iron oxides, and to a lesser extent the micaceous mineral phases, are localized within the quartz-rich groundmass to define the shadowy outlines of closely packed, shard shapes. A little relict potash feldspar may accompany the iron oxides. The fragments are rounded to sub-angular and have a size distribution in the range 2 to 0.5 mm.

The matrix is also composed in large measure of quartz with minor disseminated iron oxides and clay, but is finer-grained than in the rock fragments. Shadowy shard shapes are present but are not nearly as abundant as in the fragments. The shards are defined by a slight coarsening of grain size and by the incipient concentration of iron oxides and clay minerals about their former margins.

Crystal fragments are generally lacking in the matrix although one sample (Locality 59) contains abundant chips of quartz which range to 0.4 mm in diameter and have an undulose extinction. Sample 59 is further characterised by the greater abundance of sericite which is laced between the microcrystalline components of the matrix. The shredded flakes have a subparallel disposition which imparts a micro-foliate structure in thin section.

grades to the north into the overlying silicified, Pumiceous Tuff (pЄpt). The unit shows appreciable lensing from widths in excess of 400 m to less than 1 m.

In its lower levels (Zone 2) the Crystal Tuff is composed of a closely packed mass of quartz and feldspar crystal fragments set in a deep reddish brown, aphanitic groundmass. The crystal fragments range up to 7 mm in width and within any one area are remarkably well sorted. The feldspar crystals are equigranular, anhedral and white to cream and pale pink in colour. The quartz crystals are sub-round and glassy. Quartz and feldspar fragments are about equally abundant and compose upwards of 80% of the sample. The groundmass is very fine-grained and deep brick red. Towards the centre, the rock becomes enriched in quartz crystal fragments at the expense of feldspar, although the fragment to groundmass ratio continues to remain at a high level (in excess of 8:1). In addition, the mean grain size of the fragments decreases perceptibly and the feldspars become predominantly pink to red in colour.

There is a general decrease in the grain size and abundance of the crystal fragments accompanied by a relative concentration of quartz crystals towards the top of Zone 1 but the point at which quartz crystals cease to be conspicuous is abrupt and this, although arbitrarily defined, is taken to be the upper contact. In the region of the contact feldspar crystal fragments are not evident and the fragment to groundmass ratio falls to about 1:2.

The rock is massive, strongly jointed (Plate 18A), and lacks internal structures. A dominant blocky joint set is concordant with depositional structures in both the underlying and overlying units and thus could be related to depositional structures within the Crystal Tuff.

5 .4.3 Petrochemistry

No sample of the Porphyritic Rhyolite ($p\epsilon 1_2$) have been analysed but the petrography indicates a compositional zonation due to the introduction and removal of chemical components.

The fresh rocks probably do not differ significantly from others in the Arc Structure although the perlitic textured varieties may be richer in soda because of the unusual mantling of albite by anorthoclase. Post depositional alteration includes (see also Table 13):

1. introduction of silica and potash into the lower levels, altering both feldspars and ferromagnesian minerals. The liberated iron is localized as a replacement product of feldspars. Magnesium and calcium migrate from the system;
2. introduction of silica, magnesium and calcium into the central levels;
3. introduction of silica and potash in the upper levels.

The alteration has been initiated by the introduction of silica and potassic solutions along fractures and amygdules. Magnesium, calcium and iron are displaced and migrate within the rock unit.

5.5 Crystal Tuff ($p\epsilon ct$)

5.5.1 Field Observations

The crystal Tuff ($p\epsilon ct$) forms a distinctive and readily mapped unit. The rock is knobbly and rough (Plate 18) and contrasts with the more regular outcrop of the welded tuffs or the closely jointed outcrops of the rocks with internal structures.

The lower contact is well defined and conformable but the Crystal Tuff

PLATE 18 CRYSTAL TUFF (pЄct)

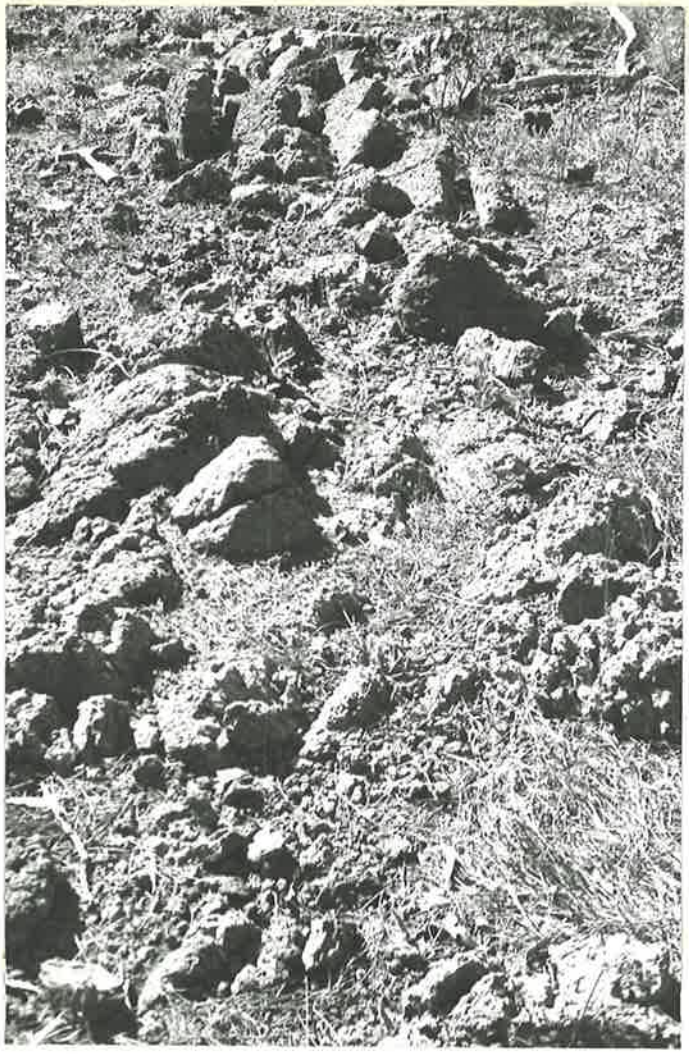
Plate 18A

Outcrop of Crystal Tuff (view looking east) blocky joint system. A dominant joint set strikes (east-west) and dips at a high angle to the north and a lesser set strikes north-south, generally with a vertical dip.

Plate 18B

Characteristic knobbly outcrop of Crystal Tuff. The speckling in shaded areas represent quartz crystal fragments.

PLATE 18.



A



B

5.5.2 Petrography

The lower part of the unit is composed of large crystals of potash feldspar, sodic plagioclase, and broken quartz crystals, in a microcrystalline groundmass (e.g. Locality 268). The feldspar crystals are subhedral to anhedral and have a size range 1.5 to 0.5 cm, whereas the quartz is more irregular in habit and has a size range 5 to 0.2 mm. Some quartz crystals are euhedral and some are splinter shaped. The larger grains are polycrystalline and formed of several anhedral crystals. The quartz is water clear but may contain a few minor inclusions of colourless silicate minerals of high relief (?apatite). The margins of the quartz fragments are sharply defined; some are straight but most are crenulate. The quartz displays a moderate to strong undulose extinction and is traversed by a network of linear or curvilinear, healed cracks, along which disseminated opaques and fine-grained silicates crystallize. The groundmass quartz crystallizes in optical continuity with the crystals at the margins of the fragments. Although the fragments are somewhat rounded the only suggestion of embayment is in the development of the crenulate margins.

The bulk of the feldspar is potassic although sodic plagioclase fragments also have a sporadic distribution. The potash feldspars are extensively altered to fibrous and shredded sericite. The largest are composed of a coarse-grained, inequigranular mosaic of crystals, each of which tends to be euhedral.

Two principle types are found. The first and most common is untwinned or twinned according to the Carlsbad Law, is strongly reddened by disseminated ?hematite and is an orthoclase (-ve $2V=71^{o}$) microperthite. The perthites are of the patch type and the exsolved plagioclase blebs are randomly distributed through the potash-feldspar host. The second type has a

PLATE 18a CRYSTAL TUFF (pЄct)

Sample 171:XN x 35

Reddened orthoclase microperthite crystal (centre of field of view) mantled by overgrowths of graphic quartz and orthoclase.



PLATE 18 a

complicated twin pattern formed of a combination of albite and pericline twin laws, and is also reddened by disseminated opaques. These crystals were possibly anorthoclase and anorthoclase-sanidine perthites, modified during their cooling history.

The least common of the feldspar phases is albite. This mineral displays albite twinning and can be distinguished from the potash-rich feldspar by a lesser degree of reddening and by its replacement by cryptocrystalline, colourless clay minerals (?illite).

The orthoclase-microperthite crystals are mantled by an intergrowth of graphic quartz and orthoclase (-ve $2V=70.5^{o}$). Apparently these crystals partially melted and recrystallized to form an eutectic intergrowth of quartz and potash feldspar during crystallization of the matrix (Plate 18a). The graphic intergrowths form radial to, and penetrate the host crystals by as much as 0.2 mm. Similar graphic intergrowths are formed within some of the crystals. In these and the peripheral intergrowths the recrystallized potash feldspar crystallizes in optical continuity with the orthoclase host.

The genetic relationships of the feldspars are complex and not easily established. In most instances the crystal fragments are discrete crystals or complex intergrowths of the one type. However, a few of the albite crystals are mantled by orthoclase microperthite (e.g. Locality 168) and there is some evidence in one of the samples (Locality 36) to suggest that the soda-rich potash-feldspar (formerly ?sanidine anorthoclase) rim potash feldspar (orthoclase microperthites). Although these relationships are by no means general it is suggested that the albite was first to crystallize, followed by the potash feldspar. The soda-rich potash feldspar may have crystallized at a late-magmatic stage prior to the extrusion of the rock.

The groundmass texture of the lower levels of Zone 2 (pЄct) is best

described as granophyric (e.g. Localities 268 and 171), and is formed essentially of euhedral to subhedral crystallites of reddened orthoclase separated by colourless, microcrystalline quartz. The granophyric intergrowth takes on a patch appearance under cross polarizers. Crystallites of reddened, non-perthitic orthoclase are set in lakes of quartz, adjacent areas of which have different optical orientations. The feldspar to quartz ratio is of the order of 60% feldspar to 40% quartz. In some places the feldspar assumes a poorly displayed, spherulitic habit.

The groundmass also contains fine chips of quartz, locally as much as 30% - (e.g. Locality 36) shredded, fine-grained, colourless muscovite, and a few, small crystals of leucoxenised opaques (?ilmenite). In some rocks (e.g. Locality 268) the shredded micas in the groundmass have a lemon-yellow to greenish-yellow colour.

Towards the top of Zone 2 (pЄct) the texture and nature of the groundmass, and the proportions of larger crystal fragments change markedly. The granophyric texture becomes progressively finer-grained and grades into the pumiceous-textured groundmass of the overlying member (Zone 1). In addition, the proportion of larger feldspar fragments decreases until the quartz exceeds feldspar.

The groundmass of Zone 1 (pЄct) is described in detail in the discussion of the Pumiceous Tuffs.

A few of the relatively large rock fragments are found in the middle to upper levels of Zone 2 of the Crystal Tuff. These are angular to subangular in habit and composed of a microcrystalline, feathery mass of quartz, the texture of which is quite distinctive when compared to that of the enclosing rock. The fragments also contain disseminated opaques and cryptocrystalline, colourless clay minerals in accessory proportions.

Feldspar crystal fragments are not found in Zone 1 and there are only a few accidental quartz crystal fragments. In this vicinity, the upper contact of Zone 2 is placed where quartz crystal fragments are no longer present. The rock is traversed by a network of fine (up to 2 cm) veinlets of late quartz (e.g. Locality 102).

At the margins of the fractures the crystals are finer grained than in the central regions and the quartz contains disseminated iron oxides which are aligned perpendicular to the walls of the fracture. A few fragments of the groundmass are incorporated in the vein quartz.

Accessory minerals are not conspicuous. A few euhedral to subhedral crystals of honey-coloured rutile, rimmed with leucoxene, are found.

5.5.3 Petrochemistry

An analysis of a sample from Locality 268 is presented in Table 4 (Page 82).

The analysed sample is representative of the lower levels of the Formation (pЄct) and is composed of abundant quartz (about 30%), orthoclase microperthite, and a few albite fragments (feldspar totalling about 40%) set in a fine-grained granophyric groundmass. The analysed rock is typical of the crystal-rich, basal member (Zone 2) described above. When the normative feldspars are recalculated to 100% and plotted in the Or-Ab-An triangular diagram (Fig. 11) the rock falls in the rhyolite compositional field along with samples from the Welded Tuff Sheet ($pЄv_3$). This is suggested by the alkali balance which contrasts with that of the potassium-rich tuffs found elsewhere in the Arc (Fig. 11).

TABLE 4: CRYSTAL TUFF (pEct)

	Analysis %		Norm %
SiO_2	78.00	Q	45.83
Al_2O_3	11.20	Co	1.88
Fe_2O_3	0.72	Or	34.28
FeO	0.48	Ab	13.54
MnO	0.01	An	1.13
MgO	0.12	En	0.30
CaO	0.24	Mn	1.03
Na_2O	1.60	Il	0.36
K_2O	5.80	He	0.01
TiO_2	0.19	Ap	0.02
P_2O_5	0.01	Sub-total	99.37
Loss on ignition	1.36	Loss on ignition	1.36
	99.73		99.73

The abundance of quartz and potash-rich feldspar is reflected in the high normative quartz and orthoclase. The lesser abundance of albite and alkali-feldspar perthite fragments is also reflected in the lower albite concentration of the norm. The normative anorthite can be accounted for as being partitioned between the modal albite and clay minerals. The metasilicate enstatite of the norm presumably represents other cations present in the clay minerals. The modal proportions of titanferous mineral phases

(leucoxene and rutile) equates approximately with the normative ilmenite. The analysed rock is distinct from much of the unit in that the feldspars are not as intensely reddened. This feature is reflected in the low normative hematite. Even so, the normative magnetite of 1.03% appears high and the normative hematite perhaps a little low to account for the modal opaque minerals.

5.6 Pumiceous Tuff (pЄpt)

5.6.1 Field Observations

The Pumiceous Tuff is a poorly exposed Formation which conformably overlies the Crystal Tuff (pЄct). From the lower contact, the rock grades upwards into coarse-grained, dark, greenish-black tuff.

The tuff is a massive, compact and fused aggregate of non-welded pumice fragments and shards and a few crystal fragments of quartz and feldspar in a fine matrix. The crystal fragments range to 2 mm in diameter and are equigranualr and anhedral. The quartz crystals are glassy while the feldspar crystals are buff and cream coloured. The pumice fragments are angular, finely striated and sometimes partly contorted but appear to be undeformed. They range to 3 cm in diameter but the matrix is composed of fine-grained, comminuted shards and pumice fragments which are varicoloured in shades of dull green, grey and black. The matrix shards are not preferentially oriented or distorted.

The pumiceous tuff changes upwards from predominantly black and dull green to fawn and brown as the abundance and mean size of the pyroclastic debris decreases. The rock is hard and fused throughout; it is weakly banded in the upper levels where crystal fragments do not form a conspicuous component. Instead it is composed of quartz dust set in an aphanitic matrix.

The contact with the overlying Welded Tuff ($p\epsilon v_2$) is not exposed although it can be located to within a few feet.

Near the base, (Zone 3 $p\epsilon pt$) the formation is locally broken by a crude blocky jointing. In the central portion (Zone 2), a platy jointing or slaty cleavage strikes east-west and dips steeply to the north. Near the upper contact (Zone 1), the jointing reverts to the blocky jointing. There is no appreciable folding within the unit.

5.6.2 Petrography

The unit can be subdivided into three Zones. The lower most (Zone 3) is a massive, fragmental rock composed of rock and crystal fragments set in a microcrystalline matrix. The second (Zone 2) is very fine-grained, and more siliceous. The uppermost Zone of the Formation (Zone 1) is a silicified pumice.

The clastic components of Zone 1 are described below.

Pumice Fragments Pumice fragments are the most abundant and conspicuous. They range from rounded (up to 2 cm diameter),to cuspate, platy and shard-like fragments (0.4 - 0.1 mm). They are tubular or micro-cellular being composed of linear aggregates of elongate pore structures (Plate 19C, 19D). In cross section the pumice fragments have a fibrous structure. There is no definite evidence to suggest that they have been subjected to partial collapse, although the pore spaces are elliptical rather than circular in plan and some fragments are contorted. This could mark the onset of incipient welding.

The devitrified pumice fragments are composed of quartz, orthoclase (verified by X-ray), clay minerals and disseminated opaques. The overall

PLATE 19 PUMICEOUS TUFF (pEpt)

A. Sample 135:PPL x 250

Details of the devitrification texture. The outer margins of the shard are formed of a narrow selvedge of yellowish-green clay minerals surrounding a zone of inwardly directed, faintly reddened orthoclase crystals. The core regions are formed of single plates or a series of plates of quartz. Rimming each shard is a narrow zone of quartz crystals which are usually elongate parallel to the edge of the fragment. This zone of quartz gradually gives way to a micro-crystalline aggregate of faintly reddened orthoclase crystals which are inwardly directed and surround a core of residual quartz.

B. Sample 135:XN x 250

Same field of view as for Plate 5C. Certain zones of recrystallization texture are shown to advantage and these are marked as for the description of Plate 5C.

C. Sample 146:PPL x 100

Cross-section of a recrystallized pumice fragment showing the retention of tubular pore spaces indicating an absence of welding phenomena. The development of a pseudo-axiolitic texture along the margins of the pores is evident. The recrystallization texture is formed of a mosaic of reddened alkali feldspar crystals and colourless quartz.

D. Sample 146:XN x 100

Same field of view as for Plate 7C in doubly polarized light.

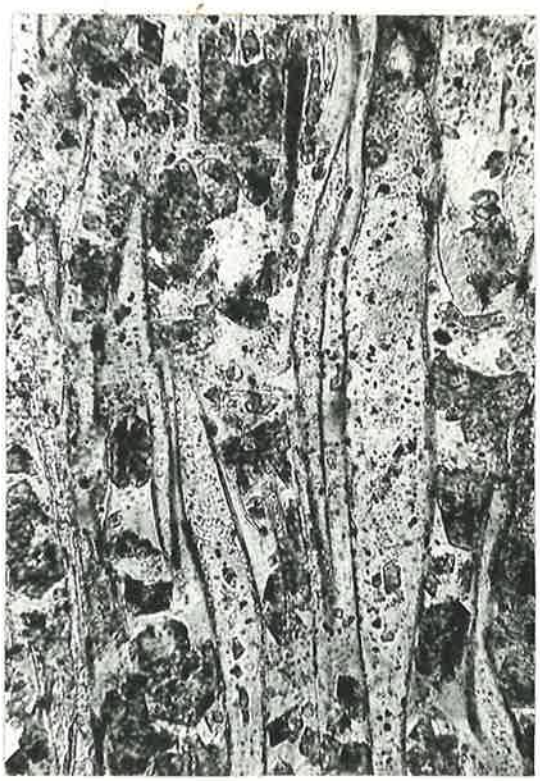


A



B

PLATE 19.



C



D

PLATE 19a PUMICEOUS TUFF (pЄpt)

Sample 134:PPL x 45

General field of view of Pumiceous Tuff showing coarse albite crystal (lower left) mantled by smoky-brown, devitrified glass; perlitic cracking in clear glass fragment (upper left); clear and smoky glass shards. Details of the devitrification textures are visible. Note the absence of welding and the perfect preservation of the vitroclastic debris.



PLATE 19 a.

texture might best be described as pseudo-axiolitic (Plate 19A, 19B). The walls of the tubular pore structures are formed of a thin layer of fibrous, matted, colourless or yellow-green illite discoloured by finely disseminated opaques. The inner surfaces of the walls are formed of a narrow zone of inwardly directed, faintly reddened, orthoclase crystals. Where the walls are close to each other the orthoclase crystals of opposing surfaces may meet, but in most instances a polygonal mosaic of microcrystalline quartz comprises the framework material. The pore spaces are filled with a finer mosaic of crystalline quartz, the individual elements of which are elongate parallel to the pore walls. In some instances the framework material consists of coarser, single plates or a series of fused plates of colourless quartz. Most of the pumice fragments are colourless but a few are smoky-brown.

Shards also are common (e.g. Locality 146), and show a wide variation in shape and size (15 to 0.8 mm) ranging from platy to Y-shaped, U-shaped, crescentic and lune-shaped. The devitrification texture (Plate 19A, 19B) is similar to that for the pumice fragments.

Devitrified Perlitic Fragments

a. Coloured fragments (Locality 135) are distinctive and characteristic. They measure up to 5 mm in diameter and are angular with sharp concave/convex margins. The smoky-brown colour increases to a dark chocolate-brown in the vicinity of a network of perlitic cracks. Between these are mosaics of platy crystals of microcrystalline, undulose extinguishing quartz, fringed by microcrystalline potash feldspar. The feldspar is somewhat darker than the quartz and in the form of elongate

grains oriented at 90° to the crack. Many of the crystals display well-developed crystal faces. The crack itself is defined by flaky, microcrystalline clay (?illite) and/or quartz. Rare, irregular crystals of leucoxenised opaque minerals (?ilmenite) are found in the quartz between the cracks.

Some of the fragments contain phenocrysts of plagioclase feldspar which are euhedral to subhedral. The rims and core regions of some of these are deeply embayed and filled with crystalline components of the groundmass. The feldspar has the composition of oligoclase ($An_{12}Ab_{88}$) and is fresh although some grains are traversed by a network of fine fractures.

b. Clear fragments (Locality 135) compositionally and structurally resemble the coloured fragments. The areas between the perlitic cracks are composed of a platy mosaic of quartz crystals, dusted with opaques and, in some cases, accessory, acicular apatite. Some fragments contain a single crystal of orthoclase in the innermost regions. As in the darker fragments the rock adjacent to the perlitic cracks is composed of orthoclase crystals oriented perpendicular to the crack. These clear fragments are richer in potash feldspar than the other fragments and the glass from which they were derived was presumably richer in alkalies.

Both the coloured and colourless fragments consist of devitrification products of a siliceous glass. The devitrification texture is the same as that displayed by the pumice fragments and shards.

Rock Fragments The rock fragments are variable in petrographic detail but all are rhyolites. Some are massive, others are flow-banded and yet

others display perlitic cooling cracks. Most are clear under the microscope, although a few are discoloured by disseminated opaques. They are angular to sub-rounded and have a size in the range 2 to 0.4 mm. They comprise less than 5% of most rocks. The following types are recognized:

a. Massive - composed of a microcrystalline mosaic of potash feldspar and quartz. These fragments display incipient development of perlitic cracks.

b. Porphyritic Rhyolites - These are formed of potash and/or soda-rich feldspar phenocrysts to which are adhering portions of devitrified, smoky-brown pumice. The phenocrysts of feldspar are similar to the crystal fragments of feldspar described below.

c. Flow-banded Rhyolites - composed of alternate, sub-parallel layers up to 0.2 mm in width. The layers are clear, crystalline quartz which is traversed by a system of perlitic cooling cracks and microcrystalline, reddened, potash feldspar (?orthoclase). In some of the potash-rich layers the feldspar forms elongate, crystals oriented in the plane of the banding.

Crystal Fragments

a. Quartz - These are not common and usually comprise less than 1% of the rock body. They are angular to sub-angular and many preserve crystal faces which indicate that they crystallized with the hexagonal symmetry of high-quartz. Some are embayed and all are water clear with a uniform extinction.

b. Feldspar - Both soda-rich plagioclase feldspars and potash-rich feldspars are present but comprise less than 2% of the rock. Potash feldspars exceed plagioclase crystals in abundance, both range in size up to 1.2mm.

Most plagioclase fragments are altered to sericite. In a few cases the crystal is replaced by a polycrystalline mosaic of quartz and by late-stage, secondary opaques. Where better preserved, (e.g. Locality 135) lamella twinning is apparent and the composition is albite (Ab_8An_{92}). Elsewhere (e.g. Locality 22) the crystals are deeply embayed and intensely reddened by iron oxides (?hematite).

Potash feldspar (strongly perthitic orthoclase) crystals may be complete and unaltered but most are embayed and partially replaced by sericite and opaques. The perthite is of patch type with small irregular blebs of albite distributed through the host. The crystals are often traversed by a network of fine fractures.

The matrix of Zone 3 (pЄpt) is a polycrystalline mosaic of interlocking quartz crystals (e.g. Locality 146) with disseminated opaques. In some areas (e.g. Locality 22) the matrix includes numerous, small shards set in cryptocrystalline material. The shards are somewhat attenuated and have a poorly defined sub-parallel orientation. They are composed of a mixture of quartz and potash feldspar which is partially replaced by yellowish-green, fibrous clay. The pumiceous tuff grades perceptibly to the north into a fine-grained vitric tuff which shows some indication of moderate welding.

The vitric tuffs (Zone 2 pЄpt) are composed of numerous, very small shards and pumice fragments. Their clastic components are similar to the underlying pumiceous tuffs (Zone 1) although more comminuted. Shards, cuspate pumiceous fragments, and a few feldspar crystal fragments are densely compacted in a matrix of altered potash feldspar and quartz. The groundmass is laced with colourless clay minerals.

The shards and pumice fragments are distorted and partially flattened, giving a foliate texture in thin section. Where the rock is least altered

the devitrification textures are the same as those of the pumiceous tuffs.

The upper levels of Zone 2 (Table 13) are traversed by a network of fine fractures along which late-stage deuteric and/or metasomatic quartz has crystallized (e.g. Locality 22). The quartz forms bladed crystals perpendicular to the length of the fracture and is discoloured by fine opaques which tend to be aligned in shadowy layers parallel to the fracture surface. There is little evidence for significant displacement.

The original vitro-clastic texture is clearly preserved in those areas enriched in silica (e.g. Locality 52). The groundmass is a mosaic of quartz crystals in which are set the shadowy outlines of shards preserved by clay minerals and disseminated opaque mineral phases. Microcrystalline "pseudo-axiolitic" orthoclase occurs on the inner side of the shard rims. The degree of perfection of the orthoclase selvedge decreases through the unit until it is almost non-existent (e.g. Locality 279). At the top, dusty opaque phases preserve the outlines of shards.

Potash-enriched varieties (e.g. Localities 233 and 228) are similar to the silica-enriched varieties though the shards and fragments in the former are reddened potash feldspar laced with disseminated opaques and cryptocrystalline clay. The matrix is cryptocrystalline and probably formed of an intergrowth of potash feldspar and clay with a little quartz. There is no indication of avenues such as fractures and vesicles along which late-stage, magmatic potash could have entered.

The upper levels of the Pumiceous Tuff (pЄpt), viz Zone 1, comprise a silicified pumice composed of elongate, tubular and globular structures set in a groundmass of microcrystalline quartz. The tubular structures have a sub-parallel orientation and display devitrification textures similar to those of the pumiceous fragments. The interstitial areas are a micro-crystalline mosaic of quartz. Almost the entire rock has this texture.

A few euhedral to subhedral phenocrysts of extensively altered albite have a sporadic distribution. Potash feldspar phenocrysts are perthitic and partially altered. A few, but by no means all, of the albite crystals are mantled by strongly perthitic potash feldspar, about 0.1 mm in width, which conforms in outline to the shape of the parent crystal. Rare ferromagnesian phenocrysts (e.g. Locality 54) are composed of yellow micaceous minerals through which are distributed abundant iron oxides. Lack of relict cleavage prevents the determination of the primary mineral but it may be an iron-rich pyroxene.

In other areas (e.g. Locality 35) silicification is more extensive and devitrification textures more diffuse; disseminated iron oxides increase in abundance, staining all of the relict potash-feldspar. In addition, the rocks are traversed by fine fractures along which microcrystalline quartz has crystallized. The presence of late-stage silica is also indicated by the formation of numerous, amygdule-like structures in some areas (e.g. Locality 196). These have a ragged habit and are filled with fibrous silica. The silica is pale fawn in thin section due to iron oxides whose grain size is so fine that optical resolution is impossible. In their best development these structures display intricately patterned agates zoned in shades of red and brown.

5.7 Welded Tuff ($p\epsilon v_2$)

5.7.1 Field Relationships

The Welded Tuff ($p\epsilon v_2$) forms a continuous unit in the western part of the Arc Structure but in the middle and east of the Central Region interfingers with the Amygdaloidal Rhyolite ($p\epsilon al$) to form an upper and a

lower Formation. The Welded Tuff ($p\epsilon v_2$) is not represented in the Eastern Region.

Superficial differences between the Welded Tuff ($p\epsilon v_2$) and the Welded Tuff ($p\epsilon v_1$) are that the phenocrysts are white and cream rather than pink, and fresh rock surfaces are mottled due to the presence of numerous recrystallized rock fragments. A weak eutaxitic texture is distinctive in the vicinity of contacts.

5.7.2 Petrography

The lower Formation [$p\epsilon V_2$ (lower) Table 13] in the eastern half of the Central Region is homogeneous. The phenocrysts of quartz are of two types. One type forms sharply angular to splinter-shaped fragments derived from formerly euhedral crystals. These have a uniform extinction but are traversed by a series of fine fractures and rimmed by a zone of reddened, fibrous, potash feldspar. They are probably related to the anhedral to subhedral phenocrysts found in the underlying units. The other type (not represented in the Welded Tuff $p\epsilon v_1$) is somewhat smaller than the first (up to 0.4 mm), spherical to ovoid in shape and displays a poorly defined concentric zonation which is outlined by disseminated opaque minerals set some distance inside the wall of the ovoid shape (Plate 20A, B). The quartz has an undulose extinction which is usually radially disposed with respect to the wall of the ovoids. These rounded quartz particles are interpreted as representing droplets of siliceous glass now crystallized. There is no evidence to suggest the former presence of alkalies in the globule.

Anhedral to subhedral albite is the most abundant feldspar phenocryst. The crystals are deeply embayed in the core regions and around their

PLATE 20 WELDED TUFF ($p\epsilon v_2$)

A. Sample 178:PPL x 250

Ovoid quartz crystal with poorly defined concentric zonation thought to represent devitrified droplets of siliceous glass (Pele's Tears).

B. Sample 178:XN x 250

Same field of view as for Plate 20A in doubly polarized light.

C. Sample 169:XN x 20

Recrystallized quartz phenocryst formed of a polygonal mosaic of quartz crystals.



A



B

PLATE 20.



C

margins. In some rocks the crystals form glomeroporphyritic clusters and may be accompanied by altered ferromagnesian minerals. The individual crystals have lamella twinning and are partially replaced by sericitic micas. A few are mantled by a rim of colourless to faintly reddened potash feldspar which usually assumes a tabular habit about a rounded or subhedral albite core.

Colourless, untwinned crystals of albite are much less common than twinned crystals. They are slightly clouded by disseminated iron-oxides and a few are incipiently altered to clay or sericite.

Pseudomorphs of lemon-yellow muscovite after primary ferromagnesians have a sporadic distribution. They comprise 2 or 3% of a sample (e.g. Locality 271). In some, relict pyroxene cleavages are pseudomorphed by dusty iron oxides which also collect about the rim of the pseudomorphs.

Opaque minerals have an erratic distribution, and may be considered among the phenocryst phases. The crystals are usually sub-rounded and at least in part, composed of leucoxene.

The groundmass is the feature which most serves to distinguish these rocks from pCv_1 in the Central and Eastern Regions. The rocks are massive and for the most part of the groundmass is formed of small crystallites of reddened potash feldspar set in a microcrystalline mass of smoky-brown quartz (Zone 1). But many have a blotchy groundmass and in some there is clear evidence for the presence of rock fragments (Zone 2). In those with a blotchy groundmass (e.g. Localities 227, 271 and 62) the blotches are composed of crystallites of potash feldspar set in cryptocrystalline illite rather than smoky-brown quartz. Disseminated iron oxides may be concentrated about these anomalous patches. Fragments of two rock types predominate. One is composed of crystallites of potash feldspar set in cryptocrystalline, colourless illite, and the other is composed of

microcrystalline-granular, colourless, quartz crystals through which are disseminated opaques.

These rocks ($p\epsilon v_2$ lower) have been subjected to late-stage alteration. The most abundant alteration products are potassium-rich and include sericite (replacing twinned and corroded albite phenocrysts), muscovite (replacing primary ferromagnesian minerals), and illite (replacing rock fragments) (X-ray and optical determinations). In a few rocks a little iron-rich chlorite forms in the groundmass and in some this mineral may be quite abundant (e.g. Locality 227). Fractures are infilled either with colourless crystalline quartz or with iron oxides (?hematite).

The rocks from the upper Formation [$p\epsilon v_2$ (upper) Table 13] Welded Tuff differ from those in the lower horizon in that snowflake texture is abundant.

At the base of this Formation (overlying the Amygdaloidal Rhyolites $p\epsilon al$), is a probable pyroclastic rock which passes rapidly to the welded tuff displaying snowflake texture.

This pyroclastic basal member (Zone 2, $p\epsilon v_2$ upper) has rock fragments and phenocrysts of quartz and quartz eyes (peles tears), albite, altered ferromagnesian minerals and opaques sporadically distributed through a microcrystalline groundmass.

The albite phenocrysts include:

1. deeply corroded crystals with lamella twinning partially replaced by colourless, sericitic micas and more rarely by iron oxides;
2. euhedral to subhedral phenocrysts which lack corrosion but which are partially replaced by sericitic micas; and

3. rare mantles of twinned albite which are reddened by disseminated ?hematite but which lack appreciable alteration.

Ferromagnesians are pseudomorphed by platy crystals of colourless to pale lemon-yellow muscovite, and a cryptocrystalline iron-rich chlorite. The two are seldom found together and the chlorite appears to develop preferentially in those crystals which are included with or related to opaques (now composed of leucoxene). A little quartz accompanies the chlorite but is not found with the muscovite.

Rock fragments are of two types. The first, and most clearly defined, is now formed of yellowish-green, non-pleochroic chlorite in which are set minute crystallites of albitic feldspar and minor crystals of microcrystalline quartz. These compose about 5% of the rock. The second type is similar to,but differentiated from,the groundmass on the basis of textural detail and by a significant increase in the degree of reddening. A few fragments are related to the phenocryst phases in the rock but for the most part they are non-porphyritic. A few ovoid quartz crystals (peles tears), are present in some fragments.

The matrix is composed of subradiating, faintly reddened, crystallites of potash feldspar set in microcrystalline quartz, disseminated opaques and minor alteration products. In some areas the crystallites of feldspar have a preferred orientation but this is neither consistent nor universal. A few,minute flakes of sericite and iron-rich chlorite are sporadically distributed and in some areas chlorite partially replaces the feldspar crystallites. Acicular apatite and minor zircon are accessory.

A network of fine fractures are filled almost exclusively with iron oxides (?hematite) but a few contain a little colourless, microcrystalline quartz and cryptocrystalline, iron-stained chlorite.

The pyroclastic basal member gives way gradationally to the snowflake-textured rhyolites (Zone 1) of the middle parts of the Upper Formation ($p\epsilon v_2$). The phenocrysts found in these rocks include:

1. sub-rounded quartz phenocrysts, some of which are incipiently embayed (high quartz?)
2. partly corroded, twinned albite phenocrysts which are incipiently replaced by sericitic micas;
3. euhedral to subhedral crystals of albite which display a chequer twin pattern and are partially replaced by sericite or quartz;
4. mantles of albite on partly corroded albite phenocrysts. The mantle feldspar is identical to the albite phenocrysts (3, above);
5. pseudomorphs after primary ferromagnesian minerals, which for the most part are composed of muscovite and iron oxides, with a little iron-rich chlorite; and
6. phenocrysts of opaque minerals (leucoxene).

The groundmass shows snowflake texture. A layered sample (Locality 251) displays the variety of snowflake texture in which sub-parallel discontinuous layers of quartz develop and in which the banding is enhanced by varying degrees of reddening of the feldspar included within the snowflake quartz.

The rocks from the surface layers of the Upper Formation do not differ significantly from those of the middle layers. They have a similar phenocryst assemblage and similar groundmass texture but they are less altered than those from the Middle Formations. A little potash-enrichment is evidenced with the minor replacement of albite phenocrysts by sericitic micas.

In the western most part of the Central Region the rocks are similar

to those from the two Formations in the east, except that the pyroclastic basal member of the upper horizon is not found in the west. Instead, the groundmass textures change quite abruptly from the Lower to the Upper Formation.

In the Western Region the corresponding rocks are characterised by a relict clastic texture, and towards the upper levels by the development of a snowflake texture. No differences in the phenocryst assemblages or in the types and degree of alteration could be detected between the Welded Tuff ($p\epsilon v_2$) of the Central Region and those of the Western Region.

5.8 Porphyritic Amygdaloidal Rhyolite ($p\epsilon a1$)

5.8.1 Field Observations

The Formation is poorly exposed. In the west sporadic outcrops of fresh rock penetrate through abundant sub-outcrop and alluvial scree. In the east, small outcrops are restricted to the contacts with the overlying and underlying rock units. The best exposures are in the Central Region on a south-sloping hill face.

The Formation is heterogeneous but a generalized stratigraphic succession can be recognized.

The upper and lower contacts are arbitrarily defined and the unit can be broadly subdivided into three members:

1. a basal welded tuff (Zone 5) which overlies the lower, red, Welded Tuff Formation ($p\epsilon v_2$) and is gradational into;
2. a central, massive perlitic and flow-banded, porphyritic rhyolite (Zones 2, 3 and 4); and

3. an upper red, amygdaloidal, porphyritic rhyolite (Zone 1) which is gradational into the upper Formation of the massive, red, Welded Tuff ($p\epsilon v_2$).

The lower contact of the Formation is taken to be that point above which a fragmental texture is apparent in the hand specimen. The placing of the contact at the point where macroscopic textural differences are apparent facilitates field mapping, although such a contact does not necessarily represent a fundamental change in the composition or petrogenesis of adjacent rock units.

A variety of porphyritic ryholites (Zone 4, 3, 2, $p\epsilon a1$) is found in the middle of the Formation. The relationships of the several types are by no means clear but it seems probable that the lower levels of the Formation are represented by a massive, red to dark-brown porphyritic rhyolite (Zone 4) which is overlain by a weakly banded, very dark grey-brown, porphyritic rhyolite (Zone 3). A distinctive feature of the rocks of Zone 3 is the abundance of brick-red feldspar phenocrysts. The banding is shadowy and defined by subtle, sub-parallel, variations in colour. A massive, dark greyish-brown rock, characterised by more or less reddened phenocrysts, could be at an equivalent stratigraphic level but is regarded, on balance, as an overlying member (Zone 2). Its distinctive feature is the development of perlitic cracks and of a few elliptical amygdules. Amygdules become increasingly abundant towards the top of the Formation (Zone 1) and in places a scoriaceous texture develops. As the amygdules increase in abundance they also become progressively flattened until they form lenticular streaks which impart a weak foliation.

The upper contact of the Formation ($p\epsilon a1$) is taken to be that point at which distorted amygdules no longer form a component of the rock. The

rocks at the top of the sequence are deep brick-red in colour and weakly porphyritic. Feldspar and quartz phenocrysts compose about 5% by volume and amygdules some 25 to 30%.

There is no evidence for folding or for tectonic deformation. In all places, where an attitude can be determined, the internal structures strike east-west and dip steeply to the north. Flaggy Jointing is prominent and concordant with the internal structures.

5.8.2 Petrography

Basal Welded Tuffs (Zone 5) These welded tuffs show a considerable variation but everywhere are characterised by the preservation of a pyroclastic texture.

In a few places (e.g. Locality 276) the rock is a welded vitric tuff and resembles the vitric tuff mapped as a discrete Formation (pЄvt) to the north and elsewhere (e.g. pЄpt Zone 2). This rock is composed of numerous, flattened and distorted shards and accessory rock fragments set in a fine-grained, microcrystalline matrix which is composed of a massive, microcrystalline-granular mosaic of quartz through which is distributed shredded clay, disseminated opaques, and fine-grained carbonate. Relict shards are recognized only by relative concentrations of clay and opaque minerals which define their outlines within the quartz mosaic.

Welded lithic tuff fragments in Zone 5 are also partially to completely replaced by carbonate, clay and opaque minerals (e.g. Locality 275). These are composed of crystal and rock fragments set in a eutaxitic-textured groundmass of flattened and distorted shards. The crystal fragments are angular to sub-angular and range in size from 0.5 to 4.0 mm. They include:

a. Quartz, subhedral to anhedral, partly embayed and rounded, with the hexagonal symmetry of high-quartz;

b. Albite which is subhedral, deeply reddened, partly altered;

c. Potash feldspar coronas which mantle albite phenocrysts and are themselves partially replaced by a mosaic of colourless quartz and colourless mica (potash-rich); and

d. Altered potash feldspar (?orthoclase). Subhedral to anhedral, extensively altered in a manner similar to that of the potash feldspar coronas.

Other rock fragments include, massive, fluidal banded and spherulitic rhyolites.

The matrix of the tuff is composed of flattened, elongate and distorted shards which have a sub-parallel orientation and display the typical streaked or eutaxitic texture of welded pyroclastic units. The shards are moulded around phenocrysts and rock fragments and are composed of a rim of dusty iron oxides and clay bordering a core of micro- or crypto-crystalline clay. Interstitial to the shards is a microcrystalline granular intergrowth of quartz and reddened potash-feldspar (?orthoclase). The reddening imparts a streaked texture to this portion of the groundmass suggesting that it too was formed of fine-grained, recrystallized, pyroclastic ejecta. The matrix also contains fine-grained, angular to sub-rounded chips of quartz and a few small crystals of leucoxenised opaques (?ilmenite). Incipient spherulitic texture develops in some places.

Massive, Banded and Perlitic "Rhyolites" (Zones 4, 3, 2 pGal) Massive rocks of rhyolitic appearance comprise the lower most member (Zone 4) and are overlain by banded (Zone 3) and perlitic (Zone 2) varieties.

The massive rhyolite (Zone 4, e.g. Locality 263) is composed of phenocrysts of quartz and feldspar set in a massive groundmass composed of an equigranular mosaic of microcrystalline quartz and micro- and crypto-crystalline potash feldspar.

The quartz phenocrysts constitute about 2 to 3% of the rock and most are rounded to sub-rounded; a few are deeply embayed; some display the hexagonal symmetry of high quartz. All are water-clear with a uniform extinction and a size in the range 0.2 to 1.5 mm.

A few of the feldspars are euhedral but most are anhedral to subhedral and are partially altered. Some are twinned according to the Carlsbad Law. Orthoclase is the common alkali feldspar (e.g. Locality 273) and forms tabular or euhedral crystals. Others are broken portions of formerly euhedral crystals. The orthoclase is reddened by disseminated opaques (?hematite) and partially altered to fibrous and flaky sericite. A more sodic variety of orthoclase (orthoclase perthite) also occurs (e.g. Locality 263). The perthite is of the patch type, with twinned, irregular blebs of albite scattered sporadically within the host but generally elongate parallel to its cleavage. Some crystals contain more than 50% of exsolved material.

Plagioclase ($Ab_{95}An_5$) may form as much as 2 to 3% of the rock. It is anhedral to euhedral, well twinned according to the albite law and is less altered (sericite) than potash feldspars. The crystals have an orthoclase microperthite mantle with an euhedral outline about the anhedral parent albite.

Small, rounded opaque mineral crystals are a third persistent phenocryst type. These are composed essentially of leucoxene with or without secondary iron oxides (?hematite).

The groundmass is generally homogeneous as an interlocking mosaic of

equigranular quartz and abundant interstitial, altered, micro- and cryptocrystalline potash feldspar. Some groundmass quartz crystallizes in optical continuity as a corona up to 0.5 mm in width around quartz phenocrysts (Plate 21A). Elsewhere patches of the quartz mosaic polarise independently. Potash feldspar forms small, tabular and euhedral crystallites enclosed within the quartz mosaic (Plate 21B). These crystallites may compose as much as 60% of the groundmass. The feldspar is reddened by disseminated opaques (?hematite) and replaced by fibrous, colourless clay.

The homogeneous texture imparts a massive character to the rock but several variations were noted. These include:

a. the development of a weak, sub-parallel layering (e.g. Locality 64) where elements of the snowflake texture form sub-parallel layers of different grain sizes. Individual "snowflakes" are loosely packed in a cryptocrystalline, clay-rich groundmass in the finer-grained layers. This zonation is probably related to primary deposition.

b. the accumulation of abundant, microcrystalline iron oxides to form subparallel streaks in the interstitial areas between the individual patches of the snowflake mosaic (e.g. Locality 236).

The fluidal banded member (Zone 3 Locality 274) is composed of quartz and feldspar phenocrysts set in a finely banded groundmass. The phenocryst phases are similar to those found in the underlying rock unit. In a few of the orthoclase perthite crystals, an area midway between the core and the rim is microperthitic suggesting that the crystals were compositionally zoned. The potash-rich phenocrysts are altered to sericite.

The banding in the groundmass is formed of alternate layers of microcrystalline and cryptocrystalline material ranging from 0.2 to 1.5 mm in width, and with a subparallel disposition, although bending and contortion is evident around phenocrysts. The most common type of layer displays

PLATE 21 AMYGDALOIDAL RHYOLITE (pЄal)

A. Sample 263:XN x 32

Snowflake texture illustrating the crystallization of groundmass quartz about quartz phenocrysts as an optically continuous corona. One quartz phenocryst is at extinction (top), one displays maximum birefringence (middle) and one is almost at extinction (bottom).

B. Sample 263:XN x 100

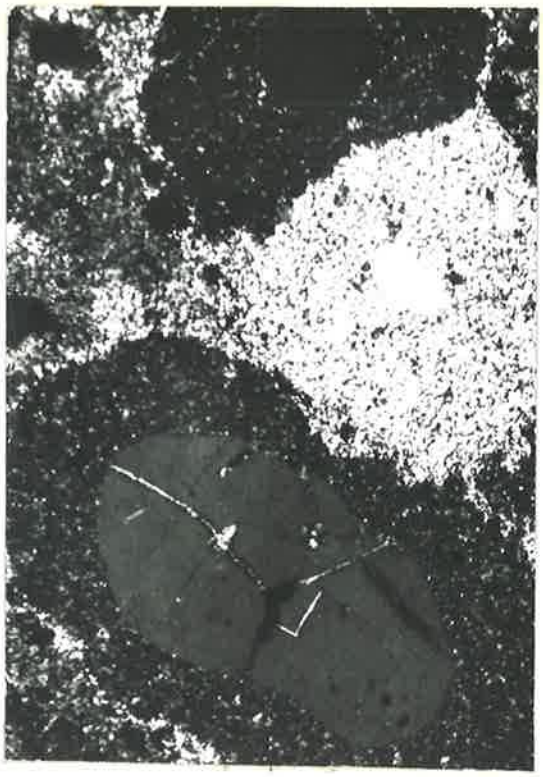
Details of snowflake texture showing crystallites of reddened potash-feldspar randomly distributed throughout an optically continuous groundmass of quartz. A quartz phenocryst (top) shows a weak zonation with a clear core and disseminated iron-oxides in the rim.

C. Sample 274:XN x 32

A devitrified, banded, porphyritic rhyolite illustrating textural variations between layers. The most common layer type (left) is formed of loosely packed snowflake (light) set in feldspar some of which is spherulitic (black). The second layer type (middle) is cryptocrystalline and composed of quartz, feldspar, and a few discrete snowflakes. Continuous bands of colourless, residual quartz (right) conform to the overall banding.

D. Sample 238:PPL x 32

Perlitic rhyolite showing dusty-iron oxides delineating perlitic cracks and enclosing quartz and reddened potash feldspar. Subparallel, elliptical amygdules are formed of an outer selvedge of iron-oxides surrounding a rim of clay (?after potash feldspar) and a core of colourless, polycrystalline quartz.

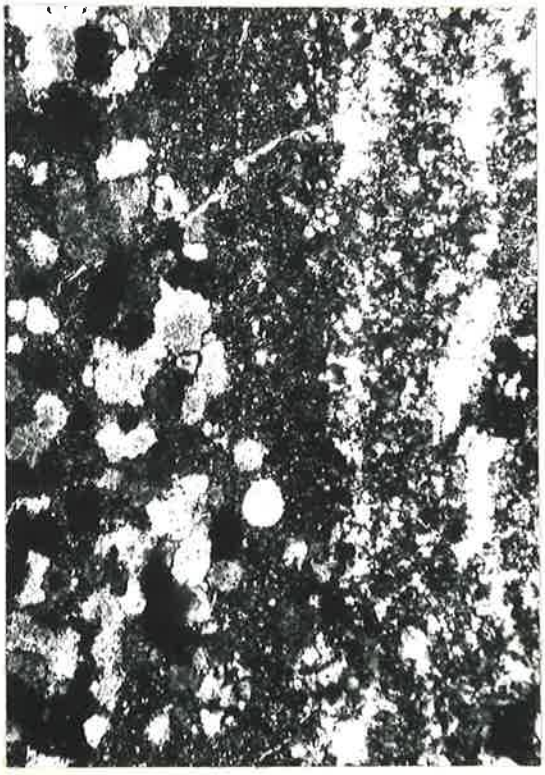


A



B

PLATE 21.



C



D

a fine-grained variety of snowflake texture (Plate 21C). The feldspar of the snowflake is potash-rich, strongly reddened, and imparts a deep yellowish-brown colouration to these layers. The feldspar is randomly distributed throughout the snowflakes but in some displays a weak spherulitic texture. It is more abundant in these than in the snowflake of the massive varieties and may form as much as 85% of each patch.

The second layer-type (Plate 21C) is cryptocrystalline and composed of quartz and feldspar through which are distributed flakes of clay and a few discrete "snowflakes". Continuous, fine bands of colourless residual quartz conform to the overall banding in the rock.

The texture displayed by the groundmass is indicative of flow and suggests that the groundmass crystallized from a fluid medium rather than directly from a pyroclastic rock.

The perlitic rhyolites (Zone 2) overlie the banded rhyolites. The rocks are all porphyritic and the phenocrysts, except for the feldspars, are similar to those in the underlying rocks. The characteristics of the feldspars are:

a. Albite - fresh and partly altered, subhedral to anhedral, in places cumulophyric (e.g. Locality 200) and with lamella twinning. Some crystals are replaced by brown, feathery illite and colourless clay minerals (e.g. Locality 264). Albite is more common than in lower zones and may compose as much as 10% of a hand specimen.

b. Orthoclase Perthites - are generally less common than albite, subhedral to anhedral in shape and partly reddened and altered to fine-grained clay minerals.

c. Orthoclase Perthite Mantles - present on a few of the albite phenocrysts are reddened and partially replaced by clay.

The groundmass is characterised by the development of perlitic cracks delineated by dusty iron oxides and enclosing areas of microcrystalline, colourless quartz and/or faintly reddened potash feldspar. In some examples (e.g. Locality

264) the iron oxides are not abundant and the cracks are formed of microcrystalline quartz enclosing areas of feldspar. However, in others, (e.g. Locality 200) iron oxides are especially abundant and form large clots in the centre of the perlitic cracks.

One sample (Locality 238) is strongly amygdaloidal (Plate 21D). Most of the amygdules are sub-spherical to elliptical although completely irregular ones are found. The elongate or elliptical varieties tend to be sub-parallel. A selvedge of iron oxides encloses a crystalline core of colourless quartz. Clay minerals are disseminated along grain boundaries within the quartz mosaic of the core but more commonly are concentrated close to the rim of the amygdule. A few euhedral to subhedral apatite crystals are the only accessory minerals.

The presence of amygdules in this rock type is their lowermost appearance in the Formation (pЄal). The overlying member contains abundant amygdules.

In the east, the perlitic rhyolites display a variation of the texture described above (e.g. Localities 40, 235 and 72). They contain rounded lobate and irregular but globular-shaped particles which range up to 22 mm in diameter. The particles have a sharp margin discoloured by finely disseminated iron oxides. The main mass of the particles consists of a feathery mosaic of quartz crystals which include dusty opaques and cryptocrystalline, potash feldspar. The crystals of the mosaic are somewhat elongate and arranged parallel to their long axes; the cryptocrystalline inclusions also tend to be aligned in this direction. There is thus imported a weak structure which is not concordant with the overall habit of the particle. A few, but not all, of the particles contained subhedral to anhedral phenocrysts of quartz and feldspar.

Amygdaloidal Rhyolites (Zone 1) The amygdaloidal rhyolites have phenocrysts of feldspar and sinuous, disc-shaped and lenticular "amygdules" set in a fine-grained, massive, quartzo-feldspathic groundmass. A weak foliation

is imparted to the rock by the sub-parallel orientation of the long axes of the"amygdules".

The feldspar phenocrysts are both potash- and soda-rich. Most of the latter display lamella twinning. These albite phenocrysts (An_8Ab_{92}) range from euhedral to subhedral and some are glomeroporphyritic. The discrete phenocrysts (An_8Ab_{92}) range from euhedral to subhedral and some are glomeroporphyritic. The discrete phenocrysts have a size distribution in the range 0.4 to 2.2 mm; the cumulophyric crystal aggregates may reach 4 mm in diameter. Many of the albite crystals are deeply embayed with sieve-textured cores. The embayments are infilled with elements of the groundmass. The crystals are partially replaced by disseminated, colourless clay and fine-grained muscovite, or by a microcrystalline, granular aggregate of quartz crystals which penetrates along grain boundaries in the cumulophyric aggregates and along cleavage traces in some of the discrete phenocrysts. Disseminated iron oxides and micas are distributed throughout the quartz mosaic.

Potash feldspar phenocrysts are much less abundant than albite and were not found in some of the samples. The mineral is commonly twinned according to the Carlsbad Law and is reddened by finely disseminated iron oxides (?hematite) in contrast to the comparatively clear albite phenocrysts. It is orthoclase and (unlike those recorded from elsewhere) does not appear to be perthitic. In general it is somewhat less altered than the albite and nowhere was it seen to be embayed.

Pseudomorphs after primary ferromagnesian phenocrysts are found in a few samples (e.g. Locality 242B). These are usually closely associated with the albite phenocrysts, in particular with the glomeroporphyritic aggregates. The pseudomorphs are essentially a yellowish-green, faintly pleochroic chlorite, a similarly coloured although more highly birefringent platy mica, opaque minerals (iron oxides) and a little quartz. The pseudomorphs have a rounded habit, with iron oxides around the margins and as an irregular,

lacy network through the crystals. Others are composed of fine-grained aggregates of chlorite and coloured mica with or without a little quartz. Relict textures do not indicate the nature of the primary mineral phase but the replacement products suggest an iron and magnesium-rich silicate (?iron-rich pyroxene). These pseudomorphs form a minor component (less than 5%) of the whole.

Opaque minerals are common (about 5%) as ragged to sub-rounded and sub-hedral crystals, many of which are magnetite, partially oxidised. A few are now composed of leucoxene and probably represent primary titanomagnetite.

The groundmass and its relationship to the "amygdules" disclose the true nature of the rock. In the lower levels (e.g. Localities 242B, 277) the groundmass is composed of sub-rounded to sub-angular, equigranular and elongate fragments which have diameters ranging from 0.4 to 2 mm. The fragments are composed of a dense mass of cryptocrystalline and microcrystalline, massive and reddened potash feldspar and quartz. Very fine-grained iron oxides (?hematite) veneer the surface of the fragments and fine-grained particles are included within them. The quartz is stained a smoky-brown and the feldspar a somewhat deeper reddish-brown. The fragments are traversed by a network of convolute and spheroidal cooling cracks along which cryptocrystalline, colourless clay minerals have crystallized. The phenocryst phases are derived from the same source as the fragments and are either contained within fragments or have portions of the material composing the fragments adhering to their surfaces. The fragments are closely compacted and there is some evidence to indicate that they have undergone a degree of flattening, in the lower levels.

The "amygdules" occupy irregular interstitial areas between the fragments. When viewed in two dimensions these are triangular and star-shaped or sinuous and lenticular (Plate 22).

In the upper levels the groundmass is completely reconstituted and

PLATE 22 AMYGDALOIDAL RHYOLITE (pEal)

In the upper levels of the unit, the amygdules are triangular and star-shaped or sinuous in two dimensions. In three dimensions they are disc-shaped or lenticular.

The amygdules are formed of a rim of microcrystalline, radially disposed quartz and iron-oxides enclosing a poly-crystalline core of quartz. A few (plate 22B) have a crystal of carbonate in the core.

The framework is completely reconstituted but was formed of sub-rounded and sub-angular rock fragments (Plate 22C) with the amygdules infilling the irregular, interstitial areas between fragments.

A. Sample 151:XN x 10

B. Sample 151:PPL x 25

C. Sample 151:PPL x 32



A

B

PLATE 22.



C

provides no evidence as to the original nature of the rock (e.g. Locality 151). Here it is a homogeneous, intensely reddened mass of cryptocrystalline potash feldspar through which is distributed a little fine-grained, discoloured quartz. The "amygdules" resemble those found in the lower levels but the variety of shapes is perhaps lacking and their sub-parallel alignment more accentuated.

The "amygdules" attain a maximum diameter of about 7 to 8 mm but more usually are in the range 1 to 2 mm. In the lower levels, the rim or skin of the amygdule is formed of a pale yellowish-green, cryptocrystalline veneer of clay minerals radiating into a crystalline core of quartz, in the centre of which may be found numerous, fine-grained silicate inclusions. The junction between the clay minerals of the skin and the quartz of the core is sharp. In the upper levels, the "amygdules" are entirely colourless, microcrystalline quartz. The rims are formed of a microcrystalline aggregate of quartz crystals and the cores of coarser-grained, bladed crystals of quartz which tend to be directed towards the centres of the "amygdules". The quartz in most places and particularly at the margins is laced with shadowy, disseminated opaques directed in towards the core regions of the "amygdules".

The cores of a very few of the "amygdules" are lined by a thin veneer of orthoclase feldspar; some are formed of microcrystalline carbonate, and a few of the larger ones are empty but by far the majority are infilled with colourless, crystalline quartz.

5.8.3 Petrochemistry

Analyses of two Amygdaloidal Rhyolites are presented in Table 5. The analysed samples (from Localities A263 and A274) represent the massive porphyritic rhyolites (Zone 4) and the banded porphyritic rhyolites (Zone 3) of the middle member respectively.

An inspection of the analyses shows that the rocks are similar

chemically except that the banded rhyolite (A274) is significantly richer in soda than is the massive sample.

TABLE 5 AMYGDALOIDAL RHYOLITE (pEal)

Analysis, %			Norm, %		
	A263	A274		A263	A274
SiO_2	77.10	75.30	Q	56.16	44.46
Al_2O_3	13.30	12.90	Co	7.27	3.93
Fe_2O_3	0.66	0.60	Or	30.73	31.91
FeO	0.44	0.40	Ab	0.51	13.54
MnO	0.01	0.01	An	0.83	1.36
MgO	0.22	0.19	En	0.55	0.47
CaO	0.18	0.30	Mn	0.93	0.60
Na_2O	0.06	1.60	Il	0.34	0.47
K_2O	5.20	5.40	He	0.02	0.19
TiO_2	0.18	0.25	Ap	0.02	0.05
			Sub-Total	97.36	96.97
LOI*	1.69	2.20	LOI*	1.69	2.20
	99.05	99.17		99.05	99.17

*LOI - Loss on ignition.

It has been noted that the tuffaceous rocks of the Arc Structure are subject to potassium enrichment with concomitant loss of soda and the analysed samples provide some evidence for this alteration. It is worthy of note, though, that these samples are not as enriched in potash and that A274 shows little depletion in soda when compared with other tuffaceous samples from the Arc Structure. The larger soda component of Sample A274 produces a greater proportion of normative albite with a corresponding decrease in normative quartz compared to the normative figures for Sample A263.

The normative compositions are similar to the modes.

Although,on the basis of their overall mineralogy and textures, most of

the rocks of the Amygdaloidal Rhyolite Formation (pЄal) must be classified as rhyolites "sensuo-stricto", there is some textural evidence to indicate that the whole succession is the product of extreme welding and recrystallization of pyroclastic rocks.

5.9 Porphyritic Rhyolite ($p\text{Є}l_3$)

5.9.1 Field Observations

The Porphyritic Rhyolite ($p\text{Є}l_3$) outcrops in the three Regions of the Arc Structure and is one of the most extensive and persistent rock units (Map 1). In the Eastern and Central Regions the lower contact is comparatively sharp and can be delineated within an interval of 1 or 2 m. In the west, the contact is less well defined but can be recognized on the basis of colour change. The rock is buff to pale-brown, fawn or pink on a weathered surface and on a fresh surface is creamy-fawn to very pale pink.

The upper contact with the Vitric Tuffs (pЄvt) is clearly defined, and conformable. A Fluidal Banded Rhyolite (pЄfbl) is interbedded with the Porphyritic Rhyolites ($p\text{Є}l_3$).

The Porphyritic Rhyolite ($p\text{Є}l_3$) is heterogeneous but three broad groupings are recognized. Near the lower contact the rocks are massive, pale fawn to buff coloured and porphyritic. The phenocrysts are principally of feldspar and are comparatively small, anhedral and white in colour. Weathered surfaces are characterised by deep pits representing phenocrysts preferentially weathered from the aphanitic groundmass.

Banding becomes perceptible at progressively higher levels (Zone 2) in the Formation. In the lower part of Zone 2 sub-parallel streaks, which alternate with massive bands in the lower part, are unlike those usually characterising an eutaxitic texture in that they are continuous for several centimetres. The streaked and massive layers are about 1 cm thick. Further into the Zone the streakiness persists but extends throughout the whole

rock. The ultimate development of the banding is in the vicinity of the fluidal banded rocks where the banding forms comparatively broad, sub-parallel layers alternating in colours of fawn, cream and red.

The banding decreases in intensity to the north of the Fluidal Banded Rhyolite (pЄfbl), the rock grading into a breccia (Zone 1) comprised of dark green, grey and khaki-coloured rock fragments compacted in an aphantic groundmass. The breccia varies along strike and contains fragments which are identical to, and reflect variations in, the underlying rock. In most areas the fragments are massive but in some are weakly banded. They have a size distribution in the range 5 mm to less than 1 mm with the finer grain sizes predominating. The fragment to matrix ratio is in excess of 8:1. The overall colour of the rock is dark grey but locally fawn and pale-grey varieties are found.

Prominent joints are related to internal structures. Blocky jointing characterises the lower, massive levels of the Formation and this gradually changes to a flaggy form in the more strongly flow-banded rocks. The overlying breccia is broken by blocky jointing. In all cases the principal joint sets and internal structures strike east-west and dip steeply to the north. Internal flow folds are also characteristic (see discussion on Structure, Section 4.2.3).

5.9.2 Petrography

In thin section the rocks show some textural variation but the most extensive rock type (massive rhyolite) is unusually uniform in texture and composition.

Massive Porphyritic Phase (Zone 3) The rocks have phenocrysts of quartz (2-3%) and feldspar (5-8%) set in a massive, microcrystalline groundmass which displays the snowflake texture.

The quartz phenocrysts are euhedral to subhedral and form bipyramidal or terminated crystals, many of which have been partially modified by round-

ing and embayment. They have a size in the range 0.1 to 0.5 mm and a sporadic distribution.

Of the feldspar phenocrysts potash feldspar crystals are most common although a few albite crystals are found.

The potash feldspar (orthoclase) appears to have undergone little, if any, exsolution. The grains are broken relicts of untwinned, formerly euhedral crystals and are partially altered to clay.

The albite phenocrysts have a similar habit to that of the potash feldspar and are subject to similar, although less extensive, alteration. The crystals have lamella twinning and most are discrete crystals, although some are mantled with a potash feldspar; both feldspar phases have a size distribution in the range 0.2 to 0.8 mm.

A third phenocryst phase is anhedral and composed of micro- and cryptocrystalline sericite and clay with included small subhedral to euhedral crystals of colourless zircon and leucoxenised opaque mineral grains (Plate 23D). The secondary sericite and clay perhaps suggests former potash feldspar but the association of opaques and zircon (presumably early products of crystallization) suggests that the pseudomorphs may represent former ferromagnesian minerals. In either case the interpretation is unable to be confirmed.

In a few samples the feldspars exhibit a glomeroporphyritic texture. Potash feldspar and to a lesser extent albite are replaced by secondary iron oxides in a few samples.

In one sample (Locality 219) a few irregular fragments composed of a polycrystalline quartz mosaic could represent former, devitrified glass fragments.

Other phenocrysts, are subhedral, leucoxenized opaques (formerly ?ilmenite).

The groundmass is a microcrystalline mosaic of quartz crystals in which are set fine-grained subhedral (rarely euhdral) potash-feldspar (?orthoclase)

crystallites giving a "snowflake texture". A spherulitic variation is found at Locality 219 (Plate 23A, B, C). In places, the rocks are very weakly layered. Massive, fine-grained, snowflake textured layers alternate with others formed of spherulitic aggregates which vary in size. The cores of the spherulites have rounded crystal(s) of colourless quartz and these are surrounded by a feathery, subradiating mosaic of quartz crystals containing numerous potash feldspar crystallites, their alteration products and disseminated opaque minerals (iron oxides).

The spherulites range in size from 0.2 to 1 mm and are loosely packed in a cryptocrystalline groundmass of colourless clay (potash rich). The larger spherulites tend to be separated by fractures along which iron-oxides have crystallized.

The more massive layers resemble the spherulitic layers in mineralogy. They lack the spherulitic texture but, subparallel to the layering, contain small elliptical aggregates of colourless, microcrystalline quartz.

At Locality 225 the massive rhyolite (Zone3) contains bombs of rock similar to that of the enclosing groundmass (Plate 24). The bombs are spherical and range up to 12 cm in diameter. They are formed of a central, reddish-brown core about 5 cm in diameter and an outer zone (about 2 to 4 cm in thickness). The outer zone is macroscopically indistinguishable from the enclosing rock although in places a weak structure concentric with the core is developed. The reddened core is massive and contains small phenocrysts of quartz which are subhedral (high temperature?) embayed, and have a straight extinction, and potash feldspars which are untwinned and extensively replaced by sericitic micas. The groundmass of the core consists of reddened snowflakes (less than 0.1 mm), through which are distributed numerous spherical, colourless quartz crystals with undulose extinction. These crystals are distinct from the phenocrystic quartz and are characterised by ragged margins round which the snowflakes tend to be radially disposed.

PLATE 23 MASSIVE PORPHYRITIC RHYOLITE ($P\epsilon 1_3$)

A. Sample 219:PPL x 32

Spherulitic texture in massive phase of porphyritic rhyolite. The spherulite consists of a core of colourless quartz surrounded by a feathery, sub-radiating mosaic of microcrystalline quartz with abundant potash-feldspar crystallites, their alteration products and disseminated iron-oxides. Iron-oxides crystallize along parting fractures between spherulites.

B. Sample 219:XN x 32

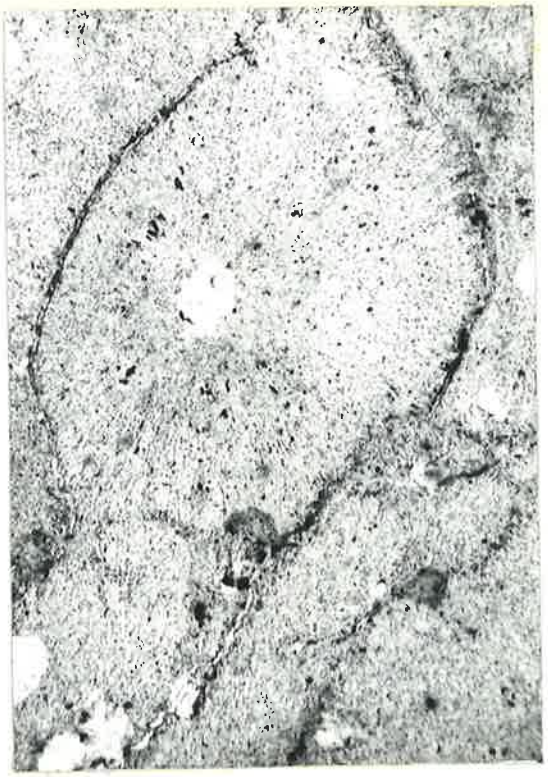
Same field of view as for Plate 12A viewed under doubly polarized light.

C. Sample 211:PPL x 32

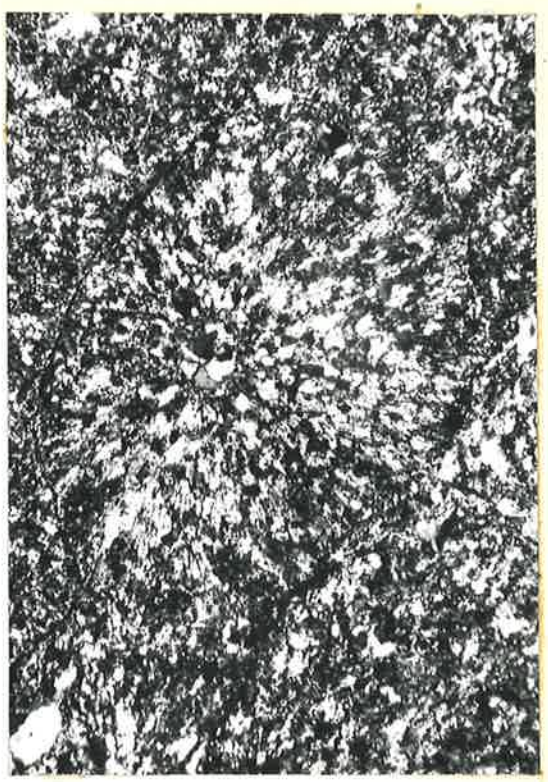
A layer of closely packed spherulites bounded by dense layers of similar mineralogy but lacking the distinctive texture. Shadowy relicts, possibly after former spherulites, can be seen in the dense layers (lower left) together with the quartz eyes (not seen).

D. Sample 254:PPL x 100

A skeletal crystal of titanomagnetite now replaced by ilmenite crystallizing along planes of octohedral symmetry in the primary crystal. The remainder is replaced by colourless, sericitic micas. The crystal is set in (visible) sericite, chlorite, iron-oxides and quartz.

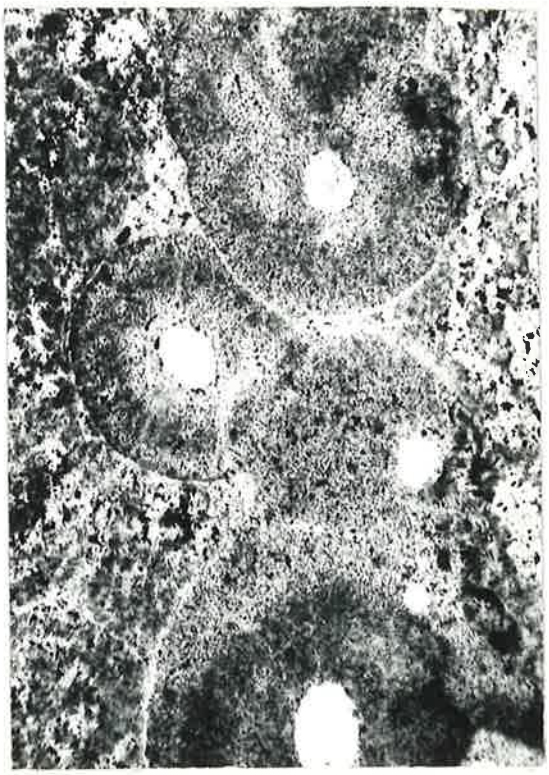


A



B

PLATE 23.



C



D

PLATE 24 PORPHYRITIC RHYOLITE ($p\epsilon l_3$)

A. Locality 225

Massive member of the Porphyritic Rhyolite ($p\epsilon l_3$) with bombs formed of rock similar to that of the host. A section through one bomb can be seen on the right side of the cluster of three in the centre of the plate. Note the sharp margin between the matrix and bomb and the central reddish-brown core.

B. Locality 311

Blocky Jointing in the massive member of the Porphyritic Rhyolite ($p\epsilon l_3$) near the contact with the Welded Tuff ($p\epsilon v_2$). The jointing is similar to that in the Welded Tuffs ($p\epsilon v$) but the unit is characterized by its buff rather than red colour and the lack of obvious phenocrysts.



A



B

PLATE 24.

The outer zone of the bombs is mineralogically similar to the core but differs in that the groundmass is formed of clusters and trains of microcrystalline quartz set in a cryptocrystalline, potash-rich groundmass. The quartz is discoloured by faint reddening which is much less marked than in the core. Numerous reddened spherulites distributed thoughout this groundmass are identical to those described from the massive member. The spherulites are in sharp contrast with the enclosing groundmass and are sized in the range 0.5 to 0.1 mm.

The rock enclosing the bombs is almost identical to their outer zone although the groundmass is somewhat coarser-grained. Small fragments which now have a spherulitic habit are abundant in the groundmass of the enclosing rock. The outer zone of the bomb is not a part of the bomb but is a chilled zone in the enclosing rock.

Banded Porphyritic Phase (Zone 2) The massive phase grades upwards into the banded phase which itself displays a gradation both across and along strike.

In the eastern portions of the Arc the rock is composed of randomly distributed phenocrysts of quartz and feldspar set in a microcrystalline, and in places spherulitic, banded groundmass.

The quartz phenocrysts vary from 1-8% by volume but no systematic variation has been found. Two types are recognized. The first, and least common, crystallized with an hexagonal symmetry suggesting high quartz. These crystals have straight extinction but show some evidence for rounding and embayment. The second type is elliptical to sub-circular in cross section and composed of either a single crystal or a mosaic of crystals each of which has a strongly undulose extinction. A few display a radial structure and some a concentric structure, but most are massive and tend to be preferentially concentrated into particular layers (e.g. Locality 211). In some areas they serve as nucleii to spherulites (e.g. Locality 212).

Feldspar phenocrysts have a random distribution and comprise some 5 to 10% of a hand specimen. No albite phenocrysts are recognized from the eastern outcrop. The potash feldspar phenocrysts are orthoclase and are altered in a similar way to those found in Zone 3 ($p\epsilon l_3$).

The groundmass consists of well defined layers from 0.2 to 1.5 mm in thickness. Texturally there are two layer types. One is a mosaic of intensely reddened feldspar crystals set in colourless, cryptocrystalline, clay minerals, and disseminated opaques. The feldspar in the other layer type is not reddened. In a few places the banding is defined by variations in the ratio of clay to feldspar.

Spherulites (as above) up to 1.0 mm in diameter are scattered though the groundmass. The only accessory minerals are euhedral to subhedral zircon and leucoxene. Zircon is colourless and leucoxene pseudomorphs a primary mineral phase (?ilmenite).

The banded phase of the Porphyritic Rhyolites ($p\epsilon l_3$) from the Central and Western Regions of the Arc Structure differs from that in the east; it resembles the massive porphyritic phase except for the banding.

The rocks are composed of phenocrysts of quartz and feldspar set in a microcrystalline groundmass with snowflake texture. Potash feldspar (orthoclase) is dominant. For the most part this mineral is partially to completely replaced by disseminated sericite and iron oxides (?hematite). Evidence for exsolution is lacking.

Mantle orthoclase is found surrounding a core composed entirely of micro- and crypto-crystalline sericite with a little quartz (Locality 254). Mantle feldspar indicates the rocks to be enriched in potash at a late stage in their crystallization and by analogy with other Formations suggests the core feldspar was albite.

The banding(Plate 25C & D) is formed by layers and elongate pods of polycrystalline, colourless quartz which are fine and discontinuous but with

PLATE 25 MASSIVE PORPHYRITIC RHYOLITE ($p\epsilon 1_3$)

A. Sample 254:PPL x 32

Structures inferred to form by viscous, fluid flow. An oblique section through a structure which takes the form of a crude cone composed of concentric semi-circles of reddened potash feldspar set in a microcrystalline groundmass of quartz and reddened, altered potash-feldspar. Layers of platy, residual quartz lie between the concentric bands. The structures are thought to form in a pressure shadow behind phenocrysts during fluid flow of a viscous medium.

B. Sample 254:XN x 32

Same field of view as for Plate 13A viewed under doubly polarized light.

C. Sample 189 :PPL x 100

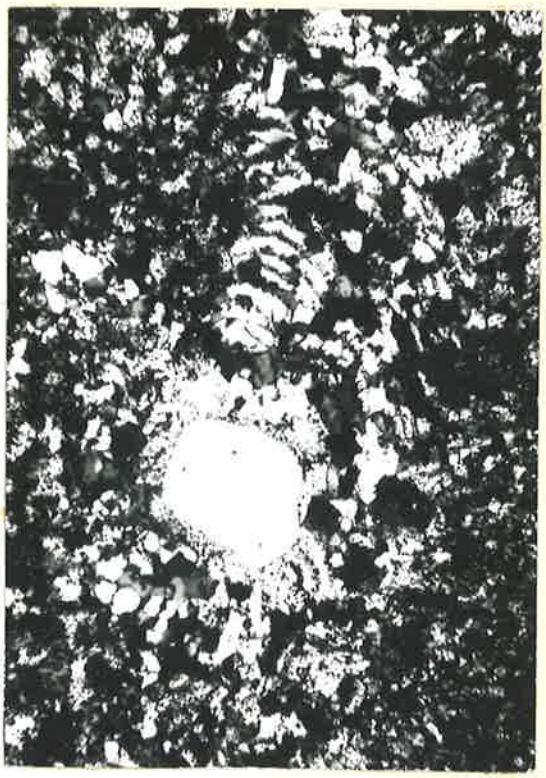
Rhythmic banding defined by discontinuous, but sub-parallel, layers of colourless quartz. The remainder of the groundmass is formed of minute snowflakes around which relatively coarse crystals of orthoclase feldspar form radially disposed overgrowths. An embayed crystal of high quartz with secondary quartz overgrowths is upper left.

D. Sample 189 :XN x 100

Same field of view as for Plate 13C viewed in doubly polarized light.



A

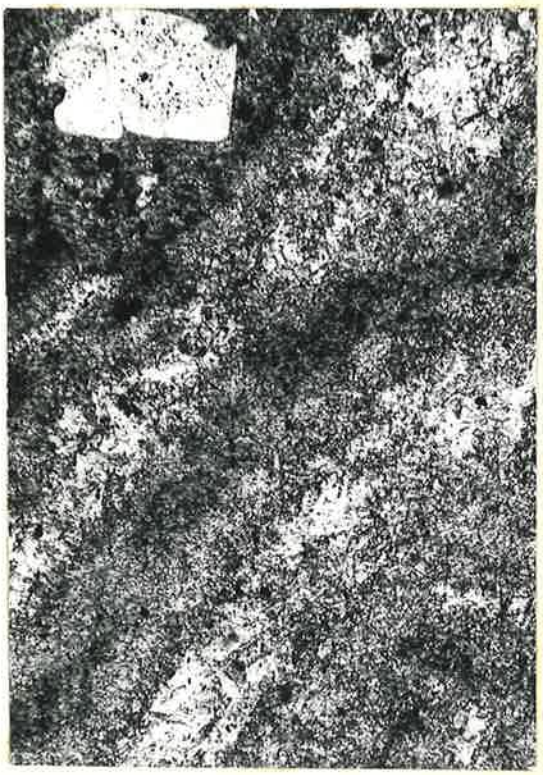


B

PLATE 25.



C



D

a sub-parallel disposition. Comparatively large crystallites of reddened potash feldspar (?orthoclase) form radially disposed overgrowths on snow-flakes in the intervening groundmass (e.g. Locality 252). The crystallites of these overgrowths penetrate and grow into the more quartzitic bands.

The layering is accentuated by varying degrees of reddening of the potash feldspar microlites.

A variation of this banded texture contains (e.g. Locality 254) structures which range to 1.55 mm in length and are formed of a series of concentric semi-circles, the diameters of which decrease in one direction (Plate 25A & B). In three dimensions each structure has the form of a crude cone and is composed of a polycrystalline mosaic of colourless quartz through which are distributed the concentric semi-circles, convex towards the apex of the cone. The semi-circular structures are composed of bands of cryptocrystalline, faintly reddened potash feldspar which bear no relationship to the residual quartz.

At another locality (Locality 312) the rock is closely jointed. Iron-rich solutions are introduced along the joint planes and replace much of the potash feldspar in the rock. The alteration penetrates to a depth of about 3 cm and iron oxides replace the potash feldspar of both the phenocrysts and the groundmass so that the rock becomes deep brick red in contrast to the usual grey and pale fawn.

Breccia Member (Zone 1) A typical rock is composed of a compact mass of rock fragments set in a small amount of fine-grained matrix. The rock fragments range up to 5 mm in diameter and exceed 95% of the whole rock.

Large, angular fragments enclosed by smaller, sub-angular to sub-rounded fragments may interlock. Textural variations along the strike of the underlying Porphyritic Rhyolites ($p\epsilon_1$3) tend to be paralleled by variation in the texture of the fragments in the breccia member.

The fragments contain a few phenocrysts of orthoclase and lesser albite,

PLATE 25a PORPHYRITIC RHYOLITE ($p\mathcal{E}l_z$)

A. Sample 148:PPL x 43

An euhedral crystal of former feldspar (?albite) now completely replaced by a mosaic of late-stage quartz. The rock is a crystallized and silicified vitric tuff.

B. Sample 148:XN x 43

Same field of view as for A above in doubly polarized light.

C. Sample 223:PPL x 10

Flow-top breccia composed of an interlocking mosaic of polygonal rock fragments of uniform composition.

D. Sample 223:XN x 35

Chilled margin to breccia fragment (diagonal across centre of photomicrograph) formed of an intergrowth of snowflakes perpendicular to the fragment wall in contrast to the normal, equigranular snowflake development in the centre of the fragment (upper left).



A

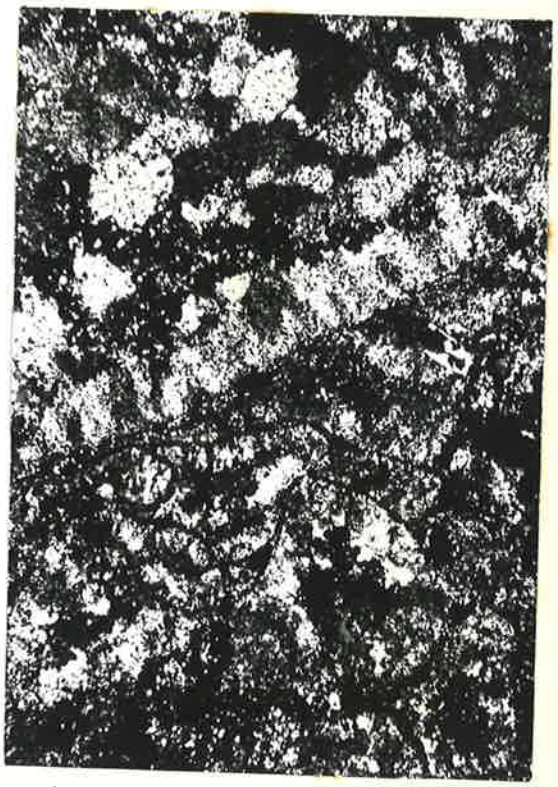


B

PLATE 25a



C



D

quartz and an unknown mineral completely pseudomorphed by sericitic micas.

The matrix of most fragments exhibits a modification of the snowflake texture. In some samples (e.g. Locality 223) disseminated iron oxides partly replace the included feldspar. For the most part the snowflakes of the fragment margins are smaller than those of the central regions and radially disposed for a distance of about 0.2 mm in from the margins. A fine veneer of dusty iron oxides (?hematite) is concentrated along the outer surface of the fragment.

Some fragments display banding due to:

a. segregation of residual quartz into sub-parallel layers;

b. preferential reddening of alternate layers of snowflakes; and

c. parallel layering of very fine-grained orthoclase crystallites within and between adjacent snowflakes.

The matrix between the rock fragments is mineralogically identical to that of the fragments, viz quartz enclosing reddened potash feldspars which are partially replaced by dusty opaques.

In some specimens (e.g. Locality 223), a few of the rock fragments are partly replaced by late-stage colourless quartz. The replacement quartz occurs in the core regions of the fragments and is accompanied by minor clay minerals.

The rock has been welded to a certain extent. In a few places pressure applied to the fragmental rock has resulted in the penetration of the sharp edge of one fragment into the flat surface of another. In other cases it can be shown that pressure on one fragment has resulted in the bending of a second. Devitrification has occurred after brecciation.

5.9.3 Petrochemistry

Three samples of the Porphyritic Rhyolites (pGl_3) were chemically analysed. The results together with the recalculated CIPW molecular norms are presented in Table 6(Page 113). The samples were collected from Localities

A253, A292 and A311.

TABLE 6 PORPHYRITIC RHYOLITE (pGl_3)

Chemical Analyses, %				CIPW Normative Analyses, %			
	A253	A292	A311		A253	A292	A311
SiO_2	76.40	76.60	75.40	Q	53.22	59.79	46.60
Al_2O_3	12.70	13.10	12.90	Co	5.98	8.23	4.66
Fe_2O_3	0.72	0.72	0.84	Or	34.28	23.64	31 91
FeO	0.48	0.48	0.56	Ab	0.51	0.51	11.00
MnO	0.01	0.01	0.06	An	0.94	1.19	0.70
MgO	0.15	0.43	0.18	En	0.37	1.07	0.45
CaO	0.23	0.28	0.18	Mn	0.80	0.51	0.90
Na_2O	0.06	0.06	1.30	Il	0.51	0.70	0.72
K_2O	5.80	4.00	5.40	He	0.17	0.37	0.22
TiO_2	0.27	0.37	0.38	Ap	0.07	0.07	0.07
P_2O_5	0.03	0.03	0.03	Sub-total	96.85	96.08	97.23
LOI*	2.35	3.65	2.00	LOI*	2.35	3.65	2.00
	99.20	99.73	99.23		99.20	99.73	99.23

* LOI - Loss on ignition.

Sample 311 (massive member) is formed of phenocrysts of quartz and altered feldspar set in a massive groundmass which displays snowflake texture. The feldspar phenocrysts include orthoclase, orthoclase microperthite and lesser albite. Alteration of both the potash-rich and soda-rich feldspars is to sericite, clay and quartz. The presence of microperthite renders the rock somewhat unusual. A third relict phenocryst phase is now composed wholly of colourless sericite and minor muscovite. Accessory crystals of colourless zircon and honey-coloured rutile, leucoxene and iron oxides are included within or associated with the sericite pseudomorphs. In a few places sericitic pseudomorphs are found in intimate association with feldspars. The groundmass of Sample A311 is composed of a polycrystalline mosaic of quartz in which are included numerous crypto- and micro-crystalline potash

feldspar crystallites.

The analysis of Sample A311 does not differ significantly from those of the tuffaceous rocks analysed from the Arc Structure. The abundance of quartz as phenocrysts and in the groundmass is reflected in the high silica and quartz of the analysis and norm respectively. Soda is comparatively high at 1.3% and is manifested in modal albite and orthoclase microperthite phenocrysts. Potash feldspars, however, comprise the major proportion of the feldspar in the total rock as indicated by the high potash (5.40%) of the analysis. The total alkali content of 6.70% is somewhat higher than that for the other two analyses (Table 6) and this is reflected in the high orthoclase and albite and comparatively low quartz and corundum values of the norm of Sample A311.

The low lime percentage is expressed by the absence of calcic feldspars and ferromagnesian minerals. Most of the normative anorthite is presumably contained in the albite phenocrysts though some may be in the clay alteration products. Low magnesia is reflected by minor, normative metasilicates representing modal alteration products. The titanium content of the analysis and ilmenite value in the norm can be directly related to the modal rutile and leucoxene. However, the high magnetite and comparatively low hematite values of the norm appear anomalous. Little magnetite is apparent in the thin section examined, whereas hematite is comparatively abundant. It appears as if the analyses for ferric and ferrous iron could be in error, although the value for total iron is probably of the correct order.

Sample A292 is a distinctive variety of the massive member(Zone 3) of the Porphyritic Rhyolites. It is composed of phenocrysts of feldspar and quartz set in a microcrystalline groundmass composed of quartz and potash feldspar with relict, perlitic cracking. The feldspar phenocrysts are intensely altered and only a few crystals could be identified as potash-rich. The feldspars are substantially replaced by a cryptocrystalline, colourless to

pale-green chlorite. Lesser amounts of quartz and colourless sericitic micas form along fractures and cleavage traces of the parent crystal.

The texture of the groundmass is controlled to a large extent by the perlitic cracking. The convolute and spheroidal cracks are delineated by accumulations of very finely divided opaque and clay minerals. A devitrified, polycrystalline mosaic of microcrystalline quartz is superimposed on, and thus post-dates, the system of cracks. The quartz is pale smoky-brown and includes potash feldspar and opaque phases. The interstitial areas, enclosed by the cracks, are infilled with a cryptocrystalline (potash-rich) colourless clay. Leucoxenised ilmenite crystals and colourless zircon crystals complete the mineral assemblage.

The chemical analysis of A292 resembles that of A311. The replacement of feldspar by chlorite rather than by potash-rich clay is reflected in the higher magnesia and the lower potash of the analysis and the higher enstatite and lower orthoclase of the norm. The lower soda content of 0.06% is reflected in the absence (apparent elimination) of modal albite and the low albite of the norm. The relatively low total alkali content and correspondingly low values for the normative feldspars is reflected in the increased normative quartz and corundum. No significance can be attached to the variations of other elements in Samples A292 and A311.

Sample A253 is representative of the banded phase (Zone 2). The analysis is again very similar to the foregoing and is almost identical with that of Sample A292 with the exception of the magnesia and alkali contents. Soda, and hence normative albite, is very low because of the almost complete elimination of modal albite. Feldspar phenocrysts are replaced by sericite rather than chlorite, corresponding to lower magnesia and at least in part, the higher potash.

Potash enrichment and soda depletion, apparent from a study of the thin sections of the tuffaceous rocks of the Arc Structure and substantiated by the above analyses, would appear to be accompanied by the migration of other ions.

5.10 Fluidal Banded Porphyritic Rhyolite (pGfb1)

5.10.1 Field Observations

The Fluidal Banded Porphyritic Rhyolites (pGfb1) are interbedded with the Porphyritic Rhyolites ($pG1_3$).

The Formation is poorly exposed. The rocks dip at a steep angle to the north (80 to 85 degrees) and are characterised by the development of a closely spaced flaggy jointing which is parallel to flow layering (see discussion on structure Section 4.2.1).

On a weathered surface the rock is pale reddish-brown with the flow banding clearly defined by differential weathering. The Zone 2 rocks have a spectacular appearance on a fresh surface with numerous phenocrysts of pale pink to red feldspar (about 30% by volume) set, with a few quartz crystals, in a strongly banded, vari-coloured groundmass. Bands are dark bottle green or deep brick-red alternating with white or cream layers. These colour differences are thought due to different oxidation states of the combined iron. The phenocrysts range in size from 6 to 2 mm and are subhedral to anhedral. Small, brick red, microcrystalline, spherulitic structures adhere to a few crystals. The laminae in the groundmass vary from less than 1 mm to 5 mm in width. The broader laminae are continuous over considerable distances although within them a subtle streakiness may

be evident. Rotation of the phenocrysts and contortion of the banding about phenocrysts is everywhere evident. Some of the laminar structures result from lateral compression.

The upper surface is composed of a blocky breccia (Zone 1) sporadically distributed. Sharply angular, banded fragments range to 7 cm in diameter and are set in an aphanitic, banded groundmass. In places the breccia fragments resemble the non-brecciated lower horizons and comprise more than 80% of the rock (e.g. Locality 218). Elsewhere (e.g. Locality 42) the upper surface resembles the brecciated top of the Porphyritic Rhyolite ($p\epsilon 1_1$) being formed of a crust of sub-spherical, globular shapes up to 2 cm in diameter. The upper surface of the globules is smooth and convex but the underside is indistinct and grades into the lava proper. A few globules are infilled with secondary quartz and probably represent bubbles formed by the rise of volatiles to the top of the flow.

Minor folding within the unit is related to flow rather than to tectonism.

5.10.2 Petrography

A typical rock from Zone 2 ($p\epsilon fb1$) is composed of phenocrysts of quartz (1%), potash feldspar (10%) and plagioclase (6%) set in a fluidal-banded groundmass.

Quartz crystals (0.1 to 0.5 mm) (e.g. Localities 262 213 and 129) possess the hexagonal symmetry of high quartz. Most crystals are modified somewhat by rounding and a few are deeply embayed. The quartz is water clear although traversed by minor fractures.

Potash feldspar and plagioclase phenocrysts are subhedral to anhedral, and range from 7 to 0.5 mm. The plagioclase (e.g. Locality 262) is albite ($Ab_{93}An_7$) with lamella twinning. Some sections are microantiperthite but this is not general; most include late-stage quartz patchily aligned along crystallographic directions of the host. The feathered terminations of these inclusions (less than 0.1 mm) indicate that they are due to replacement and are not poikilitic inclusions. Small flakes of colourless, sericite and finely disseminated opaques form minute inclusions.

The potash feldspar forms discrete subhedral to anhedral crystals, which are untwinned and faint to deeply reddened by disseminated ?hematite in contrast to the usually colourless sodic-plagioclase crystals. These potash feldspars grade from crypto-perthitic (e.g. Locality 262) to quite coarsely perthitic (e.g. Locality 213). The crypto-perthites can be recognized by the presence of an uneven or patchy extinction. The perthitic varieties contain numerous equigranular, patchy inclusions of sodic-feldspar exsolved parallel to 010 in the host.

Mantled plagioclase crystals are common. The plagioclase host-crystal is rounded and embayed and surrounded by a complete, or incomplete, potash-feldspar corona. In some cases the potash feldspar corona is one crystal containing the parent grain but more usually it forms as a series of interlocking, small crystals. Where the mantle is continuous it assumes a tabular habit of potash-feldspar and does not conform with the habit of the parent crystal.

A second generation potassic feldspar also forms a mantle to a few of the primary potash feldspar crystals. The relationships of the mantle to the host is similar to that described above for plagioclase.

Both the discrete potash feldspar and the mantle feldspar appear to be similar in composition. The large optic axial angle and the extinction angle on (010) of about 8 degrees indicates the mineral to be orthoclase. Both forms are perthitic.

Both types of orthoclase are partially replaced by quartz and in some instances the alteration was initiated along small fractures and cracks. Where the alteration is more intense, cryptocrystalline clay minerals (potash-rich) crystallize. In some rocks the crystals are traversed by a fine network of fractures containing iron oxides. In a few samples (e.g. Locality 213) barite crystallizes as ragged crystals in the core regions of the partly altered orthoclase.

Scattered through the rock in varying proportions are spherulites (e.g. Localities 213 and 128) about which the flow layering is accommodated. They may occur alone or bonded together in a complex aggregate. Each is formed of a core of colourless quartz from which radiates a polygonal mosaic of quartz crystals with included disseminated opaques and cryptocrystalline potash feldspar. Some of the spherulites have a weak concentric zonation defined by variations in the grain size of the microcrystalline quartz mosaic. The individual spherulites range in size from 0.25 to 0.1 mm but the aggregates may range up to 2 mm. Spherulites are also found adhering to and binding together quartz and feldspar phenocrysts indicating that some at least of the phenocrysts are related to the spherulites.

The groundmass has a strong fluidal structure and a general, tabular foliation defined by a series of segregated layers of quartz and potash feldspar in vari-coloured laminae 0.1 to 2 mm thick. The layers are distorted into flow folds around solid phenocrysts and spherulites (Plate 26A & B). Most quartz layers are discoloured to a pale yellowish-brown and the feldspar to a deep reddish-brown or dark green by disseminated iron oxides.

PLATE 26 FLUIDAL BANDED RHYOLITE (pЄfb1)

A. Sample 262:PPL x 35

Spherulites formed about a mass of cryptocrystalline quartz and feldspar with minor microcrystalline quartz. Particles such as these are thought to represent recrystallized rock fragments. Note the way the general tabular-foliation of the flow-banding has been distorted into flow folds about the spherulitic particles suggesting a solid mass in a fluid medium.

B. Sample 262:XN x 35

Same field of view as for Plate 15A viewed in doubly polarized light. The spherulites are composed of a polycrystalline mosaic of quartz included with abundant, reddened microlites of potash feldspar. Note the details of the flow texture and its continuity.

C. Sample 217:PPL x 10

Intermediate stage in the development of the optimum fluidal-banding texture. Quartz (colourless) and feldspar (dark) segregate into the planes of laminar flow during devitrification. Fine spherulites are present in the feldspar-rich layers.

D. Sample 110:XN x 32

Details of flow texture showing the segregation of quartz from felsic phases. The feldspar (dark) is altered to clay and discoloured by iron oxides. The quartz forms sheet-like, planar structures formed of a polycrystalline mosaic. The continuity suggests fluid flow rather than intense welding of a vitroclastic rock.



A



B

PLATE 26.



C



D

The narrow quartz layers are formed of tabular quartz crystals elongate parallel to the layering (Plate 26D), whereas the wider layers are formed of a microcrystalline aggregate of crystals elongate transverse to the layering. The feldspar-rich layers are generally of a finer grain than the quartz-rich layers. They are composed of a mosaic of reddened orthoclase crystals which tend to be equigranular but in places are elongate parallel to the layering. The feldspar is partially replaced by sericite which is streaked in the plane of the layering.

Less commonly (e.g. Locality 110) the quartz crystals of the quartz-rich layers accompany rounded to ragged clots of cryptocrystalline, colourless ?illite and the feldspar-rich layers are streaked with lens-like bodies of quartz. One unusual example (Locality 129) is even more atypical in that the banding is defined by sub-parallel "trains" of disseminated opaques which are continuous across crystal boundaries and even across quartz-rich and feldspar-rich aggregates. At Locality 129 late stage,fibrous muscovite is strongly developed parallel to the flow layering.

In some areas (e.g. Locality 217) a system of poorly preserved, spheroidal, cooling cracks is superimposed on the fluidal banding.

Euhedral crystals of colourless zircon, microcrystalline aggregates of honey-coloured rutile and euhedral to subhedral leucoxene pseudomorphs (after ?ilmenite) are accessory.

At the surface of the flow a lava breccia (Zone 1) (e.g. Locality 218) consists of blocky, sharply angular fragments up to 5 cm in diameter. It appears as if the rock was in a plastic state at the time of deformation because the fluidal banding is deformed and bent in the direction of displacement at the margins of some fragments. The fragments are embedded in a mass of cryptocrystalline potash feldspar in which are set numerous, disseminated opaques. In places this feldspar is partly replaced by cryptocrystalline clay.

5.10.3 Petrochemistry

Two samples from Localities 202 and 262 were chemically analysed (Table 7). The sample from Locality 202 was analysed by conventional techniques and that from Locality 262 was analysed on a Direct Reading Emission Spectrograph.

In thin section the rocks resemble those described above. Sample A262 is characterised by the comparative absence of disseminated iron oxides and by a relict texture of perlitic cracking superimposed on the fluidal banded groundmass. Sample A202 is characterised by an abundance of iron oxides disseminated through the feldspar rich layers of the groundmass.

TABLE 7 FLUIDAL BANDED RHYOLITE (pЄfb1)

	Analysis, %			CIPW Norm, %	
	A202	A262		A202	A262
SiO_2	72.60	74.90	Q	40.30	47.99
Al_2O_3	13.60	12.80	Co	4.52	5.07
Fe_2O_3	1.97	0.96	Z	0.10	-
FeO	0.71	0.64	Or	44.62	34.87
MnO	0.02	0.01	Ab	4.18	4.48
MgO	0.26	0.43	An	0.25	1.29
CaO	0.10	0.30	Ha	0.05	-
Na_2O	0.52	0.53	En	0.65	1.07
K_2O	7.55	5.90	Fs	-	0.10
TiO_2	0.38	0.18	Mn	1.25	1.39
P_2O_5	0.03	0.03	Il	0.72	0.34
ZrO_2	0.07	nd(a)	He	0.78	-
BaO	0.01	nd	Ap	0.07	0.07
CO_2	0.01	nd	Py	0.02	-
H_2O^+	1.65	nd	Ca	0.02	-
H_2O^-	0.65	nd	Sub-total	97.53	96.68
Cl	0.03	nd	H_2O	2.21	-
SO_3	0.03	nd	LOI	-	3.60
LOI (b)	-	3.60		-	-
	99.77	100.28		99.74	100.28

(a) nd - Not determined

(b) LOI - Loss on ignition

An inspection of the chemical analyses and the norms shows the rocks to be broadly similar and to resemble other tuffaceous rocks and lavas from the Arc, particularly in the alkali distribution. The analysis and norm of A202 differ from those of A262 in that quartz is present in slightly smaller proportions, the iron oxides and corresponding normative minerals are more abundant and the enrichment in potash is somewhat greater. These differences in chemistry are readily discerned in thin section and to a lesser extent in hand specimen.

5.11 Vitric Tuff (pЄvt)

5.11.1 Field Observations

The Vitric Tuff is better exposed than most units because its fine-grained, massive character, renders it comparatively resistant to weathering. The unit often crops out as a jumbled, blocky mass of rock, much of which is not in situ (Plate 27). The blocks are formed by a rectilinear, blocky joint system, the sets of which trend east-west and north-south. The unit lenses along strike appreciably but has an average thickness of about 15 m.

The rock is massive, aphanitic and composed of a few crystal and rock fragments set in a fine-grained matrix. Shards can be distinguished in some specimens but for the most part components of the groundmass cannot be differentiated. The freshest rocks are mid- to light-grey in colour but where chemical weathering is advanced, the rock assumes a pink to brick-red coloration. They are almost indistinguishable from recrystallized, sedimentary quartzites.

Rock fragments are uncommon. Most are small (less than 2 mm) with rare fragments up to 10 mm. The fragments are reddish-brown, fine-grained and rhyolitic. Crystal fragments of quartz and feldspar up to 3 mm in diameter are more common but still not abundant.

PLATE 27 VITRIC TUFF ($p\epsilon vt$)

A. Locality U187

A typical outcrop of vitric tuff formed of a jumbled, blocky mass of rock much of which is not in-situ. The blocks form along a rectilinear joint system (middle left). In the background (view looking south) is the typical development of spinifex over the massive red welded tuffs ($p\epsilon v_1$, $p\epsilon v_2$).



PLATE 27.

PLATE 28 VITRIC TUFF (pЄvt)

A. Sample 304:PPL x 35

Pyroclastic texture in vitric tuff. Shard shapes are set in a microcrystalline matrix of quartz and potash feldspar both of which are discoloured by disseminated iron oxides. Iron ocides concentrate about the margins of the shards.

B. Sample 304:XN x 35

Same field of view as for Plate 17A viewed in doubly polarized light. The cores of the shards are formed of microcrystalline, colourless quartz which also forms throughout the matrix.

C. Sample 44:PPL x 35

A pseudomorphed phenocryst of feldspar set in a micro-crystalline matrix in which former shards are weakly preserved.

D. Sample 44:XN x 35

Same field of view as for Plate 17C viewed in doubly polarized light. The former feldspar phenocryst is replaced by a microcrystalline granular aggregate of quartz and its outline is preserved by a veneer of iron-oxides. The matrix is composed of a somewhat coarser grained polycrystalline mosaic of quartz dusted with iron-oxides and sericite.

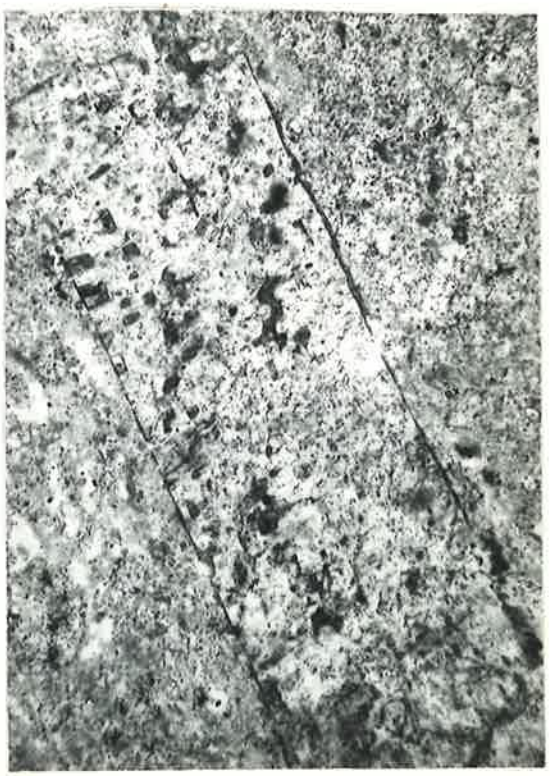


A

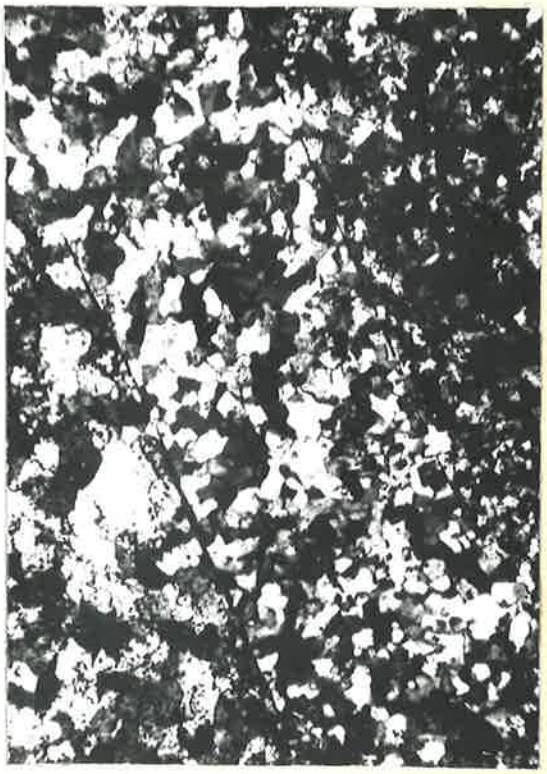


B

PLATE 28.



C



Irregularly disposed veinlets of late, white quartz up to 5 mm in width are common.

5.11.2 Petrography

The best preserved samples (e.g. Localities 148, 187 and 304) contain a few rock and crystal fragments, and numerous elongate, sinuous and cusp-shaped shards randomly distributed in a microcrystalline groundmass.

Crystal fragments (both quartz and feldspar) have a random distribution and seldom comprise more than 5% of the rock. The quartz crystals are clear, have a size distribution in the range 0.8 to 0.2 mm are rounded to sub-rounded or fragmental in habit and display sharp margins about which a fine veneer of disseminated and dusty opaques has collected. In many places the quartz crystals are surrounded by a corona of varying width ranging up to 0.5 mm, formed of sub-radiating quartz needles which have nucleated from the surrounding groundmass and crystallized in optical continuity with the parent crystal.

Both potash- and soda-rich feldspar crystal fragments (1.0 to 0.4 mm) are randomly distributed. Nearly all of the orthoclase is partially replaced by a mosaic of microcrystalline quartz, disseminated opaques and clay but what remains is perthitic and retains some crystal faces, the most distinctive being the (010) pinacoid. The perthites are of the patch type and the blebs are sporadically distributed through the crystal, which is usually clouded with iron oxides (?hematite). All crystals are fractured. The replacing quartz mosaic commonly extends beyond the margins of the parent crystal whose outline is clearly preserved,as with the quartz,by a selvedge of disseminated opaque minerals (Plate 28C & D) and microcrystalline clay. Barite is also a replacement product (Localities 256 and 305) and forms large (up to 0.4 mm), clear crystals with a ragged habit and perfect

cleavages parallel to (110) and (001). The crystals are confined to the core regions of the altered orthoclase.

Albite is a little less common than orthoclase. The fragments are completely shattered relicts of larger crystals. They have lamella twinning and less commonly Carlsbad twinning and the optic axial angles of two separate crystals were measured as 75 and 76 degrees indicating a composition of about $Ab_{95}An_5$. Many of the crystals are partially replaced by a quartz mosaic similar to that replacing the orthoclase crystal fragments but in general this feature is less well developed in the albite fragments. Barite was not found as a replacement product of albite.

Rock fragments are not common (3-4%). The most common is partially to completely collapsed pumice less than 0.8 mm in size. The pumice is formed of tubular pores (infilled with microcrystalline quartz elongate parallel to the pore walls) with walls of reddened, cryptocrystalline, potash feldspar (?orthoclase) partly replaced by a colourless clay (?illite). Small reddened, rhyolitic fragments with various textures are rare and cannot be used to characterise the unit.

The fine-grained base of the vitric tuffs is formed of a densely compacted aggregate of shard shapes. The degree of preservation of the shards is variable and ranges from well preserved (e.g. Localities 148 187 and 304) to poorly preserved and almost non-recognisable (e.g. Localities 210 255 and 310). The shards range from lune-shaped, to Y-shaped crescentic, elongate and splintered fragments. There is some evidence that the size of the shards decreases upwards through the unit from 0.3 to 0.5 mm at the base to about 0.1 to 0.3 mm at the surface.

Where the shard shapes are recognizable two principle types are present. In one the shard shapes are clearly outlined by a rim of disseminated opaques (Plate 28A & B) which surrounds a core of colourless potassium-rich, fibrous clay (?illite). In the other a mosaic of quartz crystals is

continuous across most inferred boundaries of the shards. The matrix is a massive, microcrystalline mosaic of quartz and potash feldspar (?orthoclase), dusted with disseminated opaque minerals. Potash feldspar tends to be replaced by fine clay and sericite.

With more complete devitrification the whole rock becomes a granular mosaic of microcrystalline quartz through which are distributed finely disseminated interstitial opaques and clay minerals (sericite/illite), though close inspection may reveal areas with few opaques, reflecting the former presence of shard shapes.

Where better preserved (e.g. Locality 98) the shards are distinguished from the matrix by the absence of potash feldspar.

In the eastern outcrops of the Formation there are a few, ragged, amygdule-like structures (e.g. Locality 44) whose rims have been obliterated by recrystallization. What appears to be the amygdule infilling is composed of a mass of feathery, reddened, alkali feldspar (?orthoclase) crystals radiating out from a core formed of a comparatively coarse-grained (up to 0.6 mm) mosaic of quartz through which are distributed small crystals of potash- and soda-feldspar (microchemical staining)

Sub-rounded to rounded leucoxenised opaque mineral grains (?ilmenite) disseminated opaques, and rare, colourless zircon crystals are accessory.

The rock is traversed by a series of discontinuous and irregularly disposed veinlets, which range to 2 cm but more usually are of the order of millimetres in width They are composed of a mosaic of quartz individual crystals of which extend into the tuff. In contrast to the groundmass quartz, the vein quartz is almost devoid of disseminated opaques and clay minerals.

Shards at the base of the Vitric Tuff Formation show minor distortion and flattening which is not visible in the upper horizons (e.g. Locality 44). Feldspar crystal fragments are better preserved in the east (e.g. Locality 44) than they are in the west where replacement by quartz and barite is widespread (Locality 155).

5.11.3 Petrochemistry

Two samples from Localities 304 and 260 which are representative of these rocks, have been analysed. The results are presented in Table 8.

TABLE 8 VITRIC TUFF (pEvt)

	Analysis %			CIPW Norm %	
	A304	A260		A304	A260
SiO_2	81.90	77.5	Q	68.21	54.63
Al_2O_3	8.60	12.6	Co	4.50	6.02
Fe_2O_3	0.60	0.84	Or	18.91	33.10
FeO	0.40	0.56	Ab	0.68	0.93
MnO	0.01	0.08	An	1.37	0.91
MgO	0.26	0.22	En	0.65	0.55
CaO	0.29	0.21	Fs	0.00	0.17
Na_2O	0.08	0.11	Mn	0.71	1.22
K_2O	3.20	5.60	Il	0.40	0.36
TiO_2	0.21	0.19	He	0.11	-
P_2O_5	0.01	0.02	Ap	0.02	-
LOI*	3.85	2.10	Sub-total	95.56	97.93
	99.41	100.03	LOI*	3.85	2.10
	-	-		99.41	100.03

* LOI - Loss on ignition.

Sample 304 represents the variety of Vitric Tuff in which shards are clearly recognized and which has been subjected to enrichment in silica.

The abundance of quartz and potash feldspar in Sample 304 is reflected in the high normative quartz and orthoclase. The low albite of the norm reflects the absence of soda-rich feldspar and the virtual absence of soda in the alkali feldspar. The rock is enriched in potash relative to soda. The anorthite content of the norm is at first sight anomalous. The only mineral phase which could contain calcium is the clay mineral illite. Kerr and Pill (1950) record an illite containing 1.59% CaO and other workers have reported illites with lime contents ranging up to this value. It seems probable, therefore, that nearly all the anorthite plus metasilicates of the norm are combined in the clay. The modal proportions of opaque minerals equate approximately with the iron oxides and ilmenite recorded in the norm.

Sample 260 differs from 304 in that there is less silica enrichment and more potash enrichment in the former. In addition Sample 260 is welded, a feature not recognized in 304. Whereas in the latter the shards are composed of a mass of microcrystalline quartz the majority in Sample 260 are composed of a felted mat of cryptocrystalline, colourless clay. The groundmass is composed essentially of altered potash feldspar with a little quartz. These differences in mineralogy are reflected in the norms and especially in the values of normative quartz and orthoclase. Post magmatic potash and silica enrichment has taken place in this unit and this enrichment is accompanied by migration of soda from the system.

5.12 Welded Lithic Tuff (pЄwt)

5.12.1 Field Observations

The Welded Lithic Tuff (pЄwt) conformably overlies the Vitric Tuff

($p\epsilon vt$). Although the lower contact is concealed beneath outwash channels, and the upper contact is ill-defined, the unit is moderately well exposed. Characteristic is a pronounced eutaxitic foliation due to intense welding and flattening of glass shards. The rocks are closely jointed and this structure is often related to the eutaxitic foliation.

The eutaxitic texture gradually lessens to the north where the rock grades into the massive, red, Welded Tuff ($p\epsilon v_3$). The upper contact is taken to be the point at which the eutaxitic texture can no longer be recognised in hand specimen, a textural change which is most consistent and definitive. It is usually accompanied by a colour change from multi-coloured greys, blacks and reds to the homogeneous brick-red of the overlying tuff.

Feldspar crystal fragments range up to 4 mm in diameter and compose some 15% of the coarser-grained fragmental material. The crystals are equigranular or splinter-shaped and are colourless or white and pink. Quartz crystals are much less abundant than the feldspar crystals and usually finer-grained and splinter-shaped.

Rock fragments compose 40 to 50% of the rock. They seldom exceed 15 mm in diameter and the most common size range is 5 to 10 mm; they are reddish-brown or pale brown, usually porphyritic and commonly display flow banding.

Rock fragments gradually decrease in abundance upwards until they are exceeded by the crystal fragments. Rock fragments are not found at all in the overlying Welded Tuff ($p\epsilon v_3$).

The Formation ($p\epsilon wt$) has been subjected to minor folding in the easterly outcrops. The eutaxitic or compaction foliation consistently strikes in an east-west direction and dips steeply to the north.

5.12.2 Petrography

Quartz crystal fragments (e.g. Localities 48, 209 and 222) average 0.5

to 0.1 mm but in some areas (e.g. Locality 222) range up to 5 mm. Most crystals, although somewhat rounded, have a roughly rectangular cross section or display the bipyramidal hexagonal symmetry of high quartz. A few of the more complete fragments are deeply embayed. Many are mantled by a corona of quartz (e.g. Localities 150, 289 and 258) that has crystallized from the surrounding groundmass in optical continuity with the parent crystal. The corona seldom extends more than 0.2 mm and is separated from the parent by a veneer of opaques. The corona can be further distinguished by means of its faint smoky colouration which contrasts with the crystal clear, parent quartz.

Feldspar crystal fragments are not common (less than 5%). Orthoclase is recognized by its optical properties and distinctive crystal faces but is extensively altered to microcrystalline, fibrous, clay (?illite) and strongly reddened by iron oxides (?hematite). Some crystal fragments are partially replaced by remobilised opaques (massive hematite altered to goethite).

Some altered feldspar fragments display a relict cleavage and are incipiently embayed. Embayment is rare in the potash feldspars and the altered crystals are, therefore, thought to be albite. These crystals also are replaced by a mixture of opaques (?hematite) and fine granular quartz (e.g. Locality 209) or by a mass of fine-grained, colourless, clay minerals (?illite). If these crystals were formerly albite then it is evident that migration of ions has occurred, with the introduction of potash and iron and the migration of sodium to form the alteration products, (e.g. Locality 48).

One rock (Sample 222) is a notable exception in that the feldspar crystal fragments are much less altered than those found elsewhere in this Formation and indeed elsewhere in the southern regions of the mapped area. Fresh plagioclase and potash feldspar are about equal and total 25%. The plagioclase is oligoclase ($An_{15}Ab_{85}$) with well developed lamella and less commonly the Carlsbad twinning. The potash feldspar is sanidine microperthite of the patch type, with irregular blebs of albite (?) sporadically distributed throughout the sanidine host. Most crystals are clear but minor alteration and discolouration occurs around their peripheries and to a lesser extent along cleavage traces. This rock is unusual in that the plagioclase is as calcic as oligoclase and the potash feldspar is sanidine rather than orthoclase (-ve $2V = 8^{o}$).

A second group of altered crystal fragments are rounded in shape and composed entirely of a felted mass of platy sericite. The primary nature of these fragments is uncertain (e.g. Locality 48).

Rock fragments form the most conspicuous and distinctive component of the Welded Lithic Tuff (pEwt) and may compose as much as 60% or as little as 10% of the rock. The fragments have a size distribution in the range 2.5 to 1.5 mm and most are sub-rounded to sub-angular in habit (e.g. Locality 209) although splinter shaped fragments are also known (e.g. Locality 48).

The most common are rhyolitic but their textural features tend to be constant at any one locality and to vary from one locality to another. They include:

Welded, Vitric-Crystal Tuffs In the Eastern Region (e.g. Locality 48) the fragments are composed of euhedral crystals of intensely sericitized feldspar set in an eutaxitic matrix composed of flattened and distorted shard

shapes. The flattened shards impart a foliated texture to the rock. The lithic fragments differ from the groundmass of the tuff in that the shards in the lithic fragments are replaced by secondary or late-stage opaques (?hematite) whereas the groundmass shards are replaced by quartz.

Massive Rhyolites In the central portion of the unit (e.g. Locality 222A) the fragments are non-porphyritic, essentially massive, and composed of a mosaic of quartz crystals up to 0.2 mm in diameter in which are set cryptocrystalline and partly altered potash feldspar. The fragments are discoloured by disseminated opaque minerals and in some this discolouration is streaked, suggesting a relict flow banding or relict, eutaxitic foliation. In a few fragments the quartz mosaic radiates inwards from the outer margins of the fragment indicating it to be a product of devitrification.

Devitrified Obsidian (e.g. Locality 222B). These are found in the Central Regions and are composed of a dense, cryptocrystalline mosaic of quartz and potash feldspar which is massive and featureless.

Siliceous Vitric Tuff Fragments These are identical in all respects to the more extensively altered varieties of the underlying Vitric Tuff (pЄvt). The shard structure is almost completely obliterated. It is noteworthy that some fragments have quartz veinlets indicating that silicification must have taken place prior to incorporation in the Welded Tuff (pЄwt).

Fluidal Banded Rhyolites These distinctive fragments are found in the Central Region (e.g. Locality 113) and are composed of layers of quartz or potash feldspar which, in some fragments, are tightly contorted into isoclinal-like folds. The segregation of quartz and feldspar may be related

to unequal concentrations of volatiles in the original magma, the quartz bands developing from gas-rich layers in contrast to the drier feldspathic streaks.

Altered, Vesiculated Fragments These fragments are more abundant in the Western Region (e.g. Localities 258, 150 and 289) and are composed of a cryptocrystalline mass of illite in which is set sub-rounded to elliptical amygdules. The host rock is massive and featureless whereas the amygdules are composed of microcrystalline quartz which tends to radiate from the core of the amygdule.

The matrix is the most characteristic, distinctive, and constant feature of this unit (pЄwt). In all places it is an intensely welded mass of shard structures set in a fine-grained quartzo-feldspathic groundmass. The degree of welding and reconstitution shows some variation along and across strike. The more intensely welded examples are found in the Eastern Zone (e.g. Locality 209). Here the groundmass has a foliated structure imparted by the compaction and flattening of shards and pumice fragments into more or less plate-like units (Plate 29). There is no evidence for a lineation resulting from the stretching and incipient flowage of the welded material. The intensely distorted nature of the shards becomes especially marked about phenocrysts and rock fragments where warping of the foliation occurs. The individual shards are devitrified and have a rim composed of a radial aggregate of finely fibrous feldspar crystals surrounding a core of microcrystalline quartz. The texture of the feldspar resembles the axiolitic texture of Zirkel (1876).

PLATE 29 WELDED LITHIC TUFF (pЄwt)

A. Sample 48:PPL x 35

A welded tuff (Central Zone) showing incipient development of an eutaxitic foliation. Distorted shard shapes are flattened and moulded about phenocrysts. Coarse grained shards are better preserved and formed of a margin of dusty iron-oxides about a polycrystalline core of quartz. Pseudo-axiolitic textures can be seen in a few shards. A terminated quartz phenocryst (left) and the margin of a rock fragment are in the field of view.

B. Sample 222:XN x 35

Eutaxitic foliation in welded lithic tuff. Rock fragments, some weakly banded and all extensively altered, set in a welded matrix of flattened and attenuated shard shapes. A few cuspate terminations can still be recognized on some shards. Note the streaky foliation when compared to the fluidal banded rhyolites (Plate 26).

C. Sample 209:PPL x 35

Eutaxitic foliation of fine-grained, flattened shards composed of polycrystalline quartz set in a felsic, cryptocrystalline matrix. Note the introduction of late-stage potash feldspar along veinlets parallel to the foliation. A secondary cleavage (diagonal) forms at an angle to the first and along these potash feldspar and clay minerals replace the shard texture.

D. Sample 209:PPL x 35

Same field of view as for Plate 18C viewed under double polarized light.



A



B

PLATE 29.



C



D

Elsewhere (e.g. Locality 48) the shards are better preserved and have a variety of shapes, are partly distorted and flattened, and closely compacted with a sub-parallel orientation.

In the Central Region (e.g. Localities 222 and 113) the welding is intense and the overall texture differs somewhat from that in the more easterly limits (e.g. Locality 209). The matrix has a delicate streaky lamination deceptively like the fluidal banding seen in many lavas. However, close inspection reveals the typical lens-like or eutaxitic texture (Holmes, 1920) of intensely welded tuffaceous rocks. The shard shapes are flattened and distorted beyond recognition and form sinuous and lens-like streaks composed of cryptocrystalline quartz, potash feldspar, and clay minerals. These are moulded around rocks and crystal fragments but elsewhere have a parallel orientation.

Interstitial to the flattened shards is dense, cryptocrystalline indistinct material; it is dusty brown, apparently lacks appreciable quartz and is weakly birefringent. It was probably composed of ash welded to a homogeneous glass and since devitrified. A few splinters and chips of crystal fragments are aligned in the plane of the flattening.

The matrix texture in the Western Region of exposure resembles that in the Central Region but the rocks are distinguished by an increase in the fragment to groundmass ratio from about 60% fragments to about 80% fragments. In addition the groundmass is almost colourless in comparison with the dusty-brown colouration of the rocks in the Central Region. In the West the flattened shard structures are composed of a matte of cryptocrystalline flaky clay minerals (?illite) and contain only a little quartz. The interstitial mineralogy is optically indistinct, is smoky-brown in colour and a little more coarsely crystalline than in the Central Regions of the Arc.

Accessory minerals are sparse and include rounded opaque minerals composed,at least in part,of leucoxene (?ilmenite), euhedral crystals of colourless zircon and small euhedral apatite crystals. In some rocks (e.g. Locality 209) small amounts of sphene are found.

5.13 Welded Tuff Sheet (pЄv3)

5.13.1 Field Observations

Much of the eastern area of the Complex is a massive red, welded tuff of rhyolitic composition which grades to the north into a tuff or rhyodacitic composition which is dark brownish-red in colour. In addition to the colour changes, there is a perceptible increase in the proportion of phenocrysts northwards.

In the south of the mapped area (Map 1) the tuff has sub-angular to sub-rounded feldspar crystals, rounded quartz crystals and dark, ragged mafic minerals set in a macroscopically aphanitic groundmass. The total crystal content is about 30% by volume. Potash feldspar and sodic plagioclase crystals commonly range to 7-8 mm in diameter although a few of 15 or even 20 mm are found. The crystals are milky white and buff or pink, and dull red. The potassic feldspar is usually darker in colour than the sodic plagioclase although this is not an infallible guide for the feldspar colour is largely dependent on the presence or absence of iron oxides (thin section examination).

Quartz (usually less than 2% of the whole rock) is rounded, glassy and colourless. Some of the larger crystals show a modified, terminated, habit and some are embayed.

Anhedral pseudomorphs of black and dark-green alteration products after primary ferromagnesian minerals range up to 2-3 mm in diameter and are sporadically distributed in a single hand specimen. The groundmass is deep red to brick red and massive.

In the northernmost parts of the mapped area (Map 1) the phenocrysts are of similar minerals to those in the southern areas, although constituting in excess of 40% of the rock. The crystals are milky white to buff and not red as in the south. Quartz is less, and mafic minerals more abundant. The groundmass is aphanitic but is brick red to brownish red and even dark grey. No primary depositional features have been found in the northern areas.

The outcrop throughout the area mapped is marked by the development of a persistent rectilinear joint system which trends due north-west and north-east. A second,smaller scale polygonal joint system is intersected by a low angle, almost horizontal joint system. (See structure Section 4.3.2).

5.13.2 Petrography

Thin section examination of 186 samples show subtle, but significant, variations throughout the sampled area. These variations are summarized below.

Groundmass The mineralogical similarity of the Formation precludes sub-division on the basis of mineralogy but the micro-texture of the groundmass shows considerable variation. In the rocks from the mapped area nine major textural variations are identified although there is a complete gradation between each of the described varieties and within each category variation exists in the grain size of the elements which comprise that texture.

The textural modifications are defined on the basis of the quartz and

feldspar crystal habits and their mutual relationships.

1. Granophyric (Plate 30A) The granophyric texture is composed of a microcrystalline aggregate of quartz and feldspar. The two minerals are intergrown in a similar way to that found in graphic granite so that adjacent patches extinguish simultaneously. The quartz is colourless, and displays a uniform extinction. The crystals are sharply angular and their habit is governed by the shape of the available interstitial areas between the feldspar crystals. The feldspar is probably orthoclase but is reddened so that optical identification is not possible. It forms anhedral to subhedral crystals. The granophyric texture is the coarsest grained (0.4 mm).

2. Microgranular (Plate 30B) The microgranular texture is composed of a microcrystalline granular aggregate of quartz and potash feldspar and resembles the granophyric texture but is finer grained and adjacent patches do not polarise simultaneously. The quartz is water clear, has a uniform extinction and forms equigranular, rounded crystals. The potash feldspar which is probably reddened orthoclase forms rounded, equigranular crystals which may be a little larger than the quartz. The maximum grain size is about 0.2 mm.

3. Spherulitic (Plate 30 C) The spherulitic texture is a densely packed mass of spherulites of finely fibrous, sub-radiating crystallites of reddened potash feldspar. Quartz can seldom be recognized optically in the spherulites but its presence is

PLATE 30 WELDED TUFF SHEET ($p\epsilon v_3$)

A. GRANOPHYRIC TEXTURE

Microcrystalline aggregate of quartz (clear) and reddened feldspar (stippled) with shredded mafic minerals (hatched). The quartz and feldspar are intergrown in a similar way to that found in graphic granite so that adjacent patches extinguish simultaneously.

B. MICROGRANULAR TEXTURE

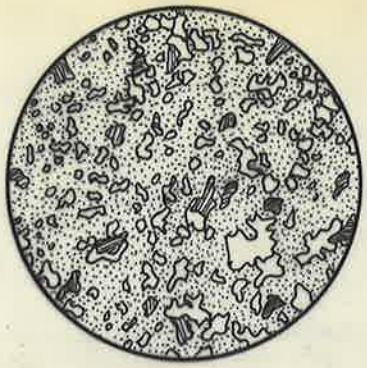
Microcrystalline granular aggregate of quartz (clear) and reddened feldspar (stippled). Adjacent patches do not polarize simultaneously and the feldspar tends to form micro-spherulitic patches.

C. SPHERULITIC TEXTURE

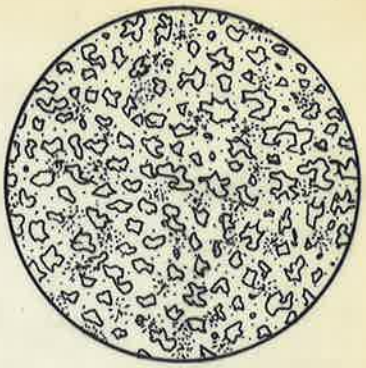
Densely packed mass of spherulites of finely fibrous, sub-radiating crystallites of reddened potash feldspar (idealized). Quartz is seldom recognized in the spherulites. Interstitial areas are infilled with a microgranular mosaic of quartz and potash feldspar.

D. SPHERULITIC MICROGRANULAR

As for C above although the spherulites are finer grained and more loosely packed.



A



B

2-mm



C



D

PLATE 30

indicated by the calculated CIPW normative analysis. The interstitial areas are infilled with a microgranular mosaic of quartz and potash feldspar.

4. Spherulitic Microgranular (Plate 30D) The spherulitic microgranular texture is intermediate between the spherulitic texture of (3), above, and the microgranular texture of (2) above. The spherulites are loosely packed in a microgranular groundmass.

5. Microlitic (Plate 31 A) The microlitic texture has fine, subradiating needles of quartz set in a mass of reddened, cryptocrystalline feldspar. The quartz needles range up to 0.3 mm in length and are composed of several, non-equally polarising quartz crystals. The material interstitial to the quartz needles is homogeneous and finely fibrous. The overall texture is a confused, unoriented aggregate.

6. Microgranular Microlitic (Plate 31B) The microgranular, microlitic texture is intermediate between (2) and (5), above. Numerous, sub-radiating quartz needles are set in a microgranular mosaic of quartz and reddened potash feldspar. The quartz needles attain 0.3mm and the elements of the microgranular groundmass are seldom more than 0.1 mm in diameter.

7. Microgranular, Microlitic, Spherulitic (Plate 31C) The microgranular, microlitic, spherulitic texture is intermediate between the textures of (4) and (6).

PLATE 31 WELDED TUFF SHEET (pCv_z)

A. MICROLITIC TEXTURE

Fine sub-radiating needles of quartz (clear) set in a mass of reddened, sometimes fibrous potash feldspar (stippled).

B. MICROGRANULAR MICROLITIC TEXTURE

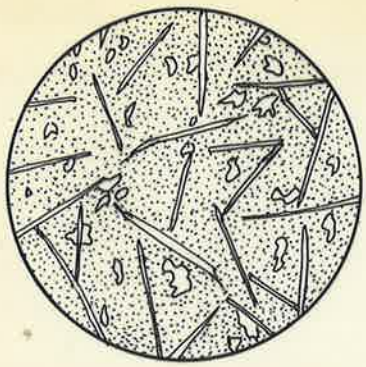
Sub-radiating quartz needles (clear) set in a micro-granular mosaic of quartz and reddened, potash feldspar (stippled). The quartz of the mosaic is not uniformly distributed.

C. MICROGRANULAR, MICROLITIC, SPHERULITIC TEXTURE

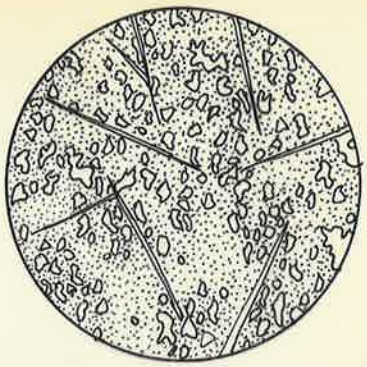
Needles of quartz (clear) set in a microgranular ground-mass that contains corroded spherulites of reddened, fibrous, potash feldspar.

D. PATCH TEXTURE

Subspherical, coalescing patches of finely intergrown, reddened, fibrous potash feldspar and quartz (stippled) set in a mass of dense reddened, potash feldspar that contains a few, discrete microcrystals of quartz.

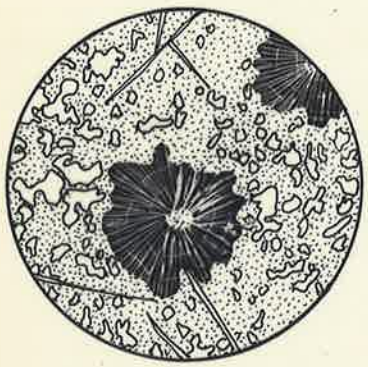


A

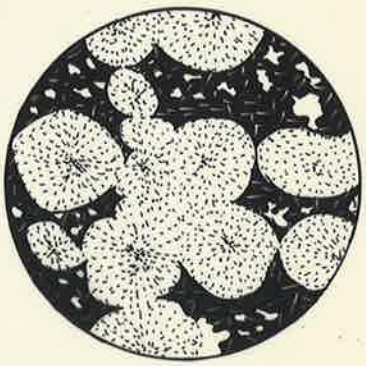


B

2 mm



C



D

PLATE 31

8. Patch (Plate 31D) The patch texture is formed of irregular coalescing patches of reddened, fibrous potash feldspar and quartz, so finely intergrown that optical identification of the feldspar is not practicable. The mosaic formed by the patches has a variable grain size which ranges up to 0.4 mm.

9. Snowflake This texture is similar to that previously described except that the feldspar has been subjected to appreciably more reddening. Rocks which display this texture are all located adjacent to or in the vicinity of the Uno Fault.

Quartz and feldspar comprise more than 90% of each of the groundmass types. Other minerals which have a sporadic distribution include alteration products after ferromagnesian minerals, opaques and accessory minerals. Mafic minerals include chlorite, amphibole, coloured micas and carbonate and form small flakes and fibrous crystals which are randomly distributed. The carbonate (identified from twelve rocks as calcite by microchemical staining techniques) forms small discrete, granular crystals and is intergrown with some of the secondary mafic silicates. Rare opaques (?magnetite) are very fine-grained and dusty.

Quartz Phenocrysts The quartz is water clear, displays a uniform extinction, is glassy, and occurs as irregular fragments, rounded grains or partly rounded bipyramids, the latter, in many cases, corroded or embayed. Dusty opaques occur at the margins of some crystals but seldom in the cores. Liquid inclusions are practically absent although a few crystals with minute globules were observed.

In many rocks the quartz phenocrysts have sharp margins but in others the margins are diffuse and ill defined. Peripheral reaction textures assume

a variety of habits, the principle ones of which include:

a. Microcrystalline graphic intergrowths (Plate 32A). The quartz of these intergrowths is optically continuous with the parent and the boundary of the grain is defined by the abrupt juxtaposition of reddened potash feldspar. There is no distinction between the quartz of the graphic intergrowth and that of the parent suggesting that the two crystallized simultaneously and therefore that the intratelluric quartz phenocryst has recrystallized at the time of crystallization of the groundmass (e.g. Locality 161).

b. Serrated margins (Plate 32B) in which microlites of reddened, potash feldspar penetrate the margins of the phenocrysts at right angles to the phenocryst surface (e.g. Locality 172).

c. Coronas of graphically intergrowth quartz and potash feldspar which is distinct from the parent. Quartz forms needles which radiate in optical continuity from the parent (Plate 32C) crystal and are intergrown with reddened potash feldspar (e.g. Locality 181).

d. Coronas of equigranular, graphic quartz and feldspar (e.g. Locality 186).

e. Coronas of reddened, cryptocrystalline potash feldspar which are notably less siliceous than the enclosing groundmass (e.g. Locality 155).

Ferromagnesian Minerals

Ferromagnesians are more abundant in the northern areas and it is here that fresh crystals are found. Fresh crystals are also found to a limited extent in the vicinity of the contact with the welded tuffs

PLATE 32 WELDED TUFF SHEET ($p\mathcal{E}v_3$)

QUARTZ PHENOCRYSTS

A. MICROCRYSTALLINE, GRAPHIC CORONA

A portion of a subhedral quartz crystal (clear, top) mantled by a microcrystalline, graphic intergrowth of quartz and reddened, potash feldspar (stippled). The quartz in the mantle is optically continuous with that of the host indicating simultaneous recrystallization of the host and crystallization of the corona. Adjacent to the corona is a mass of quartz-deficient, reddened, potash feldspar (black) indicating nucleation of quartz from the groundmass about the host phenocryst.

B. SERRATED MARGIN

A portion of an anhedral quartz phenocryst (lower) surrounded by a mantle of clusters of reddened potash feldspar microlites (black) that penetrate the phenocryst surface. The phenocryst and mantle are set in a micrographic groundmass (stippled).

C. ACICULAR QUARTZ CORONA

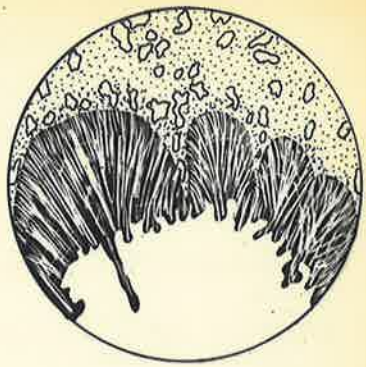
Subradiating needles of quartz radially disposed about an euhedral quartz phenocryst. The quartz needles are optically continuous with the host and have nucleated from the surrounding groundmass which is composed of reddened, potash feldspar (stippled).

D. MICROGRAPHIC CORONA

Portion of an embayed quartz phenocryst mantled by graphically intergrown quartz (clear) and reddened feldspar (stippled). Adjacent to the host the quartz of the groundmass is optically continuous with that of the host.

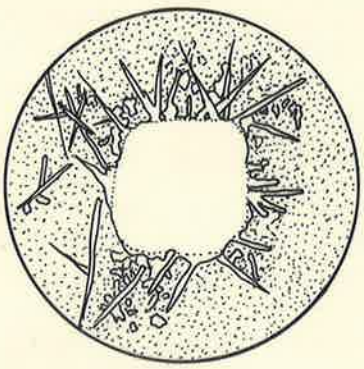


A

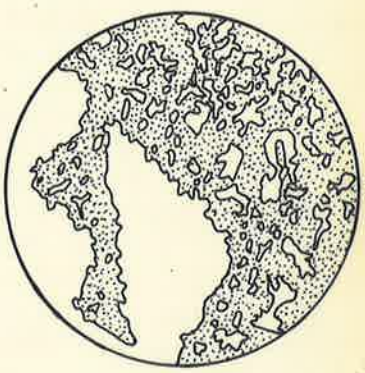


B

2 mm



C



D

PLATE 32

the Arc Structure.

Clinopyroxene (Plate 32D) occurs as anhedral, sub-rounded crystals, usually alone but rarely as cumulophyric clusters. The crystals are colourless, or very pale green in which case they display a slight but perceptible pleochroism. Refractive index and optic-axial angle determinations indicate the mineral to fall in the compositional field of the ferro-augites (Deer, Howie and Zussman, 1963, Vol. 2, p 132). The pyroxene is inclusion-free and untwinned. In addition to fresh, colourless crystals there are some with turbid patches and others which are completely altered. Some are mantled by a corona of iron oxides and leucoxene conforming to the crystal outline but separated from it by a ragged zone of pale-green chlorite. In other cases, secondary, iron-rich chlorite is accompanied by a little calcite crystallized along relict cleavage traces. The chlorite may be accompanied by a yellowish-green, or a blue-green pleochroic uralite.

Fresh pyroxene is not found in the central and southern regions but pseudomorphs are common. These crystals are often associated with plagioclase phenocrysts and contain inclusions of acicular apatite and altered titanomagnetite. Products of alteration are various but certain associations are found of which the following are most common:

a. a pale-green, weakly pleochroic, optically anomalous chlorite interleaved with calcite, with or without associated iron oxides.

b. a bright yellow-green, moderately birefringent, iron-rich chlorite which has partially replaced a strongly pleochroic, ferro-actinolite.

c. a yellowish-brown, pleochroic, moderately birefringent biotite-like mica intergrown with a pale-green strongly pleochroic, chlorite which displays a weak birefringence.

In Addition to these mineral associations, pseudomorphs composed of a single mineral phase are also found. The principle types are:

a. a blue-green, strongly pleochroic ferro-actinolite;

b. bright yellow-green, moderately birefringent, iron-rich chlorite; and

c. pale-green, faintly pleochroic, anomalous chlorite.

The sampling undertaken indicates that carbonate and chlorite are abundant in the central regions of the area studied and that the ferro-actinolite is more abundant in the southern and northern regions.

Coloured silicates in the groundmass are the same as those which form the ferromagnesian pseudomorphs. Here they form feathery and shredded crystals and microcrystalline flakes whose habit is governed by the texture of the enclosing grains. They have crystallized as a part of the groundmass and there is no reason to believe that they are the products of alteration of pre-existing mineral phases. Chlorite, ferro-actinolite and carbonate occur in this form.

Biotite is rare and forms ragged flakes, up to about 1.2 mm across, which are weakly pleochroic from pale yellow-brown to mid-brown. It shows corrosion and frayed boundaries. Very fine-grained chlorite and hornblende tends to be concentrated adjacent to the crystals and their centres are partly bleached. The alteration is culminated in relict shreds of discoloured biotite with numerous, iron oxide inclusions and bordered by iron oxides, fibrous chlorite and minor hornblende.

The small amount of biotite does not allow a detailed investigation of its properties and composition. However, two grains were selected from thin sections of different rocks and their refractive indices are tabulated below.

(Na light):	- 1.605	±0.005	1.595	±0.005
	- 1.695	±0.005	1.714	±0.005
	- 2.726	±0.005	1.720	±0.005

The biotite can be considered to have a moderate to high ferric-iron content, following Larsen et al (1937) and Deer, Howie and Zussman (1963).

Titano-magnetite occurs in small amounts and is partially to completely replaced by leucoxene, sphene and iron oxides.

Accessory Minerals Accessory minerals are perhaps more common in the Welded Tuff (pЄv3) than in the tuffs from the Arc Structure. Zircon is generally colourless, uniaxial positive, with a high refringence and very strong to extreme birefringence. A few partly altered crystals (hyacinth) are found and some display a weak zonation. Few crystals are euhedral. Some crystals occur in the groundmass but most are associated or included within pseudomorphs after primary ferromagnesian crystals.

Apatite is the most common and forms colourless, inclusion-free, euhedral crystals which are usually acicular but may be hexagonal and equidimensional.

Fluorite is present in most rocks collected from the vicinity of the Ring Structure but elsewhere its occurence is sporadic and its distribution ill defined. It is most commonly associated with the pseudomorphs after ferromagnesian silicates where it forms small octahedral to dodecahedral crystals. In addition, it may form anhedral crystals occupying interstitial areas within the groundmass. Most crystals have a non-uniformly distributed patchy violet colouration, octahedral cleavage and very low refringence. Rutile is less common than zircon, apatite or fluorite and forms elongate, bladed crystals. The mineral is honey-coloured and is fresh or partially altered to ilmenite and/or sphene.

Feldspar Phenocrysts The feldspar phenocrysts are the most abundant and conspicuous of the phenocryst phases. Sodic plagioclase, sodi-potassic and potash-rich feldspars in various stages of alteration and unmixing are represented.

The plagioclase crystals range from subhedral to anhedral and many have sharply angular or broken habits suggesting a fragmental origin.

Most crystals are embayed and some are deeply corroded. There is no evidence for compositional variations throughout the Tuff Sheet and although some phenocrysts are normally zoned, most of the crystals are homogeneous ($Ab_{90}An_{10}$ to $Ab_{100}An_{0}$).

The alkali feldspars assume a variety of habits and show exsolution to varying degrees. Most were formerly sanidine crypto- and micro-perthites which have undergone inversion to orthoclase and alteration to illite.

These feldspars are similar to those described from the underlying tuffaceous rocks.

5.13.3 Petrochemistry

Forty three samples from the Welded Tuff Sheet have been chemically analysed (Figure 10). The results are presented in Table 9 (Appendix C) and the calculated molecular norms in Table 10 (Appendix D). A discussion of the findings is presented in Section 6, (Page 155).

5.13.4 Modal Distribution of Phenocrysts in Welded Tuff Sheet ($p\epsilon v_3$)

Modal analyses (see Laboratory Techniques, Section 1.4) of plagioclase, potash feldspar, mafic and quartz phenocrysts indicate regular mineralogical gradients within the rock mass.

Trend surface analyses (Appendix A) were used to enable regional trends in the data to be established, to assess the degree by which the regional trend explains the variation in the data at each sampled point, and to

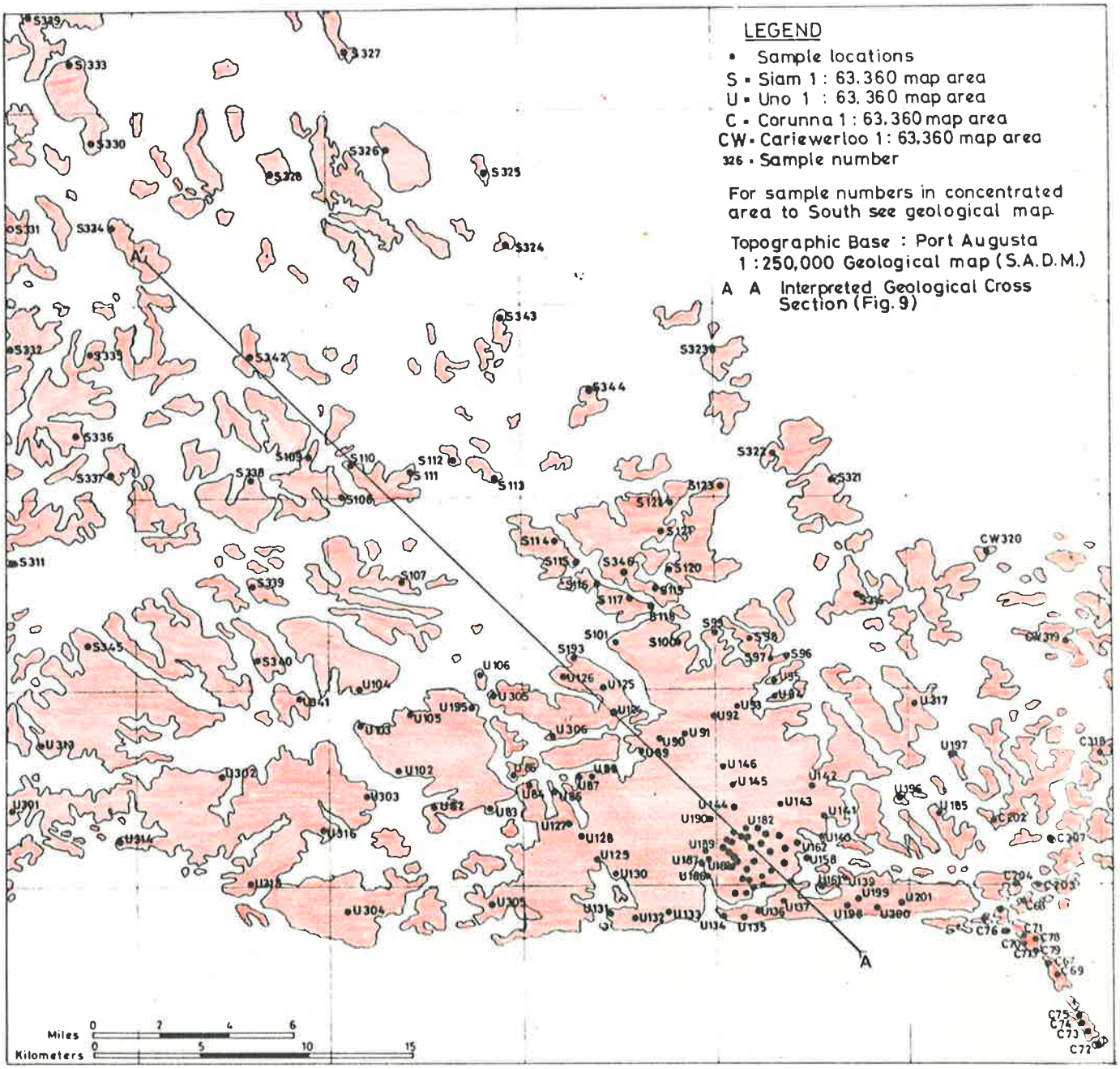


FIGURE 2: TREND SURFACE ANALYSIS
Sample Numbers and Locations

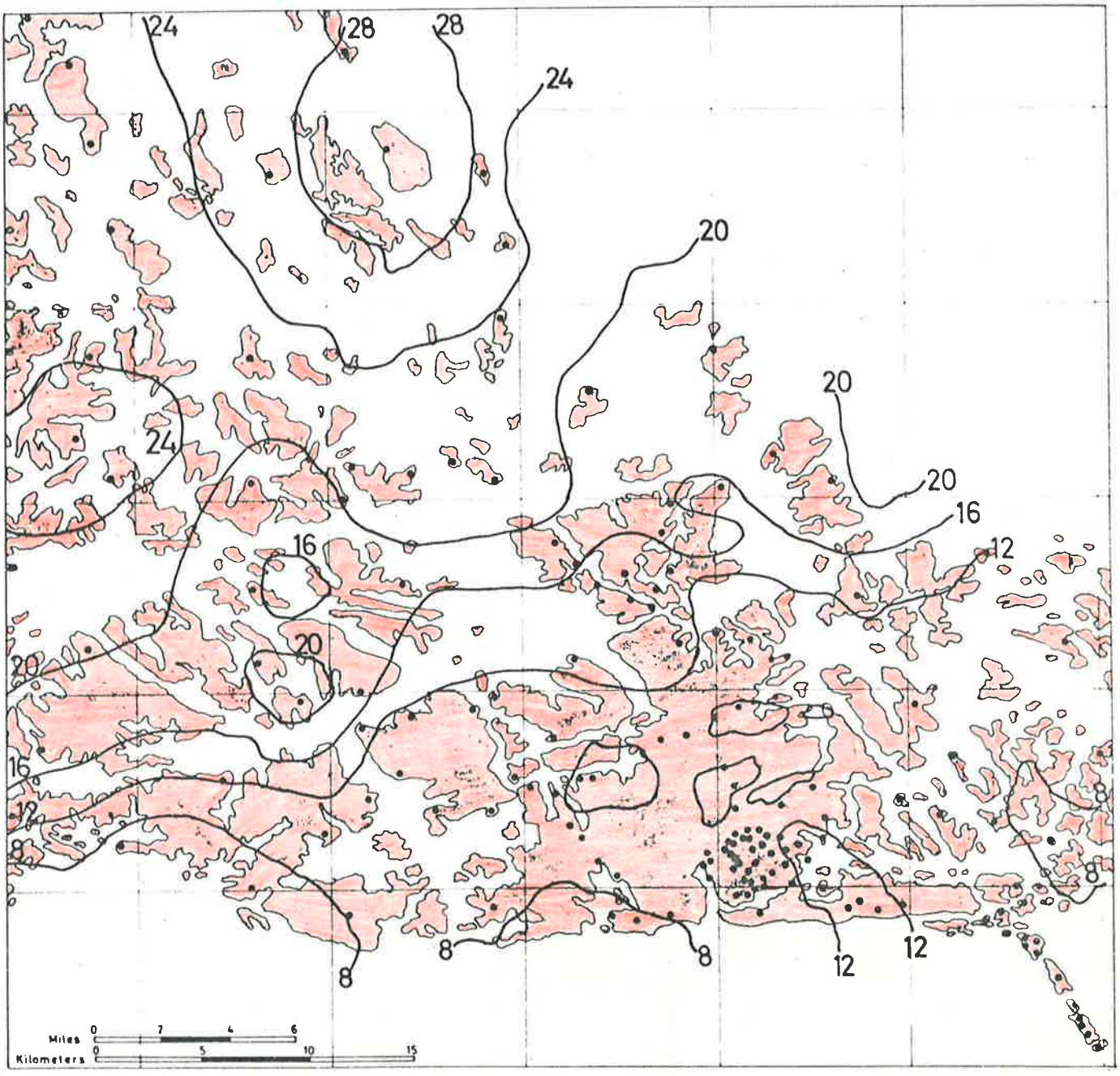


FIGURE 3: CONTOUR PLOT – PLAGIOCLASE

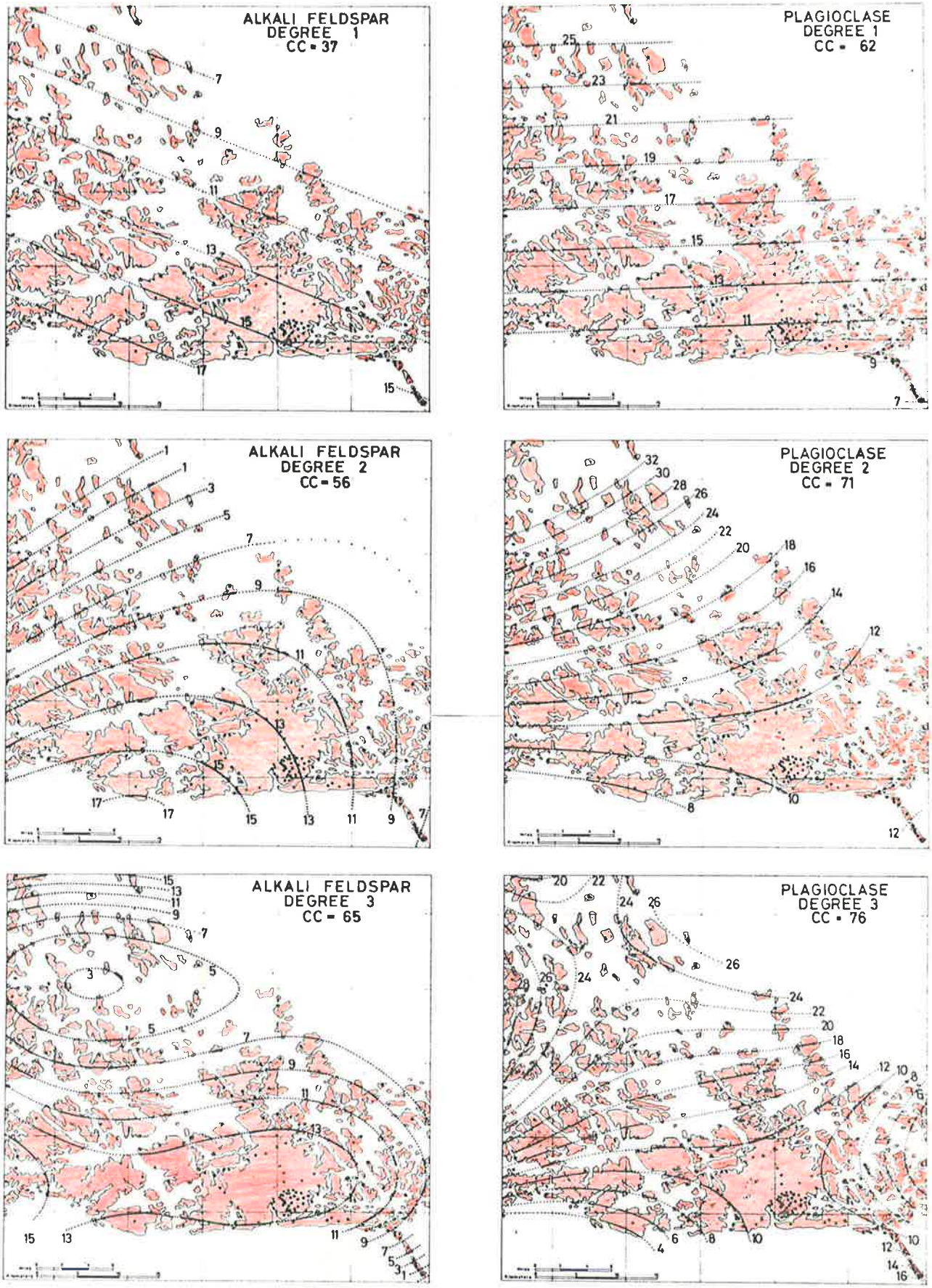


FIGURE 4: TREND SURFACE ANALYSIS
Feldspars — Run 1

obtain a quantitative appraisal of local variation.

Results Initially 180 irregularly spaced data points were considered (Fig. 2). The samples from which the data were obtained are assumed to be at (or projected on to) a constant horizontal plane. The scale of the variation noted in the preliminary examination combined with the subdued topography throughout the region suggested that the results were in no way invalidated by this assumption.

An evaluation of the fitted trend surfaces indicates that there is a marked increase from degree 1 to degree 3 in the extent to which the surfaces explain the variation in the data and that surfaces above degree 3 show little significant improvement in their degree of fit. Hence surfaces higher than degree 3 are not considered.

Table 11 lists the goodness of fit (Merriam & Harbaugh, 1968) and the standard deviations calculated for each of the fitted surfaces. First runs were completed on plagioclase and potash feldspar modal data and the results are shown in Figure 4.

The first degree or linear surface plots indicate a regional gradient in the modal feldspar data. The regional gradient for the plagioclase feldspar phenocrysts increases in a northerly direction whereas that for the potash feldspar phenocrysts increases in a south-westerly direction (Fig. 4). The goodness of fit indicated in Figure 4 and Table 12 are low for the first degree plots indicating a poor fit to the data but the coefficient of correlation shows a marked improvement as the degree of the surface increases. The coefficients of correlation are significantly higher for the plagioclase than for the potash feldspar data.

The third degree surfaces are more intricate but certain fundamental similarities are evident in the gradients of both the plagioclase and

alkali feldspar data. The goodness of fit are also high with 65% of the alkali feldspar data and 76% of the plagioclase data being explained by the fitted surfaces. These then, best indicate the regional trends displayed by the raw modal feldspar data.

TABLE 11 TREND SURFACE ANALYSIS

Mineral	Degree	Goodness of Fit			Standard Deviation		
		Run 1 %	Run 2 %	Run 3 %	Run 1	Run 2	Run 3
Plagioclase	1	63	73	78	4.32	3.96	3.65
	2	72	78	81	3.85	3.65	3.40
	3	76	82	85	3.59	3.30	3.06
Alkali feldspar	1	37	58	65	4.76	3.89	3.41
	2	56	59	65	4.25	3.85	3.40
	3	66	67	72	3.87	3.55	3.12
Mafic minerals	1	-	-	33	-	-	0.09
	2	-	-	43	-	-	0.09
	3	-	-	56	-	-	0.08
Total crystal	1	-	-	50	-	-	6.32
	2	-	-	56	-	-	6.06
	3	-	-	64	-	-	5.66
Alkali feldspar/	1	-	68	76	-	0.13	0.11
Total crystal content	2	-	72	78	-	0.12	0.10
	3	-	79	84	-	0.10	0.09
Plagioclase/	1	-	73	77	-	0.08	0.07
Total crystal content	2	-	75	78	-	0.08	0.07
	3	-	80	82	-	0.07	0.07

Although not illustrated, the trend surfaces fitted to the modal data for

mafic phenocrysts conformed in all respects with that of the plagioclase phenocrysts.

A plot of the residuals to the fitted third degree trends of plagioclase and potash feldspar shows one area in which there is a particular concentration of residuals (the Dyke Structure). The plagioclase phenocrysts are more abundant and the alkali feldspar is less abundant than predicted. Elsewhere residuals are distributed sporadically.

These results suggest that two populations of phenocryst assemblages are present. These are:

1. plagioclase, potash feldspar and mafics which display the broad regional gradients illustrated in Figure 4.
2. plagioclase (dominant), potash feldspar (minor) and mafic minerals of the Dyke Structure.

By removing the regionally anomalous data points of the Dyke Structure and refitting trend surfaces the new surfaces are found to more closely fit the modal data (Run 2, Fig. 5, Table 12). In addition, the plagioclase, potash feldspar and mafic mineral trends are more conformable.

The effect of the anomalously low potash feldspar and high plagioclase feldspar data of the Dyke Structure on the overall plotted surfaces can be seen by comparing Figure 4 and Figure 5. The degree 2 surfaces in the new data (Run 2, Table 12, Fig. 5) are almost conformable although the gradients trend in opposite directions. The degree 3 surfaces show some similarities but differ in many respects. It should be noted that again the goodness of fit is higher for the plagioclase than for the potash feldspar data.

A study of the residuals from these latter plots indicates an area due north of the Ring Structure where the plagioclase values are anomalously

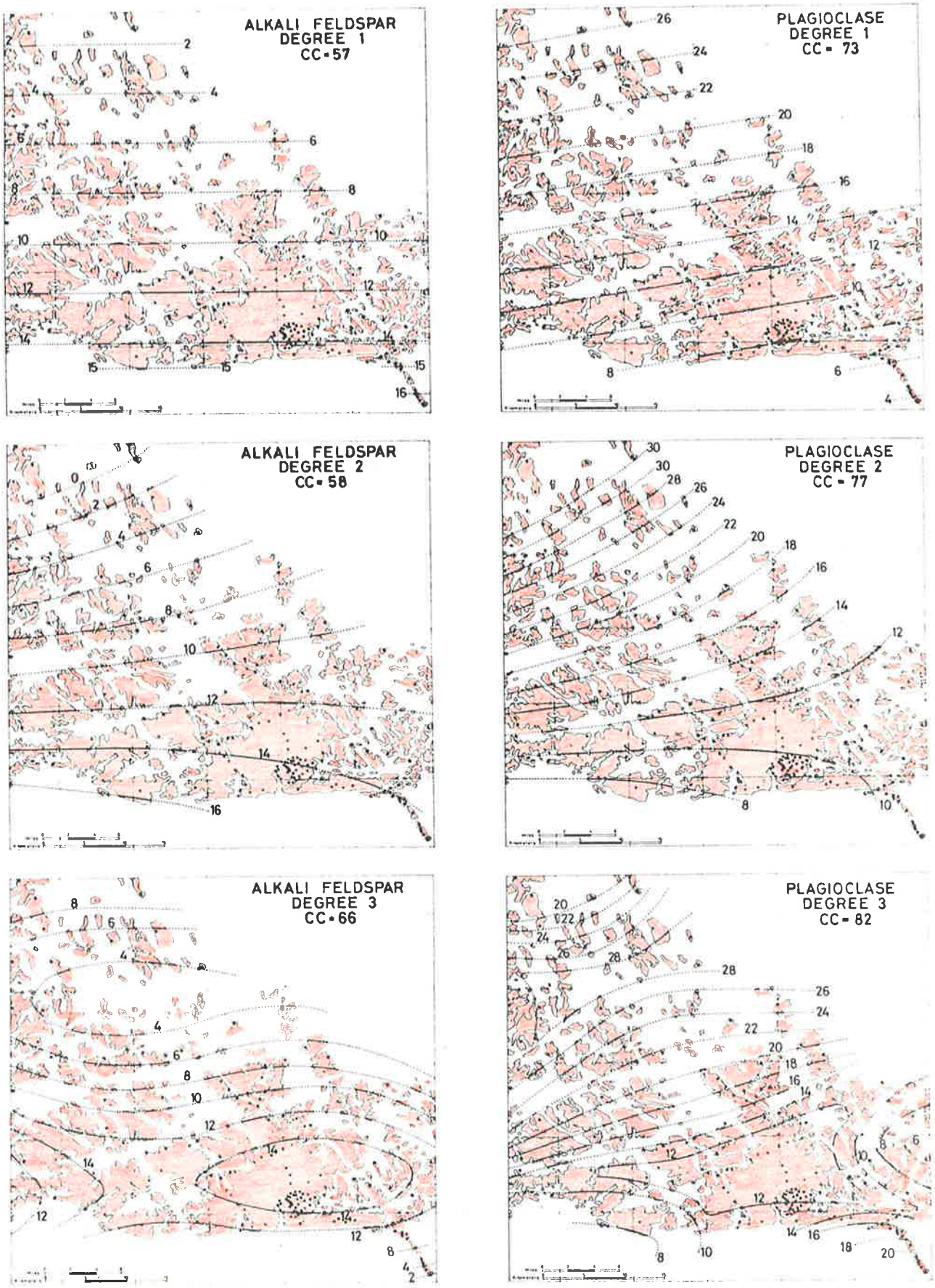


FIGURE 5: TREND SURFACE ANALYSIS
Feldspars – Run 2

high and the potash feldspar values anomalously low as compared to the regional gradients.

A third set of regional gradients was established (Fig. 6) by removing the residuals concentrated to the north of the Ring Structure and refitting the trend surfaces.

In the degree 1 and 2 plots of these revised data the two sets conform more closely than previously. Similarly, the degree 3 trends show close agreement although it is significant that the goodness of fit is again better for the plagioclase data than for potash feldspar. Trend surfaces were also fitted for the ferromagnesian phenocrysts (Fig. 7). The close conformity between these regional gradients and those of the plagioclase feldspar is noteworthy. However, the goodness of fit for the ferromagnesian data is significantly lower than those for the plagioclase. It is considered that the ferromagnesian gradients conform with those of the plagioclase and that the differences in goodness of fit is due to the precision of the data. Because the ferromagnesian minerals are very much less abundant than the plagioclase the error in the modal data is likely to be significantly higher. Hence the goodness of fit for the ferromagnesian minerals is correspondingly lower.

A study of the residuals from these revised data indicates a maximum local deviation of about plus or minus 1.5% by volume for each phenocryst component, the residuals having a random distribution within the sample area. The residuals are considered to represent sampling bias and error in analytical technique rather than to major differences in lithology.

If two or more compositionally distinct lithological units were present in the region represented by the revised data points, it would be anticipated that in the region of the contact(s) the residuals would show a marked deviation from the regional trends. No significant or systematic deviation in the residuals was established and hence it is concluded that the exposed

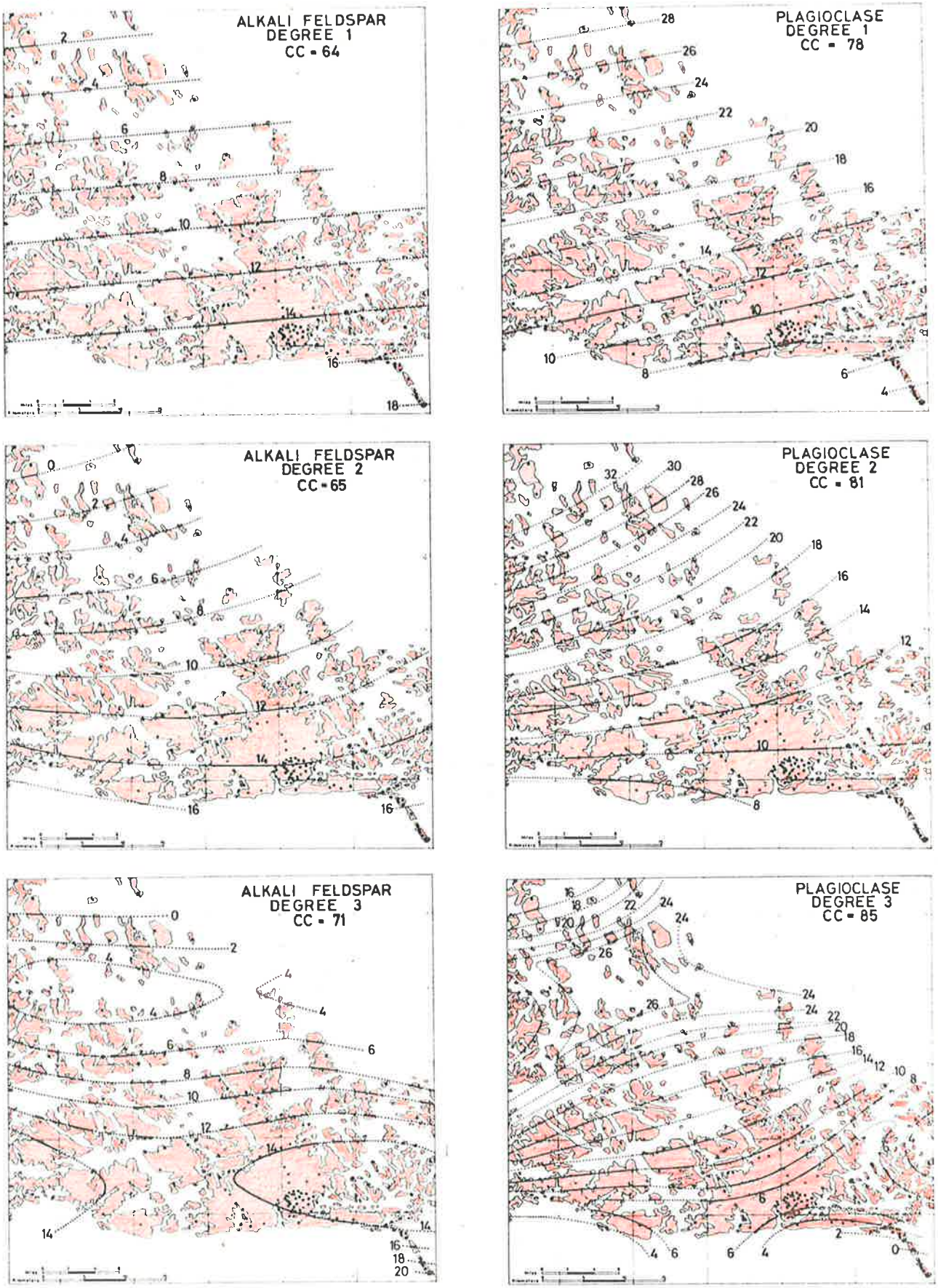


FIGURE 6: TREND SURFACE ANALYSIS
Feldspars — Run 3

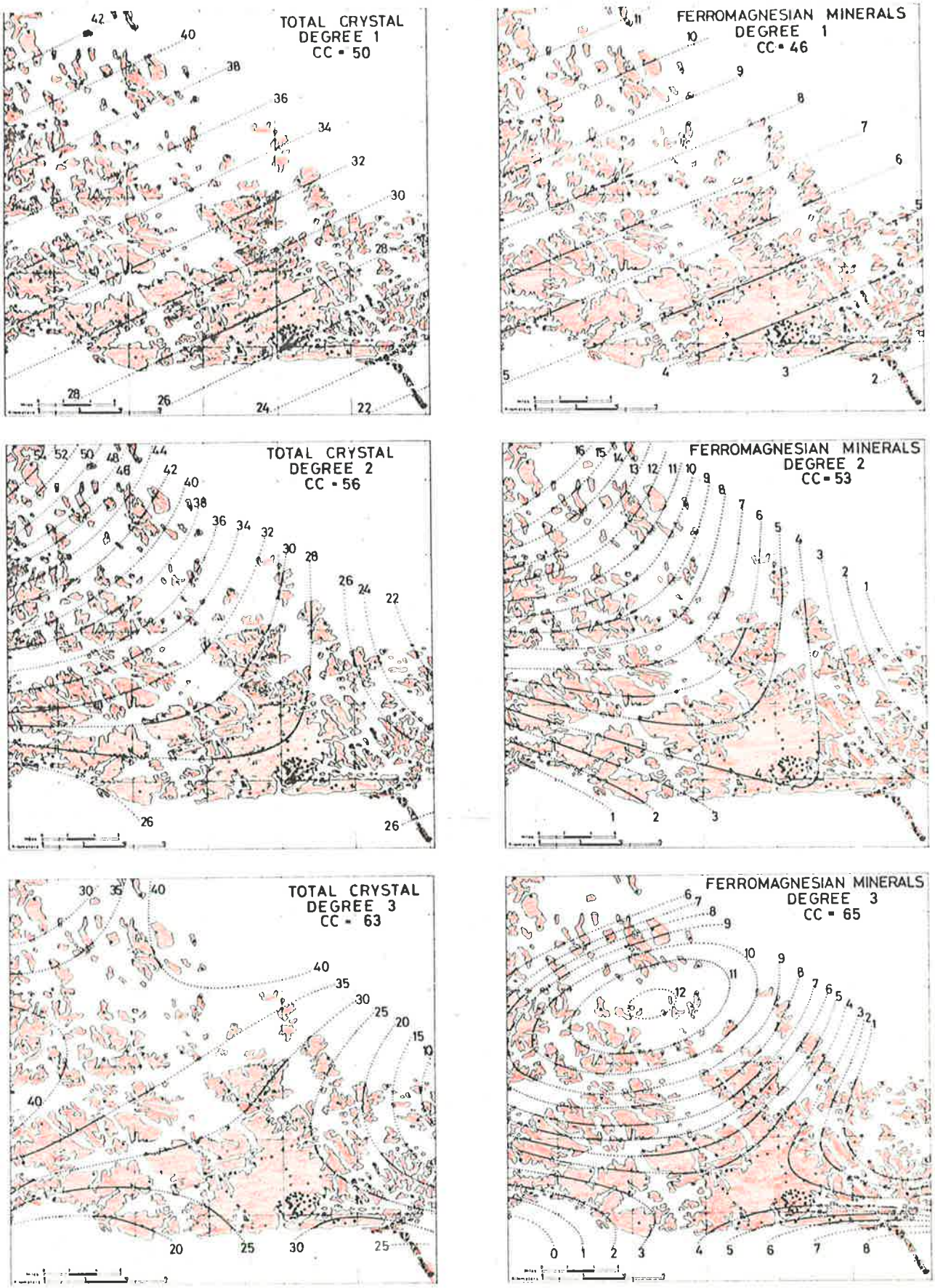


FIGURE 7: TREND SURFACE ANALYSIS
Mafics and Total Crystal — Run 3

rock type represents one continuous outpouring of igneous material.

From these observations several conclusions can be drawn:

1. The larger part of the sampled region displays pronounced gradients in the abundance of the phenocryst components. These gradients trend in a south-east, north-west direction across the region and

   a. the plagioclase phenocrysts grade from about 6% by volume in the south to about 26% by volume in the north and west and possibly decrease in volume further to the north (Fig. 6). The degree 3 trend surface explains 85% of the variation in the abundance of plagioclase phenocrysts in the sampled area;

   b. the potash feldspar phenocrysts increase in abundance from about 2% in the north to about 14% by volume along the southern margin. The degree 3 trend surfaces explain 71% of the variation in the potash feldspar data; a correlation which is significantly lower than that obtained for the plagioclase data;

   c. the ferromagnesian phenocrysts increase in abundance from about 6% by volume in the south to 12% by volume in the central, north and western areas of the sampled region. The degree 3 trend surface explains 65% of the variation in the ferromagnesian data; a correlation which is lower than that obtained for either of the feldspar data but which is considered to be due to errors inherent in the analytical technique.

   Overall the three sets of gradients are broadly conformable and intimately related.

2. The phenocryst assemblage in samples examined from the Dyke Structure differs significantly from that predicted by the trend

surface for most of the region. Plagioclase feldspar and ferromagnesian phenocrysts are significantly more abundant and potash feldspar less abundant than predicted.

3. The phenocryst assemblages in samples examined from a region immediately to the north of the Ring Structure are somewhat anomalous when compared to the regional trend. Plagioclase phenocrysts are a little more, and potash feldspar phenocrysts a little less abundant than predicted.

In order to determine the relationship between the established regional gradients for the phenocryst variations and the total crystal content of the rock body, trend surfaces were fitted to the total phenocryst data (including the quartz phenocrysts not previously considered). The results are shown in Figure 7 and Table 12. These results show that the regional gradients established independently for the modal phenocryst data generally conform to the gradients established for the total phenocryst population and that the total phenocrysts increase in abundance from about 30% by volume in the south and east of the region to greater than 40% by volume in the central, north and west of the region. The proportion of the total variation explained by the degree 3 surface is 63%.

The results suggest that the trends established for each phenocryst type may be dependent on the total phenocryst abundance and hence mutually dependent on the variations in each other. Trend surfaces were prepared to show the regional gradients of the individual phenocryst components as a ratio of the total crystal content, (Fig. 8 and Table 12).

The regional gradients established in this way closely resemble those obtained by plotting the phenocryst modal data independent of the total phenocryst content. One feature of the result is the lower goodness of fit

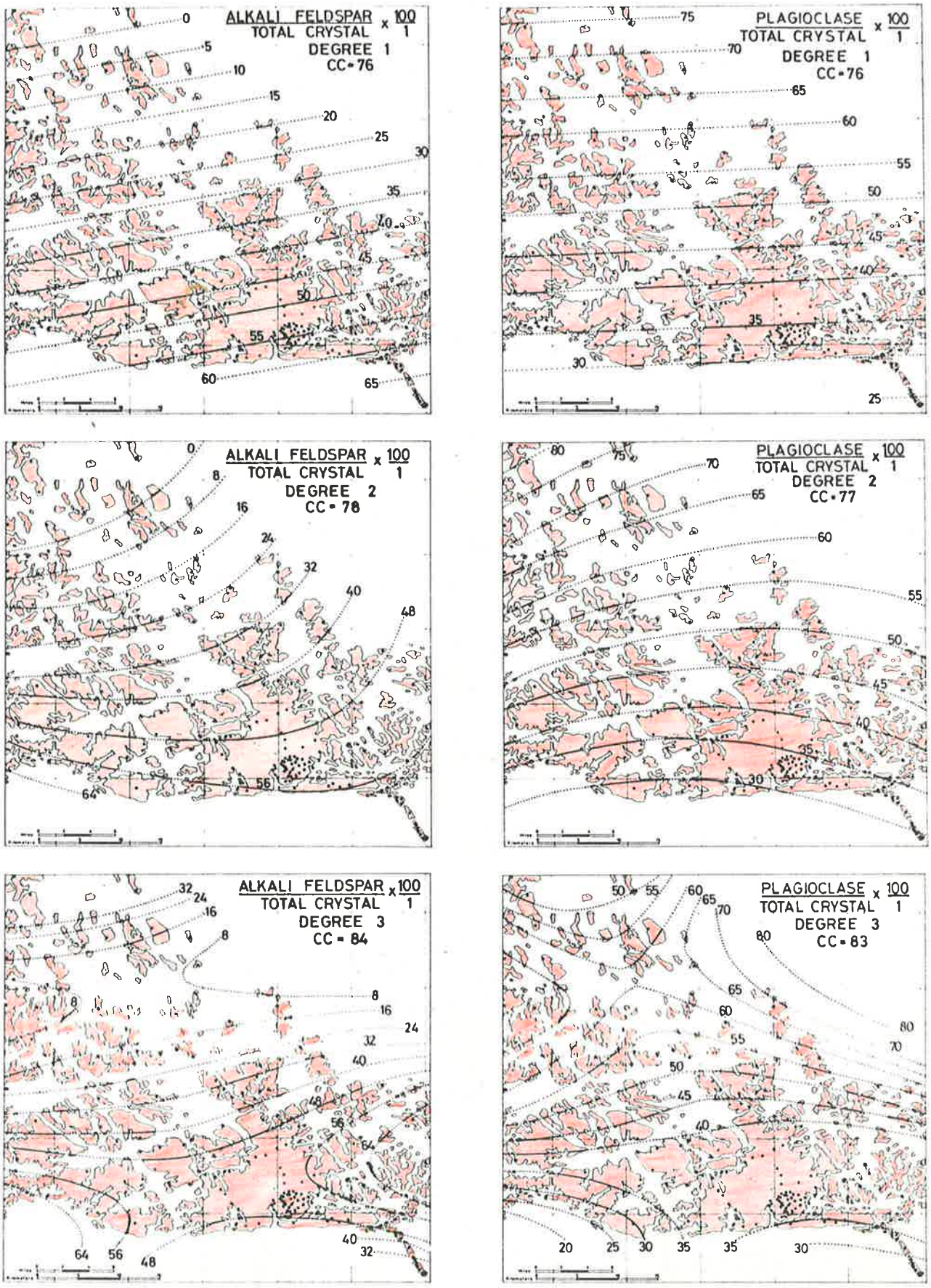


FIGURE 8: TREND SURFACE ANALYSIS
Ratio Feldspars / Total Crystal – Run 3

obtained for the plagioclase data whereas better goodness of fit is obtained for the potash feldspar data.

The improvement in the potash feldspar values indicates that the abundance of potash feldspar phenocrysts is dependent on the total abundance of phenocrysts in the rock body whereas the lower values for the plagioclase indicates that the abundance of this mineral is less dependent on the total phenocryst abundance. The results also suggest that the plagioclase and potash feldspar phenocryst abundances are mutually independent (within the limits imposed by the constant sum effect).

Statistical correlations were calculated between the three major phenocryst components in the revised data (Run 3). The results are tabulated below:

	Plagioclase	Alkali Feldspar	Mafic
Plagioclase	1.000	-0.519	0.648
Alkali feldspar	-0.519	1.000	-0.470
Mafics	-0.648	-0.470	1.000

These results show that the mafic phenocrysts have a strong positive correlation with the plagioclase phenocrysts and thus their abundances are considered to be dependent on each other. A weak negative correlation between the abundances of alkali feldspar and mafic phenocrysts suggests that these two minerals are mutually inter-dependent. The correlation between the plagioclase and potash feldspar phenocrysts is negative but its magnitude suggests some weak dependence between the two sets of data. However, the significance of this dependence is difficult to assess. The calculated means of the abundances of the phenocrysts through the region are as follows:

	%
Plagioclase	12.29
Mafic minerals	4.92
Potash feldspar	12.20

Conclusions The data are considered to be reliable and to indicate that the largest part of the sampled region represents a single lithological unit which displays a continuous gradation in the proportion of the individual phenocryst components with:

a. the plagioclase showing an increase in abundance from the south to the north and west (figure 9).

b. the ferromagnesian minerals increasing in abundance from the south to the north and west;

c. the potash feldspar showing an increase in abundance southwards from the north and west (figure 9).

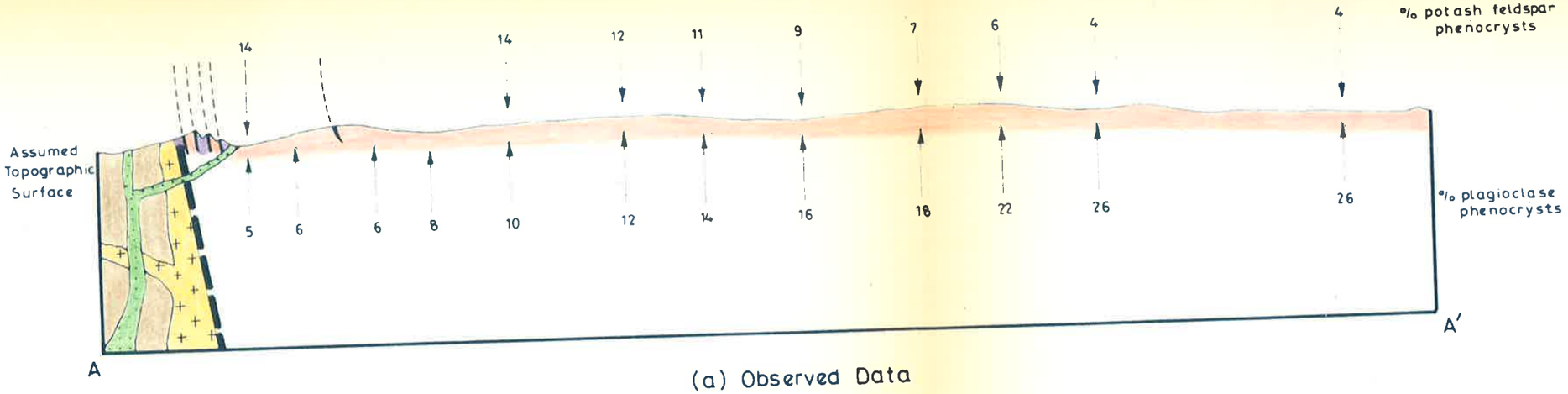
Quartz phenocrysts are present in too small a proportion (less than 2% by volume) to obtain accuracy in the data and hence to treat them statistically. However, it appears that the quartz increases in abundance as the plagioclase decreases.

Two hiatuses are present in the established trends, one in the south and one to the north and west. The reliability of the one to the north and west is questionable because of paucity of data.

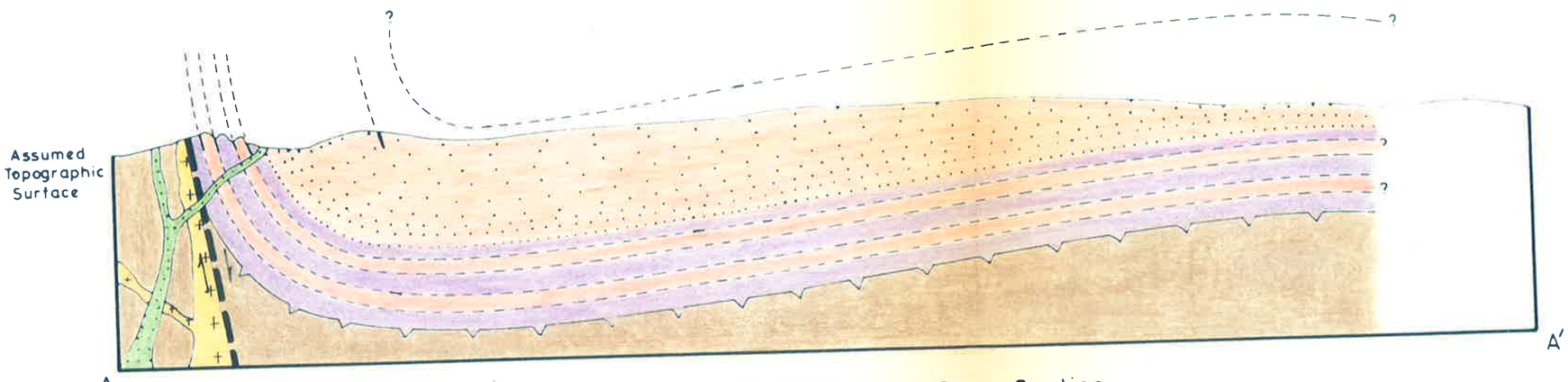
The Dyke Structure and an area to the north of the Ring Structure are mineralogically distinct from the rocks which comprise the larger area to the north and which are mineralogically distinct and anomalous when compared to the regional gradient predicted for this area.

6. CHEMISTRY AND PHYSICAL CONDITIONS OF CRYSTALLIZATION

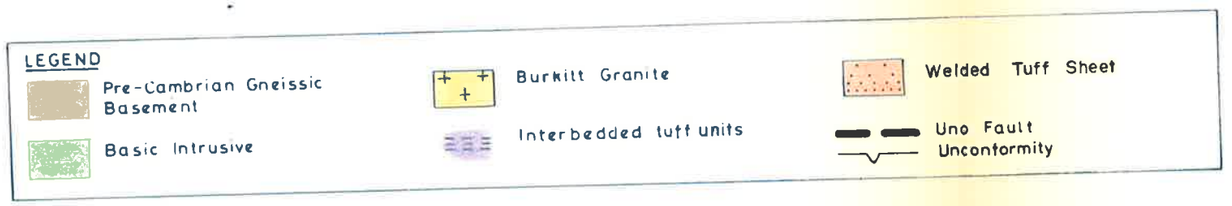
The variations in major elements are considered to be significant despite the fact that many of the rocks are subject to appreciable alteration and the basic members of the series are not represented. The alteration is especially apparent in those rocks in which relict pyroclastic and depositional textures are preserved and in these the



(a) Observed Data



(b) Interpreted Cross Section



SCALE : approx 2 miles = 1 5 cm

FIGURE 9 : DIAGRAMMATIC CROSS SECTION A—A' (fig. 2)

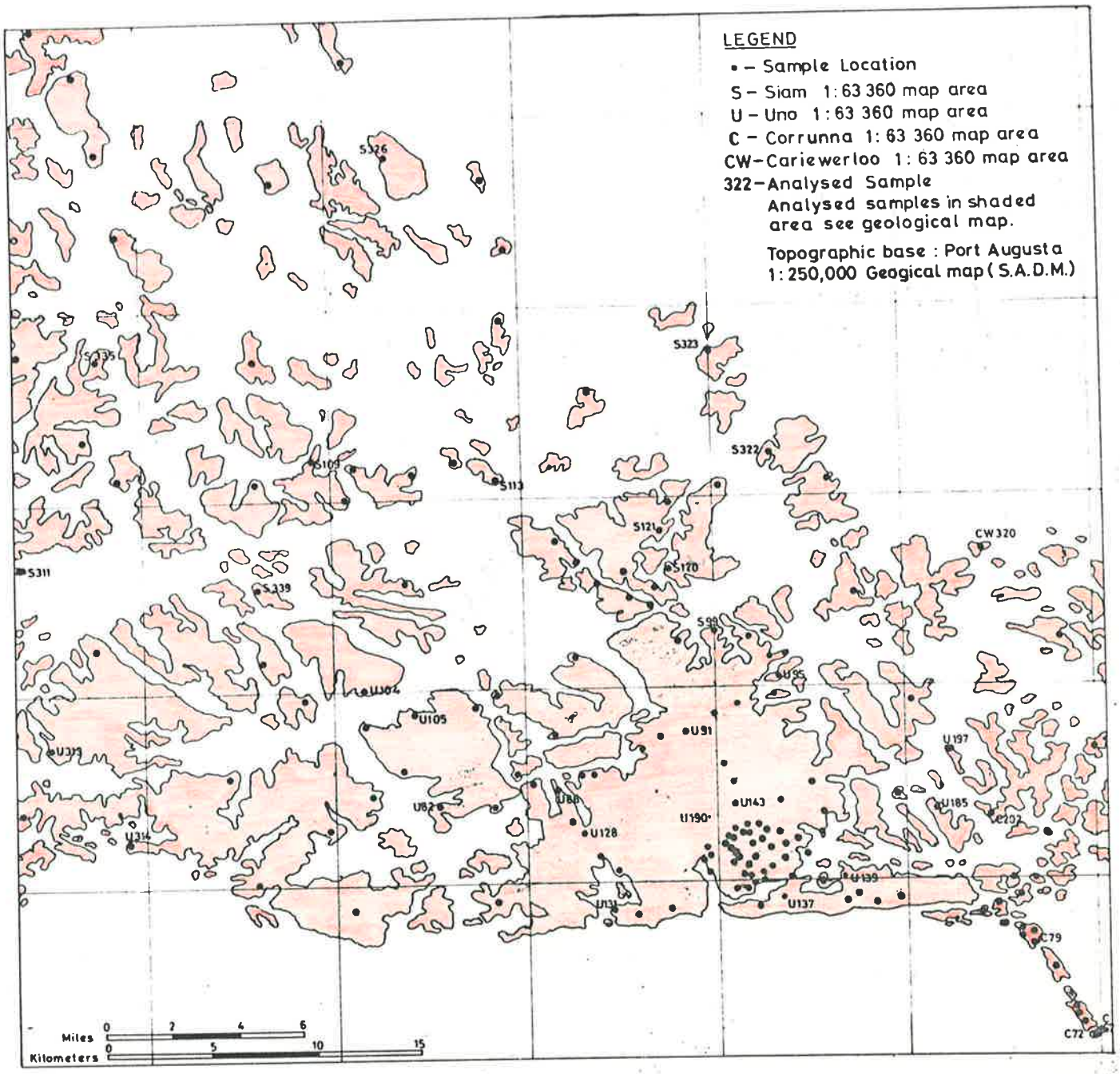


FIGURE 10 : CHEMICALLY ANALYSED SAMPLES
Numbers and Localities

anomalous alkali ratio is a conspicuous feature, although other ions do participate in the alteration.

The welded tuffs also provide evidence for some alteration but the analyses of these show a more normal alkali balance and the rocks are more nearly rhyolitic in composition (Fig. 11).

All analysed samples were taken from the surface and were selected to represent each lithological unit and chemical variation observed (Fig. 11). Sampling minimized the effects of near surface oxidation and leaching.

6.1 Major Element Variations

The major element variations when plotted against silica are shown in Figure 12. For most elements there is a wide degree of scatter, partly due to the large number of analyses, but principally to alteration. Nevertheless, there are discernible trends.

Little significance can be attached to the alumina trend.

In samples from the Welded Tuff Sheet (pCv_3) soda shows a relatively systematic distribution but many samples show enrichment in potash which is manifested in thin section by the crystallization of potash-rich minerals. Those rocks which fall in a field defined as greater than 5% K_2O and less than 72% SiO_2 have not been included in the construction of the K_2O differentiation curve (Fig. 12).

In contrast samples from the Arc Structure show anomalous values for both soda and potash and plot with a wide scatter. The total alkali content for both suites shows considerable scatter, which is a reflection of the general enrichment in potash.

A study of particular rocks and their analyses shows that the enrichment in potash is a result of deuteric alteration. Bowen (1928), Larsen et al (1938), Noble (1948) and others have advanced arguments to explain

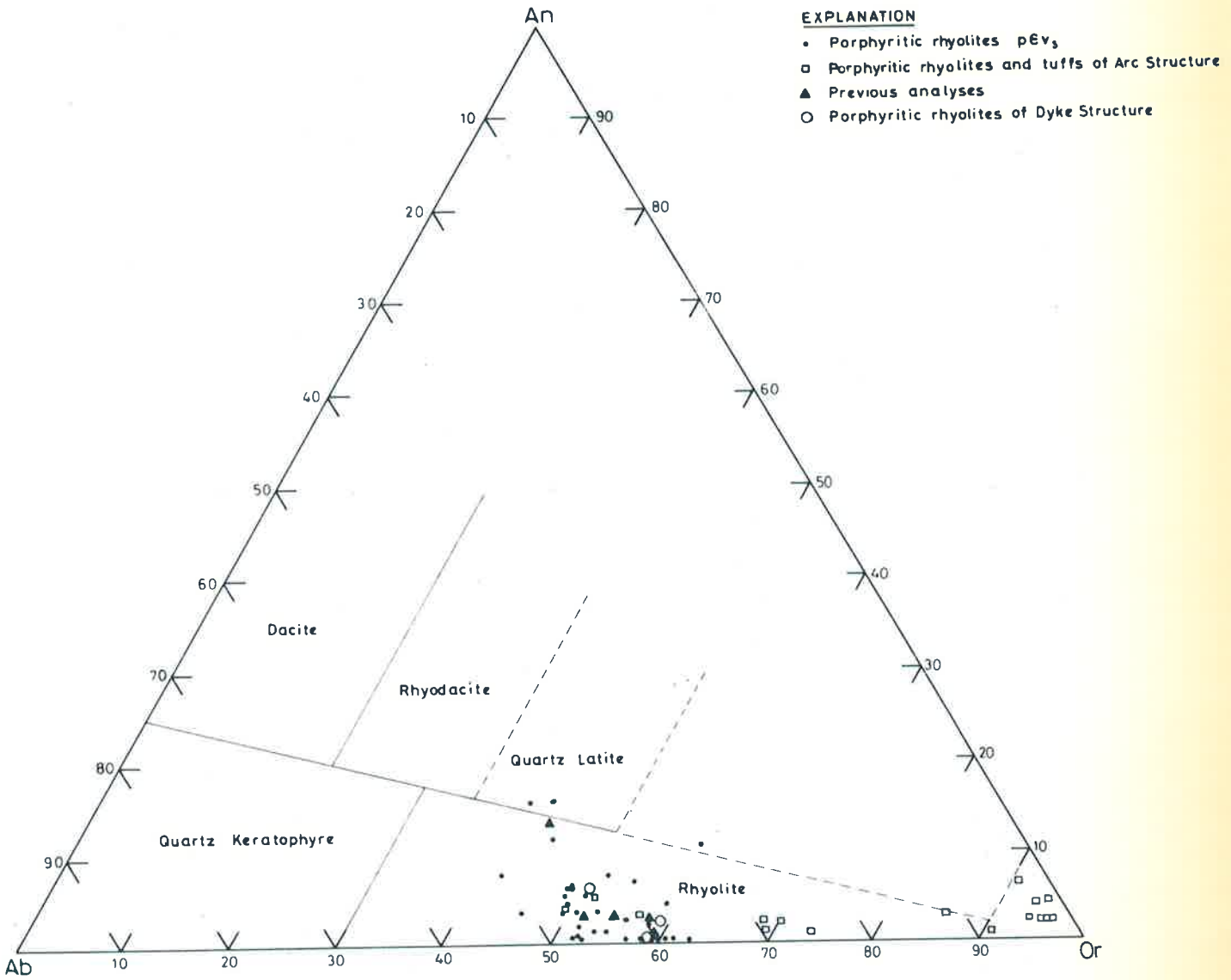


FIGURE 11: NORMATIVE Or-Ab-An RECALCULATED TO 100% (after O'Connor 1965)

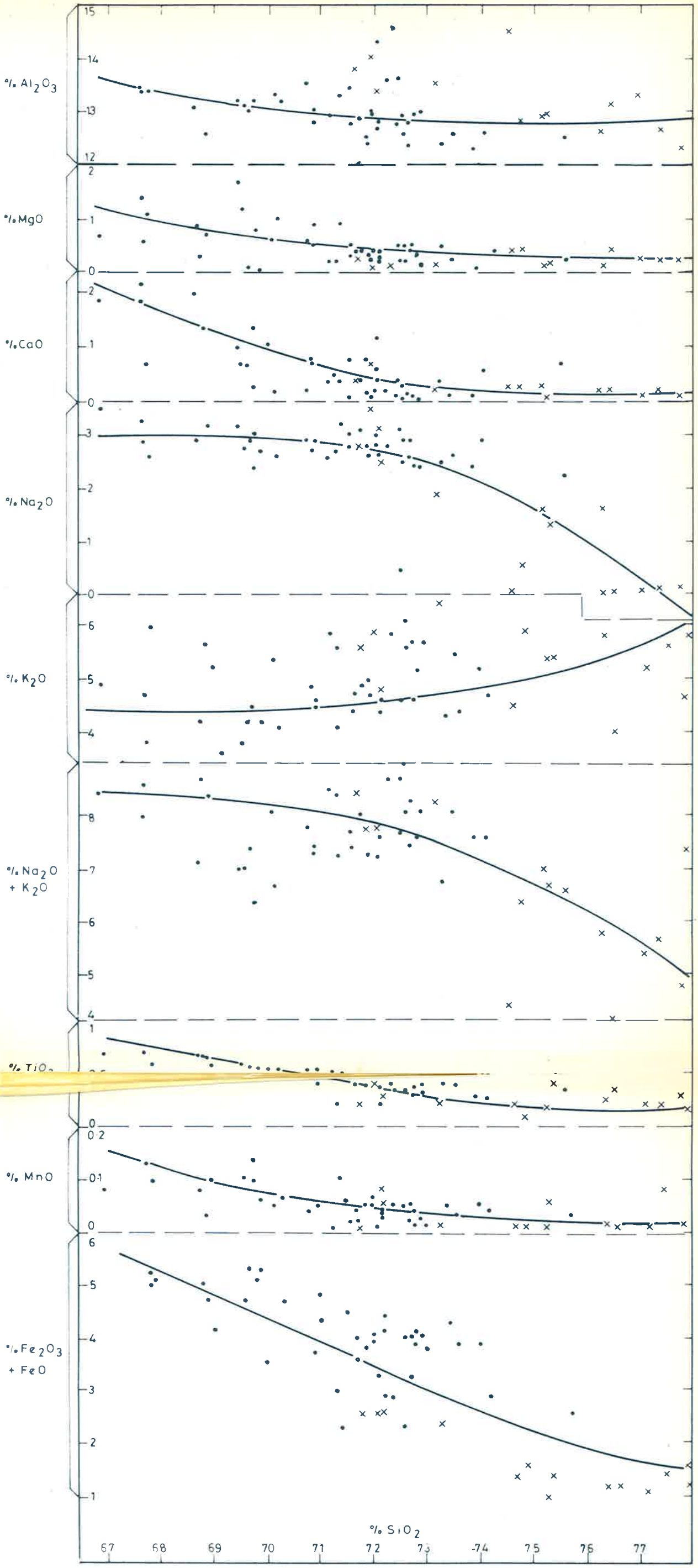


FIGURE 12: MAJOR ELEMENT VARIATION DIAGRAMS

the origins of potash-rich rocks by modifications of differentiation and fractional crystallization but these processes do not explain the present data. Scott (1966) considers potash enrichment could result from:

a. deuteric fluids which alter the original composition of aqueous-rich volcanic units by transfer, exchange, and removal of ions by an aqueous phase during cooling.

b. hydrothermal activity which changes the bulk composition by the introduction, redistribution and removal of ions.

c. weathering processes which alter pre-existing variation patterns, leach mobile ions and redistribute others by the growth of secondary minerals.

The analysed samples are not leached of mobile ions by weathering; instead, introductions of ions (e.g. potassium and silicon) into amygdules and along veins and fractures is apparent.

In some rocks it can be shown that deuteric fluids have effected the alteration by the introduction of potassium and the removal of sodium. In the more porous zones (those in which relict pyroclastic textures are preserved) the deuteric fluids have percolated through the rock unit, exchanged potassium for sodium, and carried the dissolved sodium elsewhere. In the Welded Tuff Sheet ($p\epsilon v_3$) potash enrichment is apparent towards the base but concomitant loss of soda cannot be proven.

In Fig. 12 curves for iron, magnesia and lime are more normal, although here again scatter is apparent. Thin section examination has shown that in addition to soda, also iron, lime and magnesia migrate as a result of the potash enrichment. The curves suggest that magnesia is relatively enriched with respect to lime and iron.

Titanium and manganese show the most regular variation and both show

a gradual but progressive decrease with increasing silica. The decrease in titanium towards the acid end is not distinctive of any particular differentiation series (Nockolds and Allen, 1953, 1954, 1956). The same can be said for the manganese.

The enrichment of magnesium with respect to iron is emphasised when the data are plotted on an AFM triangular diagram. The trend on this diagram conforms with the acid end of the calc-alkali series, illustrated by Nockolds and Allen (1953).

6.2 Trace Elements

A detailed study of the trace elements has not been made. In this study semi-quantitative analyses were made of a number of elements in four rocks (U183, U202, S109, C72). The following are the only elements of those sought that are present in significant proportions:

Lead:	50 to 250 ppm
Nickel:	30 to 200 ppm
Vanadium:	10 to 200 ppm
Barium:	500 to 3000 ppm
Strontium:	20 to 150 ppm
Rubidium:	600 to 800 ppm
Caesium:	250 to 300 ppm

The values appear to be higher than those obtained from other similar rock series (Nockolds and Allen, 1953, 1956).

At the writer's suggestion Mr. Russel Reid (1969) analysed ten samples collected as a part of this study, for barium. The results are presented in Table 12.

The analysed rocks represent a section from north to south through the proposed stratigraphic sequence (Table 13). Reid (op cit) found the barium to be relatively concentrated in the potash feldspar phenocrysts

Table 12: Barium Analyses

No.	Sample	Barium ppm	Potash %
1	S326	2920	4.90
2	S323	2400	3.80
3	S339	2200	4.70
4	S 99	3100	5.70
5	U104	1700	4.50
6	U105	2400	5.20
7	U 86	2300	6.10
8	U128	2300	4.70
9	U202	3900	5.00
10	C 79	7400	5.90
11	A156	3800	nd*
12	A189	2400	nd*
13	C 67	2000	4.60

* nd = not determined

(3000 ppm compared to 2000 ppm in the whole rock).

The variation of barium and potassium during differentiation is shown in Figure 13. The gradual increase in potassium during differentiation is manifested by the gradual increase in potash feldspar towards the top of the Welded Tuff Sheet ($p\epsilon v_3$). The variation in barium across the section is less regular and more complex although a general relationship with potash is found.

The early tuffaceous rocks (Analyses 11 and 12) represent the average concentration in the magma prior to differentiation. The lower values in the middle of the sequence are then due to depletion during differentiation, resulting in high concentrations in the late differentiates.

The systematic distribution in potash versus barium tends to support the stratigraphic succession proposed herein (Table 13). It is of interest to

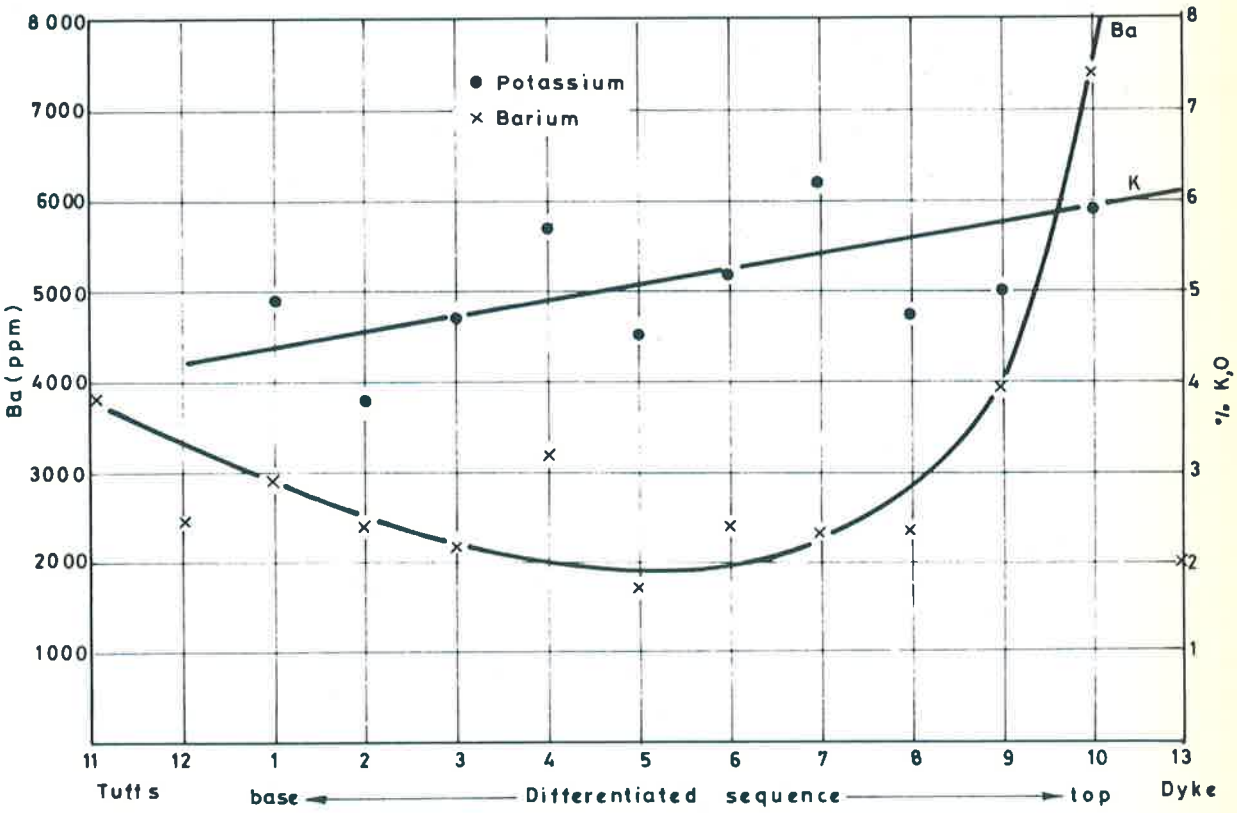


FIGURE 13: POTASSIUM AND BARIUM VARIATION

RG 5090

note that the sample analysed from the Dyke Structure (Analysis 13) equates chemically with the middle differentiates of the proposed succession. The ratio, Ba x 100 ÷ K, is not abnormally high. Deuteric processes have been operative in at least the basal parts of the succession but had they been general the ratio Ba x 100 ÷ K would probably be consistantly high. This is not established and the barium has probably not migrated on a regional scale. At the base of the exposed stratigraphy some potash feldspars are partially to completely replaced by barite whereas others in the same rock are replaced by sericite. It is suggested that the barium expelled from the potash feldspars has replaced some phenocrysts but that its movement is not widespread. Very little evidence has been found for the replacement of potash feldspar by barite in the Welded Tuff Sheet.

6.3 Physico-Chemical Conditions of Crystallization

Several factors must be considered before the analyses are compared and physico-chemical aspects of the primary magma and its subsequent history are inferred. Smith (1960) alludes to the difficulty in interpreting the pre-crystallization history of ash-flow deposits because the post-crystallization history, hydration, devitrification, alteration and recrystallization severely modifies the composition of the primary materials. In addition, Kuno (1950) and others point out that porphyritic rocks are unlikely to represent the true composition of differentiating magmatic liquids.

However, even when the above factors were taken into account it was considered that some of the chemical data might be able to be used to document aspects of the primary magma and its subsequent history. Steiner (1948), Ewart (1965) and others found that the New Zealand ignimbrites fall on differentiation curves of the associated flow rocks and thus data obtained both from ash-flow tuffs and from lava flows should be equally applicable.

6.3.1 Water-Vapour Pressure at Time of Differentiation

Following experimental demonstration of shifting of the quarternary isobaric minima in the system, $NaAlSi_3O_8$ - $KAlSi_3O_8$ - SiO_2 - H_2O (Ab-Or-Q-H_2O), with changes in water pressure (Tuttle and Bowen, 1958, p.75), several investigators have used these data to estimate water pressures and depth of formation of natural silicic magmas (Carmichael, 1962; Cornwall, 1962; Ewart, 1963; Putnam and Alfors, 1965; Bateman, 1965; Scott, 1965; Christiansen and Lipman, 1966; Lipman, 1966). Kleeman (1965) and others have discussed the inherent weaknesses of Bowen and Tuttle's diagrams for the interpretation of the physio-chemical conditions of crystallization in that it does not take into account the anorthite component of natural alkali feldspars. Many authors have warned of the need to select fresh, unaltered and uncontaminated rocks from which to obtain the relevant analytical data.

As already noted many rocks have been subjected to deuteric alteration manifested in anomalous alkali balances, (Appendix C). Others have a more normal alkali balance and for a large proportion of these there is no indication of alteration as a result of deuteric, pneumatolytic or chemical weathering processes. An attempt is therefore made to determine the water pressures during formation of the magma.

In an attempt to restrict errors (Appendix B) only those rocks have been selected in which normative anorthite is less than 2% (see Appendix D) and in which there is no evidence for alteration of the feldspar phases.

From the 56 rocks analysed only 13 appear to fit these requirements. The data from these rocks are plotted on the Q-Or-Ab diagram in Figure 14 and when linked define a clear trend (Trend 1) to intersect the molaric minima at about 600 bars pH_2O. If the data are valid then the water vapour pressure at the time of differentiation was in the range 500 to 600 bars.

These pressures are considerably lower than those inferred for rhyolitic magmas by most other authors, although they are equivalent to those deter-

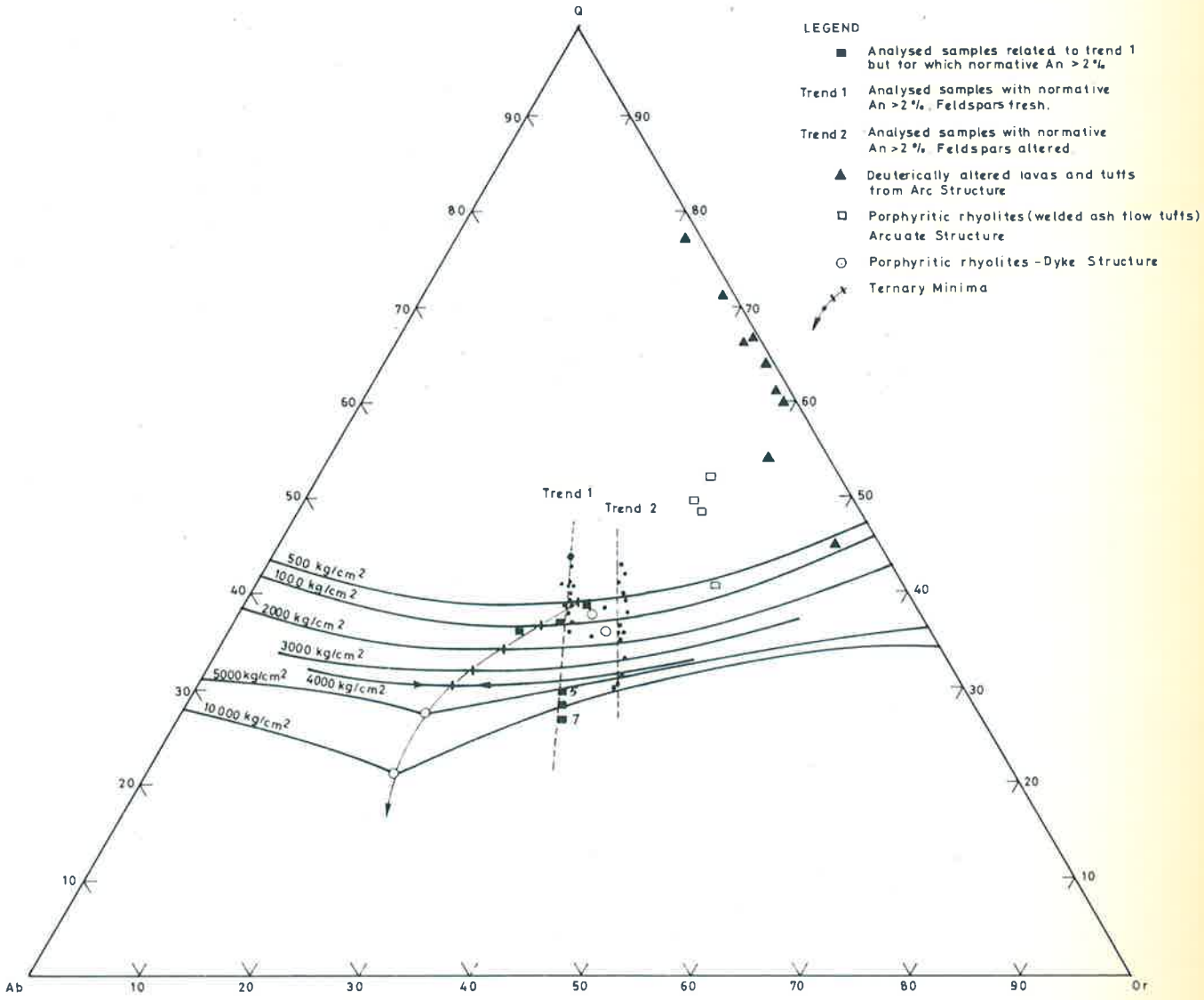


FIGURE 14: NORMATIVE Q-Or-Ab TERNARY DIAGRAM
Adapted from Tuttle & Bowen (1958)
Luth Jahns & Tuttle (1964)

TABLE 13 STRATIGRAPHIC SECTION

Summary of Lithologies

Formation	Member	Welding Zones	Welding Degree	Texture	Alteration Addition	Alteration Subtraction	Genesis	Cycle
Top								
pЄv3 Welded Tuff	crystallized tuff	1	strong	microcrystalline granular	-	-		
		2	strong	granophyric	-	-		
		3	strong	microcrystalline granular	-	-		
		4	strong	spherulitic microgranular	Mg+Ca+Fe	Na+K	Ash Flow Tuff	3
		5	moderate	snowflake, patch	K	Na		
pЄwt Welded Lithic Tuff	welded lithic tuff	1	moderate	pyroclastic	-	-		
pЄvt Vitric Tuff	vitric tuff	1	weak to moderate	vitroclastic	SiO_2+K	Na+Ca+Mg+Fe	Ash Fall Tuff	
pЄfbl Fluidal Banded Rhyolite	fluidal banded rhyolite	1	moderate	breccia	Mg+Fe	Ca+Na		
		2	strong	fluidal banded	K	Na+Mg+Fe		
pЄl3 Porphyritic Rhyolite	upper breccia	1	moderate	breccia	-	-		
	banded rhyolite	2	strong	banded snowflake	Mg+Ca+Fe	Na+K		
	massive rhyolite	3	moderate	snowflake	K	Na		
pЄv2 (upper) Welded Tuff	crystallized tuff	1	moderate	snowflake	K	Na		
		2	strong	recrystallized pyroclastic	-	-		
pЄal Amygdaloidal Rhyolite	amygdaloidal rhyolite	1	strong	recrystallized pyroclastic amygdaloidal	SiO_2+Ca+Mg	Na+K	Ash Flow Tuff	2
	perlitic and banded rhyolite	2	strong	perlitic	Mg+Ca+Fe	Na+K		
		3	strong	banded snowflake	K	Na		
		4	moderate to strong	snowflake	K	Na		
	welded tuff	5	moderate	recrystallized	SiO_2	K+Na		
pЄv2 (lower) Welded Tuff	crystallized tuff	1	strong	microcrystalline	Mg+Ca+Fe	Na		
		2	weak to moderate	recrystallized pyroclastic	K+Fe	Mg+Ca+Na		
pЄpt Pumiceous Tuff	pumice	1	fused	pumiceous	SiO_2+Mg	Na+Fe		
	vitric tuff	2	weak	vitroclastic	SiO_2+K	Na+Mg+Fe		
	pumiceous tuff	3	weak	vitroclastic	SiO_2	Na+K+Mg+Fe	Ash Fall Tuff	
pЄct Crystal Tuff	pumiceous crystal tuff	1	moderate	pyroclastic	SiO_2+Fe	K+Na		
	crystal tuff	2	strong	granophyric	-	-		
pЄl2 Porphyritic Rhyolite	vitric tuff	1	moderate	vitroclastic	SiO_2+K	Na		
	perlitic rhyolite	2	strong	perlitic amygdaloidal	Mg+Ca+SiO_2	Na		
	porphyritic rhyolite	3	moderate	banded snowflake	K+SiO_2	Na+Mg+Ca		
pЄv1 Welded Tuff	crystallized tuff	1	moderate	snowflake	K+Fe	Na+Mg+Ca	Ash Flow Tuff	
		2	strong	microcrystalline granular	Mg+Fe+Ca	Na		1
		3	strong	granophyric	-	-		
		4	strong	microcrystalline granular	Mg+Fe+Ca	Na		
		5	moderate	snowflake	K+Fe	Na+Mg+Ca		
	lapilli tuff	6	moderate	pyroclastic	K+Fe	Na+Mg+Ca		
pЄl1 Porphyritic Rhyolite	upper breccia	1	weak to moderate	breccia	K	Na+Mg+Ca+Fe		
	flow rock	2	moderate to strong	banded snowflake	K	Na+Mg+Ca+Fe		
	basal breccia	2	weak	breccia	K+SiO_2	Na+Mg+Ca+Fe		
pЄt Lithic and Lapilli Tuff	lapilli tuff	1	fused	pyroclastic	K	Na+Mg+Ca+Fe	Ash Fall Tuff	
	lithic tuff	2	fused	pyroclastic	K+SiO_2	Na+Mg+Ca+Fe		
Bottom								

mined by Lipman (1966) for some ash-flow magmas from Southern Nevada.

Two analyses, 5 and 7, have respectively 91.96% and 93.48% of the norm as quartz and feldspar and 83.86% and 86.11% of the norm as albite, orthoclase and quartz. These analyses have a comparatively high An (anorthite) content (8.10 and 7.37% as a percentage of alkalis plus silica respectively). Hence the determined water-vapour pressure may be erroneously low as the rocks deviate from the experimentally determined system. However, the error from this source is unlikely to be more than 100 to 200 bars.

Cornwall (1962) estimated water-vapour pressures of 3,000 to 4,000 bars for rhyolitic volcanis rocks from the Beatty area, Nevada. His points show much scatter and include several genetically unrelated units and thus are not amenable to interpretation from the data of Tuttle and Bowen. Ewart (1963) interprets the chemistry of Quaternary pumice falls from the Taupo area, New Zealand, as indicating that the first falls crystallized at slightly higher pressures of between 2,000 and 3,000 bars. These rocks also have a high An content which suggests that the values should be somewhat higher than determined. The compositions of the pumices (Ewart op cit) also appear unreliable because of probable groundwater leaching. Christiansen and Lipman (1966), on the basis of a single analysis, considered that a rhyolite flow in Nevada crystallized at 1,000 bars. This figure is necessarily vague because only a single analysis was considered.

6.3.2. Water Content, Temperature and Depth of Magma During Crystallization and Differentiation

Assuming that a part, at least, of the Gawler Ranges Volcanic Complex differentiated and crystallized at a water pressure in the range 500 to 800 bars, then some limiting conditions for water content, temperature and depth of the magma during crystallization and differentiation may be considered.

If the magma was saturated with water during differentiation and crystallization, equilibrium water contents and temperatures could be derived dir-

ectly from the experimental data of Tuttle and Bowen (1958; Fig. 28).

The depth of the top of the magma chamber can be inferred by assuming that the total confining pressure (equal to water pressure) is lithostatic (Lipman, 1966). Accordingly, at 500 bars water pressure the equilibrium water content of the rhyolite magma would be about three weight percent, the temperature would be about 750°C and the depth of the top of the magma chamber would be about 1.5km. At 700 bars water pressure the equilibrium water content of the rhyolitic magma would be a little less than 4 weight percent, the temperature would be about 720°C and the depth to the magma chamber would be about 3km.

Lower parts of the magma column (of which analyses 5 and 7 are probably representative) would have nearly the same partial pressure of water, assuming equilibrium diffusion of water within the magma, but the total water content would decrease downward (Kennedy, 1955; Fig. 1). In the lower parts of the column the temperatures would be higher during phenocryst crystallization as the result of a lower water content and a lower ratio of water pressure to total pressure.

The high water contents determined above accord with the presence of two phenocrystic feldspars in the rocks (Tuttle and Bowen, 1958, p 130-137) and makes the estimates of pH_2O and temperature appear reasonable.

The conclusions drawn herein must be considered with caution because of differences between natural silicic magmas and the experimentally deterimed system. However, the figures are a guide for further work.

There is field and petrographic evidence to suggest that the rocks of the Gawler Ranges are largely ash-flow tuffs. Possibly magmatic water pressures have to approach the load pressure in order to trigger an ash-flow eruption, but this has not been demonstrated. If, instead, water pressures in ash-flow magmas are generally less than load pressures then precise values for temperature, depth, and water content of the magma cannot be inferred from

presently available data although Brown (1970, Fig. 1) has established that melting can occur at 500 bars water pressure with water contents of much less than 3 weight percent when the water pressure is less than the confining pressure.

Ross (1964) has suggested that water pressures of 1 to 2% may be the maximum required to energise ash-flow eruptions and, if correct, these values would preclude saturation at confining pressures greater than a few hundred bars (Tuttle and Bowen, 1958; Fig. 28). If water contents of the Gawler Ranges rocks are similarly low the indicated water pressures would necessarily be partial pressures at considerably greater confining pressures and depths. A water content of about 1% as suggested by Ross (1964) in a magma at 500 bars partial pressure of water would indicate a depth of about 8km to the top of the magma chamber. This depth would not be totally improbable.

In any case, it seems probable that a relatively low water content was necessary for the magma to rise any distance prior, perhaps, to encountering additional free water (see Brown 1973).

Lipman (1966) concludes that-

" ... it is unclear to what extent the relatively low water pressures ... are representative of those of rhyolitic magmas. Most previously reported values are considerably higher but their interpretation is so uncertain that firm conclusions are not warranted. Possibly rhyolitic magmas that occupy shallow caldera-producing chambers, rupture their roofs and erupt at relatively low water pressures, whereas magmas confined at greater depths can develop higher water pressures before eruption. Thus ash-flow eruptions may be related to rapid expulsion of large, shallow magma bodies rather than to unusually high,magmatic water pressures."

6.3.3 Crystallization History

The plot of the compositions of the analysed rocks of the Gawler Ranges

Volcanic Complex, in terms of mormative quartz-albite-orthoclase (Fig. 14), has been referred to.

In this diagran the rock compositions are scattered widely and even the trend (Trend 1, Fig. 14) suggested earlier as reliably representing crystallization conditions ranges from the quartz side of the quartz-feldspar boundary to the orthoclase side of the locus of the ternary minima.

From none of these compositions could plagioclase be expected to initially crystallize. This is in striking contrast to the textural evidence which shows plagioclase phenocrysts, commonly corroded and embayed,and in many cases mantled by potash feldspar. The plagioclase phenocrysts never contain phenocrysts of quartz or alkali feldspar. Alkali feldspar also forms discrete crystals (compositionally similar to that of the mantle feldspar) which unlike the plagioclase is not mantled or embayed.

Textural evidence thus indicates a sequence of crystallization as follows: plagioclase ⟶ plagioclase + alkali feldspar (with earlier formed crystals dissolving) ⟶ plagioclase + alkali feldspar + quartz.

It thus seems probable that even the compositions which plot on Trend 1 in Fig. 14 are not original compositions and that these, as with the majority, have been modified.

The earlier postulated water pressures must, therefore, be accepted with caution though, in any case, a possible somewhat higher PH_2O value, consequent on a less potassic magmatic composition will cause almost negligible change to the temperature of initial crystallization (see Brown 1970, Fig. 1).

Fig. 14 clearly illustrates the enrichment in potash and silica that has affected most, if not all, samples analysed. The alteration is most intense in those lithologies from the Arc Structure and tends to decrease in intensity upwards through the pile to the Welded Tuff Sheet. Textural evidence in thin section shows late-stage,magmatic enrichment in potash and silica manifested as mantles to earlier formed crystals and this enrichment continues as a

post-extrusion, deuteric phase, as evidenced by subsequent alteration and by amygdules infilled with silica and potash-rich phases. Evidence has been presented which shows that the deuteric phenomena are more comspicuous in the rocks which retain a relict, primary texture. Enrichment in the rocks which are completely reconstituted by crystallization is probably almost due entirely to magmatic crystallization prior to extrusion.

As a result of extrusion, crystallization rapidly changes from an isobaric process at depth and elevated pressures to and adiabatic process at the surface and at atmospheric pressure.

While crystallizing at depth the hydrous and volatile substance have been held in solution by pressure. A sudden release of pressure with concomitant loss of volatile material and a drop in the water pressure promotes crystallization whether or not heat is lost from the system. As discussed above such crystallization is likely to have been already influenced by the concentration of potash and silica-rich fluids.

Boyd (1961) calculated the maximum heat losses during rise of a rhyolitic magma to the surface and showed that the important factors are cooling by evaporation and expansion of the vapour phase. Boyd (op cit) also calculated the heat loss during the emplacement of a rhyolitic pyroclastic flow and found that losses were mainly due to radiation from the exposed surface and conduction to the ground and that conduction and convection to the air were negligible.

In a magma with 3.5% initial water the maximum cooling is about 120^{o}C (Boyd, 1961; Fig. 9,10,11); however, a real magma would cool less than this, by an amount proportional to the amount of departure from reversible adiabatic expansion, violent rhyolitic eruptions cooling less than quiescent eruptions. Although actual heat loss from the magma during rise through the conduit cannot be adequately evaluated, eruption can reasonably be

assumed to have been nearly isothermal (Christiansen and Lipman, 1966).

Thus the temperature of the magma at eruption is unlikely to have been much greater than 580°C. At this temperature and at about one atmosphere pressure the magma would rapidly crystallize. The rate of crystallization would vary somewhat from place to place in a flow. In the outer regions and close to the base of a single flow chilling would occur while in the innermost portions more gradual crystallization would ensue.

Because of the great age of the Gawler Ranges rocks no glass remains. Instead widespread devitrification and crystallization has occurred.

Superimposed on the crystallization process is a post-depositional welding process. Welding must be a rapid process initiated immediately following deposition. Strongly welded zones are non-porous and late stage hydrous and volatile material continuing the enrichment process (commenced in the late-magmatic stage) has not effected the widespread replacement of soda by potash and the migration of other ions, to nearly the same extent, in the welded zones as has occurred in the porous, non welded zones.

The principal modification of the products of primary crystallization in the porous zones is a continuation of the mantling of soda-rich feldspars by potash feldspar and the sericitization of early potash feldspars and in places their replacement by barite. Migration of magnesium, calcium and iron accompanies the alteration.

The deuteric alteration decreases in intensity towards the centre of intensely welded non-porous zones.

7. THE PRIMARY ROCK TYPES AND THEIR POST EMPLACEMENT HISTORIES

An understanding of the nature of the primary rock types can be assisted greatly through an understanding of the products of alteration, welding* and crystallization.

The stratigraphic succession is shown in Table 13 which also gives the principal texture features of the various members, the degrees of welding, and the zones of chemical alteration.

Even though a wide range of textures is developed, the phenocryst components are sufficiently common and distinctive to show that the lithologies are closely related. Petrochemical studies indicate the rocks to be derived from a single magma and there is no reason to believe that more than one source was involved.

7.1 Crystallization Textures

In interpreting the stratigraphic succession and its genesis, two concepts may be considered. If rocks which display a fluidal-banding crystallize from a fluid medium, then such rocks are lavas. The succession would thus be made up of an interbedded series of pyroclastic rocks and lavas. If, on the other hand, we adhere to the concept that pyroclastic deposits can be intensely welded such that the primary texture is completely destroyed and the rocks can form a melt and, under suitable conditions can flow, then the succession represents a layered series of pyroclastic rocks subjected to varying degrees of welding, and fluid motion.

---

* Welding - Flattening of shard and pumice structures due to load compaction and internal heat without obliteration of the characteristic ash structure. Intense welding may result in extreme flattening and slight flowage and may partially obscure the original structure.

The origin of the formations in which pyro- and vitro-clastic* structures are preserved is not in question. However, snowflake, fluidal banded and perlitic textured formations and members show the characteristics of both lavas and pyroclastic deposits and their origin cannot easily be diagnosed.

7.1.1 The Snowflake Texture

Snowflake texture (Snyder, 1962, p 205-206 and 211-212) is equivalent to the informal term "patchy polarisation" used earlier by Williams et al (1966, p 123). Anderson (1969, p 2077) stated that -

> "the texture is found only in samples from volcanic units exhibiting all or most of the petrographic and field characteristics of densely welded ash-flow tuff (Ross and Smith, 1961; Smith, 1960). Rocks of definite or probable lava flow origin have not been found to exhibit snowflake texture."

This suggests that snowflake texture is produced by crystallization of densely welded ash-flow tuff but not by crystallization of glassy flow rocks.

Lofgren (1968, p 38-39) concluded that only heat, water and perhaps "some pressure" were necessary to produce the texture but that its development could not be related to definite temperatures and pressures. Anderson (1969) indicated that a conclusive answer to the origin of snowflake texture must await the accumulation of additional analytical and experimental data.

---

* Pyroclastic - The structure of unreworked solid material of whatever size explosively or aerially ejected from a volcanic vent.

* Vitroclastic - Structure typical of fine, fragmental, glassy rocks, in which shards usually have a crescentic, rudely triangular, or somewhat concave outline.

In some areas (e.g. Porphyritic Rhyolite $p\epsilon 1_1$) the rocks must be classified as rhyolites "sensuo-stricto" on the basis of their mineralogy chemistry and lack of distinctive pyroclastic textures. However, in most cases (e.g. Porphyritic Rhyolite $p\epsilon 1_2$, $p\epsilon 1_3$, Amygdaloidal Rhyolite $p\epsilon a1$) clear textural and structural evidence for a pyroclastic origin can be found. The incipient development of snowflakes in tuffaceous rocks, the transition from pyroclastic, to pyroclastics with snowflakes, to snowflake texture and the undoubted pyroclastic textures in some units all indicate that the texture is the product of the extreme welding and crystallization of pyroclastic rocks.

Features of snowflake textured rocks not previously described in the literature include the indications of flow banding and fluid motion. Flow banding indicates that the rocks had an inherent viscosity and the presence of flow-top breccias indicates that the pyroclastic ejecta was a fluidized mass of solids, enriched in volatiles with a high internal heat flow that welded, became molten and flowed prior to the deposition of overlying units. Once the deposit is molten it displays all the physical properties of a lava flow. The flow textures are not necessarily restricted to the base of individual units; a feature of welded ash-flow deposits recorded by other workers.

Banded phases of the snowflake textured rocks reach their optimum development in the Fluidal Banded Rhyolite ($p\epsilon fb1$).

7.1.2 Fluidal Banding

The Fluidal Banded Rhyolite ($p\epsilon 1_3$) possess all the features of the snowflake textured rocks, including the presence of abundant rock fragments.

Rittman (1958) described rheoignimbrites which develop when an ignimbritic tuff flow comes to rest upon a slope. A fluidised mass of solids and gas plus possible drops of magma loses most of its gaseous volatiles and settles but still is very hot. Liquefaction may occur as a secondary phenomenon in the basal part, and this will produce locally the characteristics, such as flow structure, which are normally found in lava. The mass may tend to flow and in some cases secondary lava will extrude through its own breccia cover. Rutten et. al (1971) have shown that rheoignimbrites may develop very strong fluidal laminations. General physico-chemical laws governing such eruptions have not been defined but it is evident that if rheoignimbrites do exist in nature then differentiation has been going on under conditions radically different from those occurring during magmatic differentiation; that is, at high temperatures and low (almost atmospheric) pressures.

The Fluidal Banded Rhyolites could represent a volatile-rich, siliceous magma. The spherulitic fragments and many of the phenocryst phases would then have been incorporated from earlier extruded and solidified rhyolites forming the walls of the vent or incorporated from underlying rock units after extrusion. However, the rock association and the features described are best explained in terms of rheoignimbrite petrogenesis. The spherulitic particles then represent recrystallized, but evidently immiscible, rock fragments. Many, and probably all, of the feldspar and quartz phenocrysts are related to these fragments which could represent the coarser-grained pyroclastic ejecta. The groundmass could well be the product of fluidisation of a mass of shards, pumice fragments and fine-grained pyroclastic ejecta. The chilled surface of the mobile fluid mass has brecciated under the influence of the pressure of the still-fluid lava below and the

breccia fragments are recemented by the mobile liquid. The degree of contortion of the fluidal laminae about solid particles suggests a viscous fluid.

7.1.3 Lava Textures

In two units (Porphyritic Rhyolite $p\epsilon 1_2$ and Amygdaloidal Rhyolite $p\epsilon a1$) perlitically-cracked, layers of devitrified glass overly the snowflake textured rhyolites which display fluidal banding (see Table 13). The glass layers are characterised by fragmented phenocrysts and the development of spherulites and lithophysae. Recrystallized rock fragments are recognized from some areas. Most importantly the vitric rock contains amygdules which in fact are restricted to these horizons or their vicinity. The vitric layer is a glass chilled from a melt.

7.2 Vapour Phase Crystallization

Those units in which pyroclastic, snowflake, fluidal banded and lava textures are observed have been subjected to appreciable late-stage alteration. In most cases the alteration can be related to the introduction of silica and potash, with concomitant depletion of soda and migration of magnesia, lime and iron.

A study of the petrochemistry shows that the introduction of potash and silica is greatest in those rocks which crystallize from a melt and decrease progressively as the textures change from vitric to fluidal-banded to snowflake to granophyric. (Refer sections on Petrochemistry Vitric Tuff ($p\epsilon vt$) Page 126, Fluidal Banded Porphyritic Rhyolite ($p\epsilon fb1$) Page 121, Porphyritic Rhyolite ($p\epsilon 1_3$) Page 112 and Welded Tuff ($p\epsilon v_1$) Page 60. Also refer Table 13). Soda shows its greatest depletion in the rocks which crystallize from a melt and is progressively less depleted through the same

textural range. No chemical or petrographic evidence has been found to show where the soda is localized but calcium, magnesium and iron migrate and are localized in the granophyric textured rocks. Iron appears to migrate further from its source than does magnesium which migrates further than calcium. (See discussion Petrochemistry Welded Tuff ($p\epsilon v_1$ page 60)).

The development of snowflake, banded and lava textures could be a function of the introduction of volatiles, potash and silica. As volatile enrichment progressively increases snowflake, banded and fluidal-banded textures develop. Where the volatiles reach their maximum concentration melt forms. This mechanism requires that volatile enrichment precedes the welding process and the formation of melt and is supported by the upper levels of the Amygdaloidal Rhyolites ($p\epsilon al$) where pyroclastic rocks are enriched in volatiles prior to or at the time of the welding process.

An alternative mechanism requires volatile enrichment at the time of or following the welding process and the formation of melt. Rocks which crystallize from melts may be more porous (by virtue of the perlitic cracks) and have permitted the entry of volatiles to a greater extent than other units. In either case the volatile enrichment is deuteric and parallels that of laboratory ion-exchange experiments (Orville, 1963) and predicted deuteric effects. Deuteric effects are "those that have taken place in direct continuation of the consolidation of the magma of the rock itself" (Sederholm, 1929, p 870). Reactions between a hot aqueous phase and a glassy phase are deuteric. These alterations occur after emplacement during the cooling period and result in ionic transfer and exchange between a hot fluid phase, and the unstable, reactive volcanic glass. Zones of devitrification, vapour phase crystallization and fumarolic activity are products of deuteric activity (Smith, 1960).

Types of ionic exchange and reactions are probably controlled by the temperature gradient, confining pressure, water pressure, composition of altering fluids, and composition of the volcanic glass (Scott, 1966). Scott (op. cit.) and Lipman (1965) have both shown the same inverse relationship between the distribution of sodium and potassium in ignimbrites.

7.3 Granophyric Crystallization

The red Welded Tuffs ($p\epsilon v_{1,\ 2,\ 3}$) known by the field name 'porphyry', are erected as separate units on the basis of their distinctive appearance in the field rather than on the basis of petrogenetic criteria. The textures developed within them are gradational from those in the underlying and overlying tuffaceous units. For the most part the textures developed in the vicinity of the contacts are the snowflake varieties and are distinguished from the adjacent rock units only on the basis of the greater abundance of iron oxides in the Welded Tuffs. The snowflake textures gradually give way to cryptocrystalline, microcrystalline, microlitic, and in the central portions of the thicker units, granophyric textures.

The relationship with the adjacent rock units is most clearly displayed in two areas

(1) in the subsidiary anticline to the west of the mapped area and

(2) in the unit ($p\epsilon v2$) overlying the Amygdaloidal Rhyolites.

In the west, a Welded Tuff is sandwiched between two layers of lithic tuff. The lithic tuff is unwelded except near the contact with the Welded Tuff. Along the contacts eutaxitic textures are displayed and gradually give way to an overall microcrystalline texture in the thicker parts of the Welded Tuff. The red Welded Tuffs ($p\epsilon v_2$) which overlie the Amygdaloidal Rhyolite ($p\epsilon al$) are locally amygdaloidal. The amygdules are similar to those found in the Amygdaloidal Rhyolites in that they are flattened into lenticular

and sinuous shapes which are sub-parallel. Evidence for a pyroclastic origin is nearly always lacking, although in a few samples shadowy rock fragments can be detected in thin section. For the most part the unit is micro- or crypto-crystalline. Nevertheless, it is apparent that the Welded Tuffs ($p\epsilon v_1$ and $p\epsilon v_2$) form by the recrystallization of pyroclastic rocks.

The relationship of the uppermost Welded Tuff Sheet ($p\epsilon v_3$) to the underlying rock units is similar. The contact between the Welded Lithic Tuff ($p\epsilon wt$) and the Tuff Sheet ($p\epsilon v_3$) is mapped on the basis of gradational colour changes. The Welded Lithic Tuff is pale brown to dark brown whereas the Tuff Sheet is dark reddish-brown or even black in the vicinity of the mapped contact. The colour changes correspond to a conversion from an intensely welded lithic tuff to a micro- and crypto-crystalline rock (Tuff Sheet) in which an eutaxitic texture is locally preserved. The relict pyroclastic texture, in the latter, is preserved for only a short distance from the contact (from several centimetres up to about 1.5 metres) gradually giving way to a massive rock in which relict pyroclastic textures are no longer preserved. The contact here, without snowflake or lava textures, differs from those found within the Arc structure. The transition instead is from extremely welded to crypto- and micro-crystalline tuffs.

These relationships are interpreted as indicating that the Welded Tuffs are indeed the product of crystallization of pyroclastic rocks and are intimately related to the more obviously pyroclastic rocks in the lower part of the exposed succession.

7.4 The Primary Rock Types

The petrology of each rock unit described from the Arc and representative of the lithologies found throughout the Gawler Ranges Volcanic

Complex is briefly discussed below.

7.4.1 Lithic and Lapilli Tuff (pЄt)

The basal lithic tuff has formed by the explosive brecciation of tuffaceous rocks and lavas which probably formed a roof to a magma chamber. A violent explosion(s) blew the mass of fragmented rock and ash into the atmosphere where glassy elements were cooled below their welding temperature before deposition. Slight mechanical sorting resulted from air-fall deposition.

Following pressure release the molten magma chilled forming a glassy, vesicular cap to the chamber outlet. A second set of explosions disrupted the cap and blew shards and glass beads into the atmosphere to form a shower of fine-grained particles. The shards and glass beads which were still warm were deposited as an air-fall tuff which became fused.* This mechanism explains the association of shards, subrounded glass particles and accessory rock fragments as well as the high fragment to groundmass ratio and the comparative absence of welding phenomena. After deposition and fusion the rock crystallized by devitrification.

7.4.2 Porphyritic Rhyolite ($p\text{Є}1_1$)

The basal and upper structural members of the Porphyritic Rhyolite ($p\text{Є}1_1$) indicate that this rock had the properties of a lava flow.

The basal member is the flow brecciated base of a lava which represents in part a transition from the underlying Lapilli Tuff. Prior to brecciation the initially deposited material was a chilled glass in which were incorporated a few fragments of the underlying tuff. The basal member grades continuously upward into a rock with a snowflake textured groundmass and penetrative subparallel banding. There is no evidence for a pyroclastic

---

* "Fusion" refers not to the actual melting of any constituent but to induration produced by external heating, softening and deformation of the glassy tuff (Christiansen and Lipman, 1966). This terminology avoids confusion with welded tuffs produced by compaction of thick hot ash flows (Smith, 1960).

origin. The top of the unit is a breccia that differs from the lower breccia in that the fragments are rounded rather than angular. The upper breccia represents the chilled outer surface of a fluidal lava that has ruptured through the motion of, and been invaded by, the still fluid lava below.

The rock mass has been modified by the development of secondary quartz and potash-rich alteration products, viz illite and sericite. Illite is a stable clay mineral that can form at comparatively high temperatures and in the presence of abundant K^+ ions (Krauskopf, 1967). Fractures, containing illite and minor potash feldspar within the lower breccia suggest that illite has formed, and hence the potassium been introduced, after consolidation of the rocks and prior to the complete crystallization of the glass.

7.4.3 Welded Tuff (pЄv1)

In the Eastern Zone a Lapilli Tuff forms the base of the unit. Carozzi (1960) has described a lapilli tuff composed of accretionary lapilli which exhibit a concentric texture and are formed by the gathering into clots of volcanic ash. Carozzi stated that,

> "the mechanism of accretion may take place in the air where raindrops fall across an explosion cloud, or on the ground by the rolling of lapilli nuclei over fresh ash surfaces or by the action of rain and wind on newly fallen ash".

Bordet (1945, 1951) has reported accretionary lapilli in rhyolitic tuffs as scattered spheres, entire or broken, with a diameter ranging from 1 mm to 1 cm and above, and with cores replaced by cavities.

Crystallization has destroyed much of the primary texture of the Gawler Ranges lapilli tuffs. The lapilli have formed independent of the groundmass and been incorporated by the latter but the method of formation of the lapilli remains in doubt as does the true nature of the incorporating material, i.e. a crystallized ash flow or crystallized lava.

Overlying the Lapilli Tuff in the east and the Lithic Tuff (pЄt) in the Central and Western Zones is a crystalline rock mass whose texture shows a continuous gradation from a well developed snowflake texture through a transition zone to a granophyric texture in the central levels. The sequence is reversed from the central region to the upper surface. Distinct or shadowy banding is nearly always present in the Central Zone and this resembles flow-banding suggesting crystallization from a fluid medium.

7.4.4 Porphyritic Rhyolite ($p\epsilon 1_2$)

The base of the Porphyritic Rhyolite ($p\epsilon 1_2$) is snowflake textured but usually displays a subparallel layering. The layering is closely spaced, continuous over considerable distances and is contorted about solid phenocrysts. Upwards the texture becomes streaky and resembles the eutaxitic texture of welded tuffs. However, amygdules are common indicating the rise of volatiles in a fluid medium.

A perlitic textured, lava type overlies the snowflake textured rocks. Spherulites are a conspicuous component and these could have one of two possible origins,

1. as a product of devitrification of a glass; or
2. as a product of devitrification and crystallization of rhyolitic rock fragments.

The random distribution of the spherulites, their irregular habit, and their sharp margins suggest they represent foreign particles rather than the product of 'in-situ' crystallization. In places the spherulites adhere to the surface of feldspar phenocrysts, which suggests that these too, are unrelated to the enclosing groundmass.

A lithic vitric tuff overlies the perlitic-textured rocks and shows evidence of intense welding.

The basal member of the Porphyritic Rhyolites ($p\epsilon1_2$) has behaved as a lava flow (c.f. Porphyritic Rhyolites $p\epsilon1_1$). The perlitic textured rhyolites apparently represent the maximum concentration of volatiles in a fluidized pyroclastic deposit which has since welded and crystallized. The upper tuff represents the surface layers of the pyroclastic deposit from which a large proportion of the contained volatiles have escaped and welding has not been as extreme.

This sequence should be compared with the related sequence - Porphyritic Rhyolites ($p\epsilon1_3$) higher in the succession.

7.4.5 Crystal Tuff ($p\epsilon ct$)

The abundance of crystal fragments in the basal portions of this unit suggest long-continued, intratelluric crystallization of the magma prior to eruption.

Roberts and Peterson (1961) have suggested that crystal tuffs are chemically distinct from ash flow tuffs and that the two are related to different magmatic compositions or eruptive processes. In a study of tuffaceous rocks from the Antler Peak Quadrangle, Nevada, they found that the ash-flows were rhyolitic with silica contents of 70 to 76% whereas the crystal tuffs were mostly quartz latites or dacites with silica contents of 62 to 72%. They postulated crystal settling in the magma chamber together with limited differentiation giving a magma enriched in silica, alkalies and volatile content at the top of the chamber. When the internal pressure of the chamber exceeded the confining pressure, the upper layers of the magma would be ejected to form ash-flow tuff whereas the lower volatile content of the magma at the base of the chamber would cause less disturbance of the accumulated, more basic, crystal tuffs.

A comparison of the analysis of the Crystal Tuff with other tuffaceous rocks from the Arc Structure provides no evidence to suggest that differentiation was an active process in the magma chamber of this region.

Several criteria are available for the distinction between ash-flow and ash-fall tuffs (Ross and Smith, 1961). The principal ones of these are probably:

a. that ash-fall tuffs are well sorted, whereas the ash-flow tuffs are characteristically unsorted, and,

b. that ash-flow tuffs form thick (tens of feet) non-bedded units and are usually massive, whereas ash-fall tuffs usually display pronounced bedding.

Although bedding is not a conspicuous feature of the Crystal and Pumiceous Tuffs (it may be present but obscured by poor exposure), it is thought probable, as above mentioned, that they were deposited as ash-fall tuffs. A continuous gradation from the coarsely crystalline Crystal Tuff, through the Pumiceous Tuff, to very fine-grained Vitric Tuff is established. This differentiation is related to areal deposition from a cloud of pyroclastic ejecta, with the coarser, less buoyant material falling faster than the vesicular glass ejecta. The general absence of welding suggests that the process of air-fall deposition has cooled the material below its welding temperature prior to deposition.

7.4.6 Pumiceous Tuffs (pЄpt)

The Pumiceous Tuffs are interpreted to have formed as an ash-fall rather than an ash-flow because of:

a. the high degree of sorting of the fragments,

b. the absence of significant welding.

It is evident that the rock was formed by the explosive brecciation of porphyritic glass and pumiceous rocks that chilled below their welding

temperature due to contact with the atmosphere. Fragments and groundmass were devitrified after deposition.

The devitrification textures resemble the axiolitic texture of Zirkel (1876, p 173-176) who described "linear aggregates of axially grouped fibres" as axiolites. Iddings (1899, p 419) gave a detailed description of "axiolitic structure" as follows:

> "In certain kinds of rhyolite apparently composed of welded glass fragments, there is a microspherulitic growth which bears a definite relation to the form of the supposed glass fragments. The feldspar fibres are in groups which are approximately normal to the outline of the fragments and radiate inward. Where the fragment had a rudely triangular shape the central part often attained a greater degree of crystallization than the margin and sometimes consists of distinct crystals."

The texture of these rocks is a modification of that described by Iddings in that the margins are not a microspherulitic growth but are larger crystals radiating inward towards a crystalline core.

Welding is shown by the partial collapse and contortion of the pumice rock fragments, and also by incipient attenuation and parallel orientation of shards.

The better preserved portions of the Pumiceous Tuffs have been subjected to deuteric alteration. Quartz and opaque minerals (iron oxides) partially replace feldspar phenocrysts and alteration to flaky colourless and pale greenish-yellow, clay minerals is common.

7.4.4 Welded Tuff (pЄv2)

The Welded Tuff ($pЄv_2$) is almost completely reconstituted by crystallization but a pyroclastic origin for the lower member is evidenced by the abundance of rock fragments and an eutaxitic texture developed in the

vicinity of contacts.

The upper member is separated from the lower by the Porphyritic Amygdaloidal Rhyolite (pЄal). At the base of the latter is a welded lithic tuff which gradually gives way to snowflake textures that continue to the top of the unit. The presence of 'peles tears' in rock fragments in the lithic tuff indicates derivation from rocks of the lower welded tuff horizon which exclusively contain these distinctive crystals.

7.4.8 Amygdaloidal Rhyolite (pЄal)

The basal member of the Amygdaloidal Rhyolites is a snowflake textured rock that differs little from those in other units.

The middle member is a perlitic rhyolite. A distinctive feature are globular particles which could represent,

1. former amygdules which have since recrystallized,
2. recrystallized rock fragments,
3. immiscible droplets of former glass.

Although the habit of the particles resembles that of amygdules the fact that they are porphyritic is against this possibility. The irregular, lobate and globular shape of the particles also suggests that they were not formerly solid rock fragments. Hence, the particles are considered to represent droplets of glass incorporated in the rock during its period of formation. This evidence suggests that these perlitic rhyolites may in fact be pyroclastic rocks, the ashy groundmass of which has welded to a glass and since devitrified.

The upper member is an amygdaloidal rhyolite which was a pyroclastic (Plate 22) composed of fragments of a perlitic glass which has been enriched in silica. The silica, along with less common orthoclase, opaque mineral phases and in places carbonate, infills voids between the rounded

fragments to form amygdule-like bodies. Subsequent to its deposition and enrichment in silica the pyroclastic deposit has welded as a result of its internal heat perhaps assisted by the weight of overlying material. The degree of welding increases through the member but the distinctive "amygdules" remain.

In some recent publications from New Zealand the field name "lenticulate" is used for a rock of this nature which is found in a pyroclastic association. It has been suggested, however, that this name should not be perpetuated in the literature (Branch, 1966).

This unit is gradational into a massive, red, Welded Tuff ($p\epsilon v_2$). The contact between the two is arbitrarily taken as the point where the amygdules cease to form a component of the rock.

7.4.9 Porphyritic Rhyolite ($p\epsilon 1_3$)

The basal member of the Porphyritic Rhyolite ($p\epsilon 1_3$) is a massive, snowflake textured rhyolite which contains conspicuous spherulites that are interpreted as rock fragments (Plate 23A) similar to those described from the Porphyritic Rhyolite ($p\epsilon 1_2$).

Overlying the massive member is a banded member which is formed of alternate layers of flattened spherulites, and snowflake-textured bands with abundant quartz eyes indistinguishable from those that form the cores of many spherulites. The quartz eyes in the snowflake-textured bands represent the cores of former spherulites and the snowflake-textured layers form by compaction, welding and crystallization of spherulite-rich or pyroclastic layers.

The spherulites are a function of the primary nature of the rock rather than of its subsequent history. Bombs (Plate 24) are found in the spherulite-rich zones and their presence is added evidence to support a pyroclastic origin.

Conical structures (Plate 25) are believed to form on the leeward side of solid phenocrysts as a result of fluid flow prior to crystallization. Thus the material from which at least some of the rocks from this unit crystallized was a viscous fluid prior to or during the time of crystallization.

The Fluidal Banded Rhyolite (pЄfb1) represents the optimum development of fluid flow in this environment.

The upper member of the Porphyritic Rhyolite ($p\text{Є}1_3$) is a flow breccia rather than an air-fall pyroclastic as evidenced by:

a. the fragments which are derived exclusively from the underlying rock;
b. the high fragment-to-groundmass ratio;
c. the absence of shards or other obviously pyroclastic ejecta; and
d. the angularity and interlocking nature of some of the fragment components.

In one sample (Locality 313) the fragments closely resemble the Fluidal Banded Rhyolites interbedded with the Porphyritic Rhyolites ($p\text{Є}1_3$). This is significant, for the Fluidal Banded Rhyolites outcrop only in the Central and Eastern Zones of the Arc Structure and the sample containing these fragment types is found in the Western Zone.

7.4.10 Vitric Tuff (pЄvt)

The rock is formed of ash composed of shards, minor crystals, and pumice fragments and is interpreted as an ash-fall deposit because of the sorting of the fragments, their limited variety, the abundance of shards, and the absence of significant welding. After deposition and consolidation alteration was promoted by the movement of deuteric silica along a system of small fractures and locally through small vesicles. This alteration is evidenced by the partial to complete replacement of feldspar fragments and groundmass by quartz.

Migration of alkalies also took place. The potassium in the potash feldspars crystallized as muscovite, sericite and illite. In addition, any soda combined in the potash feldspars appears to be eliminated.

7.4.11 Welded Tuff Sheet (pЄv3)

The Welded Tuff (pЄwt) represents a transitional unit between the underlying vitric Tuff (pЄvt) and the overlying Tuff Sheet ($pЄv_3$). The unit is a lithic tuff subjected to appreciable welding which increases in intensity to the north until it grades into the Tuff Sheet.

In the east (e.g. Locality 209) there is clear evidence for potassium enrichment related to minor fracturing (Plate 29) where numerous sub-parallel cracks are infilled with late-stage potash feldspar. These cracks are parallel to the foliation and were probably formed during tectonic subsidence with concomitant folding of the incompetent material. A second set of discontinuous fractures at an angle of about 30 degrees to the first represent tension cracks developed secondarily to the first cleavage (Plate 29). There is no significant displacement along either joint system. Potash feldspar is also crystallized as red feathery aggregates transverse to the cracks. Fine-grained, potassium-rich clay minerals crystallize along the secondary cleavage.

Within the Tuff Sheet no evidence for its primary nature remains. All groundmass textures are completely reconstituted. Textures in which quartz microlites are found (namely microlitic, microlitic microgranular, microgranular, microlitic spherulitic) tend to be confined to the vicinity and to the east of the Ring Structure and the snowflake and patch groundmass textures are confined to the southern margins of the Complex; the spherulitic textures to the central regions north of the Uno Fault; the granophyric textures to the north and west. These textural variations appear to reflect a general increase in grain size

of the elements of the groundmass from the south to the north, viz:

Snowflake and patch texture	south
Granophyric	↑
Microlitic, microlitic microgranular	↓
Spherulitic, spherulitic microgranular	
Granophyric	north

The local variations in groundmass textures are probably related to variations in texture within individual fault blocks. The study of groundmass textures is only sufficiently detailed in the vicinity of the Ring Structure to test the validity of this assumption. To the north of the Ring Structure is a tilted fault block which shows a variation in groundmass textures from microlitic at the base of the exposed section through microgranular to incipiently spherulitic microgranular at the top of the exposed section; a sequence which suggests that groundmass textures vary with depth in the Welded Tuff Sheet and can be correlated with rate of cooling.

7.5 Discussion

Four controls are responsible for the lithologies in the Gawler Ranges Volcanic Complex. These are:

1. primary rock type
2. concentration of volatiles
3. degree of welding
4. types of crystallization.

Through the volcanic pile there is a cyclical progression in the development of groundmass textures (Table 13). Each cycle is made up of three groups of rock textures idealized as follows:

Group 1	Group 2	Group 3
pyroclastic	snowflake	snowflake
	banded snowflake	microcrystalline
	perlitic	granophyric
	amygdaloidal	

The group 1 rocks generally lack indications of appreciable welding, are well sorted, have limited fragment materials, are bedded and form thin units. These features are ascribed to ash-fall tuffs.

Conversely the group 2 and 3 rocks contain pyroclastic ejecta which have a restricted size distribution but are heterogeneous in composition, poorly sorted and show indications of intense welding. In addition the rocks form very thick, non-bedded units. These features serve to indicate an ash-flow origin.

A cycle is then a sequence of ash-fall tuffs, ash-flow tuffs enriched in volatiles and ash-flow tuffs with a granophyric texture. Three such cycles are represented (Table 13).

The air-fall tuffs were emplaced below their welding temperature but are compacted by lithostatic load pressure. The ash-flow deposits have been emplaced as hot avalanche-like deposits or particulate flows which contained hot volatile constituents. Flowage is considered to be the principal mechanism for emplacement of these types of deposits (Fenner 1923, Marshall 1935, Gilbert 1938) and hence the presence of banding indicating flow is not unexpected. The ash-flow deposits are emplaced above their minimum welding temperature which is indicated by chemical consideration to be less than 580^{o}C (See Section 6.3.2 page 158).

The three cycles could be interpreted as forming three concordant, simple cooling units (Smith 1960) but the absence of major breaks suggests that the volcanic pile represents a single compound cooling unit.

The interaction of the four major controls on each other makes a precise demarcation of the pre- and post-cooling histories difficult if not impossible. Welding may be prolonged or be terminated by cooling or modified by crystallization. Crystallization of glassy components has taken place subsequent to or perhaps, in part, synchronous with the welding process and different environments give rise to diverse types of crystallization which can be recognized as distinct though which may overlap.

Zones of devitrification are found in the pyroclastic rocks. Devitrification involves the formation of axiolitic intergrowths in the glassy fragments and the crystallization of spherulites and lithophysae. The development of feathery and cryptocrystalline felsic minerals in pore spaces between pyroclastic debris is related to the movement of vapour and the transfer of material, viz; vapour phase crystallization. Zones of vapour phase crystallization progress from the devitrified horizon, through a snowflake texture to an horizon, which devitrified from a melt. The last of these is frequently amygdaloidal. This zone is one of active rising vapours, and changes in chemical composition take place due to the transfer of materials. Appreciable chemical differences are found between these and other zones. The zone of granophyric crystallization is represented by the red Welded Tuffs (pЄv). Here the cooling has been relatively slow and has produced a granophyric groundmass in which former pyroclastic textures are usually completely destroyed.

Overlying the exposed Welded Tuff Sheet ($pЄv_3$) which comprises such a large portion of the Gawler Ranges, there were probably considerable thicknesses of less welded tuff which have since eroded.

The widespread, welding, vapour-phase activity and crystallization has destroyed any partings between individual units and thus the geological map is more correctly an expression of the cooling history. For the most

part, however, the zones of welding and crystallization are concordant with the relict depositional textures.

8. THE GAWLER RANGES VOLCANIC COMPLEX

Widespread geological reconnaissance shows that the rock types described from the mapped area typify those exposed throughout the Complex. Except for the margins much of the Complex is flat and a two dimensional exposure of monotonous welded ash-flow tuff sheets ($p\epsilon v_3$) related in time but not in source characterise the region.

At least four and possibly more major sources for the magma are thought to exist. These are:

1. A magma chamber beneath the Ring Structure about 1.6 km north of the Uno Fault and Arc Structure. This chamber is thought to be the source of the magma for the eastern portion of the Complex.
2. A magma chamber beneath Paney Circle representing the magma source for the central portions of the Southern Belt of the Complex.
3. Hiltaba Area.
4. Kokatha Area.

At Hiltaba and Kokatha granitic stocks intrude the welded tuff sheets. The roofs to the stocks are apparently flat and their rise has caused doming of the volcanics to expose what is probably the base of the welded tuff sheet, containing abundant basic xenoliths and granitic segregations. It is suggested that the granites were intruded as a result of cauldron subsidence, along major block faults. The granite intrusions mark the close of igneous activity in the cauldron and are probably latholithic. They have similar compositions but vary in grain size both between and within single bodies. The margins are commonly porphyritic microgranites and in places are almost

transitional into the crystalline welded-tuff sheet. In other places contacts are irregular but clearly defined, and apophyses of granite intrude the tuff sheet along fractures.

Uniformity in composition is striking throughout the province, although in places alteration by deuteric fluids leads to a calc-alkaline composition. Basic rocks (hornfelsed basalts) are known from the Kokatha area and abundant basic xenoliths are found in the Hiltaba area and to a lesser extent throughout the Gawler Ranges Complex. Contemporaneous trachyandesite, trachyte and basaltic rocks are, however, rare. The basic rocks and granites form a part of the Gawler Ranges Petrographic Province.

Each of the source areas is a cauldron subsidence with peripheral upturning of the volcanic pile along faulted margins. Close similarities are found between the Hiltaba and Kokatha areas but in general the four areas differ from one another and differ in structural detail from the classical concepts of cauldron subsidence areas.

Ring fractures are inferred along the southern margin of the eastern portion of the Complex (Fig. 1B). Structural relationships to the north are concealed beneath alluvium but it is believed that faulting accompanied differential subsidence there also.

8.1 Basement Relationships

On radiometric dating (Compston et. al., 1966) and geological evidence (Section 3) the rocks south of the main boundary have the following relationships:

The Burkett Granite is the oldest, igneous rock type recognized in the immediate area (1,590 million years). Following the intrusion of the Burkett Granite into the gneissic basement the Corunna Conglomerate was deposited (1,550 million years) during the time the

Burkett granite was partially eroded. Following the deposition of the Corunna Conglomerate the main mass of the Gawler Ranges Volcanics were extruded (1,535 million years). These episodes were followed by the intrusion of the Gawler Ranges Volcanic Complex into both the Burkett Granite and the Corunna Conglomerate (1,490 million years). The barite veins and attendant mineralization are related to the late phase of the Gawler Ranges Volcanics exposed in the Dyke Structure (Reid 1968).

The alignment of the Burkett Granite along the approximate trace of the Uno Fault and the post-emplacement shearing indicates that the granite was emplaced along a pre-existing basement fracture prior to the extrusion of the Complex to the north. After the extrusion of the volcanics, subsidence along the pre-existing structural feature occurred with the concomitant, cataclastic deformation of the granites emplaced along it.

Previously, (Port Augusta 1:250,000 mile sheet, S.A. Department of Mines, 1968) all basic dykes of Eyre Peninsula were mapped as intruding the Older Precambrian rocks and the Moonabie Formation and were thought to be Carpentarian in age.

These are now considered to belong to the Cleve Metamorphics, Southern Eyre Peninsula. The basic dykes in the vicinity of the Uno Fault and within the Complex are not metamorphosed or deformed and thus belong to a younger series emplaced subsequent to differential subsidence along the fault.

If the Gawler Ranges Volcanics were extruded during a single short episode dated at 1,530 million years (Compston et. al., 1966) then these basic dykes are younger than this date.

9. THE SOURCE MAGMA

The mechanism of formation of ash-flows is reasonably well understood (Marshall, 1932; Vlodavels, 1957; Hay, 1959; Maucher, 1960; Steiner, 1960; McTaggart, 1960, 1962; Fitch, 1961; Brown 1962; Rast 1962; Ewart, 1965; Branch, 1967). Ash-flows are distributed in a very fluid manner over the surface of the earth and are presumed to be highly mobile as they intrude the earths crust. The completely liquid magma must rise under tension to a shallow magma chamber before it starts to solidify. A shallow magma chamber is supported by the present physico-chemical data (Section 6.3.1) which suggest that the water vapour pressure at the time of differentiation was about 600 bars, the temperature about 730^{o}C and the depth to the top of the magma chamber about 2.4 km.

It is quite evident that a considerable quantity of acid magma is required to form the extensive ash-flows and late-stage granites that make up the Gawler Ranges Volcanics. The vast amounts of acid magma associated with only minor amounts of trachyandesite, andesite and basalt suggests the source of the magma to be the lower crust. It is proposed that the acid magma was generated by fractional melting (partial fusion) of contaminated basic rocks (Kleeman, 1965) in the lower crust due to an increase in heat flow from the mantle during the orogenic phase of the development of the Adelaide Geosyncline. The earliest sediments recorded from the Adelaide Geosyncline are Willouran in age(1,340 - 1,490 million years) and hence the orogenic phase would have commenced somewhat earlier.

Ringwood (1962) states that in a normal orogenic cycle,

> "a period of acute crustal instablity occurs..... This is accompanied by diastrophism, magmatism, and strong differentiation so that the low melting fraction of the upper mantle becomes concentrated towards the surface".

This could be related to convection overturn near the end of the orogenic cycle which Verhoogen (1954) maintains will lead to partial melting and magma formation.

In the tectonically unstable zone near the geosyncline, where temperatures are higher and melting more complete basic magmas could be expected to form and may be manifested in the basic lavas of Roopena, Depot Creek, Wooltana, Kokatha and elsewhere. Further away from the developing geosyncline, beneath the adjacent semi-stable continental block, the lower crust would be less affected by orogenic forces and fractional melting would be slower. Pockets of acid magma would coalesce and accumulate to form a widespread magma chamber in the lower crust, doming the crust above. A similar source was suggested by Branch (1967) for the Georgetown Inlier in Queensland.

At the close of the orogenic phase of geosynclinal development the relaxation of compressional forces and the doming effect of the generated magma would place the semi-stable block in a state of tension. Reactivation of major basement faults would allow a rise of the magma and its intrusion as granite bodies (Burkett Granite). A concomitant drop in vapour pressure in the chamber would permit the accumulation of volatiles near the top of the chamber and this volatile-rich magma would be erupted as ash-flows. The magma is erupted in a series of intermittent bursts. Explosive eruption of the vent results in the accumulation of thin, well sorted air-fall tuffs which are followed by volatile-rich ash-flows. Blocking of the vent results in a period of pressure build-up. The vent erupts for a second time and a further series of ash-fall and ash-flow tuffs is extruded. Three such cycles have been mapped but no doubt numerous cycles are present. The process eventually culminates in the outpouring of a vast fluidized pyroclastic flow.

Cauldron subsidence accompanied the vacation of the magma chamber. Finally, still liquid magma filled spaces remaining after crustal blocks below the base of the ash-flow deposits had subsided. This magma crystallized as granite bodies beneath the protective covering of the thick ash-flows, (Branch 1967).

Thus it is hypothesised that the magma from which the Gawler Ranges Volcanics crystallized was formed by partial melting of the lower crust beneath the semi-stable continental platform adjacent to the developing Adelaide Geosyncline. The magma was injected in a fluid state to the upper crustal levels where crystallization was initiated and enrichment in volatiles promoted immense ash-flow eruptions. The available radiometric age data, although sparse, can be used to support this hypothesis.

10. BACKGROUND AND ACKNOWLEDGEMENTS

The writer's interest in the Gawler Ranges was generated during a brief visit on behalf of the South Australian Department of Mines in October 1965. Subsequently the writer undertook several reconnaissance trips to the region during his vacations and eventually selected the eastern area of the Ranges for a research topic. Field work for the preparation of the geological map and sample collection was undertaken during vacations from the writer's regular employ.

Some of the laboratory work was completed using a South Australian Mines Department Grant to the Australian Mineral Development Laboratories (Amdel). The remainder of the research was completed on a part time basis while the writer was employed as a Senior Mineralogist at Amdel in South Australia and as a Project Geologist with Anaconda Australia Inc. in Western Australia.

The writer wishes to acknowledge the assistance of the Director of the South Australian Department of Mines in financing the preparation of about half of the 700 thin sections examined and for financing the chemical and trend surface analysis; the Director of Amdel for the use of laboratory equipment; the Directors of both organizations for permission to present these data for the degree of M.Sc.; the Chief Geologist, Anaconda for drafting and typing facilities; Dr. R. Oliver (University of Adelaide) for his supervision, his enthusiasm, constructive criticism and advice; Mr. B.P. Thomson (Supervising Geologist Regional Mapping, S.A.D.M.) for his assistance and advice; the staff of the Analytical Chemistry Section (Amdel) for the Chemical Analyses; the staff of the Operations Research Group (Amdel) for running the trend surface analyses; the staffs of Amdel and Anaconda for their encouragement in all phases of the work; and lastly to my wife without whose patience and encouragement none of this would have been possible.

10. REFERENCES

ANDERSON, E.M. (1936). The Dynamics of the Formation of Cone Sheets, Ring Dykes and Cauldron Subsidences. Roy. Soc. Edin. 56, (2), 128-157.

ANDERSON, J.E. (1969). Development of Snowflake Texture in a Welded Tuff, Davies Mountains, Texas. Geol. Soc. Am. Bull. 80, 2075-2080.

BARTH, T.F.W. (1963). Theoretical Petrology. A Textbook on the Origin Evolution of Rocks. 2nd Edition, John Wiley and Sons, 414 p.

BATEMAN, P.C. (1965). Geology and Tungsten Mineralisation of the Bishop District, California. US Geol. Survey, Prof. Paper 470, 208 p.

BELOUSSOV, V.V. (1972). Basic Problems in Geotechnics. Ed. John. C. Maxwell, trans. from Russian Paul J. Broneer. Int. Series in Earth Sciences, McGraw Hill Book Coy.

BORDET, P. (1945). Traces de Goutles de Pluie dans les Tufs Rhylitiques de 1'Esterel. Soc. Geol. Franc, Comptes Rendu somm, 34-35.

BORDET, P. (1951). Etude Geologique et Petrographique de 1'Esterel. Me Carle Geol. det Francis Paris Imprimevie Nationale, 216 pp.

BOWEN, N.L. (1928). The Evolution of Igneous Rocks, Princetown.

BOYD, F.R. (1961). Welded Tuffs and Flows in the Rhyolitic Plateau of Yellowstone Park, Wyoming. Geo. Soc. Am. Bull., 72, 387-426.

BRADLEY, W.C. (1973). Large-scale Exfoliation in Massive Sandstones of the Colorado Plateau. Geo. Soc. Am. Bull., 74, 519-528.

BRANCH, C.D. (1966). The Volcanic Cauldrons, Ring Complexes and Associated Granites of the Georgetown, Inlier, Queensland. Bur. Min. Resourc. Aust. Bull. 76.

BRANCH, C.D. (1969). Genesis of Magma for Acid Calc-Alkaline Volcano-Plutonic Formations. Tectonophysics 4, (1), 83-100.

BROWN, G.C. (1970). A comment on the Role of Water in the Partial Fusion of Crustal Rocks. Earth and Planetry Science Letters. 9, 355-358.

BROWN, G.C. (1973). Evolution of Granite Magmas at Distructive Plate Margins. Nature Physical Science, 241. (106), 26-28.

BROWN, H.Y.L. (1894). Report of Government Geologist for year ended June 30th 1894. Parl. Pap. S.A. (25), 26p.

BROWN, M.C. (1962). Nuees Ardentes and Fluidisation. Am. J. Sci. 260, (6), 467-470.

BUDDINGTON, A.F. (1959). Granite Emplacement with Special Reference to North America. Bull. Geol. Soc. Am. 70, (6), 671-748.

CARMICHAEL, I.S.E. (1962). A Note on the Composition of Some Natural Acid Glasses. Geol. Mag. 99, 253-264.

CAROZZI, A.V. (1960). Microscopic Sedimentary Petrography. John Wiley and Sons Inc., NY.

CHAPMAN, C.A. and RIOUX, R.L. (1958). Statistical Study of Topography, Sheeting and Jointing in Granite, Acadia National Park, Maine. Am. Jour. Sci., 256, 111-127.

CHAYES, F. (1949). A Simple Point Counter for Thin Section Analysis. Am. Min. 34, 1-11.

CHAYES, F. (1954). The Theory of Thin Section Analysis. Jour. Geol. 62, 92-101.

CHAYES, F. (1961). Numerical Petrography. Carnegie Inst. Wash. Year Book, 60, 158-165.

CHAYES, F. and SUZUKI, J. (1963). Geological Contours and Trend Surfaces. Jour. Pet. 4, 307-312.

CHRISTIANSEN, R.L. and LIPMAN, P.W. (1966). Emplacement and Thermal History of a Rhyolite Lava Flow near Fortymile Canyon, Southern Nevada. Geol. Soc. Am. Bull. 77 (7), 671-684.

CLARK, R.H. (1960). Andesite Lavas of the North Island, New Zealand. Int. Geol. Congr. 21st, Copenhagen, 1960. Rept. Session Norden 13, 123-131.

CLOUGH, G.T., MAUFE, H.B. and BAILEY, E.B. (1909). The Cauldron Subsidence of Glen Coe and Associated Igenous Phenomena. Geol. Soc. Lon. Quart. Jour., 65, 611-678, 629-631.

COMPSTON, W., CRAWFORD, A.R. and BOFINGER, V.W. (1966). A Radiometric Estimate of the Duration of Sedimentation in the Adelaide Geosyncline, South Australia. Jour. Geol. Soc. Aust. 13, (1), 229-276.

CORNWALL, H.R. (1962). Calderas and Associated Volcanic Rocks near Beatty, Nye County, Nevada. In Engel, A.E.J., James, H.L. and Leonard, B.F., eds, Petrological Studies. A Volume in Honour of A.F. Buddington. Geol. Soc. Am., 357-371.

CRAWFORD, A.R. (1962). A Preliminary Account of the Gawler Ranges Volcanic Complex, South Australia. Unpub. Report S.A. Geol. Surv.

CRAWFORD, A.R. (1963). Large Ring Structures in a South Australian Pre-Cambrian Volcanic Complex. Nature, 197, (4863), 140-142.

DAWSON, K.R. (1958). An Application of Multivariate, Variance Analysis to Mineralogical Variation, Preissac-Lacorne Batholith, Abitibi County, Quebec. Can. Mineral. 6, 222-233.

DAWSON, K.R. and WHITTEN, E.H.T. (1962). The Quantitative Mineralogical Composition and Variation in the Lacorne, La Motte, and Preissac Granite Complex, Quebec, Canada. Jour. Pet. 3, 1-37.

DEER, W.A., HOWIE, R.A. and ZUSSMAN, J. (1963). Rock Forming Minerals. Five volumes.

DE SITTER, L.U. (1956). Structural Geology. McGraw-Hill Book Co. Inc., Lon., N.Y., Tor., 552 p.

EWART, A. (1963). Petrology and Petrogenesis of the Quaternary Pumice Ash in the Taupo Area, New Zealand. Jour. Pet. 4, 392-431.

EWART, A. (1965). Mineralogy and Petrogensis of the Lohakamaru Ignimbrite in the Maraetai Area of the Taupo Volcanic Area, New Zealand. N.Z. Jour. Geol. Geophys. 8, (11), 611-677.

FENNER, C.N. (1923). The Origin and Mode of Emplacement of the Great Tuff Deposit in the Valley of Ten Thousand Smokes. Natl. Geog. Soc., Contrib. Tech. Papers, Katmai Ser., (1), 74 p.

FITCH, F.J. (1961). Origin of Ignimbrites. Nature, 190, (4780), 995-996.

GABRIEL, A. and COX, E.P. (1929). A Staining Method for the Quantitative Determination of Certain Rock Minerals. Am. Min., 14, 290-292.

GILBERT, C.M. (1938). Welded Tuff in Eastern California. Geol. Soc. Am. Bull., 49, (12), 1829-1862.

GILBERT, G.K. (1904). Domes and Dome Structure of the High Sierra. Geol. Soc. Am. Bull. 15, 29-36.

GRANT, F. (1957). A Problem in the Analysis of Geophysical Data. Geophysics 22, 309-344.

GREEN, D.H. and RINGWOOD, A.E. (1967). An Experimental Investigation of the Gabbro to Eclogite Transition and its Petrological Applications. Geochim. et Cosmochim. Acta 31, (5), 767.

GREENWOOD, R. (1951). Younger Intrusive Rocks of the Plateau Province, Nigeria compared to the Alkali Rocks of New England. Bull. Geol. Soc. Am. 62, 1151-1178.

HACK, J.T. (1966). Circular Patterns and Exfoliation in Crystalline Terraine, Grandfather Mountain Area, North Carolina. Bull. Geol. Soc. Am. 77, 975-986.

HAMILTON, W.B. (1956). Variations in Plutons of Granitic Rocks of the Huntingdon Lake Area of the Sierra Nevada, California. Bull. Geol. Soc. Am. 67, 1585-1598.

HARDIE, W.B. (1963). Explosion Breccias Near Stob Mhic Mhartuin, Glen Coe, Argyll, and their Bearing on the Origin of the Nearby Flinty Crush Rock. Edin. Geol. Soc. Trans., 19, 426-438.

HATCH, F.H., WELLS, A.K. and WELLS, M.K. (1960). The Petrology of the Igenous Rocks. Thomas Murby & Co.

HAY, R.L. (1959). Formation of the Crystal-Rich Glowing Avalanche Deposits of St. Vincent, British West Indies. J. Geol. 67, (5), 540-562.

HILLS, E.S. (1959). Cauldron Subsidence, Granitic Rocks and Crustal Fracturing in South-eastern Australia. Geol. Rundschau 47, (2), 543-561.

HILLS, E.S. (1963). Elements of Structural Geology. Metheun & Co. Ltd., London.

HOLMES, A. (1920). The Nomenclature of Petrology. Thomas Murby and Co., London, 284 p.

HOUSER, F.N. and POOLE, F.G. (1959). "Granite" Exploration Hole, Area 15, Nevada Test Site, Nye County, Nevada. Interim Report, Part A, Structural, Petrographic and Chemical Data. U.S. Geol. Survey Open File Report, TEM- 836A.

HUNT, C.G. (1938). A Suggested Explanation of the Curvature of Columnar Joints in Volcanic Necks. Am. Jour. Sci., 36, (5), 142-149.

IDDINGS, J.P. (1886). The Columnar Structure in the Igneous Rock on Orange Mountain, New Jersey. Am. Jour. Sci. 31, (3), 321-331.

IDDINGS, J.P. (1899). Geology of Yellowstone National Park. U.S. Geol. Survey Mem. 32, part 2, chapt. 10, 256-430.

IZETT, G.A. (1960). "Granite" Exploration Hole, Area 15, Nevada Test Site, Nye County, Nevada. Interim Report, Part C, Physical Properties. Trace Elements Memorandum Report 836-C, U.S. Geol. Survey Open File Report TEM - 836 - C.

JACK, R.L. (1912). The Geology of Portions of the Counties of Le Hunte, Robinson and Dufferin with Special Reference to Underground Water Supplies. Bull. Geol. Surv. SA No. 1.

JACK, R.L. (1917). The Geology of the Moonta and Wallaroo Mining District. Bull. Geol. Surv. SA No. 6.

JACK, R.L. (1922). The Iron Ore Resources of South Australia. Bull. Geol. Surv. SA No. 10.

JAHNS, R.H. (1943). Sheet Structure in Granites: Its Origin and Uses as a Measure of Glacial Erosion. Jour. Geol. 51, 71-98.

JAMES, A.V.G. (1936). Factors Producing Columnar Structure in Lavas and its Occurrence Near Melbourne, Victoria. Jour. Geol. 28, 458-469.

JOHNS, R.K. and SOLOMON, M. (1953). The Age of the Gawler Ranges Porphyry. Proc. Roy. Soc. S. Aust., 76, 41-44.

KENNEDY, G.C. (1955). Some Aspects of the Role of Water in Rock Melts. In Poldervaart, Arie. Ed. Crust of the Earth. A Symposium. Geol. Soc. Am. Spec. Paper 62, 489-503.

KRAUSKOPF, (1967). Introduction to Geochemistry. McGraw Hill Book Coy (NY).

KRUMBEIN, W.C. (1956). Regional and Local Components in Facies Maps. Bull. Am. Ass. Pet. Geol. 40, 2163-2194.

KRUMBEIN, W.X. (1959). Trend Surface Analysis of Contour-Type Maps with Irregular Control-Point Spacing. Jour. Geophys. Research 64, 823-834.

KRUMBEIN, W.C. (1960). The "Geological Population" as a Framework for Analysing Numerical Data in Geology. Liverpool, Manchester Geol. Jour. 2, 341-368.

KRUMBEIN, W.C. (1963). Confidence Intervals on Low-Order Polynomial Trend Surfaces. Jour. Geophys. Research 68, (20).

LARSEN, L.H., IRVING, J., GONYER, F.A. and LARSEN, E. (1938). Petrologic Results of the Study of the Minerals from the Tertiary Volcanic Rocks of the San Juan Region, Colorado. Am. Min., 23, 417-429.

LARSEN, L.H. and POLDERVAART, A. (1961). Petrologic Study of Bald Rock Batholith, near Bidwell Bar, California. Bull. Geol. Soc. Am. 72, 69-92.

LINK, R.F. and KOCH, G.S. (1962). Quantitative Areal Modal Analysis of Granitic Complexes: Discussion. Bull. Geol. Soc. Am. 73, 411-414.

LIPMAN, P.W. (1965). Chemical Comparison of Glassy and Crystalline Volcanic Rocks. U.S. Geol. Survey Bull. 1201-D, 1-24.

LIPMAN, P.W. (1966). Water Pressures During Differentiation and Crystallization of Some Ash-Flow Magmas from Southern Nevada. Am. Jour. Sci. 264, (10), 810-826.

LIPMAN, P.W. (1966). Mineralogical and Chemical Variations within Ash-Flow Sheets, Aso Caldera, South-western Japan, and Elsewhere. (Abs.) Program. Ann. Meeting Geol. Soc. Am. San Francisco.

LOFGREN, G.E. (1968). Experimental Devitrification of Rhyolite Glass. Stanford Univ., PhD dissert., 19 p.

MANDELBAUM, H. (1963). Statistical and Geological Implications of Trend Mapping with Non-orthagonal Polynomials. Jour. Geophys. Research 68, (2), 505-519.

MARSHALL, P. (1932). Notes on Some Volcanic Rocks of the North Island of New Zealand. N.Z. J. Sci. Tech. B. 13, 198-202.

MARSHALL, P. (1935). Acid Rocks of the Tampo-Rotorua Volcanic District, Roy. Soc. N.Z. Trans. 64, pt 3, 323-366.

MATHES, F.E. (1930). Geologic Histroy of the Yosemite Valley. U.S. Geol. Survey Prof. Paper 160, 137 p.

MAUCHER, A. (1960). Der Permishe Vulkanismus in Sudtirol und das Problem der Ignimbrite. Geol. Rundschau 49, (2), 487-498.

MAWSON, O. (1926). Brief Resume of Present Knowledge Relating to Igneous Rocks of South Australia. Aust. Inst. Adv. Sci. XVIII.

McTAGGART, K.C. (1960). The Mobility of Nuees Ardentes. Am. Jour. Sci., 258, (5), 369-382.

McTAGGART, K.C. (1962). Nuees Ardentes and Fluidisation - A Reply. Am. J. Sci. 260, (6), 470-476.

MIESCH, A.T. (1967). Theory of Error in Geochemical Data. Statistical Studies in Field Geochemistry. U.S. Geol. Surv. Prof. Paper 574A, 17 p.

MILLER, R.L. (1956). Trend Surfaces: Their Application to Analysis and Description of Environments of Sedimentation. Jour. Geol. 64, 425-446.

NOBLE, J.A. (1948). High Potash Dykes, in the Homestake Mine, Lead, South Dakota. Bull. Geol. Soc. Am. 59, 927-939.

NOCKOLDS, S.R. and ALLEN, R. (1953). The Geochemistry of Some Igneous Rock Series. Geochim. et Cosmichim Acta 4, 105-142.

O'CONNOR, J.T. (1965). A Classification for Quartz-Rich Igenous Rocks Based on Feldspar Ratios. U.S. Geo. Survey Prof. Paper 525B, 79-84.

OLDHAM, C.H.G. and SUTHERLAND, D.B. (1955). Orthogonal Polynomials. Geophysics 20, 295-306.

ORVILLE, P.M. (1963). Alkali-Ion Exchange between Vapour and Feldspar Phases. Am. Jour. Sci., 261, 357-364.

PARKIN, L.W. (1969). (ed). Handbook of South Australian Geology. S.A. Dept. of Mines, 286 p.

PEIKERT, E.W. (1963). Three-Dimensional, Specific Gravity Variation in the Glen Alpine Stock, Sierra Nevada, California. Bull. Geol. Soc. Am. 73, 1437-1442.

PUTMAN, G.W. and ALFORS, J.T. (1965). Depth of Intrusion and Age of the Rocky Hill Stock, Tulare County, California. Geol. Soc. Am. Bull., 76, 357-364.

RAST, N. (1962). Textural Evidence for the Origin of Ignimbrites. Liverpool Manchester Geol. J. 3, (1), 97-108.

REID, R.B. (1968). A Survey of Australian Barite Deposits. Unpub. B.Sc. (Hons) Thesis, Univ. Adelaide.

REYNOLDS, D.L. (1956). Calderas and Ring-Complexes. Nederl. Geol.-Mijinb. Genoot. Verh., Geol. Serv. (16), 355-379.

RICHEY, J.E. (1961). Scotland: The Tertiary Volcanic District. Geol. Survey Gt. Brit., Handbooks. Brit. Regional Geol., 1961, 120 p.

RITTMAN, A. (1952). Nomenclature of Volcanic Rocks. Bull. Volcanologique, 12, 75-102.

RITTMAN, A. (1958). Cenni Sulle Colate Di Ignim-briti. Boll. Del. Sed. Acad. Gioenia di Sc. Nat. in Catania. IV, (IV), 10, 524-533.

ROSS, C.S. (1964). Volatiles in Volcanic Glasses and Their Stability Relations. Am. Min. 49, 258-271.

ROSS, C.S. and SMITH, R.L. (1961). Ash-Flow Tuffs: Their Origin, Geologic Relations and Identification. U.S. Geo. Surv. Prof. Paper 366, 81 p.

RUTTEN, M.G. and VAN EVERDINGEN, R.O. (1961). Rheo-Ignimbrite of the Ramnes Volcano, Permian, Oslo Graben. Geologic en Mijnboum JAAR. 40, (2), 49-57.

SAHA, A.K. (1954). The Granodiorites Around Bahalda Road, Mayurbhanj. Geol. Min. Metall. Soc. India Quart. Jour. 36, 87-104.

SCOTT, R.B. (1965). Formation and Crystallization of Ignimbritic Magmas under High Water Pressure. (Abs). Geol. Soc. Am. Program Ann. Meeting Kansas City, 147-148.

SCOTT, R.B. (1966). Origin of Chemical Variations within Ignimbrite Cooling Units. Am. Jour. Sci. 264, 273-288.

SEDERHOLM, J.J. (1929). The Use of the Term Deuteric. Econ. Geol. 24, 869-871.

SEGNIT, R.W. (1937). Geology and Development of Groundwater in the Robinson Fresh Water Basin, Eyre's Peninsular. Part 1. Geology and Hydrology. Bull. Geol. Surv. S.A. 17, 3-48.

SMALE, D. (1965). The Petrology and Age Relationships of Rocks in the Moonabie Range, South Australia. Trans. Roy. Soc. S. Aust. 90, 153-165.

SMITH, R.L. (1960). Ash Flows. Geol. Soc. Am. Bull., 71, 795-842.

SMITH, R.L. (1960). Zones and Zonal Variations in Welded Ash Flows. U.S. Geol. Survey Prof. Paper, 354F, 149-159.

SNYDER, J.L. (1962). Geologic Investigations, Central Davis Mountains, Texas. Texas Jour. Sci., XIV, (2), 197-215.

STEINER, (1960). Origin of Ignimbrites of the North Island, New Zealand. A New Petrogenic Concept. N.Z. Dept. Sci. and Inc. Res. Bull. 86, 41.

STEWART, D.B. (1958). System $CaAl_2Si_2O_8$ - SiO_2 - H_2. (Abs.) Geol. Soc. Am. Bull., 69, 1948.

SUBRANDAMUM, A.P. (1956). Mineralogy and Petrology of the Sittampundi Complex, Salen District, Madras, India. Bull. Geol. Soc. Am. 67, 317-390.

SUZUKI, Y. (1953). Studies of Variations in Mineral Composition of Some Granodioritic Masses in Japan and Korea. Jour. Fac. Sci. Hokkaido Univ. (Ser. IV), 8, 277-288.

TAUBENECK, W.H. (1957). Geology of the Elkhorn Mountains, North-eastern Oregon, Bald Mountain Batholith. Bull. Geol. Soc. Am. 68, 181-238.

TAUBENECK, W.H. (1963). Distribution of Accessory Minerals in Zoned Granitic Intrusions, North-eastern Oregon. (Abs.) Geol. Soc. Am. Spec. Paper 73, 97-98.

TAUBENECK, W.H. (1967). Notes on the Glen Coe Cauldron Subsidence, Argyllshire, Scotland. Geol. Soc. Am. Bull., 78, (11).

THOMSON, B.P. (1966). The Lower Boundary of the Adelaide System and Older Basement Relationships of South Australia. Jour. Geol. Soc. S.A. 13, (1), 203-228.

TSUYA, H. (1930). The Volcano Komagatake, Hokkaido, Its Geology, Activity and Petrography. Tokyo Univ. Earthquake Research Inst. Bull., 8, 238-270.

TUTTLE, O.F. and BOWEN, N.L. (1958). Origin of Granite in the Light of Experimental Studies in the System $NaAlSi_3O_8$ - $KAlSi_3O_8$ - SiO_2 - H_2O. Geol. Soc. Am. Mem., 74, 153 p.

VISTELIUS, A.B. (1962). Phosphorous in Granitic Rocks of Central Tien Shan. Geochemistry 1962, 131-151.

VLODAVETS, V.I. (1957). On the Origin of the Rocks Usually called Tuff-Lava and Ignimbrite. Tr. Lab. Vulkanol. Akad. Nauk. SSSR, 14, 36-47.

WENTWORTH, C.K. and WILLIAMS, H. (1930). The Classification and Terminology of the Pyroclastic Rocks. Nat. Research Council Bull. 89, 19-53.

WHITTEN, E.H.T. (1957). The Gola Granite (County Donegal) and its Regional Setting. Proc. Royal Irish Acad., 58B, 245-292.

WHITTEN, E.H.T. (1959). Compositional Trends in a Granite: Modal Variation and Ghost-Stratigraphy in Part of the Donegal Granite, Eire. Jour. Geophys. Research 64, 835-848.

WHITTEN, E.H.T. (1960). Quantative Evidence of Palimpsestic Ghost Stratigraphy from Modal Analysis of a Granitic Complex. Int. Geol. Congr. Rept. 21st Ses. Copenhagen, (4), 182-193.

WHITTEN, E.H.T. (1961a). Quantitative Areal Modal Analysis of Granitic Complexes. Bull. Geol. Soc. Am., 72, 1331-1360.

WHITTEN, E.H.T. (1961b). Systematic Quantitative Areal Variation in Five Granitic Massifs from India, Canada and Great Britain. Jour. Geol. 69, 619-646.

WHITTEN, E.H.T. (1962a). Sampling and Trend-Surface Analysis of Granites. A Reply. Bull. Geol. Soc. Am. 73, 415-418.

WHITTEN, E.H.T. (1962b). A New Method for Determination of the Average Composition of a Granite Massif. Geochem. et Cosmochim. Acta 26, 545-560.

WHITTEN, E.H.T. (1966). Application of Quantitative Methods in the Geochemical Study of Granite Masses. Studies in Analytical Geochemistry (6).

WILLIAMS, H., TURNER, F.J. and GILBERT, C.M. (1955). Petrography: San Francisco. W.H. Freeman and Co., 406 p.

WILLIAMS, I.A. (1965). The Comparative Accuracy of the Methods for Determining the Percentages of the Several Components of an Igneous Rock. Am. Geol. 35, 34-46.

WILLIAMS, P.L. (1960). A Stained Slice Method for Rapid Determination of Phenocryst Composition of Volcanic Rocks. Am. Jour. Sci., 258, 148-152.

WILSON, G. (1946). The Relationships of Slaty Cleavage and Kindred Structures to Tectonics. Proc. Geol. Assoc. 57, 263-302.

WINCHEL, A.N. and WINCHEL, H. (1951). Elements of Optical Mineralogy. Fourth Edition (2). Descriptions of the Minerals. John Wiley and Sons Inc., N.Y.

ZIRKEL, K. (1876). Microscopical Petrography. U.S. Geol. Expl. 40th Parallel Report (King) 6, 297 p.

ZIRKEL, K. (1877). Ueber Die Krystallinischen Gesteine Langs des 40. Ber. Sachs. Gesell. Wiss., Leipzig, XXIX, 216-20.
Idem: Lehrbuch. 11, (1894), 244-248.

Additional References

KLEEMAN, A.W. (1965). The Origin of Granitic Magmas. I. Geol. Soc. Aust. 12, 35-52.

HARBAUGH and MERIAM. Computer Applications in Stratigraphic Analysis, 67-70 (John Wiley).

APPENDIX A

CONTOUR MAPS AND STATISTICAL EVALUATION OF GEOLOGICAL DATA

Modal data form the basis of most quantitative work but with the introduction of rapid analytical techniques the variation of major and trace elements is being increasingly studied. Examples of the types of quantitative data that can be gained from the study of a single rock mass were provided by Houser and Pool (1959) and Izett (1960) who recorded quantitative data concerning more than 120 variables for a single core drilled through granodiorite of the Climax Stock, Nevada.

Several workers have contoured quantitative modal data to express geographical areal variation in a rock mass (Suzuki, 1953; Saha, 1954; Hamilton, 1956; Taubeneck, 1957; Whitten, 1957; Dawson, 1958; Larsen and Poldervaart, 1961; Vistelius, 1962; Taubeneck, 1963, and others). Contour maps have also been used to express geographical area variation in bulk chemistry.

Although contour maps tend to create an impression of quantitative objectivity, the construction is, essentially, a subjective operation (Chayes, 1961, p 163; Dawson and Whitten, 1962, p 3) and preconceived ideas gained from field observations or other sources can be infused in the basic data. Krumbein (1960, p 361) suggested that an interpretative method is to be preferred for most maps because it permits inclusion of the "geologists' judgement of the grain of the maps". Even so, surveys of recent literature indicate that for the interpretation of geological data it is preferable to use a technique which eliminates the subjective elements inherent in contour diagrams.

A.1 Trend Surface Analysis

Most texts utilising statistics have discussed the problems of approximating a curve to a set of data points. It is common practice to use a quantitative technique such as the method of least squares to develop the regression line. With the advent of high speed, electronic computers this method has been extended to mapped data (trend surface analysis) and the method has found increasing acceptance for synthesising and obtaining reliable quantitative inferences from areal data collected from large rock bodies.

The early literature on the subject includes papers by Oldham and Sutherland (1955), Krumbein (1956), Miller (1956) and Grant (1957). The general method for contour maps with irregular control point spacing was given by Krumbein (1959). In igneous petrology, the method has been used by Whitten (1959, 1961) and Dawson and Whitten (1962). The reliability of trend surfaces as compared to geological contours has been discussed by Chayes and Suzuki (1963). Confidence limits on low-order polynomial trend surfaces have been computed by Krumbein (1963).

The method of trend analysis, currently applied to geological problems, is a form of multiple regression wherein polynomial or other mathematical surfaces are fitted to map data by least squares techniques. Confidence limits placed on the computed surfaces express the degree to which a surface fits the given data points. The trend surface expresses the measured variable (dependent variable Xn) as a function of two orthogonal, geographical co-ordinates (independent variables U and V), so that $Xn = f\ (UV)$ and computes the polynomial functions which best

fit the data by the least squares, regression technique.

Several objectives can be achieved by this technique but chief among these is the separation of total map variability into regional and local components. The departures from the regional trend (local components or residual) are the differences between the actual value and the calculated regional surface value at each data point.

Regional trend surfaces are classified according to the degree or order, and are expressed by mathematical equations. The most usual surfaces fitted to modal data are first, second and third degree which correspond to linear, quadratic and cubic polynomials of the function -

$$Xn = f(UV)$$

The precise form of the calculated surface is that for which the sums of squares for the residuals, of the differences between the observed and computed values, have a minimum value. The trend surface therefore contains the regional or systematic component of the variability of the data, while the residuals include local or erratic values unrelated to the principal distribution. The linear or first degree trend components reflect the broadest scale gradients across a map area; successively higher degree trends reflect more and more detailed variability and thus smaller scale features. It is generally supposed that the second degree component adequately represents the regional trend and that higher degree surfaces become too complex and isolate too much of the local noise to enable adequate interpretations about the regional trend. Ultimately the selection of the appropriate surfaces to be fitted to any set of data is dependent on the quality of the data and on its overall bias, variable bias or variable precision.

Krumbein (1959), Whitten (1966) and Miesch (1967) have discussed the types of data amenable to trend surface analysis. Because trend surface analysis may be viewed as an empirical tool or as a descriptive technique in geological data analysis, the data errors involved are not subject to unusual requirements. Miesch (op cit) has pointed out that the overall bias in a set of data merely reflects the estimation of the constant term in the computed regression equation and the values on the contours of the regression surface. He has also shown that variable precision results in unequal reliability of the locality means described by the fitted surface and that these effects are the same as if the data were merely contoured. Miesch (op cit, p A15) concludes that -

> "when neither overall bias, nor variable precision of the errors is of large magnitude, the data, in so far as the error is concerned, are suitable for interpretation on either statistical or substantive grounds although statistical methods are more likely to overcome the effects of unbiased error".

Whitten (1961, 1962) and Link and Koch (1962) have indicated that modal variables at the hand specimen level commonly have large variances but that this does not imply that the gradient across a map area is unreal. However, such a surface may be a poor predictor of precise composition at the local level.

The objective of the least squares method is to make the sum of the squared residual values the least possible and hence the significance of the predicted trends in unsampled areas can be obtained from the proportion of the sum of squares associated with a surface. Nevertheless, it is important to distinguish between the usefulness of a trend surface as a predicting device and as an indicator of regional gradient.

Whitten (1966) has indicated that relatively few data points are required to define a regional trend but that closely spaced sample sites are essential if interest attaches to the deviations (local variations or residuals).

Two statistical expressions used to empirically define the degree to which the computed surfaces fit the original data are:

a. The coefficient of correlation is expressed as -

$$100 \left[1 - \frac{\Sigma (Z \text{ obs}^* - Z \text{ trend})^2}{\Sigma (Z \text{ obs}^* - Z \text{ obs}^*)^2} \right]$$

b. The standard deviation is the standard deviation between the data values computed for the surface and the actual values.

---

obs* - observed value at data point.

APPENDIX B

CALCULATION OF WATER PRESSURES DURING FORMATION OF THE MAGMA

The method employed involves the calculation of the normative Al (albite), Or (orthoclase) and Q (quartz) of each analysis to 100% and plotting the results on a triangular diagram showing the experimentally determined isobars. The water pressure value can then be obtained in two ways (Lipman, 1966):

1. If both feldspar and quartz phenocrysts are present and can be presumed to have been in equilibrium with a residual liquid, now represented by a fine-grained or glassy groundmass, the groundmass composition should plot on the isobar indicating the water pressure at time of phenocryst growth. Ideally, this approach requires only a single anaylsis.

2. Alternatively, plots of bulk rock composition of a rock series, presumed to be related to a single line of liquid descent, can be used to establish a differentiation trend. Depending on the initial composition of the series its trend may indicate, either by intersecting the line of isobaric minima, or by bending to follow an isobaric line toward the minimum, the water vapour present at the time of differentiation. This approach yields a water pressure for the time of differentiation rather than for the time of phenocrysts crystallisation.

The assumptions and errors inherent in the methods include:

a. That the groundmass or bulk-rock compositions result from fractionation under conditions of crystal-liquid equilibrium.

If equilibrium was not achieved or if fractionation resulted from other mechanisms such as assimilation, volatile transfer, liquid immiscibility, etc., then the data of Tuttle and Bowen have no relevance.

b. The influence of calcium, iron and magnesium on the system. The effect of anorthite can be predicted qualitatively. As the quartz-feldspar field surface in the quartz and three-feldspar tetrahedron shifts towards the three-feldspar surface with increasing water pressure (Tuttle and Bowen, 1958; Stewart, 1958), projection of an analysis that contains appreciable anorthite onto the Ab-Or-Q face of the tetrahedron will yield an erroneously low water pressure value. The effect of iron and magnesium is more difficult to predict; at the very least variations in these constituents modify the amount of Q (quartz). The oxidation state of iron, which is especially variable in volcanic rocks and increases during devitrification, is critical, as in the norm calculations ferric iron goes into Mg (magnetite) or Hm (hematite) whereas ferrous iron goes into Hy (hypersthene) and requires silica which otherwise would go into Q (quartz).

c. Water is treated as the sole contributor to the total vapour pressure, and the effects of other volatile constituents undoubtedly present in natural magmas are not taken into account. Such effects are probably small but they cannot be evaluated quantitatively.

APPENDIX C

TABLE 9 WELDED TUFF SHEET ($p\epsilon v_3$)

Chemical Analyses

TABLE 9: CHEMICAL ANALYSES - WELDED TUFF SHEET (pEv3)

Sample	S109	A1747/61	S323	S121	S113	Jack (1917)	A1746/61	S335	U313	U104	U120	C72	S322	S326	U139
	Analyses, %														
Method of Analysis	2	1	3	3	3	1	1	3	3	3	3	2	3	3	3
SiO_2	67.00	67.80	67.80	67.90	68.80	68.90	69.00	69.60	69.70	69.80	69.90	70.20	70.30	70.90	71.00
Al_2O_3	13.60	13.40	13.40	13.40	13.10	14.43	12.60	13.20	13.10	13.00	13.20	13.20	13.30	13.50	13.00
Fe_2O_3	1.97	1.41	1.90	3.30	2.00	1.91	1.64	1.90	2.90	1.90	4.20	1.02	4.20	3.40	1.50
FeO	3.65	3.59	3.30	1.75	3.00	2.80	2.56	2.80	2.40	3.20	1.10	2.55	0.54	0.33	2.80
MnO	0.08	0.12	0.13	0.11	0.08	0.03	0.11	0.11	0.14	0.10	0.06	0.05	0.07	0.04	0.05
MgO	0.74	0.61	1.10	1.10	0.96	0.33	0.73	1.70	1.20	0.15	0.85	0.60	1.00	0.66	0.56
CaO	1.94	2.26	1.90	0.72	2.00	0.92	1.49	1.00	0.73	0.79	0.37	1.12	0.21	0.26	0.84
Na_2O	3.50	3.30	2.90	2.60	2.90	3.07	3.20	3.20	2.80	2.90	2.20	2.70	2.60	2.90	2.90
K_2O	4.95	4.70	3.80	6.00	4.20	5.70	5.20	3.80	4.20	4.50	4.20	5.40	4.10	4.90	4.50
TiO_2	0.75	0.67	0.72	0.62	0.72	0.69	0.62	0.64	0.64	0.61	0.65	0.60	0.63	0.59	0.39
P_2O_5	0.24	0.19	0.12	0.13	0.13	0.19	0.15	0.11	0.12	0.10	0.09	0.13	0.09	0.07	0.06
L.O.I.*	-	-	1.80	2.40	1.30	-	-	1.60	1.90	1.60	2.30	-	2.20	1.80	1.50
ZrO_2	0.07	-	-	-	-	-	-	-	-	-	-	0.06	-	-	-
BaO	0.01	-	-	-	-	-	-	-	-	-	-	0.02	-	-	-
CO_2	0.04	0.08	-	-	-	0.23	0.70	-	-	-	-	0.71	-	-	-
H_2O	1.39	1.65	-	-	-	1.16	1.65	-	-	-	-	1.47	-	-	-
Cl	0.04	-	-	-	-	0.03	-	-	-	-	-	0.04	-	-	-
SO_3	0.04	-	-	-	-	0.15	-	-	-	-	-	0.03	-	-	-
Total	100.01	99.78	99.17	100.03	99.19	100.54	99.65	99.66	99.83	99.65	99.12	99.90	99.24	99.35	99.10

* Loss on ignition

Continued ..

TABLE 9: CONTINUED

Sample	C67	C79	Jack (1917)	U311	U190	U162	U204	U143	U128	U193	U202	U188	U131	Jack (1917)	U183
Method of Analysis	3	3	1	3	3	3	4	3	3	3	3	3	3	1	2
	Analysis, %														
SiO_2	71.00	71.30	71.48	71.50	71.70	71.70	71.80	71.90	72.00	72.00	72.10	72.20	72.20	72.22	72.40
Al_2O_3	12.80	12.90	14.73	13.30	13.40	12.80	13.80	12.90	12.50	12.50	13.00	12.80	12.70	14.35	13.60
Fe_2O_3	4.50	1.60	1.14	3.20	2.70	1.90	1.56	2.10	2.00	3.10	2.90	3.20	2.40	1.22	1.89
FeO	0.33	1.40	1.16	1.30	0.97	2.10	1.04	1.70	2.00	0.89	0.47	0.97	2.00	1.69	1.07
MnO	0.05	0.01	0.10	0.06	0.02	0.04	0.01	0.05	0.05	0.06	0.01	0.03	0.04	0.02	0.05
MgO	0.99	0.29	0.25	0.97	0.53	0.37	0.21	0.44	0.30	0.39	0.42	0.43	0.24	0.30	0.11
CaO	0.88	0.40	0.54	0.45	0.13	0.80	0.45	0.49	0.84	0.24	0.12	0.28	0.60	1.22	0.24
Na_2O	2.70	2.60	2.74	3.20	3.00	2.80	2.80	3.10	2.60	2.80	2.60	2.80	3.00	2.50	2.85
K_2O	4.60	5.90	5.68	4.10	4.70	4.40	5.60	4.90	4.70	5.00	5.00	4.40	4.60	5.12	5.90
TiO_2	0.60	0.59	0.35	0.49	0.37	0.37	0.23	0.37	0.39	0.35	0.36	0.36	0.35	0.42	0.39
P_2O_5	0.11	0.09	0.04	0.08	0.05	0.05	0.04	0.05	-	0.05	0.03	0.05	0.06	0.70	0.05
L.O.I.*	-	-	-	1.40	1.50	1.80	1.53	1.30	1.70	2.00	2.00	1.50	1.40	-	-
ZrO_2	-	-	-	-	-	-	-	-	-	-	-	-	-	-	0.08
BaO	-	-	-	-	-	-	-	-	-	-	-	-	-	-	0.02
CO_2	-	-	0.12	-	-	-	-	-	-	-	-	-	-	0.22	0.08
H_2O	1.80	2.10	1.40	-	-	-	-	-	-	-	-	-	-	0.80	1.26
Cl	-	-	0.04	-	-	-	-	-	-	-	-	-	-	0.02	0.02
SO_3	-	-	0.14	-	-	-	-	-	-	-	-	-	-	0.06	0.04
Total	100.36	99.18	99.91	100.05	99.07	99.13	99.07	99.30	99.08	99.38	99.01	99.02	99.59	100.86	99.91

* Loss on ignition

Continued ..

TABLE 9: CONTINUED

Sample	U202	U197	U137	U186	U185	S99	S320	U191	U82	U95	U105	S339	U314
	Analysis, %												
Method of Analysis	2	3	3	3	3	3	3	3	3	3	3	3	3
SiO_2	72.60	72.60	72.70	72.70	72.80	72.80	72.90	73.00	73.40	73.60	74.00	74.20	75.70
Al_2O_3	13.60	12.80	12.90	12.60	12.80	12.40	12.90	13.00	12.40	12.60	12.30	12.60	12.50
Fe_2O_3	1.64	2.20	2.00	2.30	3.40	3.90	3.80	3.50	2.90	3.20	3.50	1.70	2.20
FeO	0.71	1.80	1.30	1.70	0.48	0.47	0.23	0.31	1.40	0.71	0.49	1.20	0.45
MnO	0.02	0.05	0.02	0.05	0.01	0.04	0.02	0.01	0.05	0.03	0.05	0.04	0.03
MgO	0.26	0.55	0.24	0.57	0.56	0.40	0.38	0.14	0.51	0.29	0.19	0.39	0.20
CaO	0.10	0.45	0.14	0.33	0.14	0.15	0.15	0.05	0.43	0.09	0.10	0.63	0.74
Na_2O	0.52	3.10	2.50	2.90	2.90	2.60	2.40	2.40	2.50	2.60	2.40	2.90	2.20
K_2O	7.55	4.60	5.60	6.10	4.60	5.70	5.20	5.70	4.30	5.50	5.20	4.70	4.40
TiO_2	0.38	0.37	0.37	0.39	0.34	0.39	0.39	0.37	0.41	0.38	0.30	0.34	0.39
P_2O5	0.03	0.05	0.06	0.06	0.05	0.06	0.08	0.02	0.06	0.07	0.06	0.04	0.05
L.O.I.*	-	1.50	1.30	-	2.00	1.60	1.70	1.60	1.86	1.80	1.60	1.90	1.80
ZrO_2	0.07	-	-	-	-	-	-	-	-	-	-	-	-
BaO	0.01	-	-	-	-	-	-	-	-	-	-	-	-
CO_2	0.01	-	-	-	-	-	-	-	-	-	-	-	-
H_2O	2.21	-	-	1.20	-	-	-	-	-	-	-	-	-
Cl	0.03	-	-	-	-	-	-	-	-	-	-	-	-
SO_3	0.03	-	-	-	-	-	-	-	-	-	-	-	-
Total	99.77	100.07	99.13	100.90	100.08	100.51	100.15	100.10	100.16	100.86	100.19	100.64	100.66

* Loss on ignition.

APPENDIX D

TABLE 10 WELDED TUFF SHEET ($p\epsilon v_3$)

C.I.P.W. Normative Analyses

TABLE 10: CIPW NORMATIVE ANALYSES - WELDED TUFF SHEET. ($p\mathcal{E}v_3$)

	Analysis, %.														
	S109	A1747/61	S323	S121	S113	Jack (1917)	A1746/61	S335	U313	U104	U120	C72	S322	S326	U139
Quartz	21.76	23.89	28.95	27.00	29.22	26.95	27.39	30.84	33.77	31.00	39.22	31.66	37.80	33.93	32.92
Corundum	-	-	1.35	1.63	0.46	2.57	0.98	2.27	2.91	2.16	4.58	2.88	4.42	3.12	1.98
Zircon	0.10	-	-	-	-	-	-	-	-	-	-	0.09	-	-	-
Orthoclase	29.25	27.78	22.46	35.46	24.82	33.69	30.73	22.46	24.82	26.59	24.82	31.91	24.23	28.96	26.59
Albite	29.32	27.92	24.54	22.00	24.54	25.76	27.08	27.08	23.69	24.54	18.62	22.55	22.00	24.54	24.54
Anorthite	6.94	7.87	8.64	2.72	9.07	1.87	1.99	4.24	2.84	3.27	1.25	0.25	0.45	0.83	3.78
Halite	0.07	-	-	-	-	0.05	-	-	-	-	-	0.07	-	-	-
Diopside:Wo	0.37	0.67	-	-	-	-	-	-	-	-	-	-	-	-	-
En	0.12	0.18	-	-	-	-	-	-	-	-	-	-	-	-	-
Fs	0.26	0.53	-	-	-	-	-	-	-	-	-	-	-	-	-
Hypersthese: En	1.72	1.34	3.49	2.74	2.39	0.82	1.82	4.23	2.99	2.86	2.12	1.49	2.49	1.64	1.39
Fs	3.73	4.02	3.54	-	2.82	2.48	2.53	2.72	1.22	3.49	-	2.94	-	-	3.35
Magnetite	2.86	2.04	2.75	4.20	2.90	2.77	2.38	2.75	4.20	2.75	1.86	1.48	0.14	-	2.17
Ilmenite	1.42	1.27	1.37	1.18	1.37	1.31	1.18	1.22	1.22	1.16	1.23	1.14	1.20	0.78	0.74
Hematite	-	-	-	0.40	-	-	-	-	-	-	2.92	-	4.10	3.40	-
Apatite	0.56	0.44	0.28	0.30	0.30	0.44	0.35	0.26	0.28	0.23	0.21	0.30	0.21	0.16	0.14
Pyrite	0.03	-	-	-	-	0.11	-	-	-	-	-	0.02	-	-	-
Calcite	0.09	0.18	-	-	-	0.52	1.59	-	-	-	-	1.61	-	-	-
Rutile	-	-	-	-	-	-	-	-	-	-	-	-	-	0.18	-
Total	98.60	98.13	97.37	97.63	97.89	99.34	98.00	98.06	97.93	98.05	96.82	98.40	97.04	97.55	97.60

Continued

TABLE 10: CONTINUED

	Analysis, %														
	Jack (1917)	U183	U202	U197	U137	U86	U185	S99	S320	U91	U82	U95	U105	S339	U314
Quartz	37.04	32.97	40.30	34.88	36.16	30.79	37.33	35.11	38.37	36.96	40.89	37.00	39.81	37.38	44.32
Corundum	4.69	2.41	4.52	2.02	2.62	0.77	2.92	1.82	3.24	2.84	3.00	2.37	2.69	1.69	2.89
Zircon	-	0.12	0.10	-	-	-	-	-	-	-	-	-	-	-	-
Orthoclase	30.26	34.87	44.62	27.19	33.10	36.05	27.19	33.69	30.73	33.69	25.41	32.50	30.73	27.78	26.00
Albite	21.01	23.97	4.18	26.23	21.15	24.54	24.54	22.00	20.31	20.31	21.15	22.00	20.31	24.54	18.62
Anorthite	0.09	0.39	0.25	1.91	0.30	1.24	0.37	0.35	0.22	0.12	1.74	0.01	0.10	2.86	3.34
Halite	0.03	0.03	0.05	-	-	-	-	-	-	-	-	-	-	-	-
Diopside: Wo	-	-	-	-	-	-	-	-	-	-	-	-	-	-	-
En	-	-	-	-	-	-	-	-	-	-	-	-	-	-	-
Fs	-	-	-	-	-	-	-	-	-	-	-	-	-	-	-
Hypersthene: En	0.75	0.27	0.65	1.37	0.60	1.42	1.39	1.00	0.95	0.35	1.27	0.72	0.47	0.97	0.50
Fs	1.44	-	-	0.97	0.16	0.67	-	-	-	-	-	-	-	0.31	-
Magnetite	1.77	2.48		1.25	3.19	2.90	3.33	0.59	0.52	-	-	3.49	1.25	0.87	2.46
Ilmenite	0.80	0.74	0.72	0.70	0.70	0.74	0.65	0.74	0.53	0.68	0.78	0.72	0.57	0.65	0.74
Hematite	-	0.18	0.78	-	-	-	2.99	3.54	3.80	3.50	0.49	2.34	2.90	-	1.91
Apatite	1.63	0.12	0.07	0.12	0.14	0.14	0.12	0.14	0.19	0.05	0.14	0.16	0.14	0.09	0.12
Pyrite	0.04	0.03	0.02	-	-	-	-	-	-	-	-	-	-	-	-
Calcite	0.50	0.18	0.02	-	-	-	-	-	-	-	-	-	-	-	-
Rutile	-	-	-	-	-	-	-	-	0.11	0.01	-	-	-	-	-
Total	100.05	98.76	97.54	98.57	97.83	99.70	98.08	98.91	98.45	98.50	98.36	99.06	98.59	98.74	98.86

Continued

TABLE 10: CONTINUED

	Analysis, %												
	C67	C79	Jack (1917)	U311	U190	U162	U204	U143	U128	U193	U202	U188	U131
Quartz	34.64	32.43	32.55	35.01	35.33	35.65	32.80	33.15	35.97	35.62	37.04	37.97	35.13
Corundum	2.04	1.73	3.52	2.97	3.26	2.10	2.41	1.73	1.61	2.17	3.16	3.04	1.84
Zircon	-	-	-	-	-	-	-	-	-	-	-	-	-
Orthoclase	27.19	34.87	33.57	24.23	27.78	26.00	33.10	28.96	27.78	29.55	29.55	26.00	27.19
Albite	22.85	22.00	22.89	27.08	25.39	23.69	23.69	26.23	22.00	23.69	22.00	23.69	25.39
Anorthite	3.65	1.40	1.66	1.71	0.32	3.64	1.97	2.10	4.17	0.86	0.40	1.06	2.58
Halite	-	-	0.07	-	-	-	-	-	-	-	-	-	-
Diopside: Wo	-	-	-	-	-	-	-	-	-	-	-	-	-
En	-	-	-	-	-	-	-	-	-	-	-	-	-
Fs	-	-	-	-	-	-	-	-	-	-	-	-	-
Hypersthene: En	2.47	0.72	0.62	2.42	1.32	0.92	0.52	1.10	0.75	0.97	1.05	1.07	0.60
Fs	-	0.29	0.80	-	-	1.75	0.26	0.87	1.47	-	-	-	1.19
Magnetite	-	2.32	1.65	2.97	2.12	2.75	2.26	3.04	2.90	2.05	0.50	2.18	3.48
Ilmenite	0.80	1.12	0.66	0.93	0.70	0.70	0.44	0.70	0.74	0.66	0.68	0.68	0.66
Hematite	4.50	-	-	1.15	1.24	-	-	-	-	1.69	2.55	1.70	-
Apatite	0.26	0.21	0.09	0.19	0.12	0.12	0.09	0.12	-	0.12	0.07	0.12	0.14
Pyrite	-	-	0.10	-	-	-	-	-	-	-	-	-	-
Calcite	-	-	0.27	-	-	-	-	-	-	-	-	-	-
Rutile	0.18	-	-	-	-	-	-	-	-	-	-	-	-
Total	98.56	97.08	98.47	98.65	97.57	97.33	97.54	98.00	97.38	97.38	97.01	97.52	98.19

APPENDIX E

SAMPLE LOCATIONS OF ROCK UNITS EXAMINED IN THIN SECTIONS

LITHIC AND LAPILLI TUFF ($p\epsilon t$)

Samples 1, 3, 15, 17, 24, 30, 31, 55, 56, 192, 193, 194, 195, 245b, 352, 190, 191, 307, 313, 318, 320, 321, 324.

PORPHYRITIC RHYOLITE ($p\epsilon l_1$)

Samples 2, 6, 8, 11, 12, 14, 16, 25, 195, 226.

PORPHYRITIC RHYOLITE ($p\epsilon l_2$)

Samples
snowflake textured, 60, 166, 167, 248, 298.
perlitic textured, 61, 137, 249, 299, 53, 199, 229, 267.
lithic vitric tuff, 59, 107, 232.

CRYSTAL TUFF ($p\epsilon ct$)

Samples 36, 58, 171, 268, 102, 134.

PUMICEOUS TUFFS ($p\epsilon pt$)

Samples 22, 52, 135, 146, 138, 145, 228, 233.

AMYGDALOIDAL PORPHYRITIC RHYOLITE ($p\epsilon al$)

Samples 275, 276, 273, 263, 64.

VITRIC TUFF ($p\epsilon vt$)

Samples 44, 45, 118, 128, 148, 210, 255, 256, 304, 305, 310, 311, 187.

WELDED TUFF ($p\epsilon v_2$)

Samples 74, 99, 62, 243, 38, 227, 271.

PORPHYRITIC RHYOLITE ($p\epsilon l_3$)

Samples
massive phase 188, 189, 220, 309, 311, 316, 219.
banded phase 211, 212, 115, 162, 170, 252, 253, 254, 288, 293, 306, 312.
breccia member 42, 221, 223, 313.

FLUIDAL BANDED PORPHYRITIC RHYOLITE ($p\epsilon fbl$)

Samples 262, 110, 128, 213, 129, 217, 218, 202.

WELDED LITHIC TUFF ($p\epsilon wt$)

Samples 47, 48, 113, 190, 191, 209, 222, 260, 289, 150, 258.

WELDED TUFF SHEET($p\epsilon v_3$)

Samples S329, S327, S333, S330, S328, S326, S325, S331, S334, S324, S332, S335, S342, S343, S344, S323, S336, S337, S338, S109, S108, S110, S111, S112, S113, S123 S321, S311, S345, S339, S340, S107, S193, S101, S114, S115, S116, S117, S118, S100, S99, S97, S98, S96, S119, S120, S121, S123, S124, S340, S316, CW320,Cw379,S322, U104, U106, U126, U125, U95, U313, U301, U314, U302, U341, U316, U313, U303, U304, U305, U102, U103, U105, U195, U304, U305, U306, U124, U83, U84, U85, U86, U87, U88, U89, U90, U91, U92, U93, U94, U317, U197, U196, U185, U127, U128, U129, U130, U131, U132, U133, U134, U135, U136, U137, U138, U139, U140, U141, U142, U143, U144, U145, U146, U182, U190, U189, U188, U187, U186, U204, U205, U206, U207, U208, U97, U28, U257, U138, U163, U164, U165, U167, U168, U170, U169, U149, U183, U184, U185, U174, U181, U180, U179, U150, U151, U152, U153, U154, U155, U156, U157, U158, U162, U166, U140, U148, U159, U160, U161, U141, U182, U173, U172, U171, U178, C318, C202, C207, C203, C204.

LEGEND

Geological boundaries

Faults observed

inferred

Fold Axis, inferred

Trend lines, joint patterns (photo interpretation)

Layering

inclined 70°

vertical

Joints (major)

inclined 70°

vertical

Spherical Projection Joint Systems (equal area, lower hemisphere)

Key > 5%

4 – 5%

3 – 4%

2 – 3%

1 – 2%

< 1%

Welded Tuff Sheet	$p\epsilon v_3$	Crystal Tuff	$p\epsilon ct$
Welded Lithic Tuff	$p\epsilon wt$	Porphyritic Rhyolite	$p\epsilon l_2$
Vitric Tuff	$p\epsilon vt$	Porphyritic Rhyolite	$p\epsilon l_1$
Porphyritic Rhyolite	$p\epsilon l_3$	Lithic Tuff	$p\epsilon lt$
Fluidal Banded Rhyolite	$p\epsilon fbl$	BURKITT GRANITE	$p\epsilon b$
Welded Tuff	$p\epsilon v$	Basic Intrusives	$p\epsilon df$
Amygdaloidal Rhyolite	$p\epsilon al$	CLEVE METAMORPHICS	
Pumiceous Vitric Tuff	$p\epsilon pt$	MIDDLEBACK GROUP	

MAP 2

TECTONIC MAP ARC AND ENVIRONS

GAWLER RANGE VOLCANIC COMPLEX

SOUTH AUSTRALIA

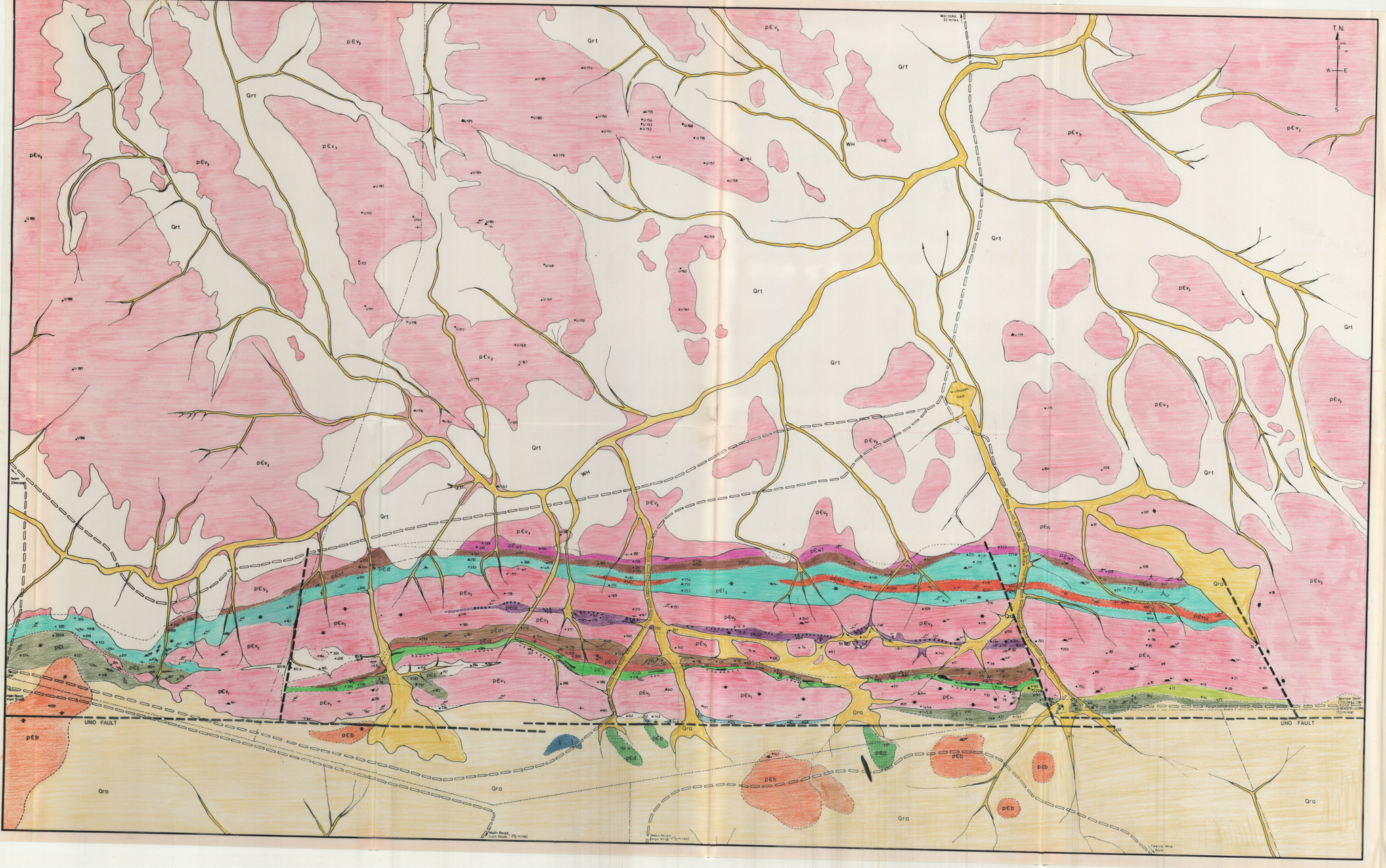
1 MILE

0 440 880 1320 1760 yards

1 Km

0 200 400 600 800 1000 metres

RG 5039



LEGEND

Recent

- Qra — Fluviatile sands and gravels of the modern drainage

Pleistocene

- Qrt — POORAKA FORMATION: Gravels sands and clayey soils

Carpentarian

GAWLER RANGE VOLCANICS

- pEv3 — Welded Tuff Sheet: Massive for most part deep reddish brown
- pEwt — Welded Lithic Tuff: Brown to dark grey, eutaxitic texture
- pEvt — Vitric Tuff: Fine grained, pale grey, locally vitroclastic
- pEl3 — Porphyritic Rhyolite: Massive and banded, pale pink to red
- pEfbl — Fluidal Banded Rhyolite: Vari coloured, prominant segregated flow-banding
- pEv — Welded Tuff: Brick red to pink, local banding and eutaxitic texture
- pEpl — Porphyritic Amygdaloidal Rhyolite: Dark red, welded, locally perlitic
- pEpl — Pumiceous Vitric Tuff: Dark grey-greenish grey, locally vitroclastic
- pEct — Rhyolitic Crystal Tuff: Red, massive, conspicuous quartz feldspar
- pEl2 — Porphyritic Rhyolite: Pale pink to red, locally banded
- pEl1 — Porphyritic Rhyolite: Dark grey, massive
- pEct — Lithic Tuff: Dark to pale-grey, welded, non-welded
- pEs — Silicified Breccia: Volcanic rock, brecciated, silicified

- pEb — BURKITT GRANITE: Massive, hornblende granite locally syenitic
- pEd — Basic Intrusives: Intruding Lower Proterozoic and Gawler Range volcanics
- CLEVE METAMORPHICS: Foliated granite gneisses

Lower Proterozoic

- MIDDLEBACK GROUP: Banded jaspilites

Geological Boundaries: observed / inferred

Faults: observed / inferred

Folds

Bedding: inclined / vertical

Joints (major): inclined / vertical

Quartz veins

Amygdules

Blocks

Tracks

Fence

Sample Localities: petrographic • 137; chemically analysed ▲ 304

Drainage: direction flow

WH — Water hole

MAP 1
GEOLOGY ARC AND ENVIRONS
GAWLER RANGE VOLCANIC COMPLEX
SOUTH AUSTRALIA

SCALE
1:10,000

0 200 400 600 800 1,000 1,200 1,400 1,760 yards

0 100 200 300 400 500 600 700 800 900 1000 metres